WOODHEAD PUBLISHING SERIES IN ELECTRONIC AND OPTICAL MATERIALS

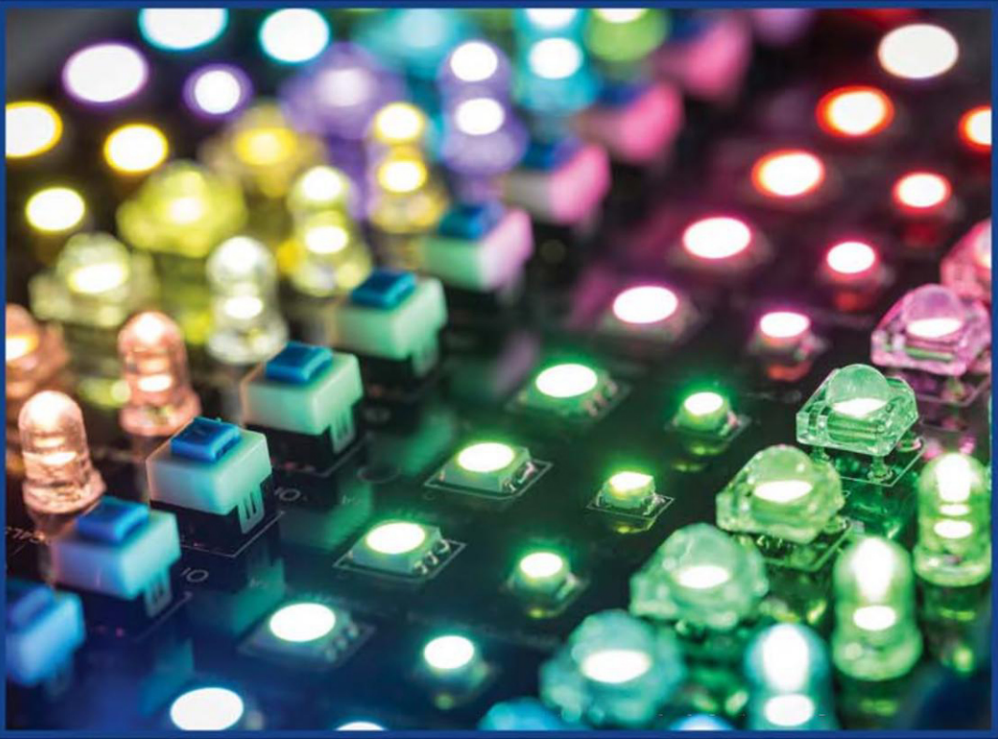

THE FUNDAMENTALS AND APPLICATIONS OF LIGHT-EMITTING DIODES

THE REVOLUTION IN THE LIGHTING INDUSTRY

GOVIND B. NAIR
S. J. DHOBLE

ELSEVIER

Woodhead Publishing Series in Electronic and Optical Materials

The Fundamentals and Applications of Light-Emitting Diodes

The Revolution in the Lighting Industry

Govind B. Nair

S. J. Dhoble

ELSEVIER

WP

WOODHEAD PUBLISHING

An imprint of Elsevier

Woodhead Publishing is an imprint of Elsevier
The Officers' Mess Business Centre, Royston Road, Duxford, CB22 4QH, United Kingdom
50 Hampshire Street, 5th Floor, Cambridge, MA 02139, United States
The Boulevard, Langford Lane, Kidlington, OX5 1GB, United Kingdom

Notices
Knowledge and best practice in this field are constantly changing. As new research and experience broaden our understanding, changes in research methods, professional practices, or medical treatment may become necessary.

Practitioners and researchers must always rely on their own experience and knowledge in evaluating and using any information, methods, compounds, or experiments described herein. In using such information or methods they should be mindful of their own safety and the safety of others, including parties for whom they have a professional responsibility.

To the fullest extent of the law, neither the Publisher nor the authors, contributors, or editors, assume any liability for any injury and/or damage to persons or property as a matter of products liability, negligence or otherwise, or from any use or operation of any methods, products, instructions, or ideas contained in the material herein.

Library of Congress Cataloging-in-Publication Data
A catalog record for this book is available from the Library of Congress

British Library Cataloguing-in-Publication Data
A catalogue record for this book is available from the British Library

ISBN: 978-0-12-819605-2

Publisher: Matthew Deans
Acquisitions Editor: Sabrina Webber
Editorial Project Manager: Emily Thompson
Production Project Manager: Surya Narayanan Jayachandran
Cover Designer: Greg Harris

Typeset by TNQ Technologies

Part One

Fundamentals

Introduction to luminescence

1

1.1 Characteristics and quality of light

The quality and quantity of the lumen output originating from a light source justifies the imperial amount of research dedicated to improve the efficiency of the luminaire. Time has witnessed many drastic improvements in the lighting industry. From the dawn of life on the earth, the role of the ultimate source of light has been redeemed by the sun. Unconditionally, the sun provides the best quality light that is still unmatched with the present-day luminaires. The eminence of light can only be determined by the eye that perceives it. Apparently, the features of a luminaire are adjusted to give a pleasant perception to the human eye. To optimize the lighting systems from the perception of a human eye, several quantitative metrics were developed.

The interpretation of a light source by a human eye differs from individual to individual due to the differences in their physiology and, consequently, the quantified perception is likely to change from person to person. To standardize the perceptual responses to light stimuli, a statistical analysis was prepared involving several human subjects. Based on those results, the photometric standards for different sources of light were put forward. The part of the eye that is most sensitive to light is the human retina, which consists of two types of cells, *viz*., the rod cells and the cone cells. Rod cells and cone cells are together known as the photoreceptors. It is estimated that 120 million rod cells and 60 million cone cells exist in the retina. The rod cells are more sensitive than the cone cells and are sensitive to the entire range of the visible light spectrum. On the other hand, the cone cells are sensitive to only a small range in the visible light spectrum and they are characterized into three types depending on their sensitivity to red, green, and blue light spectrum. The cone cells are functional at high light-levels while the rod cells show their functioning at low light-levels. At intermediate light-levels, both of them function together. Based on the light-levels, the vision regimes are categorized into three types, namely photopic vision, scotopic vision, and mesopic vision. The cone cells mediate the photopic vision, and the rod cells mediate the scotopic vision while the mesopic vision relates to light-levels between the photopic and scotopic vision regimes [1].

Radiometric and photometric units are, in general, used to characterize the physical properties of electromagnetic radiation that is significant to the optical quantities for light-emitting diode (LED) metrology. Light is characterized by radiometric units in terms of physical quantities, for instance, the radiant flux, photon energy, and the number of photons. Ideally, the radiometric quantities are four in number, and those are listed as radiant flux, radiant intensity, irradiance, and radiance. Radiant flux is the net power emitted per unit time by a light source and is expressed in the units of watt (W). Another quantity is the radiant intensity, which is expressed in units of

The Fundamentals and Applications of Light-Emitting Diodes. https://doi.org/10.1016/B978-0-12-819605-2.00001-X

watt per steradian (W/sr) and it is defined as the power emitted per unit solid angle. The radiant power is measured using a detector with an active area, which is positioned at some distance from the point source of light. The ratio of the radiant power and the area of the detector is the irradiance, which is measured in the units of watt per square meter (W/m^2). The radiant power emitted from an area per unit solid angle is called radiance, and it is generally measured for extended light sources. Radiance is measured in the units of watts per steradian per square centimeter ($W/sr\ cm^2$). Nevertheless, human eyes fail to have any perception of radiations other than the visible light, and hence, these radiometric units have less significance while considering the light perception by a human eye. In this regard, the photometric units came to the picture and played a great role in the standardization of the perception of light by human eyes [2]. The photometric quantities such as luminous intensity, luminous flux, illuminance, and luminance define the quality of light originating from a source. The luminous intensity represents the light intensity of an optical source as perceived by the human eye and is expressed in the units of candela (cd). A unit candela is defined as the luminous intensity obtained when a monochromatic light source emitting an optical power of (1/683) watt at 555 nm into the solid angle of 1 steradian (sr). The luminous flux is another photometric quantity, which is expressed in the units of the lumen (lm). It represents the light power of a source as perceived by the human eye. Technically, the lumen can be defined as the luminous flux achieved after a monochromatic light source emits an optical power of (1/683) W at 555 nm. On associating the definitions of lumen and candela, it is found that 1 lumen per steradian is equal to 1 cd. When the luminous flux is measured per unit area, the quantity is expressed in terms of illuminance. Lux is the unit used to measure illuminance and it is equal to lm/m^2. Yet another photometric quantity is the luminance, which is expressed in the units of cd/m^2. Luminance is defined as the ratio of the emitted luminous intensity to the projected surface area in a certain direction. All the earlier mentioned metrics are useful while defining only the quality of light from a source and do not necessarily describe the actual merit of a luminaire.

1.2 Conceptual background of luminescence

Luminescence is a cold-body radiation or the spontaneous emission of light from a source that does not accompany heat with it. Technically, luminescence is defined as "*the emission of light by bodies*, *which is in excess of that attributable to black body radiation*; *and persists considerably longer than the periods of electromagnetic radiations in the visible range after the excitation stops*" [3]. The materials exhibiting this phenomenon are called as luminescent materials, or simply phosphors. When a phosphor is stimulated by an excitation source, it absorbs the energy from that source and remits it in the form of light. This light can be either in the ultraviolet (UV) region, visible region, or infrared region. On providing proper stimulus to the phosphor, the electronic system of the material gets excited from the ground state to the higher energy state and, finally, decays from this higher energy state to a lower energy state with the emission of photons/light. The wavelength of the emitted light is the characteristic of the material and not of the excitation source or stimulus. Depending on the type of stimulation, luminescence can be broadly classified as shown in the Table 1.1.

Table 1.1 Classification of luminescence on the basis of the excitation source.

Type of luminescence	Source of excitation	Example
Photoluminescence	Low-energy photons	LED phosphors [4]
Electroluminescence	Passage of electric current	InGaN blue light emitting diodes [5]
Chemiluminescence	Chemical reaction	Luminol derivatives for biosensor applications [6]
Bioluminescence	Biochemical reactions in living organisms	Luciferase enzymes as probes for molecular imaging [7]
Thermoluminescence	Release of absorbed light from traps or defects on heating	Luminescence on applying thermal energy to the γ-irradiated $CaSO_4$:Dy phosphor [8]
Cathodoluminescence	Bombardment of high energy electrons	Cathodoluminescence spectroscope for nanoscale optical tomography [9]
Radioluminescence	Ionizing radiations	$NaGdF_4$/Tb@CaF_2 core/shell nanocrystals as X-ray luminescence imaging probe [10]
Ionoluminescence	Ion beams	Proton-beam induced luminescence in diamonds [11]
Electrochemiluminescence	Electrochemical reactions	Electrochemiluminescence of tris (2,2′-bipyridyl)ruthenium(II) in high performance liquid chromatography [12]
Candoluminescence	Exposure to high temperature	Flame-excited emission of SnO_2 [13]
Mechanoluminescence	Release of absorbed light from traps or defects as a result of mechanical stress	Luminescence on applying mechanical stress on the UV-irradiated $SrAl_2O_4$:Eu^{2+},Dy^{3+} phosphor [14]
Triboluminescence	Breakage of bonds in a material due to rubbing, scratching or crushing	Luminescence arising from the friction of corundum rod on $Sr_3Ga_4O_9$:Bi^{3+} phosphor [15]
Piezoluminescence	Induced pressure	Piezoluminescence from $LiTaO_3$:Pr^{3+} phosphor [16]
Fractoluminescence	Breakage of bonds in a material due to fractures	Luminescence from the three-point bending fracture of crystalline quartz [17]

Continued

Table 1.1 Continued

Type of luminescence	Source of excitation	Example
Lyoluminescence	Dissolution of irradiated solute in a liquid solvent	Luminescence obtained on dissolving γ-irradiated $GdCa_4O(BO_3)_3$ in dil. HCl [18]
Sonoluminescence	Implosion of bubbles in a liquid due to sound	Sonoluminescence from nanodispersed suspensions of $Cr(CO)_6$ in 74% H_3PO_4 [19]
Crystalloluminescence	Crystallization of a substance	Luminescence emerging from the crystallization of benzanilide from organic solvents of uranine, eosine, 9,10-dibromoanthracene [20]
Cryoluminescence	Cooling of a substance	ZnS phosphors excited by infrared radiations showed increase in luminescence on cooling to temperatures ~50 K [21]

Depending on the duration of the decay lifetime, luminescence can also be classified as fluorescence and phosphorescence. Fluorescence is a temperature-independent process, with a decay lifetime of less than 10^{-8} seconds. The term *fluorescence* was coined by G.G. Stokes in 1852 while investigating the ability of fluorspar and uranium glass to convert the UV light into blue light [22]. Irrespective of the intensity of the excitation source or the temperature, fluorescence shows an immediate exponential decay as soon as the excitation is shut down. On the contrary, phosphorescence bears a longer decay lifetime greater than 10^{-8} seconds. This process depends on the intensity of the excitation source and the temperature. When the excitation source is cut off, the phosphorescent material shows a long afterglow that can continue to last from about a few seconds to several hours. Afterglow is the slow decay of the luminescence emission resulting from the complex kinetics occurring in the luminescent material. The presence of electron or hole traps, lattice defects, impurities, or activators present in the lattice lead to the formation of metastable states that delay the luminescence emission from the material. The prerequisite for the afterglow is the thermal activation of metastable states. The difference between fluorescence and phosphorescence on the basis of its decay lifetime seemed to be unacceptable in the case of certain luminescent materials. Eu^{2+}-doped phosphors often exhibit fluorescence with a long lifetime of the order of few microseconds [23], while ZnS exhibited violet phosphorescence with a short lifetime of the order of few nanoseconds [24,25]. In 1929, F. Perrin came up with a better understanding of the distinction between fluorescence and phosphorescence [26]. He proposed that the excited species in phosphorescence pass through an intermediate state before emission. The precise distinction between the two processes is pointed out under the framework of molecular photochemistry.

In phosphorescence, the spin multiplicity involves a change from the triplet to the singlet state or vice versa, whereas the spin multiplicity is retained in the fluorescence process.

1.3 Luminescence mechanisms

The theory behind the luminescence mechanisms observed in solid materials can be best understood from the band theory of solids. An isolated atom consists of an electron cloud present in the orbitals around the nucleus. These orbitals are analogous to the planetary orbits around the sun. The difference between these two systems lies in the type of force acting on them: Gravitational force is responsible for the planetary motion around the sun, while electromagnetic force is responsible for the electronic motion around the nucleus. The electrons are allowed to occupy only the discrete orbitals wherein the electrons can revolve without any loss of energy. The laws of quantum mechanics govern the rules for determining the energy states of these allowed orbitals. As per Pauli's exclusion principle, an orbital can be shared at the most between two electrons of opposite spins. However, all the orbitals are not equidistant from the nucleus. Some electrons occupy the lower energy orbitals that are near the nucleus while others occupy the orbitals far away from the nucleus as the orbitals near the nucleus are already filled. By providing a radiation pulse, the electron in the occupied energy levels can be dislodged and vacancies can be created in them. These electronic transitions can be a result of the absorption of energy by material from one of the excitation sources such as photons, electrons, ionizing radiations, and mechanical stress. This will lead to the occupation of the electron vacancy in the lower energy level by an electron in the outermost level. The transition of an electron from the higher energy level to the lower energy level leads to an emission of photon energy, which is equivalent to the energy difference between the two energy levels. In certain cases, the energy difference between the higher and the lower energy states are spaced in such a way that the electron transition results in the emission of photon energy within the visible light spectrum.

1.3.1 Photoluminescence

Photoluminescence occurs when photonic energy excites a material and compels it to release photons of higher or lower values of energy than that which is absorbed. The curiosity of finding the underlying mechanism behind the luminescence phenomenon is always a topic of keen interest among the researchers. As a result, several theories describing the luminescence mechanisms were developed and still, research is going on. Mechanisms, by which photoluminescence phenomenon is observed, can be broadly classified as intrinsic luminescence and extrinsic luminescence [27].

1.3.1.1 Intrinsic luminescence

Several phosphors have shown the ability to produce luminescence on its own without being activated by any impurity ion-doping in them. Such materials are known as self-

luminescent materials, and the phenomenon is called self-luminescence or intrinsic luminescence. Self-luminescent materials enjoy the advantage of lower energy losses, which is generally observed during the energy transfer among the doped luminescent ions. Intrinsic luminescence can be either due to the defects present in the material, or it may be due to the charge-transfer (CT) transition between a ligand O^{2-} ion and the metal ion. The mechanism of intrinsic luminescence is dependent on the type of host material.

Defect-assisted luminescence: Ideally, defect-assisted luminescence systems do not require an activator ion and such systems come under the category of intrinsic luminescence. Even in the absence of an activator ion, such materials can show luminescence by creating electron−hole pairs that act as luminescence centers at certain sites in the host matrix. One of the most promising examples of defect-assisted luminescence is the BCNO phosphor [28]. BCNO has the potential to tune its emission color from violet (400 nm) to near-red (650 nm) region of the visible-light spectrum by varying the carbon content in them. The carbon impurities can be introduced into the phosphor by using polyethylene glycol (PEG) as the carbon source. With an increasing PEG concentration, the nitrogen and boron atoms in the crystals of turbostratic boron nitride (t-BN) were substituted by carbon atoms. This led to the rearrangement of the chemical composition and position of atoms in the phosphor, which was accompanied by the shift in the photoluminescence emission peaks, as shown in Fig. 1.1. BCNO exhibited high external quantum efficiency values, particularly in the blue and green region, and hence, it forms an attractive material for the fabrication of white light-emitting diodes (WLEDs). The presence of carbon impurities has also proved the tuning of luminescence emission from 370 to 620 nm in the case of spherical ZrO_2 particles [29]. BPO_4 showed a weak purplish-blue emission centered at 409 nm. However, after doping Ba^{2+} ions, oxygen-related defects were created in the BPO_4 lattice that acted as additional emission centers in the lattice [30]. As a result, the intensity of the emission peaks enhanced and this was accompanied by a red shift in the peak position. Most of the materials exhibiting defect-assisted luminescence are eco-friendly, nontoxic, and produced from inexpensive raw materials. These features have emphasized the acceleration of these luminescent materials as a replacement for expensive rare-earth-based phosphors.

Charge-transfer (CT) transition: CT transition is the most common type of intrinsic luminescence. It is mostly observed in host lattices involving niobates $(NbO_4)^{3-}$, vanadates $(VO_4)^{3-}$, molybdates $(MO_4)^{2-}$, and tungstates $(WO_4)^{2-}$. In these cases, the photon energy is absorbed by the host due to the electron transfer from O^{2-} ligand to the metal ion, which may be Nb^{5+}, V^{5+}, Mo^{6+}, or W^{6+}. In general, charge-transfer can occur due to the electron transition either from metal to ligand ions or from ligand to metal ions, and hence, they are subsequently termed as metal-to-ligand charge transfer (MLCT) and ligand-to-metal charge transfer (LMCT), respectively [31]. Most of the inorganic phosphors are known to exhibit the LMCT type of charge-transfer band (CTB). For instance, $Ca_{0.5}Y_{(1-x)}(WO_4)_2{:}xEu^{3+}$ and $Ca_{0.5}Y_{1-x}(WO_4)_2{:}xTb^{3+}$ phosphors exhibit LMCT from O^{2-} to W^{6+} resulting in a strong absorption in the UV region [32]. $Y_2WO_6{:}Sm^{3+}$ phosphor showed a strong absorption band in the 300−380 nm region, which is also attributable to the charge transfer from the 2p

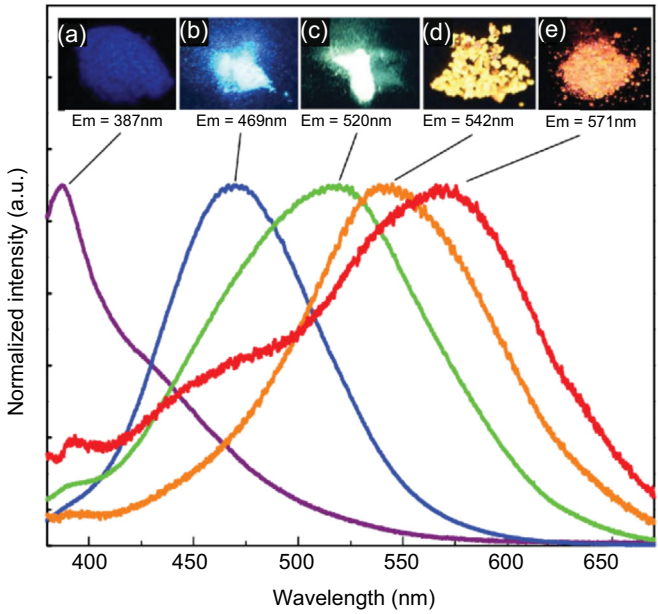

Figure 1.1 Digital photographs and PL emission spectra of 365 nm NUV-excited BCNO phosphor prepared under different conditions. The PEG/B ratio, operating temperature, and heating time were set as (a) 2×10^{-3}, 900°C, 30 minutes; (b) 2×10^{-3}, 800°C, 30 minutes; (c) 4×10^{-3}, 700°C, 60 minutes; (d) 4×10^{-3}, 700°C, 45 minutes; (e) 4.4×10^{-3}, 700°C, 30 minutes.

orbitals of O^{2-} to the 5d orbitals of W^{6+} within the $(WO_4)^{2-}$ group [33]. All these phosphors will continue to show the UV absorption even in the absence of any rare-earth activator ion. On similar terms, phosphors such as $M_{1-x}MoO_4:Eu_x$ (M = Zn, Mg, Ni, Ca, and Co) [34], $Sr_{1.98}Sm_{0.02}CaMoO_6$ [35], $Sr_9Eu_2W_{4-x}Mo_xO_{24}$ [36], and Y_2SiO_5 [37] also showed LMCT, which is not a characteristic of the rare-earth ions present in them.

CTBs can sometimes arise as a result of the rare-earth activator ions that are doped into a host lattice. The most widely observed example is that of Eu^{3+} ions that most commonly demonstrate LMCT from the filled $2p^6$ orbitals of O^{2-} to the vacant $4f^7$ orbitals of Eu^{3+} ions. The peak position of the CTB can vary depending on the bandgap of the host in which the activator ion is doped [38]. When the activator ion is doped into a certain host lattice, all the energy levels of the activator will be positioned within the bandgap of the host. LMCT is not just limited between the O^{2-} and Eu^{3+} ions, but other electronegative anions such as fluorides, chlorides, bromides, iodides, nitrides, sulfides, selenides, antimonides, tellurides, arsenides, and phosphides also demonstrate LMCT with Eu^{3+} ions. One factor that presents the CTB of Eu^{3+}

with an edge over its characteristic 4f−4f transitions is that the former one is allowed as per the Laporte selection rules, while the latter one is forbidden. This forms the reason for the occurrence of very intense CTB as compared to the narrow bands arising from the 4f−4f transitions. The luminescence efficiency of Gd_2O_3:Eu^{3+}, Y_2O_3:Eu^{3+}, and Lu_2O_3:Eu^{3+} phosphors increased following their excitation by 260 nm CT excitation band, which is attributed to the LMCT from O^{2-} to Eu^{3+} [39]. The charge transfer absorption energy can vary with the size of the crystalline material as the bandgap shows the variation with the crystal size. Shang et al. have reported the effect on the CT excitation band when the size of the Y_2O_3:Eu^{3+} phosphor was decreased to nanoscale [40]. As a result, there was a decrease in the CT energy and a redshift in the CT excitation spectrum. The energy of the CT transition largely depends on the nearest neighbors of the metal ion and the optical electronegativity of the ligands [41]. Temperature can also influence the position of the CT band and cause its luminescence quenching [42].

The coating of organic materials on inorganic phosphor can lead to the shifting of LMCT absorption toward the near-UV (NUV) region. LMCT absorption is significant for white NUV-LED technology from the point of view that the phosphor absorbs light in the UV region that overlaps with the NUV-LED emission [43]. In MLCT transition, electrons are transferred from metal ions to ligands. MLCT transition is rarely observed as compared to the LMCT transition. Ce^{4+} and Yb^{3+} show MLCT type of transition. In Sr_2CeO_4 phosphor, MLCT emission is observed at 467 nm as a result of the electron transfer from Ce^{4+} to O^{2-} ions [44]. MLCT transition is mostly observed in organometallic compounds. Apart from lanthanides, Mn^{2+} metal ions also show MLCT absorption in the UV region, which can be attributed to the electron transfer from Mn^{2+} to O^{2-} [45].

1.3.1.2 Extrinsic luminescence

Extrinsic luminescence involves the process of luminescence from an optically inactive host matrix, which is doped with an activator ion in optimized concentrations typically quantified in the values of a few mole percent. Extrinsic luminescence is also termed as center luminescence. In this type of luminescence, only the activator ion takes part in the luminescence process and the host lattice does not produce any luminescence on its own. The role of the host lattice is only to provide a favorable environment for the activator ions to luminesce.

The excitation and emission spectra of an externally doped luminescent ion can either be narrow or broad. Generally, narrow bands are observed if there is less or no electron−phonon coupling of a luminescent ion in a host lattice. On the other hand, broad bands are observed when the ground state and the excited state of the ion have different types of chemical bonding. In other words, the coupling of vibrational bands with the electronic transitions of the luminescent ion causes the broadening of the excitation and the emission bands. This concept can be visualized from the configurational coordinate model as shown in Fig. 1.2. The two electronic states are represented by the ground state parabola and the excited state parabola under adiabatic approximation. These two parabolas consist of a number of vibrational energy levels associated with the two electronic states. When there is an electronic transition

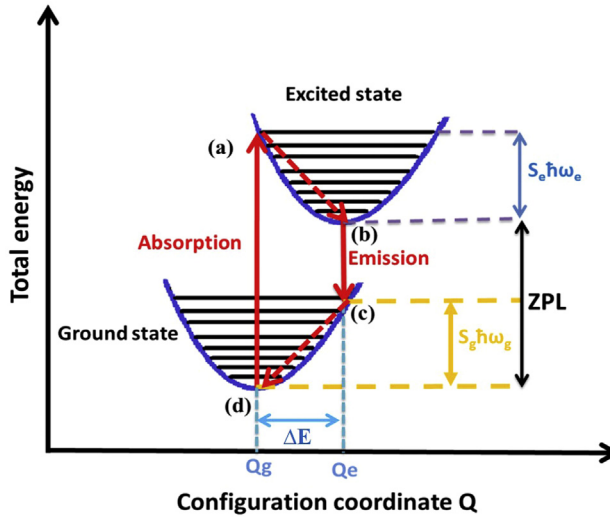

Figure 1.2 Configurational coordinate model [Reproduced with permission from Ref. [120], Copyright 2016, Elsevier B.V.].

between the ground state and the excited state, there is a change in the configuration coordinate, the chemical bonding character, and the metal−ligand distance. The metal−ligand distances for the completely relaxed excited state and the ground state are represented by Q_e and Q_g, respectively.

When the luminescent center absorbs energy from an external source, the lattice undergoes an expansion and initiates an electronic transition from the lowest vibrational energy level of the ground state parabola to the vibrational level of the excited state parabola. In Fig. 1.2, the vertical arrows indicate the absorption and emission of energy by the excited state parabola. The difference between the absorption and emission energies is termed as the Stokes shift (ΔE). The Stokes shift is quantified by another electron-vibrational interaction parameter, known as Huang-Rhys factor (S). It indicates the average number of phonons of energy ħω and gives a measure of the strength of the electron−lattice coupling [46]. $S_e\hbar\omega_e$ and $S_g\hbar\omega_g$ are phonon energies for excited state and ground state, respectively. For stronger electron−phonon coupling, the emission and the excitation spectra become broad [47,48]. The point at which the excitation and the emission bands intersect is known as the zero-phonon line (ZPL) position.

Energy transfer between the luminescent ions: An activator ion absorbs the energy from an external source and emits a characteristic light with a different energy. Part of the absorbed energy is transferred nonradiatively among other activator ions in the host. Sometimes, the absorption of energy by the activator ion is too weak, and this leads to very weak or no radiative emission. In such a scenario, there is a need to introduce another species of ions that could efficiently absorb the energy and transfer it to the activator ions for them to radiatively emit the energy. This new species of ions that are codoped along with the activator ions are known as sensitizer ions. As the name suggests, sensitizer ions produce a sensitizing action in the luminescence process by

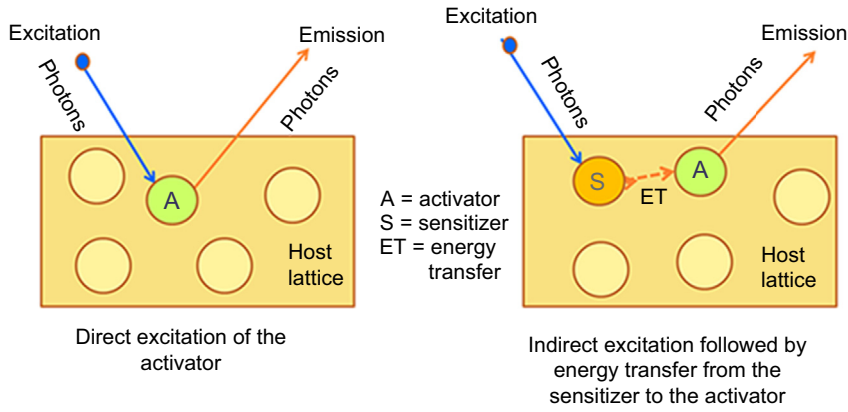

Figure 1.3 Energy transfer between the sensitizer and activator ions.

acting as a bridge for the activator ions to efficiently absorb the energy provided by an external source. As shown in Fig. 1.3, a sensitizer ion absorbs the energy and gives an indirect excitation to the activator ion by transferring its energy to the activators. Generally, trivalent lanthanide ions (Dy^{3+}, Tb^{3+}, Eu^{3+}, etc.) exhibit weak absorption in the UV region owing to their parity-forbidden 4f−4f transitions. This also forms the reason for their weak and narrow-band emission in the visible light spectrum. On the other hand, Eu^{2+} and Ce^{3+} exhibit parity-allowed 4f−5d transition, and that results in broad as well as intense absorption and emission bands for these ions. Hence, Eu^{2+} and Ce^{3+} ions can form efficient sensitizers to the lanthanide ions such as Dy^{3+} and Tb^{3+} [49,50]. An important condition for the energy transfer to take place between the sensitizer and the activator ions is that there should be a spectral overlap between them. In other words, the emission spectrum of the sensitizer must overlap with the excitation spectrum of the activator ion [51]. In addition, there should be some physical interaction between the sensitizer and the activator ions. There are two types of interaction by which energy transfer between two ions can be possible. One is the exchange interaction and the other one is the electrostatic interaction. In exchange interaction, an electron is transferred from a sensitizer ion to an activator ion in an excited state and then, from the activator ion to sensitizer ion in the ground state. In electrostatic interaction, sensitizer induces a dipole oscillation on the activator ion by which energy is transferred.

Persistence luminescence: In persistence luminescence, a material is subjected to high-energy excitation and the emission of light persists for a long time even after the excitation source is removed. This type of luminescence is also called as afterglow phosphorescence, or long-lasting phosphorescence. In the case of persistence luminescence that occurs in inorganic phosphors, the long decay time is due to the forbidden transition within the luminescent center. Optical storage, display, safety signs, and biomedical imagining are some of the applications of persistence luminescence [52].

Donor−acceptor pair luminescence: This type of luminescence is usually seen in semiconductor materials that are doped with acceptor-type and donor-type impurities.

In this type of luminescence, the distance between donor−acceptor ions decides the peak maxima of the emission and the excitation spectra. ZnS:Ag,Cl [53] and ZnS:Cu,Au,Al [54] are some of the examples of the compounds that show donor−acceptor-type of luminescence.

1.3.2 Electroluminescence

Electroluminescence (EL) is an optical process that leads to the generation of photons as a result of the radiative recombination of holes and electrons during the passage of an electric current through a material. EL is broadly classified into two types: (1) low-field EL, wherein the injection of minority charge carriers takes place, and (2) high-field EL, wherein the majority charge carriers are accelerated to high optical energies [55]. Low-field EL is more commonly observed in p−n junction semiconductors like LEDs, whereas high-field EL is more common in electroluminescent displays made of phosphor or organic luminescent materials. For low-field electroluminescence to take place, the recombination of the electrons and holes in the semiconductor material must occur, for which they must be separated from each other before recombination. The electrons and holes are separated from each other by creating a p−n junction through doping. On the other hand, high-field EL occurs in phosphors when the strong electric field accelerates the electrons in the material to very high energies that are capable of exciting the luminescent centers in the phosphor. The excited states of the luminescent center undergo relaxation to give out an EL emission. High-field EL devices can be further divided into AC-operated and DC-operated devices. The phosphors for EL displays are either used in the form of powder or in the form of thin films. As the name suggests, the electric field in the active region of high-field EL devices are very high and range in the order of 10^6 V/cm, whereas the electric field in the low-field devices like LEDs is just a few volts per cm. The former shows less sensitivity to temperature, while the latter is highly influenced by the temperature [56]. The working principle of semiconductor LEDs will be discussed in Section 2.4.2 of Chapter 2.

1.4 Luminescence from rare-earth ions and transition metal ions

1.4.1 Rare-earth ions

Lanthanides form the most significant class of luminescent dopants that are introduced in inorganic solids for LEDs. Lanthanide elements have a typical characteristic to get excited by absorbing UV or near-UV light and then bring out the emission in the form of visible light. Lanthanides are part of the f-block series of elements and are more commonly known as the rare-earths. Although actinides also come under this series, they are neatly ignored from being a part of pc-LEDs. Citing the radioactive nature of these elements, actinides are never preferred in phosphors. There are 15 elements under the lanthanide series that extend from lanthanum (La) to lutetium (Lu). The elements in the extreme ends of the series are La and Lu, which possess empty and filled

4f orbitals, respectively. As a result, they do not produce any f−f or f−d transitions capable of producing luminescence. In contrast, all the other elements of the lanthanide series are characterized by an incompletely filled 4f orbital. As a result, the host lattice shows very small influence on the optical transitions occurring within the 4f orbital. Except for La and Lu, all of the elements in the lanthanide series are capable of exhibiting luminescence. The lanthanide elements are capable of showing their emissions in their +3 oxidation state. Eu has an additional feature of exhibiting luminescence in both +2 and +3 oxidation states [48,57−63].

Most of the lanthanides (in their trivalent state) show sharp line spectra owing to these transitions. However, these transitions are spectroscopically forbidden and hence, appear with a weak intensity most of the time. However, the admixture of forbidden 4f−4f transitions with the allowed transitions, for example, 4f−5d transitions, makes it possible for the former to occur. The symmetry of the crystal environment can also affect the selection rules controlling the transitions. A transition may be either of magnetic-dipole nature, an electric-dipole nature, or a combination of both. A magnetic-dipole transition is independent of the symmetry and its strength does not change with the site symmetry. In contrast, the electric-dipole transition is greatly influenced by the crystal site symmetry, and its strength increases when the lanthanide ion occupies a site with noninversion symmetry. The electrons in the 4f orbitals are arranged in discrete energy levels that are unaffected by the crystal field environment due to the strong shielding of the outer orbitals. This also remains the reason for the trivalent lanthanides exhibiting similar energy level diagram in its free-ion state as well as when doped into a certain host matrix. Except Ce^{3+}, all other trivalent lanthanides show their narrow-band excitation and emission peak positions with a variation of $\pm$ 500 cm^{-1} from that of a free ion. The electronic transitions corresponding to the absorption and emission processes in a lanthanide ion occurs from different energy levels. Hence, the spectral positions of absorption and emission also differ. The difference between the peak positions of the absorption and the emission spectra is termed as the Stokes shift.

Although all the lanthanides from Ce^{3+} to Yb^{3+} can show luminescence, not all are favorable for LED phosphors. Trivalent ions such as Yb^{3+}, Tm^{3+}, Er^{3+}, Ho^{3+}, and Nd^{3+} are more inclined to exhibit upconversion luminescence and are totally out of the frame of LED phosphors. The most prominently used lanthanides for LED applications are Ce^{3+}, Sm^{3+}, Eu^{3+}, Eu^{2+}, Tb^{3+}, and Dy^{3+}. Hence, we shall limit our discussion only to these lanthanides. Depending on the type of electronic transitions exhibited by the ions, they may be classified into two subsections as follows:

1.4.1.1 4f−4f transition

Ce^{3+} is the simplest of all the lanthanides (Ln^{3+}) under our discussion. It has only one 4f electron and hence, only a single discrete 4f energy level. Barring Ce^{3+}, all other lanthanides possess numerous discrete 4f energy levels. These levels undergo further splitting due to the crystal field. The excitation and the emission spectra in these ions are ascribed to the intra 4f−4f transitions, which are parity forbidden. However, the Ln^{3+} ions interact with the lattice vibrations or the crystal field that

cause its 4f states to interact with other Ln^{3+} states having opposite parity. This leads to the formation of mixed-parity states and the selection rules forbidding the 4f−4f transitions are relaxed, as a result of which, the parity-forbidden 4f−4f electric-dipole transitions become allowed. Consequently, these transitions are better known as forced electric-dipole transitions or induced electric-dipole transitions. The admixture of the states with opposite parity decides the intensity of the emission band. The 4f energy levels are well shielded by the filled $5s^2$ and $5p^6$ orbitals. Hence, the electronic transitions occurring within the 4f orbitals are unperturbed by the crystal environment. This forms the reason that the peak positions of the excitation and the emission narrow-bands occurring in Ln^{3+} ions do not vary much with respect to the host lattice.

1.4.1.2 4f−5d transition

Different from other lanthanides discussed earlier, Ce^{3+} and Eu^{2+} exhibit broad excitation and emission bands corresponding to the parity-allowed $4f^n$−$4f^{n-1}5d$ electronic transitions. The spectroscopic features of the 4f−5d transitions are strongly influenced by the crystal environment. This means that the intensity and the energy of the transition are strongly affected by the crystal field strength, crystal lattice symmetry, nature of bonds (covalence/ionic), atomic coordination, bond strength, etc. The excitation and emission properties of Ce^{3+}- and Eu^{2+}-doped phosphors can be determined directly from their 4f and 5d energy levels, as their luminescence is greatly depending on their intrinsic interaction with the host lattice. In the free-ion state, the energy gap between the 4f ground state and 5d excited state of Ce^{3+} and Eu^{2+} ions are 50,000 and 34,000 cm^{-1}, respectively [46,64]. When these ions are doped into a certain host matrix, the energy gap between the two levels is significantly decreased due to the centroid shift and the crystal field splitting [65]. The 5d orbitals experience a centroid downshift depending on the host in which the ion is doped. It can also be associated with the covalency of the host. This is because the centroid experiences downshift due to the reduction of the interelectronic repulsion, which in turn is ascribed to the sharing of electrons between the activator ions and the surrounding ligand anions. Thus, the degree of centroid downshift determines the covalency of the host. As the anion polarizability, symmetry, covalency, and crystal field of the host lattice significantly influence the 5d orbitals of Ce^{3+} and Eu^{2+}, their excitation and emission spectra can be tuned by bringing about structural change or variation in the chemical composition of the host. The structural modification in the host compound can be achieved by performing crystal-site engineering, anionic substitution, cationic substitution, cationic−anionic substitution, control of doping concentration, or mixing of multiple phases [66]. In the crystal-site engineering approach, the activator ions (Ce^{3+} or Eu^{2+}) are introduced into different cationic sites available in the host [67]. These cationic sites bear different coordination environments and hence, the emission properties of the activator ions will also experience an essence of spectral tuning. The exceptional luminescence properties of Ce^{3+} and Eu^{2+} have also rendered them as excellent sensitizer ions for the trivalent lanthanides such as Dy^{3+}, Tb^{3+}, and Sm^{3+} and transition metal ions such as Mn^{2+} and Mn^{4+}.

1.4.2 Transition metal ions

The activator ions doped into a solid host lattice experience a local crystalline environment that has an immense influence on the luminescence properties of that activator ion. The activator ion in the crystalline host acts as a luminescence center. This activator ion may be a transition metal ion or a rare-earth ion. They are generally coordinated by ligands in a host lattice. The attraction between the positively charged activator ion and the negatively charged nonbonding electrons of the ligands gives rise to a crystal field interaction between the activator ion and the ligand. This interaction leads to the splitting of d-orbitals of the luminescent center (transition metal ion or rare-earth ion). Any perturbation in the crystal environment is bound to affect the spectroscopically active d orbitals of the transition metals more than that of the rare-earths. As a result, transition metal ions experience much stronger crystal field effects.

Mn^{4+} ions are the most investigated transition-metal ions for LED phosphors. Mn^{4+} ions are known to produce efficient, sharp, red luminescence in the spectral range of 600−750 nm [68,69]. It contains three electrons in its unfilled 3d shell. Mn^{4+}-doped phosphors have gained great attention due to the easy availability of raw manganese ores and cheap production costs. Mn^{4+} exhibits several unique features that enable Mn^{4+}-doped phosphors to meet the requirements of an ideal red-emitting phosphor for LEDs. Mn^{4+} ion possesses high effective positive charge, and as a result, it experiences strong crystal field effects. Mn^{4+} ions always exhibit the case of a strong crystal field. Analysis of the emission spectra can be used to distinguish between the weak and strong crystal field cases [70]. The spin-allowed $^2T_{2g} \rightarrow {}^4A_{2g}$ transition will give rise to a broad emission band in the case of a weak crystal field. On the other hand, a spin-forbidden $^2E_g \rightarrow {}^4A_{2g}$ transition will give rise to sharp emission peaks in the case of a strong crystal field. Consequently, the sharp lines corresponding to the spin-forbidden $^2E_g \rightarrow {}^4A_{2g}$ transition are, generally, found to dominate the Mn^{4+}-emission spectrum. The $^4A_2$ state is a spin-quartet orbital singlet arising that forms the ground state of Mn^{4+}. The Mn^{4+}-excitation spectrum clearly shows two broad bands corresponding to the spin-allowed $^4A_{2g} \rightarrow {}^4T_{2g}$ and $^4A_{2g} \rightarrow {}^4T_{1g}$ (^4F) transitions, whereas a third spin-allowed $^4A_{2g} \rightarrow {}^4T_{1g}$ (^4P) transition is often hidden within the host-lattice absorption or the charge-transfer transitions [71]. Thus, Mn^{4+}-doped phosphors can efficiently absorb in the UV to the blue region because of their broad excitation bands arising in that region and emit sharp emission lines in the red region. This also validates its suitability to be used in LED phosphors pumped with NUV or blue LEDs and can be easily blended with yellow or green phosphors with minimal reabsorption effects during their blending. The $^2E_g \rightarrow {}^4A_{2g}$ transition shows a wide variation in the energy when doped in different hosts. For instance, Mn^{4+} shows $^2E_g \rightarrow {}^4A_{2g}$ emission at 16,181 cm^{-1} (618 nm) for Na_2SiF_6:Mn^{4+} [72], 15,360 cm^{-1} (651 nm) for $Sr_4Al_{14}O_{25}$:Mn^{4+} [73], 15,220 cm^{-1} (657 nm) for Mg_2TiO_4:Mn^{4+},Bi^{3+} [74], and 13,792 cm^{-1} (725 nm) for $SrTiO_3$:Mn^{4+} [75]. This variation in energy of the $^2E_g \rightarrow {}^4A_{2g}$ emission transition cannot be ascribed to the variation of the crystal field as the energy of this transition in the d^3 electronic configuration is independent of the crystal field effects [71]. It depends more on the covalency or iconicity of the Mn^{4+}-ligand bonding in the host.

If the $^2E_g \rightarrow {}^4A_{2g}$ emission energy is above 15,000 cm^{-1}, then the host is considered as ionic, and if this energy value is below 15,000 cm^{-1}, then the host is considered as covalent. This feature of Mn^{4+} allows its application as a trustworthy indicator to determine the ionic or covalent nature of a host. Mn^{4+} ions are most commonly doped in oxides and fluorides for obtaining red-emitting LED phosphors. Oxides prove to be more thermally and chemically stable hosts for Mn^{4+} as compared to fluorides. It is proved that Mn^{4+} ions can stably exist only in an octahedral site of the host lattice [76]. In most of the cases, the nearest six neighbors of the Mn^{4+}-octahedral site form a distorted octahedron around Mn^{4+} ions. Mn^{4+} ions show a distinct $^2E_g \rightarrow {}^4A_{2g}$ transition in the crystal field that is octahedrally symmetric and this transition corresponds to deep red luminescence with narrow-band emission peaks in the range 600−750 nm with high quantum efficiency [77−82]. Although the emission peaks corresponding to $^2E_g \rightarrow {}^4A_{2g}$ transition is spin forbidden, their excitation peaks lying in the near-UV region and the blue region correspond to the spin-allowed $^4A_{2g} \rightarrow {}^4T_{2g}$ and $^4A_{2g} \rightarrow {}^4T_{1g}$ transitions, respectively. The excitation peaks are broad and can be easily excited by InGaN chips [80,83,84]. This is a noteworthy feature required for a phosphor to be used in pc-LEDs. However, the main difficulty lies in controlling the valence state of Mn ions that are doped in the host material. Mn can exist in 2+, 3+, 4+, 6+, and 7+ oxidation states, and the synthesis temperature has a huge effect on the occurrence of a particular valence state of Mn ions [72]. Mn^{4+} emission is tuned depending on the host material in which it is doped. When the host material is highly ionic, as in the case of fluorides, the prominent emission peak is obtained in the range 600−630 nm [78,82,85−89]. A number of complex alkaline metal fluorides have been reported to be excellent host materials for Mn^{4+} doping. Jiang et al. have synthesized the hexagonal phase of $BaSiF_6$:Mn^{4+} phosphors by the hydrothermal method [85]. Its room temperature emission spectrum consists of narrow-band peaks at 615 nm, 632 nm, and 648 nm, with an exceptionally intense and prominent peak at 632 nm. The peak at 615 nm gradually disappears when the emission spectrum is measured at 78 K and this peak has been associated with the anti-Stokes vibronic sidebands related to the excited state ^2E of Mn^{4+} ions [85]. On the other hand, the prominent emission band is obtained in the range 630−700 nm when the host material is covalent, as in the case of oxides [73,74,80−82,90]. The crystal field effect is found to strongly affect the luminescence of Mn^{4+} ions doped in oxides such as $Sr_4Al_{14}O_{25}$, Ba_2GdNbO_6, and $Mg_7Ga_2GeO_{12}$ [73,80,81,90,91]. Mn^{2+} is also likely to show red luminescence in some cases. Different from Mn^{4+}, a broad emission band is obtained for Mn^{2+}-doped phosphors [92,93].

Another form of manganese showing photoluminescence properties is in its +2 state (Mn^{2+}). Mn^{2+} ion possesses five electrons in the unfilled 3d shell. The orbital singlet $^6A_1$ state forms the ground state for Mn^{2+}, and it is not split by the crystal field. However, under a strong crystal field, the spin-sextet $^6A_1$ does not remain the ground state and instead, spin-doublet $^2T_2$ becomes the ground state. Mn^{2+} ions can substitute either an octahedrally-coordinated site or a tetrahedrally-coordinated site. In both cases, Mn^{2+} shows the spin-forbidden $^4T_1 \rightarrow {}^6A_1$ transition. However, the emission color for this d−d transition is found to vary depending on the strength of the crystal field. When the crystal field strength is stronger, the Mn^{2+}-emission occurs in the

orange to red region. On the contrary, green emission is observed when the crystal field strength is weak. In general, an octahedrally coordinated site is found to experience a much stronger crystal field as compared to a tetrahedrally coordinated site. Hence, octahedrally coordinated Mn^{2+} often shows red emission, while the tetrahedrally coordinated Mn^{2+} shows green emission. Nevertheless, Mn^{2+} suffers from the fact that it has weak narrow excitation bands in the 400−520 nm range and hence, is incapable to show an efficient green or red emission unless it is sensitized by Eu^{2+} or Ce^{3+} ions [70,94–97].

Cr^{3+} ions also produce luminescence in the red or near-infrared (NIR) region [98,99]. Although these ions are mostly investigated for solid-state lasers, they are sometimes considered as a potential luminescent ion for preparing phosphors for NIR-LEDs [100,101]. Cr^{3+} ions share the same electronic configuration as that of Mn^{4+}, that is, d^3 configuration. The ^4F level of Cr^{3+} undergoes crystal field splitting at the octahedral site into $^4A_2$, $^4T_2$, and $^4T_1$ states. The $^4A_2$ state forms the ground state for Cr^{3+}. The ^4P level remains unsplit by the octahedral crystal field and it transforms into another $^4T_1$ state. Thus, two $^4T_1$ states are existing in Cr^{3+}. The spin-allowed $^4A_2 \rightarrow {}^4T_2$ and $^4A_2 \rightarrow {}^4T_1$ give rise to two broad absorption bands in the visible region. Generally, Cr^{3+} ions occupy sites with octahedral coordination. When Cr^{3+} ions occupy weak crystal field sites, $^4T_2 \rightarrow {}^4A_2$ transition is observed in the form of broad emission bands. On the contrary, $^2E \rightarrow {}^4A_2$ transition is observed in the form of sharp emission lines when the Cr^{3+} ions occupy strong crystal field sites [102].

Other non-rare-earth activated phosphors were discovered and have attracted much attention in the field of energy-efficient LED lighting. For instance, Bi^{3+}, when mixed into different matrix materials, can realize multiple luminescence intensities ranging from 400 to 700 nm [103]. Bismuth is one of the posttransition metals, which are elements situated on the periodic table between the transition metals and metalloids. The tunable emission results from the susceptibility of bismuth naked 6s electrons to the crystal field surrounding Bi^{3+}. The multitude of bismuth states complicates, but enriches, the luminescence possibilities from bismuth-activated materials that exhibit emissions from the ultraviolet to the infrared. The outer orbitals responsible for luminescence are unshielded and strongly influenced by the surrounding environment so that their energies are host dependent [104,105].

1.5 Historical background

1.5.1 The advent of light

Light is one of the most essential requirements for the existence of light on earth. Light has triggered the cycle of the ecosystem that enabled plants to synthesize their food and also provide food for other living organisms in the environment. The very first light rays originated from the big bang explosion that occurred almost 14 billion years ago. The explosion led to the formation of an infinite dense universe in a very hot state that began to expand over time. The continued process of expansion is still ongoing, and this has tremendously lowered the temperature and density of the universe. The light that emerged from the big bang explosion was the first light that existed in the universe. This light is present in the universe as cosmic background radiation and is filled throughout the

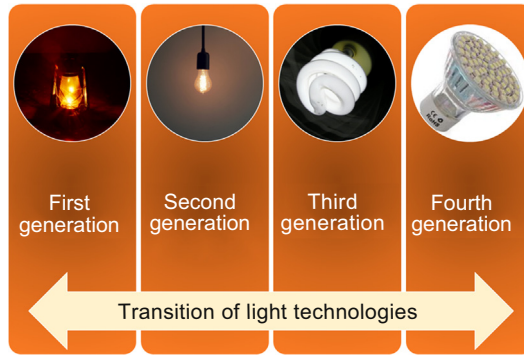

Figure 1.4 Different phases of lighting technologies classified into four generations.

universe. At the time of big bang, the light emerged as a visible light that slowly shifted to microwave radiation with time [106]. Thus, the cosmic background radiation is now invisible to the human eye. The ever-expanding universe gave birth to several galaxies, and each galaxy is formed by numerous stars. The stars themselves are a source of light. The nuclear fusion of hydrogen atoms on the surface of a star produces both heat and light. In the galaxies, some planets revolve around a star and they are collectively termed as the solar system. In our solar system, the sun forms the core around which planets revolve. The earth is the only existing planet in this solar system that has life on it. The sun, being a star, also produces heat and light through the nuclear fusion of four hydrogen atoms to form a helium nucleus. At present, the sun is the most powerful source of natural light that is available on the earth. Sunlight is utilized by both flora and fauna, equally. Mankind has always depended on sunlight for their day-to-day life. However, sunlight is available only during the daytime and the night is often left in darkness. At times, the moon shines its light on earth. But, this source of light cannot be reliable in every night. The waxing and waning cycles disable the moon to provide a consistently bright light on earth. The amount of sunlight received on the earth is also not the same everywhere. A tremendous amount of sunlight is received in the regions covering the equator and the surrounding areas. However, there are several areas on earth, such as the polar regions, that receive a deficient amount of sunlight. The circumstances led humans to think for an alternative source of light that could shine both in the day and night and also provide light in the areas where sunlight is scarce. Many of the artificial light sources were discovered or invented accidently. However, with time, these sources developed into more promising alternatives that could even surpass the naturally available sunlight. The artificial light sources are classified into four generations on the basis of their working principles. The subsequent subsections shall be giving a brief introduction to the different generations of lighting that man has developed and utilized over time. Fig. 1.4 shows the classification of lighting technologies into four generations.

1.5.2 The first generation of lighting

The earliest form of lighting came in the form of fire torches. The torch was a log of wood that was wrapped with pieces of rag and immersed in some flammable liquid.

This enabled the log of wood to carry fire for a prolonged period. The fire itself was an accidental discovery by the Homo Erectus at around 1.5 million years ago [107]. Although several mysteries and theories are surrounding the origin of the fire, it is widely believed that lightning struck on a tree or a bush brought out the idea about the fire in humans. Man started creating fire by rubbing flint stones or dry twigs. He used this fire to set up campfires to obtain warmth and light in cold chilling nights. Soon it was realized that fire can be used to cook food and also keep the wild animals at bay. They started using campfires to protect themselves and their family by frightening off these animals. While roaming around the forest, man used fire torches to lighten their path. When he started building houses, he found that campfires cannot be used to eliminate darkness from their homes. These houses were mainly constructed from logs of wood and hence, there was a risk of houses catching fire if campfires are set inside their homes. To make it possible for holding the fire inside houses without posing any hazard to their dwelling, man developed lamps from clay. He started using oils and fats as fuel for the fire to burn in these lamps. The biggest advantage of oil lamps was that these gave out a controllable flame and were much smaller in size. The very first oil lamps were made at around 70,000 BCE. Hollow stones and shells were filled with moss that was soaked with animal fats to ignite the fire. With the advancement of mankind, stones were replaced by metals and the lamps began to gain shape in the molds instead of pottery wheels. Lamps were mainly fueled by oils extracted from nuts and seeds. Nuts such as almonds, walnuts, and seeds such as castor, sesame, flax, and olive were preferred for their oil. Oil lamps were also ignited using animal fats such as whale blubber, shark liver, fish oil, bee wax, and butter. The earliest oil lamps appeared like an open dish that could hold the oil and a small protruding to place the wick. An added advantage of oil lamps was its facile operation and safety as compared to fire torches. In addition, oil lamps left very less residue after burning and are often reusable to a large number of times. However, the tediousness of placing the wick in the oil and frequently adjusting the wick's position inspired the Romans to invent candles at around 500 BCE. Candles are designed in such a way that a long wick is enclosed inside a cylindrically-shaped wax- covering. This design ensured that the wick will automatically burn to its end without any manual adjustment.

By the end of the 18th century, ancient forms of oil lamps were rapidly replaced by Argand lamps. These lamps were much brighter than the earlier used lamps and produced lumens equivalent to that produced by six candles. These lamps carried a sleeve-shaped wick mounted in such a way that air can steadily flow through the center and around the wick toward the cylindrical chimney. This ensured that the flame burned steadily and brightly. Argand lamps were fueled by olive oil, seal oil, whale oil, or vegetable oil. The fuel reservoir is mounted above the burner, and the fuel supply was achieved by means of gravity feed. As the vegetable oil was too heavy to rise to the wick, it was essential to keep the oil reservoir above the burner. This also proved to be a disadvantage as the lamps became very heavy and expensive than the primitive oil lamps. By the middle of the 19th century, kerosene lamps started gaining popularity and soon replaced the expensive Argand lamps. In those days, kerosene was a cheaper fuel than vegetable oil and the low viscosity of kerosene enabled it to quickly rise

towards the wick in the lamp. Kerosene lamps are the simplest, but best among the oil lamps. Still, there are several parts of the world where electricity is still a myth or non-affordable and people resort to kerosene lamps for lighting.

1.5.3 The second generation of lighting

With the advent of electricity, the use of oil lamps gradually decreased. In the second quarter of the 19th century, lamps based on electricity started showing up. The very first electricity-driven lighting came in the form of gas discharge lamps in the early 18th century. Francis Hauksbee was the first to demonstrate the working principle of the gas discharge lamp in 1705. Inside a partially evacuated gas globe, he placed a small amount of mercury and supplied static electricity to it. These efforts produced light that was bright enough to let a person read using it. Later on, Vasily V. Petrov described the principle of electric arc lamps in 1802 and at the same time, Sir Humphry Davy successfully demonstrated its working more convincingly. Sir Humphry Davy is credited with the invention of carbon arc lamps in the early 19th century. He made use of the charcoal sticks and a two-thousand-cell battery to create an arc across a 10-cm gap. Carbon arc lamps are considered as the first electric light with practical applications. It marked its entry into commercial lighting for streets and buildings from the mid-19th century to the early 20th century, until its replacement by more advanced incandescent bulbs. Since its inception in the lighting industry, many variants of gas-discharge lamps have come into existence. In 1857, Heinrich Geissler constructed the Geissler tubes that comprised colorful artistic cold-cathode tubes filled with different gases. These tubes were found to glow with different colors. Heinrich Geissler, a German glassblower, is considered as the father of low-pressure gas-discharge lamps. Inert gases such as xenon, krypton, argon, and neon as well as carbon dioxide were found to be suitable for Geissler tubes.

When several inventors were busy improving the gas-discharge lamps and arc lamps, there were some others who were working on the development of electric bulbs working on the principle of incandescence. Although Thomas Alva Edison is credited with the successful invention of incandescent bulbs, there was a long chain of struggles by many scientists who laid stepping stones for the invention. At about 1802, Humphry Davy again marked the beginning of the incandescent lamps by reporting a glow from a platinum strip on passing an electric current through it. The glow did not last for long but laid the foundation for the future of electric bulbs working on incandescence. The experiments on incandescence were performed with platinum and iridium for the next 70 years. Frederick de Moleyns made use of an evacuated glass bulb in which a platinum filament was kept. His experiment was partially successful but faced issues like the blackening of the bulb that caused the blocking of the light output. The issue related to the blackening of the bulb can be sorted out by making proper vacuum inside the glass bulb. In addition, there was a need to replace the expensive platinum and iridium wire strips by some easily available and cheap material. Electric bulbs lasting with a more reasonable number of hours were developed by Thomas Edison and Joseph Swan independently. Joseph Swan made use of the carbonized paper filament in a partial vacuum bulb to produce light with lesser success.

On the other hand, Edison figured out a way to develop a complete vacuum inside the bulb and managed to place a carbonized sewing thread as filament inside the bulb. He used a mercury vacuum pump created by Hermann Sprengel, and this proved to be highly effective in creating a vacuum inside the bulb. His success with the experiment led to the commercialization of the incandescence bulbs for general lighting. Edison further improved the lamp's working life by introducing the carbonized bamboo strips as filaments. Larger pieces of bamboo were cut into small square-shaped filaments and directly electroplated them to the lead in wires. This way the high costs for platinum clamps were also avoided. He also considered using carbon paste as an adhesive between bamboo and lead in wires. Filaments made of cellulose were also used by Joseph Swan, while Edison continued with the use of bamboo filaments. In 1902, tantalum filaments were started being used due to its superior properties than all other existing filaments. Tantalum was also the first metal to be used as filaments. Most metals failed to show incandescence when heated and got destroyed very easily. On the other hand, tantalum has a very high melting point and presented a sustainable performance without getting damaged. Tantalum continued its reign until the ductile tungsten gained popularity. Tantalum filament-based bulbs exhibit greater brightness with lower energy consumption. In 1904, Austro-Hungarian inventors Alexander Just and Franjo Hanaman developed sintered tungsten filaments that enhanced the efficiency of the bulb to a very large extent. However, this tungsten filament failed to find a practical application due to its brittleness. In 1908, ductile tungsten was developed by William Coolidge and this revolutionized the future of incandescent bulbs. Ductile tungsten filaments were efficient, durable, and long lasting. Ductile tungsten filaments started gaining popularity soon after its development and by 1911, almost every incandescent bulb came up with a ductile tungsten filament. The ductile tungsten-based incandescent bulbs continued to rule till the end of the 20th century till its phasing-out and the arrival of fluorescent lamps.

1.5.4 The third generation of lighting

Before the phasing-out of the incandescent bulbs, the third generation of lighting also started showing up. This era was completely dominated by the fluorescent lamps (FL) and compact fluorescent lamps (CFLs). However, the idea for fluorescence lamps was visualized much earlier in the mid-19th century. Alexander Becquerel, a French Physicist, studied the phenomena of fluorescence and phosphorescence and put forward the idea of constructing the fluorescent tubes in 1887. He applied a coating of luminescent materials on the electric discharge tubes and observed fluorescence from them. Although this setup has a short operating life and poor efficiency, it was known to be the prototype of the modern fluorescent lamps. Still, it took almost three decades to get a complete design of fluorescent lamps that could be brought for commercial applications.

The idea of fluorescent lamps was taken to a further step by Nikola Tesla and Thomas Edison separately. In 1893, Tesla became the first to demonstrate his electrodeless induction lamp that was coated with greenish phosphors. Although this design seemed to be different from the modern fluorescent lamps, it inspired the development of

modern induction lamps to a great extent. However, the high-frequency ballasts used in modern fluorescent lamps is a successor to those used in Tesla's lamp. On the parallel, Edison observed luminescence from calcium tungstate phosphors coated inside a glass tube by passing X-rays through it. This lamp showed unpleasant color with a short life. However, Edison soon abandoned his work on this lamp after one of his colleagues fell ill and died due to exposure of X-rays. In 1894, Daniel McFarlane Moore developed a lamp that consisted of carbon dioxide and nitrogen gas-filled tubes of 5-cm diameter and 2-m length. These lamps were called Moore lamps and showed much greater efficiency than the early incandescent bulbs. However, the enormous size, massive expense, and difficulty in its installation led to very early extinction of Moore lamps from the market. In 1901, Peter Cooper Hewitt created the first commercial mercury-vapor lamp operating at a lower voltage. This is considered as the foundation for the development of modern fluorescent lamps. His lamp emitted a bluish-green color, which was unpleasant and nonsuitable for practical applications despite its superior efficiency. However, the combination of electrodes and ballasts used in this lamp was later employed for fluorescent lamps too. In 1915, Georges Claude developed the neon lamp, which is a simple version of the fluorescent lamp with neon and argon gases inside the glass tube. However, the breakthrough came in the year 1926, when Edmund Germer and his coworkers successfully coated phosphors inside the glass tube and utilized the UV rays from the mercury vapor lamp to excite the phosphor for obtaining light suitable for lighting. The General Electric (GE) company bought the patent rights for Germer's lamp and started working on it to make it viable in the market. In 1934, George Inman of the GE Company along with his coworkers brought about several modifications and improvements in the lamp. By 1938, GE Company started selling the fully developed fluorescent lamps in the market. During World War II, the demand for lighting increased, and thereby the production of long-tube-like fluorescent lamp fixtures rapidly increased. During the oil crisis in the early 1970s, there were attempts made by the major manufacturers to shrink the size of fluorescent lamps to make it more convenient for household lighting. This ultimately led to the development of CFLs by Edward Hammer in 1976. Philips, a major manufacturing company for lighting, was the first to develop electronic ballasts for CFL. They also started using rare-earth-activated phosphor coatings to provide a warm white color hue to the lighting. Soon CFLs became popular in the commercial market. With the rising popularity of CFLs, the 21st century witnessed a huge surge of CFLs in the market and a noteworthy reduction in its cost. There was a small time gap when the rare-earth supplies were globally hit by the crisis and this affected the CFL prices to go up for a short duration. The reign of fluorescent lamps and CFLs continued until consumers became aware of the environmental and health hazards arising from the mercury vapor/waste due to improper disposal of these lamps [108]. This also paved the way for the more advanced and energy-efficient fourth generation of lighting.

1.5.5 The fourth generation of lighting

The past few decades witnessed a major revolution in the lighting industry with the advent of LEDs. The development of LEDs did not occur in a single night, but it

took the hardships of several decades to expand its wings in the lighting industry. The scientific society slowly garnered all the necessary ingredients to pave way for the most economic, energy-efficient, and incredible form of artificial lighting. All these started with the breakthrough discovery of EL by Henry Joseph Round, an English engineer by profession, in the year 1907 [109]. He observed yellow emission from a piece of silicon carbide (SiC) through a cat's whisker detector on passing an electric current through SiC. Nevertheless, working with SiC seemed to be very difficult in those days and the observed yellow light appeared to be very dim to observe. This compelled to cease any further research on electroluminescence from SiC. Later on, Oleg Vladimirovich Losev, a Russian scientist, reported several articles in Russian, English, and German journals regarding the invention of LEDs in 1927 [110]. He anticipated a reverse effect of Einstein's photoelectric effect that may be leading to his observations. However, his work did not produce any practical applications and it remained shelved for several years. Numerous experiments were carried out on zinc sulfide with several dopants in the late 1920s−1940s. In 1936, George Destriau, a French physicist, discovered electroluminescence from zinc sulfide crystals that were doped with copper ions [111]. He applied a strong alternating electric field to the samples that were suspended in castor oil between two mica platelets. However, these materials also proved less worthy due to their low light output and this fact diminished the curiosity among the researchers to undertake further research on these materials.

Till the dawn of 1950, SiC and the semiconductors belonging to II−IV groups were the most researched materials for electroluminescence. The new era of LED technology and its modernization was marked by the arrival of group III−V semiconductors. Rubin Braunstein, an American physicist, claimed that diodes made from semiconductor alloys such as GaAs, SiGe, GaSb, and InP could produce infrared emissions [2].

In 1961, while working in the Texas Instruments, James Biard and Gary Pittman observed the emission of infrared light from GaAs on passing an electric current through it. Based on their findings, they received a patent on 8th August 1962. Following this, Texas Instruments began to manufacture the infrared emitting diodes that carried a pure GaAs crystal. Such diodes exhibited an emission at 900 nm wavelength. A new milestone in the history of LEDs came with the discovery of the first visible LEDs in the year 1962. Nick Holonyak Jr. developed an LED that showed red-light emission while he was working as a consulting scientist in General Electric Company [112]. He reported on the coherent visible red-light emission from the GaAsP junctions and was later titled as the "Father of the Light Emitting Diode." His discovery was published in the first volume of *Applied Physics Letters*; his paper was co-authored by S.F. Bevacqua. His devices worked as LEDs and emitted visible light at room temperatures although a coherent emission was observed only at low temperatures. He had used vapor-phase epitaxial growth of GaAsP over GaAs substrates, a method well suited for the large-scale growth of wafers.

The Monsanto Company was the first organization to start the commercial manufacturing of visible red LEDs using GaAsP in 1968. Until 1968, the visible and infrared LEDs were not at all affordable, and each unit costed around US$200, thereby, limiting its practical use in the commercial market [2]. However, a new era of solid-state lighting started with the low-cost production of LEDs based on GaAsP p−n junctions grown on GaAs substrates in the factory set up by the Monsanto

Company in 1968. This initiated the replacement of the incandescent and neon indicator lamps with the LEDs wherever it was possible. The Monsanto Company collaborated with Hewlett−Packard (HP) Corporation to produce LED and LED displays from GaAsP. HP was supposed to manufacture the LEDs and the Monsanto Company was expected to supply the GaAsP raw material. However, HP felt the inadequacy of depending on a single source of GaAsP material for producing LEDs and backed out from their ties with the Monsanto Company. Later, HP started growing its GaAsP material.

The market emerged with major advances in the seven-segment numeric displays, indicator lamps, and the more advanced alphanumeric displays. In 1972, M. George Craford invented the first yellow LED that had employed an n-doped GaAsP active region grown on a GaAs substrate. He achieved improved brightness in red and orange-red LEDs that increased by a factor of 10. He was formerly a graduate student of Holonyak. His initial days in business went in the Monsanto Company where he managed all the optoelectronic research until the company sold it off in 1979. Later on, he joined HP and led its research in the LEDs. He soon became the key innovator in the research [113].

Ralph Logan et al. reported their pioneer work on the manufacture of GaP-based green and red LEDs with high efficiency [114]. They grew an n-type GaP layer onto ZnO-doped GaP wafers that were polished out of large solution grown wafers to form junctions. This team discovered the process for manufacturing this novel material while they were working in AT&T Bell Laboratories in Murray Hill, NJ, in the early 1960s. The Bell Laboratories decided to manufacture these LEDs at its facility in Reading, PA. N-doped GaP, which gave a green emission and ZnO-doped GaP, which gave a red emission proved to be equally bright, efficient, and useful.

In 1987, a research team in Eastman Kodak demonstrated devices with appropriately low operation voltages and attractive electroluminescence efficiencies by exploiting suitable small-molecule materials and structures by using two-layer organic LEDs [115]. In 1990, a Cambridge research team reported the polymer-based LEDs [116].

The first high-brightness blue LED was demonstrated by Shuji Nakamura of Nichia Corporation in 1994 and was based on InGaN [117]. Critical developments in GaN nucleation on sapphire substrates and the p-type doping of GaN were demonstrated by Isamu Akasaki and Hiroshi Amano [118]. The trio of Shuji Nakamura, Isamu Akasaki, and Hiroshi Amano received the 2014 Nobel Prize in Physics for their outstanding invention that led to the development of WLEDs. Until then, WLEDs suffered due to the missing blue LED that was indeed necessary to obtain white light by mixing red, green, and blue light. In 2015, a group of German scientists came up with a prototype of bio-LEDs, which are hybrid devices that utilized the blue LEDs to excite protein rubbers to emit red/green/white light. The luminescent proteins are introduced into a polymer matrix to produce luminescent rubber, which is then packaged with a UV-LED or a Blue-LED. At about the same time, halide perovskites started gaining attention for their luminescent properties. In 2014, the first organometal halide perovskite LED with an ITO/PEDOT:PSS/$CH_3NH_3PbBr_3$/F_8/Ca/Ag structure was demonstrated [119]. These innovations are still in their early stages and further developments are required before considering them to build commercial LEDs.

1.6 Conclusions

The evolution of lighting technologies, since time immemorial, has witnessed several challenges and efforts to meet the requirements of mankind. Each time, the lacunas left out by the existing light source were filled up by the newer technology and this led to the phasing-out of the reign of the first three generations of a light source to a great extent. At present, the lighting industries are ruled by LED luminaires and this will continue to exist for a long time until an innovation strikes the world with its superior efficiency and durability.

References

[1] E. Kandel, Principles of Neural Science, fifth ed., McGraw Hill Professional, 2013.
[2] E.F. Schubert, Light-Emitting Diodes, Second ed., Cambridge University Press, New York, 2006.
[3] K.N. Shinde, S.J. Dhoble, H.C. Swart, K. Park, Phosphate Phosphors for Solid-State Lighting, Springer, London, 2012, https://doi.org/10.1007/978-3-642-34312-4.
[4] S. Ye, F. Xiao, Y.X. Pan, Y.Y. Ma, Q.Y. Zhang, Phosphors in phosphor-converted white light-emitting diodes: recent advances in materials, techniques and properties, Mater. Sci. Eng. R Rep. 71 (2010) 1−34, https://doi.org/10.1016/j.mser.2010.07.001.
[5] S. Nakamura, InGaN/AlGaN blue-light-emitting diodes, J. Vac. Sci. Technol. A 13 (1995) 705, https://doi.org/10.1116/1.579811.
[6] C. Dodeigne, Chemiluminescence as diagnostic tool. A review, Talanta. 51 (2000) 415−439, https://doi.org/10.1016/S0039-9140(99)00294-5.
[7] R. Strack, Harnessing fungal bioluminescence, Nat. Methods 16 (2019), https://doi.org/10.1038/s41592-019-0311-4, 140−140.
[8] J.A. Wani, M.S. Atone, S.J. Dhoble, The influence of different synthesis routes on thermoluminescence of $CaSO_4$: Dy, P, Ce phosphors, Adv. Mater. Lett. 4 (2013) 363−367, https://doi.org/10.5185/amlett.2012.10433.
[9] A.C. Atre, B.J.M. Brenny, T. Coenen, A. García-Etxarri, A. Polman, J.A. Dionne, Nanoscale optical tomography with cathodoluminescence spectroscopy, Nat. Nanotechnol. 10 (2015) 429−436, https://doi.org/10.1038/nnano.2015.39.
[10] Y. Ren, H. Winter, J. Rosch, K. Jung, A. Duross, M. Landry, G. Pratx, C. Sun, PEGylated β-$NaGdF_4$:Tb@CaF_2 core/shell nanophosphors for enhanced radioluminescence and folate receptor targeting, ACS Appl. Nano Mater. (2019), https://doi.org/10.1021/acsanm.9b00629.
[11] C. Manfredotti, E. Vittone, A. Lo Giudice, C. Paolini, F. Fizzotti, G. Dinca, V. Ralchenko, S.V. Nistor, Ionoluminescence in CVD diamond and in cubic boron nitride, Diam. Relat. Mater. 10 (2001) 568−573, https://doi.org/10.1016/S0925-9635(00)00604-X.
[12] W.-Y. Lee, Tris (2,2'-bipyridyl)ruthenium(II) electrogenerated chemiluminescence in analytical science, Mikrochim. Acta 127 (1997) 19−39, https://doi.org/10.1007/BF01243160.
[13] P.L. Provenzano, G.R. Jindal, J.R. Sweet, W.B. White, Flame-excited luminescence in the oxides Ta_2O_5, Nb_2O_5, TiO_2, ZnO, and SnO_2, J. Lumin. 92 (2001) 297−305, https://doi.org/10.1016/S0022-2313(00)00264-7.

[14] H. Lv, Z. Pan, Y. Wang, Synthesis and mechanoluminescent property of (Eu^{2+}, Dy^{3+})-co-doped strontium aluminate phosphor by soft mechanochemistry-assisted solid-state method, J. Lumin. 209 (2019) 129−140, https://doi.org/10.1016/j.jlumin.2019.01.026.
[15] X. Wang, P. Boutinaud, L. Li, J. Cao, P. Xiong, X. Li, H. Luo, M. Peng, Novel persistent and tribo-luminescence from bismuth ion pairs doped strontium gallate, J. Mater. Chem. C 6 (2018) 10367−10375, https://doi.org/10.1039/C8TC04012E.
[16] G. Qiu, H. Ye, X. Wang, H. Fang, Y. Li, X. Yao, Intense piezoluminescence in $LiTaO_3$ phosphors doped with Pr^{3+} ions, Ceram. Int. 45 (2019) 8553−8560, https://doi.org/10.1016/j.ceramint.2019.01.173.
[17] Y. Kawaguchi, Fractoluminescence spectra in crystalline quartz, Jpn. J. Appl. Phys. 37 (1998) 1892−1896, https://doi.org/10.1143/JJAP.37.1892.
[18] G.C. Mishra, S.J. Dhoble, A. Srivastava, S. Dwiwedi, R.S. Kher, Study of lyoluminescence of gamma-irradiated $GdCa_4O(BO_3)_3$:Ce phosphors: mass of solute and pH of solvent as a key factor, Optik 158 (2018) 826−830, https://doi.org/10.1016/j.ijleo.2017.12.189.
[19] G.L. Sharipov, B.M. Gareev, A.M. Abdrakhmanov, Sonoluminescence of suspensions of insoluble chromium carbonyl nanoparticles in water and inorganic acids, Tech. Phys. Lett. 44 (2018) 1072−1073, https://doi.org/10.1134/S1063785018120350.
[20] G.P. Safonov, V.Y. Shlyapintokh, S.G. Entelis, Crystalloluminescence of organic compounds, Nature 205 (1965) 1203−1204, https://doi.org/10.1038/2051203a0.
[21] P. Jaszczyn-Kopec, H. Kallmann, B. Kramer, Cryoluminescence of ZnS phosphors, Phys. Rev. 165 (1968) 901−908, https://doi.org/10.1103/PhysRev.165.901.
[22] G.G. Stokes, On the change of refrangibility of light, Philos. Trans. R. Soc. Lond. 142 (1852) 463−562, https://doi.org/10.1098/rstl.1852.0022.
[23] S. Ray, P. Tadge, S.J. Dhoble, G.B. Nair, A. Singh, A.K. Singh, M. Rai, T.M. Chen, V. Rajput, Structural and spectroscopic characterizations of a new near-UV-converting cyan-emitting $RbBaScSi_3O_9:Eu^{2+}$ phosphor with robust thermal performance, J. Alloys Compd. 713 (2017) 138−147, https://doi.org/10.1016/j.jallcom.2017.03.366.
[24] L. Ma, K. Jiang, X. Liu, W. Chen, A violet emission in ZnS:Mn,Eu: luminescence and applications for radiation detection, J. Appl. Phys. 115 (2014) 103104, https://doi.org/10.1063/1.4868221.
[25] K. Era, S. Shionoya, Y. Wasfflzawa, H. Ohmatsu, Mechanism of broad-band luminescences in ZnS phosphors—II. Characteristics of pair emission type luminescences, J. Phys. Chem. Solid. 29 (1968) 1843−1857, https://doi.org/10.1016/0022-3697(68)90168-6.
[26] F. Perrin, La fluorescence des solutions, Ann. Phys. 10 (1929) 169−275, https://doi.org/10.1051/anphys/192910120169.
[27] Y.Q. Li, N. Hirosaki, R.J. Xie, T. Takeda, M. Mitomo, Photoluminescence , and application in white LEDs, Chem. Mater. 19 (2008) 6704−6714, https://doi.org/10.1021/cm801669x.
[28] T. Ogi, Y. Kaihatsu, F. Iskandar, W.-N.N. Wang, K. Okuyama, Facile synthesis of new full-color-emitting BCNO phosphors with high quantum efficiency, Adv. Mater. 20 (2008) 3235−3238, https://doi.org/10.1002/adma.200702551.
[29] C. Zhang, C. Li, J. Yang, Z. Cheng, Z. Hou, Y. Fan, J. Lin, Tunable luminescence in monodisperse zirconia spheres, Langmuir 25 (2009) 7078−7083, https://doi.org/10.1021/la900146y.
[30] C.K. Lin, Y. Luo, H. You, Z. Quan, J. Zhang, J. Fang, J. Lin, Sol−Gel-Derived BPO_4/Ba^{2+} as a new efficient and environmentally-friendly bluish-white luminescent material, Chem. Mater. 18 (2006) 458−464, https://doi.org/10.1021/cm052109h.

[31] G. Blasse, B.C. Grabmaier, Luminescent Materials, Springer-Verlag, New York, 1994, https://doi.org/10.1007/978-3-642-79017-1.
[32] V. Mahalingam, J. Thirumalai, R. Krishnan, S. Mantha, Up/down conversion luminescence and charge compensation investigation of $Ca_{0.5}Y_{1-x}(WO_4)_2$:xLn^{3+} (Ln = Pr, Sm, Eu, Tb, Dy, Yb/Er) phosphors, Spectrochim. Acta Part A Mol. Biomol. Spectrosc. 152 (2016) 172−180, https://doi.org/10.1016/j.saa.2015.06.129.
[33] H. Qian, J. Zhang, L. Yin, Crystal structure and optical properties of white light-emitting Y_2WO_6:Sm^{3+} phosphor with excellent color rendering, RSC Adv. 3 (2013) 9029, https://doi.org/10.1039/c3ra40742j.
[34] A. Kumar, J. Kumar, Perspective on europium activated fine-grained metal molybdate phosphors for solid state illumination, J. Mater. Chem. 21 (2011) 3788, https://doi.org/10.1039/c0jm03708g.
[35] L. Wang, H.M. Noh, B.K. Moon, S.H. Park, K.H. Kim, J. Shi, J.H. Jeong, Dual-mode luminescence with broad near UV and blue excitation band from Sr_2CaMoO_6:Sm^{3+} phosphor for white LEDs, J. Phys. Chem. C 119 (2015) 15517−15525, https://doi.org/10.1021/acs.jpcc.5b02828.
[36] X. Wang, Y. Huang, Y. Moon, S. Il, H. Jin, The influence of Mo^{6+} doping on the luminescence properties of red-emitting phosphor $Sr_9Eu_2W_4À_xMo_xO_{24}$ (x = 0 − 4), Ceram. Int. 38 (2012) 4991−4995, https://doi.org/10.1016/j.ceramint.2012.02.094.
[37] G. Ramakrishna, H. Nagabhushana, D.V. Sunitha, S.C. Prashantha, S.C. Sharma, B.M. Nagabhushana, Effect of different fuels on structural, photo and thermo luminescence properties of solution combustion prepared Y_2SiO_5 nanopowders, Spectrochim. Acta Part A Mol. Biomol. Spectrosc. 127 (2014) 177−184, https://doi.org/10.1016/j.saa.2014.02.054.
[38] A. Durugkar, S. Tamboli, N.S. Dhoble, S.J. Dhoble, Novel photoluminescence properties of Eu^{3+} doped chlorapatite phosphor synthesized via sol-gel method, Mater. Res. Bull. 97 (2018) 466−472, https://doi.org/10.1016/j.materresbull.2017.09.043.
[39] I.G.N. Silva, L.C. V Rodrigues, E.R. Souza, J. Kai, M.C.F.C. Felinto, J. Hölsä, H.F. Brito, Low temperature synthesis and optical properties of the R_2O_3:Eu^{3+} nanophosphors (R^{3+}: Y , Gd and Lu) using TMA complexes as precursors 40 (2015) 41−48.
[40] C.Y. Shang, X.Q. Wang, H. Kang, D.M. Han, Charge transfer energy for Y_2O_3:Eu^{3+} nanophosphor, J. Appl. Phys. 109 (2011), https://doi.org/10.1063/1.3581056.
[41] R. Reisfeld, C.K. Jørgensen, Lasers and Excited States of Rare Earths, Springer Berlin Heidelberg, Berlin, Heidelberg, 1977, https://doi.org/10.1007/978-3-642-66696-4.
[42] W.H. Fonger, C.W. Struck, Eu^{+35}D resonance quenching to the charge-transfer states in Y_2O_2S, La_2O_2S, and LaOCl, J. Chem. Phys. 52 (1970) 6364−6372, https://doi.org/10.1063/1.1672952.
[43] Q. Dai, M. Foley, C. Breshike, Ligand-passivated Eu: Y_2O_3 nanocrystals as a phosphor for white light emitting diodes, J. Am. Chem. Soc. 133 (2011) 15475−15486. http://pubs.acs.org/doi/abs/10.1021/ja2039419.
[44] T. Hirai, Y. Kawamura, Preparation of Sr_2CeO_4 blue phosphor particles and rare earth (Eu, Ho, Tm, or Er)-doped Sr_2CeO_4 phosphor particles, using an emulsion liquid membrane system, J. Phys. Chem. B 108 (2004) 12763−12769, https://doi.org/10.1021/jp040220p.
[45] Y. Chen, Y. Li, J. Wang, M. Wu, C. Wang, Color-tunable phosphor of Eu^{2+} and Mn^{2+} codoped $Ca_2Sr(PO_4)_2$ for UV light-emitting diodes, J. Phys. Chem. C 118 (2014) 12494−12499, https://doi.org/10.1021/jp502571c.

[46] G.B. Nair, S.J. Dhoble, Assessment of electron-vibrational interaction (EVI) parameters of YAG:Ce^{3+}, TAG:Ce^{3+} and LuAG:Ce^{3+} garnet phosphors by spectrum fitting method, Spectrochim. Acta Part A Mol. Biomol. Spectrosc. 173 (2017) 822−826, https://doi.org/10.1016/j.saa.2016.10.049.

[47] J. García Sol´ e, L.E. Bausá, D. Jaque, An Introduction to the Optical Spectroscopy of Inorganic Solids, John Wiley and Sons Ltd., West Sussex, 2005. http://onlinelibrary.wiley.com/book/10.1002/0470016043.

[48] G.B. Nair, P.D. Bhoyar, S.J. Dhoble, Exploration of electron-vibrational interaction in the 5d states of Eu^{2+} ions in $ABaPO_4$ (A = Li, Na, K and Rb) phosphors, Luminescence 32 (2017) 22−29, https://doi.org/10.1002/bio.3143.

[49] G.B. Nair, S.J. Dhoble, White light emission through efficient energy transfer from Ce^{3+} to Dy^{3+} ions in $Ca_3Mg_3(PO4)_4$ matrix aided by Li^+ charge compensator, J. Lumin. 192 (2017) 1157−1166, https://doi.org/10.1016/j.jlumin.2017.08.047.

[50] Q. Guo, L. Liao, L. Mei, H. Liu, Y. Hai, Color-tunable photoluminescence phosphors of Ce^{3+} and Tb^{3+} co-doped $Sr_2La_8(SiO_4)_6O_2$ for UV w-LEDs, J. Solid State Chem. 225 (2015) 149−154, https://doi.org/10.1016/j.jssc.2014.12.017.

[51] G.B. Nair, S.J. Dhoble, Highly enterprising calcium zirconium phosphate [$CaZr_4(PO_4)_6$: Dy^{3+}, Ce^{3+}] phosphor for white light emission, RSC Adv. 5 (2015) 49235−49247, https://doi.org/10.1039/C5RA07306E.

[52] Y. Li, M. Gecevicius, J. Qiu, Long persistent phosphors—from fundamentals to applications, Chem. Soc. Rev. 45 (2016) 2090−2136, https://doi.org/10.1039/C5CS00582E.

[53] Y. Nakanishi, G. Shimaoka, H. Tatsuoka, H. Kuwabara, Preparation of ZnS:Ag,Cl thin films emitting blue luminescence, Thin Solid Films 187 (1990) 323−329, https://doi.org/10.1016/0040-6090(90)90053-G.

[54] M. Bredol, J. Merikhi, C. Ronda, Defect chemistry and luminescence of ZnS: Cu, Au, Al, Berichte Der Bunsengesellschaft Für Phys. Chemie. 96 (1992) 1770−1774, https://doi.org/10.1002/bbpc.19920961149.

[55] F. Williams, High-field electroluminescence, J. Lumin. 23 (1981) 1−16, https://doi.org/10.1016/0022-2313(81)90188-5.

[56] P.J. Dean, Comparisons and contrasts between light emitting diodes and high field electroluminescent devices, J. Lumin. 23 (1981) 17−53, https://doi.org/10.1016/0022-2313(81)90189-7.

[57] H. Yu, B. Yao, D. Deng, L. Chen, H. Zhao, Y. Li, Y. Hua, S. Xu, Novel tunable red to yellow emitting (Ca, $Ba)_4(PO_4)_2O:Eu^{2+}$ phosphor for blue-excited white light emitting diodes, Ceram. Int. 43 (2017) 1038−1043, https://doi.org/10.1016/j.ceramint.2016.10.036.

[58] N.V. Rebrova, A.Y. Grippa, A.S. Pushak, T.E. Gorbacheva, V.Y. Pedash, O.G. Viagin, V.L. Cherginets, V.A. Tarasov, V.V. Vistovskyy, A.P. Vas'kiv, S.V. Myagkota, Crystal growth and characterization of Eu^{2+} doped RbCaX 3 (X = Cl, Br) scintillators, J. Cryst. Growth 466 (2017) 39−44, https://doi.org/10.1016/j.jcrysgro.2017.03.016.

[59] M. Dalal, V.B. Taxak, J. Dalal, A. Khatkar, S. Chahar, R. Devi, S.P. Khatkar, Crystal structure and Judd-Ofelt properties of a novel color tunable blue-white-red $Ba_5Zn_4Y_8O_{21}$: Eu^{3+} nanophosphor for near-ultraviolet based WLEDs, J. Alloys Compd. 698 (2017) 662−672, https://doi.org/10.1016/j.jallcom.2016.12.257.

[60] X. Sun, C. Li, L. Yu, H. Qi, Y. Gao, F. Gao, C. Wu, Y. Luo, J. Zhang, Preparation and luminescence properties of $Sr_2Eu_xLa_{1-x}AlO_5$ phosphor, J. Lumin. 157 (2015) 197−200.

[61] C. Bernard, G. Boulon, Eu^{3+} luminescence from different sites in scheelite-type cadmium molybdate red phosphor with vacancies, J. Mater. Chem. C 3 (2015) 8582−8594, https://doi.org/10.1039/C5TC01109D.
[62] B. Poornaprakash, P.T. Poojitha, U. Chalapathi, S.-H. Park, Achieving room temperature ferromagnetism in ZnS nanoparticles via Eu^{3+} doping, Mater. Lett. 181 (2016) 227−230, https://doi.org/10.1016/j.matlet.2016.06.033.
[63] S. Tamboli, P.D. Bhoyar, S.J. Dhoble, Analysis of electron-vibrational interaction in the 5d states of Eu^{2+} ions in $A_3P_4O_{13}$ and $A_3(PO_4)_2$ (A=Sr, Ba) phosphors, J. Lumin. 184 (2017) 23−28, https://doi.org/10.1016/j.jlumin.2016.12.003.
[64] G.B. Nair, H.C. Swart, S.J. Dhoble, Analysis of the electron-vibrational interaction in the 5d states of Eu^{2+} ions in $LiSrPO_4$ host matrix, J. Lumin. 214 (2019) 116564, https://doi.org/10.1016/j.jlumin.2019.116564.
[65] Z. Xia, Q. Liu, Progress in discovery and structural design of color conversion phosphors for LEDs, Prog. Mater. Sci. 84 (2016) 59−117, https://doi.org/10.1016/j.pmatsci.2016.09.007.
[66] G. Li, Y. Tian, Y. Zhao, J. Lin, Recent progress in luminescence tuning of Ce^{3+} and Eu^{2+}-activated phosphors for pc-WLEDs, Chem. Soc. Rev. 44 (2015) 8688−8713, https://doi.org/10.1039/c4cs00446a.
[67] B. Wang, Z. Wang, Y. Liu, S. Duan, Z. Huang, M. Fang, Valent control and spectral tuning by cation site engineering strategy in Eu doped $Sr_{1-x}Ba_xAl_2Si_2O_8$ phosphor, J. Alloys Compd. 806 (2019) 529−536, https://doi.org/10.1016/j.jallcom.2019.07.235.
[68] R. Cao, W. Wang, J. Zhang, S. Jiang, Z. Chen, W. Li, X. Yu, Synthesis and luminescence properties of Li_2SnO_3:Mn^{4+} red-emitting phosphor for solid-state lighting, J. Alloys Compd. 704 (2017) 124−130, https://doi.org/10.1016/j.jallcom.2017.02.079.
[69] T. Lesniewski, S. Mahlik, M. Grinberg, R.-S. Liu, Temperature effect on the emission spectra of narrow band Mn^{4+} phosphors for application in LEDs, Phys. Chem. Chem. Phys. 19 (2017) 32505−32513, https://doi.org/10.1039/C7CP06548E.
[70] Q. Zhou, L. Dolgov, A.M. Srivastava, L. Zhou, Z. Wang, J. Shi, M.D. Dramićanin, M.G. Brik, M. Wu, Mn^{2+} and Mn^{4+} red phosphors: synthesis, luminescence and applications in WLEDs. A review, J. Mater. Chem. C 6 (2018) 2652−2671, https://doi.org/10.1039/C8TC00251G.
[71] M.G. Brik, A.M. Srivastava, On the optical properties of the Mn^{4+} ion in solids, J. Lumin. 133 (2013) 69−72, https://doi.org/10.1016/j.jlumin.2011.08.047.
[72] H.-D. Nguyen, C.C. Lin, M.-H. Fang, R. Liu, Synthesis of Na_2SiF_6:Mn^{4+} red phosphors for white LED applications by co-precipitation, J. Mater. Chem. C 2 (2014) 10268−10272, https://doi.org/10.1039/C4TC02062F.
[73] Y.D. Xu, D. Wang, L. Wang, N. Ding, M. Shi, J.G. Zhong, S. Qi, Preparation and luminescent properties of a new red phosphor ($Sr_4Al_{14}O_{25}$:Mn^{4+}) for white LEDs, J. Alloys Compd. 550 (2013) 226−230, https://doi.org/10.1016/j.jallcom.2012.09.139.
[74] Z. Qiu, T. Luo, J. Zhang, W. Zhou, L. Yu, S. Lian, Effectively enhancing blue excitation of red phosphor Mg_2TiO_4:Mn^{4+} by Bi^{3+} sensitization, J. Lumin. 158 (2015) 130−135, https://doi.org/10.1016/j.jlumin.2014.09.032.
[75] M.G. Brik, N.M. Avram, Microscopic analysis of the crystal field strength and electron-vibrational interaction in cubic $SrTiO_3$ doped with Cr^{3+}, Mn^{4+} and Fe^{5+} ions, J. Phys. Condens. Matter 21 (2009), https://doi.org/10.1088/0953-8984/21/15/155502.
[76] Y. Li, S. Qi, P. Li, Z. Wang, Research progress of Mn doped phosphors, RSC Adv. 7 (2017) 38318−38334, https://doi.org/10.1039/C7RA06026B.

[77] A.M. Srivastava, M.G. Brik, Crystal field studies of the Mn^{4+} energy levels in the perovskite, $LaAlO_3$, Opt. Mater 35 (2013) 1544−1548, https://doi.org/10.1016/j.optmat.2013.03.021.

[78] Y.K. Xu, S. Adachi, Properties of Na_2SiF_6:Mn^{4+} and Na_2GeF_6:Mn^{4+} red phosphors synthesized by wet chemical etching, J. Appl. Phys. 105 (2009) 013525, https://doi.org/10.1063/1.3056375.

[79] R. Hoshino, S. Adachi, Optical spectroscopy and degradation behavior of $ZnGeF_6 \cdot 6H_2O$:Mn^{4+} red-emitting phosphor, J. Lumin. 162 (2015) 63−71, https://doi.org/10.1016/j.jlumin.2015.02.011.

[80] S.J. Kim, H.S. Jang, S. Unithrattil, Y.H. Kim, W. Bin Im, Structural and luminescent properties of red-emitting $SrGe_4O_9$:Mn^{4+} phosphors for white light-emitting diodes with high color rendering index, J. Lumin. 172 (2016) 99−104, https://doi.org/10.1016/j.jlumin.2015.11.042.

[81] A. Fu, C. Zhou, Q. Chen, Z. Lu, T. Huang, H. Wang, L. Zhou, Preparation and optical properties of a novel double-perovskite phosphor, Ba_2GdNbO_6: Mn^{4+}, for light-emitting diodes, Ceram. Int. 43 (2017) 6353−6362, https://doi.org/10.1016/j.ceramint.2017.02.044.

[82] M.G. Brik, S.J. Camardello, A.M. Srivastava, Influence of covalency on the Mn^{4+} $^2Eg \rightarrow {}^4A_{2g}$ emission energy in crystals, ECS J. Solid State Sci. Technol. 4 (2015) R39−R43, https://doi.org/10.1149/2.0031503jss.

[83] L.-L. Wei, C.C. Lin, M.-H. Fang, M.G. Brik, S.-F. Hu, H. Jiao, R.-S. Liu, A low-temperature co-precipitation approach to synthesize fluoride phosphors K_2MF_6:Mn^{4+} (M = Ge, Si) for white LED applications, J. Mater. Chem. C 3 (2015) 1655−1660, https://doi.org/10.1039/C4TC02551B.

[84] B. Wang, H. Lin, J. Xu, H. Chen, Y. Wang, $CaMg_2Al_{16}O_{27}$:Mn^{4+}-based red phosphor: a potential color converter for high-powered warm W-led, ACS Appl. Mater. Interfaces 6 (2014) 22905−22913, https://doi.org/10.1021/am507316b.

[85] X. Jiang, Y. Pan, S. Huang, X. Chen, J. Wang, G. Liu, Hydrothermal synthesis and photoluminescence properties of red phosphor $BaSiF_6$:Mn^{4+} for LED applications, J. Mater. Chem. C 2 (2014) 2301, https://doi.org/10.1039/c3tc31878h.

[86] L. Lv, X. Jiang, S. Huang, X. Chen, Y. Pan, The formation mechanism, improved photoluminescence and LED applications of red phosphor K_2SiF_6:Mn^{4+}, J. Mater. Chem. C 2 (2014) 3879, https://doi.org/10.1039/c4tc00087k.

[87] S. Adachi, T. Takahashi, Direct synthesis of K_2SiF_6:Mn^{4+} red phosphor from crushed quartz schist by wet chemical etching, Electrochem. Solid State Lett. 12 (2009) J20, https://doi.org/10.1149/1.3039192.

[88] D. Sekiguchi, S. Adachi, Synthesis and photoluminescence spectroscopy of $BaGeF_6$:Mn^{4+} red phosphor, Opt. Mater. 42 (2015) 417−422, https://doi.org/10.1016/j.optmat.2015.01.039.

[89] J. Long, X. Yuan, C. Ma, M. Du, X. Ma, Z. Wen, R. Ma, Y. Wang, Y. Cao, Strongly enhanced luminescence of $Sr_4Al_{14}O_{25}$:Mn^{4+} phosphor by co-doping B^{3+} and Na^+ ions with red emission for plant growth LEDs, RSC Adv. 8 (2018) 1469−1476, https://doi.org/10.1039/C7RA11967D.

[90] C. Wu, J. Li, H. Xu, J. Wu, J. Zhang, Z. Ci, L. Feng, C. Cao, Z. Zhang, Y. Wang, Preparation, structural and photoluminescence characteristics of novel red emitting $Mg_7Ga_2GeO_{12}$:Mn^{4+} phosphor, J. Alloys Compd. 646 (2015) 734−740, https://doi.org/10.1016/j.jallcom.2015.06.166.

[91] L. Meng, L. Liang, Y. Wen, A novel red phosphor Na^{+}, Mn^{4+} co-doped $Sr_4Al_{14}O_{25}$ for warm white light emitting diodes, Mater. Chem. Phys. 153 (2015) 1−4, https://doi.org/10.1016/j.matchemphys.2014.12.041.
[92] R. Cao, Z. Shi, G. Quan, Z. Hu, G. Zheng, T. Chen, S. Guo, H. Ao, Rare-earth free broadband $Ca_3Mg_3P_4O_{16}$:Mn^{2+} red phosphor: synthesis and luminescence properties, J. Lumin. 194 (2018) 542−546, https://doi.org/10.1016/j.jlumin.2017.10.079.
[93] R. Kasahara, K. Tezuka, Y.J. Shan, Preparation and luminescence properties of a red phosphor $Ba_5Ta_4O_{15}$:Mn^{2+}, Optik 158 (2018) 1170−1178, https://doi.org/10.1016/j.ijleo.2017.12.175.
[94] J. Zhang, F. Zhang, L. Han, Investigation on luminescence of red-emitting $Mg_3Ca_3(PO_4)_4$:Ce^{3+},Mn^{2+} phosphors, J. Rare Earths 33 (2015) 820−824, https://doi.org/10.1016/S1002-0721(14)60490-7.
[95] J. Zhou, T. Wang, X. Yu, D. Zhou, J. Qiu, The synthesis and photoluminescence of a single-phased white-emitting $NaAlSiO_4$:Ce^{3+}, Mn^{2+} phosphor for WLEDs, Mater. Res. Bull. 73 (2016) 1−5, https://doi.org/10.1016/j.materresbull.2015.08.006.
[96] M. Jiao, Y. Jia, W. Lü, W. Lv, Q. Zhao, B. Shao, H. You, $Sr_3GdNa(PO_4)_3F$:Eu^{2+},Mn^{2+}: a potential color tunable phosphor for white LEDs, J. Mater. Chem. C 2 (2014) 90−97, https://doi.org/10.1039/C3TC31837K.
[97] W. Tang, Z. Zhang, Realization of color tuning via solid-solution and energy transfer in $Ca_{3-x}Sr_x(PO_4)_2$:Eu^{2+},Mn^{2+} phosphors, J. Mater. Chem. C 3 (2015) 5339−5346, https://doi.org/10.1039/C5TC00562K.
[98] R. Zhong, J. Zhang, Red photoluminescence due to energy transfer from Eu^{2+} to Cr^{3+} in $BaAl_{12}O_{19}$, J. Lumin. 130 (2010) 206−210, https://doi.org/10.1016/j.jlumin.2009.09.021.
[99] B. Malysa, A. Meijerink, T. Jüstel, Temperature dependent Cr^{3+} photoluminescence in garnets of the type $X_3Sc_2Ga_3O_{12}$ (X = Lu, Y, Gd, La), J. Lumin. 202 (2018) 523−531, https://doi.org/10.1016/j.jlumin.2018.05.076.
[100] R.E. Samad, G.E.C. Nogueira, S.L. Baldochi, N.D. Vieira Jr., Development of a flashlamp-pumped Cr:LiSAF laser operating at 30 Hz, Appl. Opt. 45 (2006) 3356, https://doi.org/10.1364/AO.45.003356.
[101] Q. Shao, H. Ding, L. Yao, J. Xu, C. Liang, Z. Li, Y. Dong, J. Jiang, Broadband near-infrared light source derived from Cr^{3+} -doped phosphors and a blue LED chip, Opt. Lett. 43 (2018) 5251, https://doi.org/10.1364/OL.43.005251.
[102] Q. Shao, H. Ding, L. Yao, J. Xu, C. Liang, J. Jiang, Photoluminescence properties of a $ScBO_3$:Cr^{3+} phosphor and its applications for broadband near-infrared LEDs, RSC Adv. 8 (2018) 12035−12042, https://doi.org/10.1039/C8RA01084F.
[103] M. Li, L. Wang, W. Ran, Q. Liu, C. Ren, H. Jiang, J. Shi, Broadly tunable emission from $Ca_2Al_2SiO_7$:Bi phosphors based on crystal field modulation around Bi ions, New J. Chem. 40 (2016) 9579−9585, https://doi.org/10.1039/C6NJ01755J.
[104] H.C. Swart, R.E. Kroon, Ultraviolet and visible luminescence from bismuth doped materials, Opt. Mater. X 2 (2019) 100025, https://doi.org/10.1016/j.omx.2019.100025.
[105] A. Yousif, R.M. Jafer, S. Som, M.M. Duvenhage, E. Coetsee, H.C. Swart, Ultra-broadband luminescent from a Bi doped CaO matrix, RSC Adv. 5 (2015) 54115−54122, https://doi.org/10.1039/C5RA09246A.
[106] A.A. Penzias, R.W. Wilson, A measurement of excess antenna temperature at 4080 Mc/s, Astrophys. J. 142 (1965) 419, https://doi.org/10.1086/148307.
[107] S.R. James, R.W. Dennell, A.S. Gilbert, H.T. Lewis, J.A.J. Gowlett, T.F. Lynch, W.C. McGrew, C.R. Peters, G.G. Pope, A.B. Stahl, S.R. James, Hominid use of fire in the

lower and middle pleistocene: a review of the evidence, Curr. Anthropol. 30 (1989) 1−26, https://doi.org/10.1086/203705.
[108] A.R. Kadam, G.B. Nair, S.J. Dhoble, Insights into the extraction of mercury from fluorescent lamps: a review, J. Environ. Chem. Eng. 7 (2019) 103279, https://doi.org/10.1016/j.jece.2019.103279.
[109] H. Round, A note on carborundum, Electr. World 49 (1907) 309−310.
[110] O.V. Lossev, CII. Luminous carborundum detector and detection effect and oscillations with crystals, Lond. Edinb. Dublin Philos. Mag. J. Sci. 6 (1928) 1024−1044, https://doi.org/10.1080/14786441108564683.
[111] G. Destriau, Recherches sur les scintillations des sulfures de zinc aux rayons α, J. Chim. Phys. 33 (1936) 587−625, https://doi.org/10.1051/jcp/1936330587.
[112] N. Holonyak, S.F. Bevacqua, Coherent (visible) light emission from $Ga(As_{1-x}P_x)$ junctions, Appl. Phys. Lett. 1 (1962) 82−83, https://doi.org/10.1063/1.1753706.
[113] G.B. Nair, S.J. Dhoble, A perspective perception on the applications of light-emitting diodes, Luminescence 30 (2015) 1167−1175, https://doi.org/10.1002/bio.2919.
[114] R.A. Logan, p-n junctions in GaP with external electroluminescence efficiencies ∼ 2% at 25°C, Appl. Phys. Lett. 10 (1967) 206, https://doi.org/10.1063/1.1754913.
[115] C. Adachi, T. Tsutsui, S. Saito, Organic electroluminescent device having a hole conductor as an emitting layer, Appl. Phys. Lett. 55 (1989) 1489−1491, https://doi.org/10.1063/1.101586.
[116] X.-Y. Deng, Light-emitting devices with conjugated polymers, Int. J. Mol. Sci. 12 (2011) 1575−1594, https://doi.org/10.3390/ijms12031575.
[117] S. Nakamura, M. Senoh, T. Mukai, P-GaN/N-InGaN/N-GaN double-heterostructure blue-light-emitting diodes, Jpn. J. Appl. Phys. 32 (1993) 8−11.
[118] I. Akasaki, H. Amano, Breakthroughs in improving crystal quality of GaN and invention of the p-n junction blue-light-emitting diode, Jpn. J. Appl. Phys. 45 (2006) 9001−9010, https://doi.org/10.1143/JJAP.45.9001.
[119] Z.-K. Tan, R.S. Moghaddam, M.L. Lai, P. Docampo, R. Higler, F. Deschler, M. Price, A. Sadhanala, L.M. Pazos, D. Credgington, F. Hanusch, T. Bein, H.J. Snaith, R.H. Friend, Bright light-emitting diodes based on organometal halide perovskite, Nat. Nanotechnol. 9 (2014) 687−692, https://doi.org/10.1038/nnano.2014.149.
[120] S. Tamboli, P.D. Bhoyar, S.J. Dhoble, Analysis of electron-vibrational interaction in the 5d states of Eu^{2+} ions in $A_3P_4O_{13}$ and $A_3(PO_4)_2$ (A=Sr, Ba) phosphors, Journal of Luminescence 184 (2017) 23−28, https://doi.org/10.1016/j.jlumin.2016.12.003.

Fundamentals of LEDs

2

2.1 Overview of LEDs

Light-based technologies gained lots of recognition from all over the world, considering their importance for the future development of the global society on countless levels. This also led to the celebration of the International Year of Light in 2015. The global bodies have stressed on the awareness of science and technologies affiliated to light for addressing challenges such as sustainable development, energy and community health, as well as for improving the quality of life. Light-based technologies have been considered vital for the existing and future advances in energy, medicine, information and communications, fiber optics, agriculture, mining, astronomy, architecture, archaeology, entertainment, art, and culture, as well as many other industries and services. Ramifications were significant in introducing many advances in this technology. Currently, the most significant and popular devices among the light-based technologies are the light-emitting diodes (LEDs) that provide direct conversion of electrical energy into light. It is foreseen as the ultimate lamp in the future surpassing all other conventional sources that have proven their inefficiency in maximum conversion of electrical energy into light [1]. The improving performance of LEDs, since 1984, showed sustainable progress in the lighting systems from red-only LED arrays to high density, multicolor LED chip-on-board technologies. The development of blue-green LEDs based on aluminum gallium indium nitride (AlGaInN) in the early 1990s led to progress in the industries related to lighting and display devices due to the availability of low-voltage light sources in all the three primary colors (red, green, and blue) that helped in the direct penetration into multibillion-dollar markets in indoor agricultural production as well as medical treatment and phototherapy. Solid-state lighting is based on the LEDs that are p−n junction semiconductor chips forward-biased to emit light. Their emission wavelength immensely depends on the composition of the semiconductor chip and the forward bias voltage. GaN [2,3], InGaN [4,5], AlGaN [6,7], and AlInGaP [8] were some of the LED chips that have been used to produce different wavelengths of emission. However, there is a limit to the wavelength range covered by such semiconductor chips. To conquer the pitfalls accompanied by these LED chips and to provide a better spectrum of light emission, down-converting phosphors and quantum dots were introduced into the field. The quest for the improvement did not end here and it continued with the involvement of organic and biological materials in LED devices. This further enhanced the efficiency levels of LEDs but not without compromising on the device stability.

The Fundamentals and Applications of Light-Emitting Diodes. https://doi.org/10.1016/B978-0-12-819605-2.00002-1

More recently, LEDs with a combination of organic−inorganic perovskite materials is being explored, and it is assumed to conquer the commercial markets after its shortcomings are addressed and eliminated.

2.2 Merits and opportunities

Although LEDs are the latest entrants in the field of lighting, they have strongly surpassed other artificial light sources with their attractive and magnificent features. They are inherited with loads of merits and are promising candidates to future's low budget scheme on lighting. LEDs produce more lumens per watt than the incandescent bulbs can do; this makes it viable in battery-powered or energy-saving devices. LEDs can emit light of an intended color without the use of color filters that traditional lighting methods require, which proves to be more efficient and can lower the initial costs. The solid package of the LED can be designed to focus its light. Incandescent and fluorescent sources often require an external reflector to collect light and direct it in a useable manner. When used in applications where dimming is required, LEDs do not change their color tint as the current passing through them is lowered, unlike incandescent lamps, which turn yellow. LEDs are ideal for use in applications that are subject to frequent on−off cycling, unlike fluorescent lamps that burn out more quickly when cycled frequently, or high-intensity discharge (HID) lamps that require a long time before restarting. LEDs, being solid-state components, are difficult to damage with external shock. Fluorescent and incandescent bulbs are easily broken if subjected to external shock. LEDs can have a relatively long useful life. Reports estimate 100,000 hours of life for an LED lamp as compared to 10,000 hours of a fluorescent lamp or 1000 hours of an incandescent lamp. Even after completing its stipulated working hours, LED lamps continue to illuminate but at a lower intensity. Their long lifespan make them highly reliable. They do not require any type of maintenance throughout their lifetime. LEDs mostly fail by dimming over time, rather than the abrupt burn-out as found in the incandescent or HID bulbs. This provides extra safety for any area illuminated by LEDs. Even if the LEDs dim over time, they never fail completely like HID sources before their stipulated lifespan. LEDs need to be replaced only after they reach 30% lumen depreciation. It normally takes 17−20 years for quality LEDs to reach this stage of depreciation. LEDs light up very quickly. They do not need a starter or a ballast to start its operation. Being low-voltage electronic components with simple mechanism, they are easily operated with simple and cheap solutions. They are very efficient even in harsh conditions. A typical red indicator LED will achieve full brightness in microseconds. LEDs used in communication devices can have even faster response times. LEDs can be very small and are easily populated onto printed circuit boards. LEDs operate in weak-current electrical and electronic systems at low input voltage and are potentially safe to use. LEDs do not contain mercury, unlike compact fluorescent lamps, and hence, are stated as environment-friendly. They are featured with the absence of harmful ultraviolet and infrared emissions,

minimum heat emission, and nonbreakable glass tubes. They are mechanically robust and resistant to vibrations and impact. They are moisture-resistant electronic components able to operate at high humidity with no change in the operating parameters. Low power consumption reduces the load on power stations that in turn reduces harmful emissions in the atmosphere, and this acts as a prerequisite for mitigation of the global greenhouse effect. Their features indirectly benefit the global environment, and they are fully recyclable. Another important advantage is that LEDs are available in many colors and they do not need any type of filter to sort out different colors. Different combinations between monochrome LEDs can emit light with adjustable color, including white. LED luminaires can produce light in the entire color temperature range including those that are unachievable by conventional lamps. They emit light with constant temperature regardless of the intensity. Various LED bodies allow varied spatial distribution of illumination that may be either uniform distribution in all directions or concentrated into a narrow shaft of light. As opposed to conventional lights, there are no complex mirror lenses and reflector structures leading to loss of light. In addition, their miniature size allows for very compact light sources with low material consumption and aesthetic lighting fixtures. The volume of the emitting zone of the powerful white LED is several thousand times smaller than that of conventional lamps. Due to the low operating temperature and the nature of the materials employed, LEDs are found to be fire-safe.

2.3 Considerations while using LEDs

LEDs must satisfy some basic requirements before considering their commercialization in the global market. The materials needed to fabricate LEDs must be checked for their safety and their effects on human health. A large number of LED devices are checked for their quality and passed as safe for use under normal conditions. Different from fluorescent lamps, LEDs do not contain mercury and hence, are safer to use. However, some other elements such as copper, lead, and arsenic must be maintained below the regulatory limits laid down by the global bodies. LED phosphors must exhibit an overlapping between their excitation spectra and the emission spectra. Generally, emission spectra are in the region 420−490 nm and 360−400 nm for blue LED and near UV LED, respectively. LEDs must have their emission spectra in the green and red region for blue LED, whereas for near UV LED the emission spectra must lie in the red, green, and blue region. High quantum efficiency must be exhibited by phosphors for their use in LED. They must maintain their luminescence efficiency while working at differing temperatures. For this purpose, phosphors must have a very high thermal quenching temperature. They must be physically and chemically stable during the fabrication of LEDs. Their color rendering index (CRI) must not be less than 80.

2.4 Semiconductor physics of LEDs

The very first LEDs that were introduced to the world were nothing but semiconductor diodes capable of emitting light as a result of the passage of an electric current through it. More specifically, LEDs are photonic devices that carry out the conversion of electrical energy into optical radiation. Technically, they are p−n junction diodes that operates in the forward-biased condition. Generally, p−n junction diodes are constructed using silicon (Si) or germanium (Ge) as they permit the efficient flow of electric current through them without causing any damage to themselves and they are less sensitive to temperature. Such pure semiconductors are called intrinsic semiconductors. The doping of trivalent impurity ions such as boron, gallium, or aluminum into an intrinsic semiconductor leads to the formation of a p-type semiconductor, while the doping of pentavalent impurity ions like phosphorus, arsenic, antimony, or bismuth into an intrinsic semiconductor leads to the formation of an n-type semiconductor. However, Si- and Ge-based semiconductors are unable to convert electrical energy into light; rather they convert them into heat. In addition, these materials have an indirect energy gap that results in poor efficiencies. Hence, Si and Ge are totally ignored in the construction of LEDs. Soon, direct energy gap materials like GaAs came to the limelight for their higher quantum efficiencies and were used in the fabrication of LEDs [9]. Thereafter, advancements in research made it possible to produce efficient electroluminescence from indirect energy gap materials such as GaP, GaAsP, and AlGaP. The breakthrough moment in the LED industry came with the invention of InGaN chips that made it possible to cover the blue region of the electromagnetic spectrum [10]. The subsequent chapter 3 shall give a detailed description of the semiconductor materials for LEDs. In this section, we shall limit ourselves to a brief discussion on the general construction and working of semiconductor LEDs.

2.4.1 General construction

Although the basic structure of an LED is similar to a p−n junction diode, the construction of an LED is quite different from a normal diode. A schematic representation of an LED structure can be seen in Fig. 2.1(a). The symbolic representation of an LED in electronic circuits is given in Fig. 2.1(b). The semiconductor die consists of three different layers that are deposited on the substrate. The top layer is the p-type region; the midlayer is the active region, while the bottom layer is the n-type region. The p-type and n-type regions have holes and electrons, respectively, whereas the active region has both of these charge carriers. The anode is connected from the bottom of the substrate, while the cathode is connected to the top surface of the p-layer using a wire bond. The semiconductor die is rested on the anvil that connects the die with the anode. There is a reflector cup attached beneath the die to reflect all possible light toward the top. The whole setup is surrounded by a hemispherical-shaped transparent casing made up of hard plastic epoxy resin, which acts as a shielding to protect the LED from any shocks or vibrations and other effects from the surrounding. It is crucial for the encapsulating resin to possess a high refractive index, optical transparency,

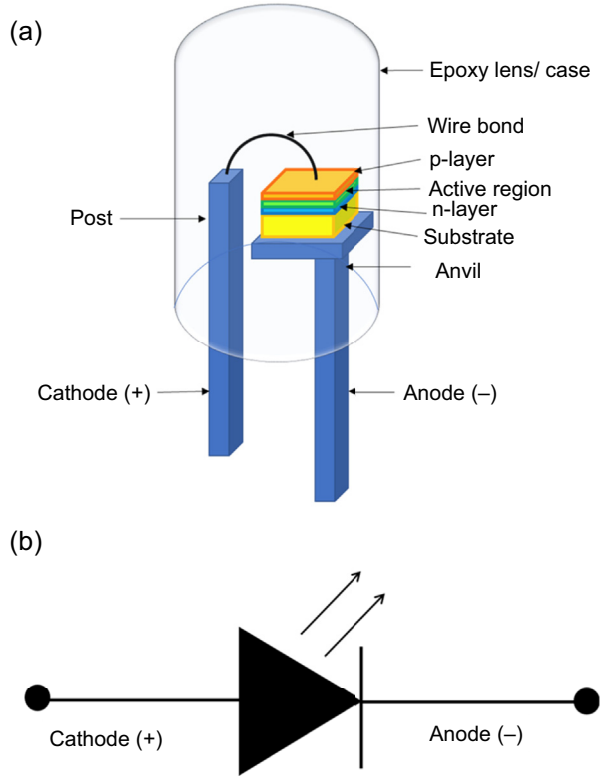

Figure 2.1 (a) Schematic representation of an LED structure (Reproduced with permission from Ref. [39], Copyright 2020, Elsevier B.V.). (b) Symbolic representation of an LED in electronic circuits.

temperature stability, and chemical inertness and to be airtight. The top portion of the casing is designed in such a way that the light reflected away from the reflector cup is focused by the dome-shaped lens to give maximum brightness. Some LEDs bear a cylindrical or rectangular casing with a flat-surfaced top. From the bottom of the casing, two electrodes are seen protruding from inside. These electrodes represent the cathode and anode terminals of the LED. LEDs will work only if it is forward biased, and hence, it is essential to identify the electrodes accurately before installing LEDs into a circuit. Consequently, in most cases, the anodes are found to be a bit longer than the cathode terminal to make a distinction between them. Sometimes, a notch or a flat spot is also provided on the cathode terminal. In high-power LEDs, a thermal sink is also provided for the heat dissipation.

2.4.2 Working principle

LEDs belong to the family of luminescent devices that works on the principle of electroluminescence. Electroluminescence was discovered by H.J. Round in 1907 during

his experiments on the passage of electric current through the contact of carborundum [11]. For LEDs to exhibit electroluminescence, it is necessary to put them in forward-biased condition, that is, the positive terminal of the battery should be connected to the p-type region and the negative terminal to the n-type region. If the terminals are connected vice versa, the diode will be set into the reverse-bias mode and will stop functioning. In the forward-bias mode, the free holes from the p-region and the free electrons from the n-region start flowing toward the p−n junction. Although both p-type and n-type regions are conducting, their junction is nonconductive. The region near this junction is called the depletion region. The depletion region, also known as the active region, is a nonconducting zone positioned between the p-type and n-type regions, wherein the positively charged holes and the negatively charged electrons attract and annihilate each other through a process known as recombination. The positive charge attracts the electrons from the n-type region towards the p-type region and repels the holes from the p-type region towards the junction, while the negative charge repels the electrons from the n-type region towards the junction. This results in the narrowing of the depletion region and the potential barrier across the junction lowers down, thereby enabling more electrons to cross the junction from the n-type to the p-type region. The flow of electrons from the n-type to p-type region leaves behind positively-charged holes in the n-type region, which then recombines with the available free electrons in the local region to give out emission of radiative energy. The electrons that tunneled the potential barrier across the junction and traveled to the p-type region also radiatively recombined with the holes. Most of the recombination takes place in the depletion region itself. The crossing of the charge-carriers from their respective regions to the other side increases as the width of the depletion region reduces with the recombination of holes and electrons. The energy of the emitted photon is a characteristic of the semiconducting material with which the diode is manufactured and it depends upon the energy band gap of that material. The electrons hop from hole to hole in the diode to maintain the flow of current through the circuit. A pictorial representation of the working principle of an LED is shown in Fig. 2.2. If the LED is forced into the reverse-bias mode, the photon energy stops radiating from the LED. This is because the positive terminal connected to the n-type region starts attracting all the electrons away from the junction, while the negative terminal connected to the p-type region repels the electrons away from the junction towards the n-type region and attracts the holes from the junction towards the p-type region. This causes a rise in the barrier potential across the junction and the widening of the depletion region.

2.5 Device fabrication

2.5.1 Substrate materials

The foremost phase in the development of an LED is distinguishing the vital materials required at various stages of fabrication. Before beginning the manufacturing process, the most essential part is the selection of the substrate for deposition.

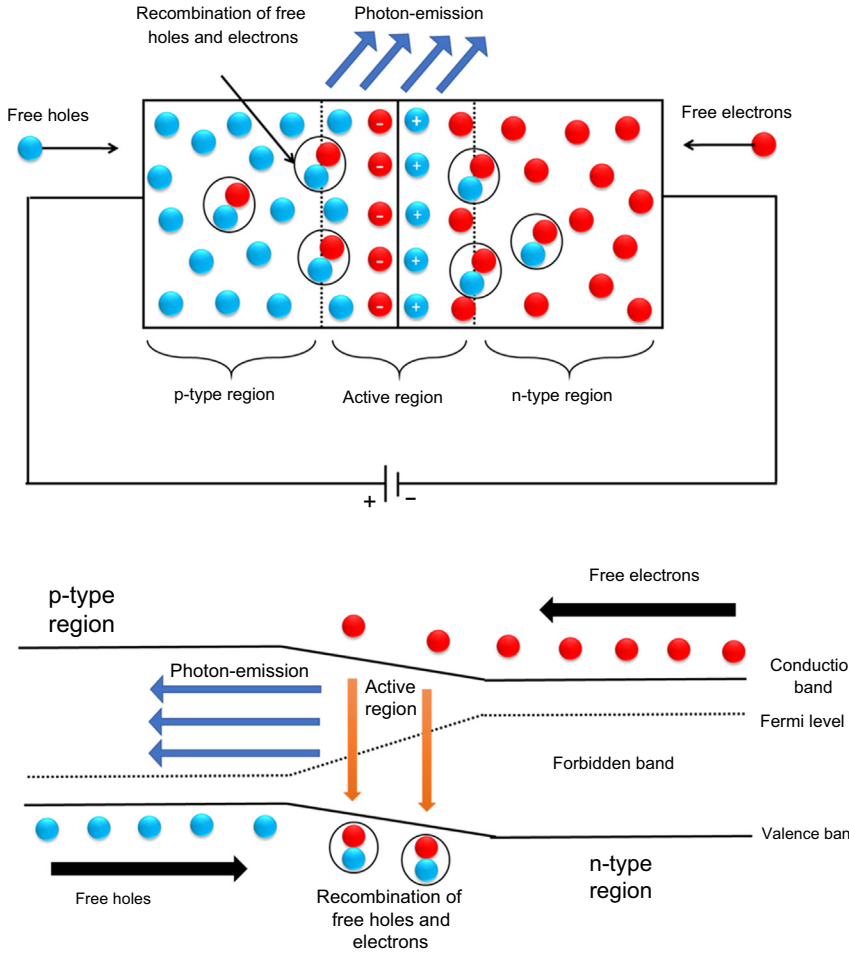

Figure 2.2 Working principle of an LED.

For manufacturing an LED, the number of substrates is very few in options; especially for high-power GaN-based LEDs, the options are restricted between gallium nitride (GaN), silicon carbide (SiC), sapphire, and silicon (Si).

GaN has gained huge recognition as one of the most promising materials for semiconductors with wide bandgap. It is especially known for its direct bandgap of 3.39 eV at room temperature, which is favorable for applications in light-emitting devices such as laser diodes and LEDs that emit ultraviolet, violet, and blue color emissions. In 1969, the first single-crystal film of GaN was reported by Maruska and Tietjen [12]. They made use of a vapor-phase growth technique to produce colorless GaN, which was suitable for electrical and optical evaluation. Assuming that GaN will not decompose at temperatures up to 600 °C, they limited the growth temperatures below 600 °C to produce polycrystalline GaN. However, they soon raised the growth temperature

from 600 to 850 °C after realizing that the decomposition would be suppressed by growth in an ammonia environment. All these attempts led to the growth of n-type GaN films although no intentional doping was introduced. The p-type GaN films were almost impossible to obtain by these methods. Generally, single-crystalline GaN is prepared by employing a homoepitaxial growth on GaN substrate or a hetero-epitaxial growth on silicon/silicon carbide/sapphire substrate. However, there is a large lattice mismatch and difference in the thermal expansion coefficients between the gallium nitride and the sapphire substrate that created many obstacles in the production of defect-free high-quality GaN films with a flat surface. The lattice mismatch results in microscopic defects, known as threading dislocations, in GaN films that lead to an undesirable decrease in the LED lifetime and luminosity. Under such circumstances, the search for alternatives to sapphire substrate began. One such alternative was silicon carbide (SiC) that has relatively close association with the crystal structure of gallium nitride. Soon sapphires were replaced by SiC, and this led to a significant decrease in the defect density and improved longevity as well as efficacy. However, the expenses around the production of sapphire and silicon carbide substrates were tough to handle, and their manufacture is critically challenging. It is quite difficult to meet the high-profile demands and manufacture LEDs in massive numbers using sapphire or silicon carbide substrates, unless measures are adopted to improve their product consistency and quality in conjunction with larger diameters. One way to improve the light extraction by reducing the epilayer defect densities is to create the patterning of the substrate. Patterned sapphire substrates (PSS) involve nanoscale patterning of the sapphire substrate surface. Such substrates provide better performance with reduced cost and simplified manufacturing [13−15]. Mid- and low-power LEDs are widely manufactured using these substrates for backlighting applications. However, uncertainties still prevail over the performance achieved through PSS. With a vision to reduce the manufacturing expenses, silicon substrates were brought forward. Silicon is the mainstay of the semiconductor chip-fabrication industry. Unfortunately, there is a mismatch between the crystal structures of silicon and GaN and, this case was found to be worse than silicon carbide and sapphire substrates. In addition, silicon substrates tend to reabsorb the emitted photons, which would have otherwise escaped from the device and contributed to the overall luminosity of the LED.

All these drawbacks could be effectively minimized by introducing homoepitaxial growth on GaN substrates. This would effectively eliminate any possibility of a lattice mismatch between the epilayer and the substrate, thus, making way for simplified epitaxial growth processes and device structures. An unsuccessful attempt was made my Maruska to prepare a p−n junction out of GaN by introducing Zn into it as a dopant. Zn was heavily doped into GaN with an objective to produce p-type GaN. However, heavy doping of Zn compelled the GaN films to turn insulators rather than demonstrating p-type conduction. Zn forms an effective radiative center in GaN that can emit blue light at 2.86 ± 0.02 eV [3]. Zn acts a deep acceptor that makes the GaN crystal insulating. There is a drastic change in the electronic concentration with increasing Zn-concentration. This also results in the shifting of photoconductivity peak to higher energies by about 70 meV and the disappearance of the sensitivity to visible radiation [16]. Pankove et al. studied the optical properties of GaN thin film

and reported an exponential rise in the absorption edge of GaN to a value of about 4×10^5 cm^{-1} at 3.5 eV at room temperature [2]. This suggested the existence of direct optical transition and a high joint density of states in GaN. Blue electroluminescence center at 475 nm was obtained from an assembly consisting of an insulated Zn-doped layer connected with two surface probes in GaN [17]. The first current-injected GaN light emitter was fabricated by Pankove et al. and it emitted blue and green light [18]. This assembly was a metal−insulator−semiconductor diode that consisted of an undoped n-type layer, an insulating Zn-doped layer, and an indium surface contact. Blue and violet electroluminescence was achieved from Mg-doped GaN films, which were prepared by metalorganic halide vapor phase epitaxy technique [19]. Mg-doped GaN films that were prepared by the low-energy electron-beam irradiation (LEEBI) treatment were able to realize distinct p-type conduction [20]. Although remarkable enhancement in the photoluminescence efficiency and drastic fall in the resistivity were obtained by this treatment, it suffered a drawback that a very thin region from the GaN epitaxial wafer's surface showed strong p-type conduction. This is because the penetration depth of the incident electrons from the LEEBI influences the low-resistivity region of the Mg-doped GaN film. This created a huge obstacle in the fabrication of several kinds of light-emitting devices due to the scarce availability of p-type regions on the surface of GaN films. Nakamura et al. put forward a suggestion to obtain highly p-type Mg-doped GaN films by thermally annealing them in N_2-ambient atmosphere at temperatures $>700\,^{\circ}C$ [21]. They were successful in establishing the mechanisms of LEEBI treatment and thermal annealing on GaN films [22]. They assumed that the weak blue emissions in photoluminescence measurements and high resistivity are due to the formation of acceptor-H neutral complexes in GaN films. There is a lowering of resistivity of p-type GaN films when subjected to thermal annealing in the nitrogen-ambient atmosphere. This is due to the removal of atomic hydrogen from the acceptor-H neutral complexes.

2.5.2 Packaging materials

The selection of packaging materials requires high attention to the mechanical support and protection that should be offered to a semiconductor die by these materials. These materials must not reduce the light intensity of the LED die by absorbing the light emitted from the die. They must ensure optimum light extraction by being transparent to the emitted light and yield high light output. The LED package consists of external contact pads for electrical and thermal connection to the die. Generally, copper is used to make the contact patterns on the front and rear of the substrate. Several mid- and low-power LEDs use cheap plastic packaging materials to deliver a high power LED package with high efficacy in varied sizes. Plastic-leaded chip carrier (PLCC) package was used in a great number of luminaires owing to their improved efficacy, increased lumen output, and low cost. Another version of the PLCC package is the quad flat no-lead (QFN) plastic package. Both PLCC and QFN packaging has several features in common barring the fact that PLCC have leads while QFN has pads located on the base of the package. An alternative to these packaging techniques is the chip-on-flex (COF) technology, which is much cheaper

than the former ones. Here, the LED die is directly mounted on a ceramic or a metal core printed circuit board (MCPCB). Normally, an MCPCB is assigned with the task of dissipating the heat from the LED to the heat sink. The circuit layer is bonded with the base metal made of aluminum using a thermal interface layer, for which a dielectric polymer layer with high thermal conductivity is used. The upper metal circuit layer is made of copper. Chip-in-flex, which is an extension of the COF approach, shortens the signal path down to the substrate level, reducing the interconnect length [23]. Fig. 2.3 exhibits some of the examples of packaging technologies used in LED fabrication.

2.5.3 Phosphors or quantum dots

A large share of the cost of a packaged LED depends on the phosphor materials or the down-conversion materials and the associated matrix materials that have been embedded in the package. A phosphor needs to get excited by a near-UV or blue light from the LED die and then, emit its characteristic light in the visible part of the electromagnetic spectrum. This forms the primary requirement for a phosphor to be used in an LED package. LED phosphors generally consist of a wide bandgap host material that is doped with some activator ions. The luminescence centers in a phosphor are generally localized at the sites occupied by dopant ions in a host matrix. Sometimes, coactivator or sensitizer ions are added along with the activator ions to enhance the overall emission from the phosphor. The sensitizer and the activator ions may either be a lanthanide ion or a transition metal ion. Lanthanide ions are the most preferred activators due to their ability to give emissions from ultraviolet to near-infrared regions of the electromagnetic spectrum. Actinides are generally ignored from the phosphor configuration owing to their radioactivity and the hazards arising from it. Some transition metals such as Mn, Cr, and Bi are also known to produce photoluminescence emission in the visible region. However, there are certain other metals such as Fe, Co, and Ni, which act as luminescence quenchers and extinguish the luminescence properties.

The selection of a phosphor for an LED package requires its compatibility with the LED to be proven at its best. Although most phosphors claim to showcase excellent luminescence efficiency during their initial tests, they fail to withstand the harsh temperature conditions experienced within the LED package. A phosphor must be both thermally and chemically stable and possess uniform particle size with well-controlled morphology. They must exhibit consistency in their luminescence performance within the LED package for a prolonged duration of several years. It is also essential that the color coordinates of the emitted light remain consistent and the alterations in the CIE coordinates as well as the lumen output should be minimum with time. A hypothesis based on the ab initio calculations suggests that host materials with highly rigid structure and larger bandgap can be more efficient phosphors for LEDs [24]. Apart from phosphors, another class of materials with nanodimensional semiconductor crystals started gaining acceptance in the LED package. These nanocrystals are called quantum dots (QD), and their dimensional

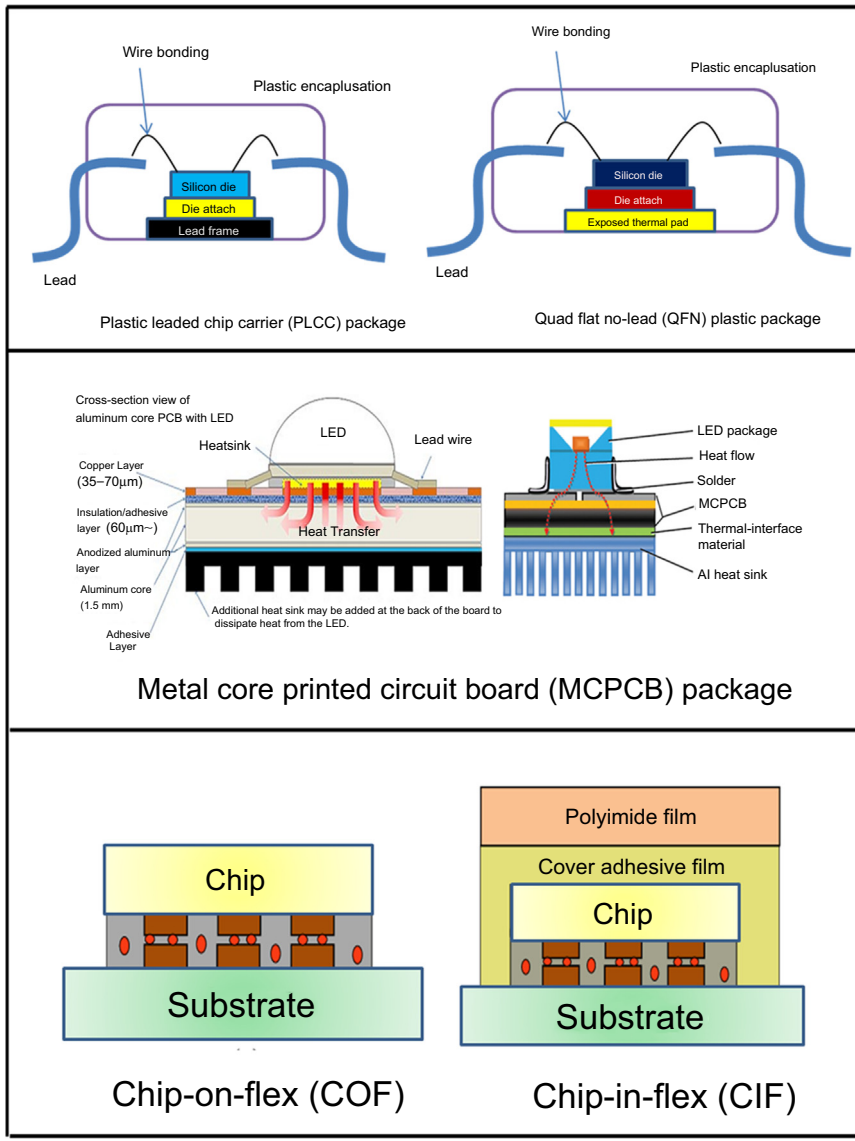

Figure 2.3 Different types of LED packaging.

variations could effectively tune their absorption and emission bands [25]. Thus, it is possible to extract the color emission of the desired wavelength just by varying the size of the quantum dots. However, the passivation of QD surface is essential to avert the luminescence quenching or spectral shifts, which may arise due to the recombination of delocalized charge carriers at the surface. For this purpose, quantum dots need to be grown as a shell over a core. Quantum dots exhibit a blue shift with

decreasing size, that is, the color emission peak shifts from red to blue with decreasing QD size. QDs are tinier than a virus. Yet, their lifetime is found to be longer when their size is larger.

2.5.4 Encapsulation materials

The protection of the LED package from the hazards posed by the moisture or other contaminations is entrusted to the encapsulation materials. The electronic circuits are volatile to moisture and dust particles and are prone to damage under thermal or mechanical stress. The materials employed for encapsulation ensure that the LED package is isolated from any mechanical or thermal stresses. The encapsulant acts as a protective shield for the LED die against the mechanical and chemical tensions from the environment and also helps to enhance the extraction of generated photons. Before depositing over the LED die, the phosphor material is dispersed within the encapsulant matrix. Epoxy or silicone are highly stable to heat and intense blue emission exposures, and hence, they are the most widely used encapsulants. Nevertheless, the performance of silicone encapsulants is being pushed beyond its limits by the high thermal loads induced by high-power LEDs. This is risking them to issues like cracking, discoloration, and degradation. Good long-term stability against such exposures is exhibited only by certain premium grades of silicone. However, these high-grade silicone matrix materials are very expensive and challenging to consider if the overall manufacturing cost of LEDs is to be kept low. Spin on glass was proposed as an alternative to silicone encapsulants to produce remarkable light attenuation in comparison to silicone for prolonged lighting duration [26]. Yet, they too suffer from a disadvantage that can be observed in the form of low brightness.

2.5.5 Luminaires

LED luminaires can be sensed as a stunning compilation of the mechanical, electronic, electrical, and optical designs shaped out of numerous research outputs. An LED fixture consists of an arrangement of LEDs with components such as heat sink, driver circuits, and optical lenses, all of which are assembled in a unit. There is a general misconception on the heating issues of an LED. It is often assumed that LED luminaires do not get heated-up on operation. However, the fact is that LEDs often heat up when it draws more power and the heat that is generated must be dissipated out from the LED package. There is no proper system configured with the LED package to drain out this excess heat. Hence, a heat-sink is positioned at the bottom of the LED to dissipate the heat into the surrounding environment and protect the electric components from any thermal damage. Heat-sink protects the LED package from self-damage due to overheating and thereby, enhances the lifespan of the luminaire. It ensures proper thermal management of the luminaire. Apart from this, heat-sinks also provide attractive appearance to the LED luminaire. Heat-sinks are available in various innovative and attractive designs that offer a magnificent look to the luminaire. In general, LED fixtures possess metal fins, whereas aluminum fins or ceramic fins are used in high-power LEDs. Ceramic fins have low thermal capacity and have tiny pores

that facilitate easy dissipation of heat; hence, they are more effective than the metal fins. Graphene films have also garnered huge reputation as an excellent heat-sink [27]. Graphene exhibits fourfold better thermal conductivity compared to copper. Originally, certain malfunctions persisted with the addition of more layers of graphene. The weak adhesive forces of graphene posed a big issue and this was due to the weak van der Waals forces that formed the bonds in graphene. This issue was soon recognized and resolved by managing to produce strong covalent bonding between the surface and the graphene film by adding (3-aminopropyl) triethoxysilane.

LED luminaires are available in a variety of designs such as retrofitted light bulbs, tube lights, spotlights, downlights, and strip lights as shown in Fig. 2.4. It is unworthy to use small-chip packaged LEDs for lighting as they are deficient of proper thermal management systems. For such applications, high-power LEDs must be preferred. High-power LEDs are capable of performing for an extended period without experiencing any damage. They produce continuous light output with desirable light characteristics and are specially designed to maintain their performance throughout their lifespan. The quality of the components included in an LED package decides the quality of the luminaire and it is a matter of foremost concern to obtain luminaires with top-class performance. The deciding factors behind the quality of an LED luminaire are the design of the fixture, illumination produced, thermal management, low cost, and the long lifespan. Hence, it is highly recommended to opt for the standard luminaires manufactured by reputed companies.

Figure 2.4 Different types of LED luminaires.

2.6 Characteristics of LED phosphors

LED phosphors must satisfy several requirements before considering it in an LED package. Different standards and recommendations are used to measure the eligibility of the phosphors. At present, the only internationally recognized agency to provide standard recommendations for LED measurements is the CIE (Commission Internationale de I'Eclairage). In this section, some of the characteristics that are considered as the basic requirement for an LED phosphor and the standards associated with it are discussed.

2.6.1 Temperature quenching

Phosphors find it quite difficult to maintain the efficiency and performance under different thermal conditions. In most cases, there is a drastic drop in their efficiency, when the operating temperature reaches a critical limit. Generally, the operating temperatures of an LED can exceed 150 °C and the phosphor encapsulated on the LED die is subjected to tolerate these harsh thermal conditions. Under such circumstances, the quality of the phosphor starts degrading and the overall light output is affected. This can be witnessed in the form of change in the color point, drop in the efficiency, and the intensity. The drop in the quantum yield should not exceed 10% at 150 °C. It is also essential that the color point do not vary with the variation in the temperature. High-power LEDs draw a huge amount of power for their operation and hence, their temperatures go much higher than 150 °C. The temperature is elevated due to the high input-power densities in the chip, and this heat is transferred to the phosphor and the encapsulant that are in close contact with the chip. Consequently, the phosphors used for high-power LEDs must have much better thermal stability than that used for ordinary LED packages. One way to avoid the ill-effects of heat on the phosphor is by adopting the strategy of the remote phosphor-coating on the inner walls of the epoxy lens. Although the remote phosphor technique will evade the rapid degradation of phosphor, it suffers from the disadvantage that light output is poorer than that obtained when the phosphor is directly encapsulated on the die. The lifespan of the phosphor can be fundamentally reduced due to the thermal quenching effect. It may even put an end to the color emission of the phosphor.

The thermal quenching of the phosphor can lead to certain serious effects such as a spectral shift in the emission peak and a decline in the overall color emission of the phosphor. A strong thermal quenching behavior was exhibited by $Ba_2SiO_4:Eu^{2+}$ phosphor whose integrated intensity at 150 °C was 28% of that observed at room temperature [28]. The thermal stability of $Ba_2SiO_4:Eu^{2+}$ phosphor was improved by bringing about a structural modification in the lattice. Shao et al. proposed the idea of introducing Sr^{2+} ions at some of the Ba^{2+} sites. The idea prospered and they were successful in optimizing the thermal stability of the phosphor by maintaining a 1:1 ratio of Ba^{2+} and Sr^{2+} ions. The drop in the luminescence intensity with the increasing temperature is a general phenomenon. However, Xia et al. reported an unusual behavior in $Ba_2Y(BO_3)_2Cl:Eu^{2+}$ wherein the luminescence intensity

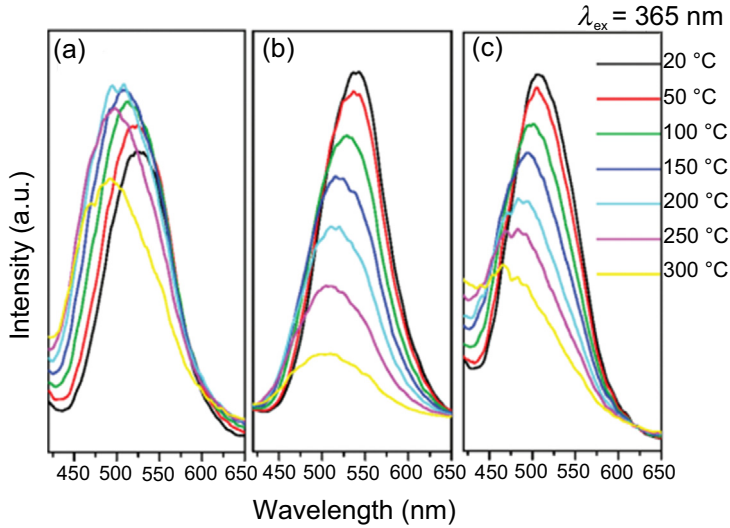

Figure 2.5 Emission spectra of (a) $Ba_2Y(BO_3)_2Cl:Eu^{2+}$, (b) $Ba_2Gd(BO_3)_2Cl:Eu^{2+}$, and (c) $Ba_2Lu(BO_3)_2Cl:Eu^{2+}$ phosphors at different temperatures from 20 to 300 °C under the excitation of 365 nm.
Reproduced with permission from Z. Xia, X. Wang, Y. Wang, L. Liao, X. Jing, Synthesis, structure, and thermally stable luminescence of Eu2+ -doped Ba2Ln(BO3)2 Cl (Ln = Y, Gd and Lu) host compounds, Inorg. Chem. 50 (2011) 10134−10142. https://doi.org/10.1021/ic200988w. Copyright 2011, American Chemical Society.

proportionally increased with temperature up to 200 °C, as shown in Fig. 2.5. The integrated intensity for $Ba_2Y(BO_3)_2Cl:Eu^{2+}$ at 200 °C was noted to be 136% of that observed at room temperature [29].

2.6.2 Luminous efficacy

The most convenient term to evaluate the number of lumens produced at the expense of electric power is the luminous efficacy. The maximum luminous efficacy value for the photopic vision was determined by Pulli et al. as 683.002 lumens per watt [30]. The green light with an emission peak at 555 nm is the most sensitive to the human eye. Hence, the luminous efficacy value for the photopic vision was calculated using only the 555 nm light. However, to obtain a higher color rendering index (CRI), it is essential to obtain the spectral dispersion over the entire range of visible light spectrum. Thus, the color-rendering index and the luminous efficacy contradict each other. There is a significant effect of the size of the phosphor particle on the luminous efficacy [31]. The particles will scatter more light when their size is smaller. The backscattered light is then reabsorbed by the Blue LED chip in the package, thereby leading to a drop in the luminous efficacy. In addition, there is a critical effect of temperature on the luminous efficacy. There is often a decline in the efficacy of the phosphor with rising temperatures.

With time, the term "lumens" has fallen out from the list of metrics to assess the actual efficiency of an LED luminaire. Lumens are unable to measure the perceived brightness of the LED. This factor can be understood by taking an example. Consider two LED luminaires emitting a similar number of optical watts. The first luminaire takes the color rendition into account and emits photons of lower energy (longer wavelength) with deep red tones. On the other hand, the second luminaire completely ignores the aspect of color rendition but emits the same number of optical watts as the first one. The first luminaire is heavily penalized in terms of the lumen output.

Better accuracy in the assessment of the efficiency of an LED luminaire can be achieved by calculating the number of optical watts produced for every unit of electrical watt provided as an input to the luminaire. This new metric provides more information about the luminaire's efficiency and is termed as "White Efficiency." This metric is a physical quantity measuring the conversion efficiency of the electric input power into optical output power in the form of white light. It also describes the amount of electric input power that is lost in the form of heat. In practical devices, the heatsinks are limited and there is a substantial amount of heat generated in the driver circuit, due to which, the phosphor's efficiency and performance are adversely affected. Hence, it is essential to understand the conversion ratio of input power into heat in the luminaire and this piece of information can be recognized from White efficiency. From the knowledge gained from this metric, the energy loss in the luminaire can be effectively reduced by bringing about certain modifications in its design.

2.6.3 Color rendering index

Color rendition is an important aspect of a light source that describes an object under illumination defining the true reflection of its colors. The metric that defines the color rendition property of a light source is expressed in terms of the color rendering index (CRI). In general, CRI is denoted by R_a. The quality of the light is considered to improve the luminaire's CRI to higher values. The value of CRI for a light source is determined by considering the broad daylight from the sun as the reference. An object portrayed in broad daylight has 100% CRI. Thus, the light source is found to have characteristics similar to broad daylight if it can exhibit 100% CRI. Greater the value of CRI, greater will be the probability of obtaining a light spectrum closer to broad daylight. Apart from the luminous efficacy and brightness of a luminaire, the color rendering index of the luminaire must also be sufficiently high. From Fig. 2.6, the variation in the color appearance of an object exposed under light sources with different CRI values can be witnessed. The cost of a luminaire is proportional to the value of CRI of that luminaire.

LED phosphors involving the rare-earth ions as dopants often add to the overall manufacturing cost of the luminaire. As a result, manufacturers often compromise with the quality of the phosphor to lower the overall luminaire cost. In this pursuit, the CRI of the luminaire gets ignored and the integrated color emission of the luminaire is adversely affected. As a result, the white light produced from the LED appears differently at various spots, thus giving a clear indication of the degraded quality of

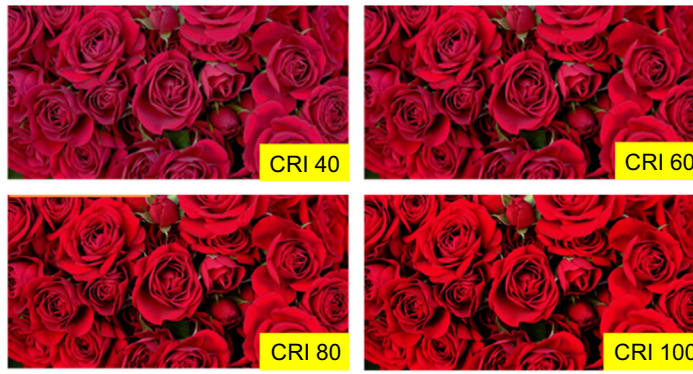

Figure 2.6 Variation in the color appearance of the object illuminated by light sources with different color rendering index (CRI) values.

light. It is ultimately a challenge for LED manufacturers to maintain the same color purity and CRI. High-quality phosphors possess high CRI value that enables the luminaire to emit in the desired color region almost throughout its lifespan.

In the recent, CIE addressed the shortcomings of color rendering index that often led to a mismatched perception for solid-state lighting sources against the perception made by a human eye [32]. CRI has failed to accurately define the color gamut and describe the color fidelity of a light source. Consequently, the scientific society was compelled to adopt a new and more accurate metric to quantify the color fidelity of a light source. CIE released a technical report to introduce the color fidelity index (R_f) as the new metric to fill the gaps left out by CRI. Technically, it is defined as a measure to describe "how closely the color appearances of the entire sample set are rendered on average by a test light as compared to those under a reference illuminant" [32]. Yet, it is too early to rule out the CRI, as the color fidelity index does not perform as a replacement to the existing CRI, nor does it describe the minimum performance standards or specifications of a light source.

2.6.4 CIE chromaticity coordinates

In 1913, the CIE, also known as the International Commission on Illumination, was founded as an international independent body to universally standardize the metrics related to light and exchange ideas pertaining to the science of light, color, vision, and lighting. To give analog and digital representations of colors, CIE introduced the concept of color spaces. Till now, three models for the color spaces were proposed by CIE, namely CIE 1931, CIE 1960, and CIE 1976, which are displayed in Fig. 2.7. The color space model proposed in 1931 was the first complete representation of the colors perceived by human eye quantitatively linked with the distribution of wavelengths in the visible light spectrum. This model was created after a series of independent experiments by W.D. Wright and J. Guild [33,34]. The CIE 1931 color space makes use of the tristimulus values X, Y, and Z to define the composition of

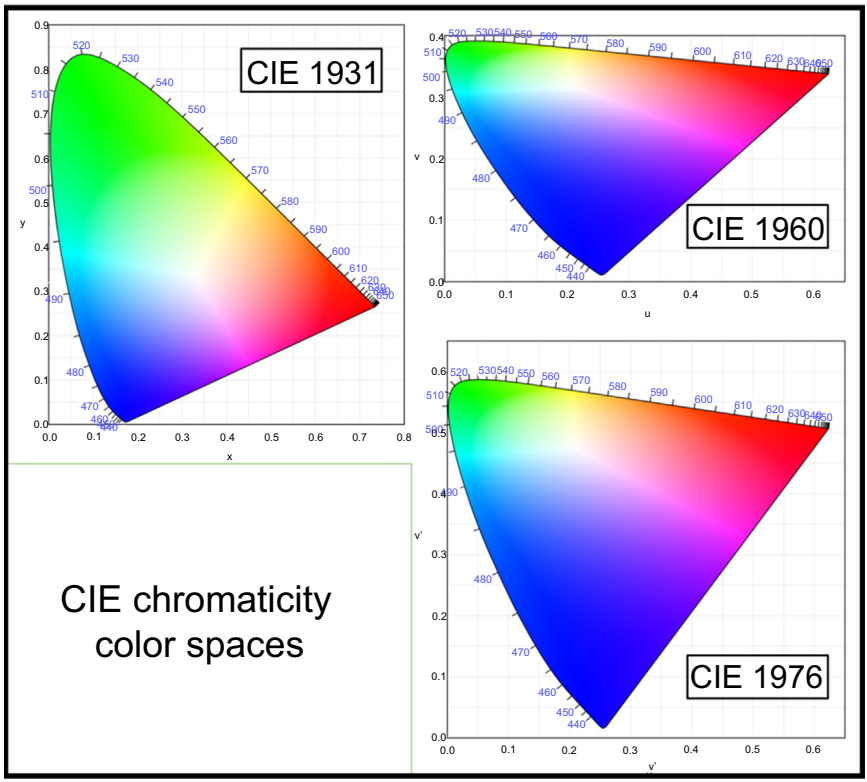

Figure 2.7 Color space models proposed by CIE.

colors. The ratio of X, Y, or Z to their sum ($X + Y + Z$) leads to a new set of coordinates (x, y, z), which are known as the CIE chromaticity coordinates. As the sum of x, y, and z is always unity, each color can be sufficiently represented by using only (x, y) coordinates on the 1931 CIE color space. There were some minor issues with the uniformity of the 1931 color space. These were tried to be rectified in the subsequent models that came up in 1960 and 1976. Nevertheless, the modifications were not enough to pull out the 1931 color space from the limelight, which is still more popularly used than the latter ones.

2.6.5 Correlated color temperature

The color appearance of a light source is, usually, described by correlating it with the temperature of an ideal blackbody radiator. Thus, the color appearance of the light source is measured in terms of the color temperature and is expressed in the units of kelvin (K). However, such kind of terminology is appropriate only if the light source emits thermal radiation. One such example is the incandescent bulb that uses 90% of its energy to emit heat. The color temperature failed to find significance in case of the

light sources that gave cold light emission, such as luminescence. In such cases, the terminology was modified as correlated color temperature (CCT). For light sources emitting cold light, the temperature of the emitted light is not a true color temperature. Instead, the temperature of the light is decided depending upon the wavelength of the emitted light. The CCT of the light source is rated as warm light if the emitted light has wavelength nearer to red/infrared region. On the contrary, the CCT of the light source is rated as cool light if the emission is near the blue region of the electromagnetic spectrum. It is quite necessary to note that the temperatures depicted for warm and cool light are contradicting to their nomenclatures. A warm light falls in the temperature range of 2500−3500 K, while the cool light has correlated color temperatures above 5000 K [35,36].

2.6.6 Quantum efficiency

The efficiency of a phosphor is considered to be of prime importance before involving it in the fabrication of an LED device. Sometimes, those phosphors that show unmatched efficiency out of the package can be slightly inefficient within the LED package. Hence, different terminologies were stated to describe the phosphor efficiency in different stages of fabrication. The term quantum efficiency or the quantum yield is often used to describe the phosphor's efficiency. Quantum yield can be defined as the ratio of the number of photons emitted to the number of photons absorbed by the phosphor. On the other hand, the efficiency of an LED chip is expressed in terms of the external quantum efficiency (EQE). This term signifies the efficiency of the chip to convert the electrons into photons. Precisely, it can be defined as the ratio of the number of photons emitted from the LED to the number of electrons passing through the device. An EQE of an LED depends upon the injection efficiency, internal quantum efficiency, and extraction efficiency by the following relation:

$$\text{External Quantum Efficiency} = [\text{Internal Quantum Efficiency}] \times [\text{Injection Efficiency}] \times [\text{Extraction Efficiency}]$$

The electrons injected into the active region of the LED chip are required to tunnel through the device to undergo electron−hole recombination for producing photons. The ratio of the number of electrons passing through the device to the number of electrons injected into the active region gives the injection efficiency. Nevertheless, it is not necessary that all the electron-hole recombinations will lead to the generation of photons. Those that can produce electrons are known as radiative recombinations. The ratio of all the radiative electron−hole recombinations in the active region to the total number of recombinations occurring between the electron−hole pairs is known as the internal quantum efficiency or the radiative efficiency. The photons, which are produced from the radiative electron−hole recombinations in the active region, escape from the LED chip. The proportion of such photons produced in the active region and that are able to escape from the device is called extraction efficiency.

The energy conversion efficiency of a device that is required in converting the electrical power into optical power is called the wall-plug efficiency or radiant efficiency of the device. The optical output power is the radiant flux output of the device, which is measured in watts. The radiant efficiency can be correlated to the external quantum efficiency by the following relation:

$$\text{Wall} - \text{Plug Efficiency} = [\text{External Quantum Efficiency}] \times [\text{Feeding Efficiency}]$$

where the feeding efficiency is defined as the ratio of the mean energy of photons emitted by the device to the total energy acquired by the electron−hole pair from the power source.

2.6.7 Life span

Despite being hailed as the most energy-efficient and long-lasting lighting, LEDs fail to complete its life span with full performance. It is observed that LED luminaires do not burn out completely, rather they start dimming over time and continue its operation with reduced lumen output. Every lamp has a critical point at which the lumen output undergoes depreciation by 30%. This point is rated as the lifespan of the luminaire. Thus, an LED luminaire will continue to illuminate, even after reaching its stipulated lifespan of 1,00,000 hours but with a lower lumen output. However, it is observed that some LED luminaires completely fail to operate before reaching its lifespan. In such cases, external factors such as the operating voltage, operating temperature, manufacturing defects, exposure to voltage spikes, mechanical shocks, and vibrations are responsible for the degradation of luminaires. Failure of the heat-sink inside the LED package also forms a major factor responsible for the breakdown of the LED luminaire. Even though the luminaire has a high-quality LED chip and phosphor to boast, it may not withstand the high operating temperatures and could breakdown very early in the absence of a decent-quality heat-sink. The electronic circuit in the device also forms an integral part of the LED package. Ignoring the complexities associated with the device electronics, the lifespan of an LED luminaire can be extended by operating under ambient conditions where it can cool down easily.

Another cause that leads to LED failure is the degradation of phosphor or yellowing of the epoxy resin. There is degradation or discoloration of epoxy resins after repeated exposures to high operating temperatures and radiations. An instance of the yellowing of epoxy resin can be seen in Fig. 2.8 [37]. In some cases, white LEDs (WLEDs) employ blending of tricolor (red, green, blue or *simply* RGB) phosphors or chips to produce white light of desired color temperature. In such cases, the degradation of each of the phosphor or chip is different from one another. As a result, there is a significant change in the color output of the WLEDs after a certain period of operation [38]. This has inspired researchers to work on single-phased materials that can emit white light by absorbing the near-UV radiations from the LED chip. To some extent, this will certainly be a solution to the problems discovered in tricolor WLEDs.

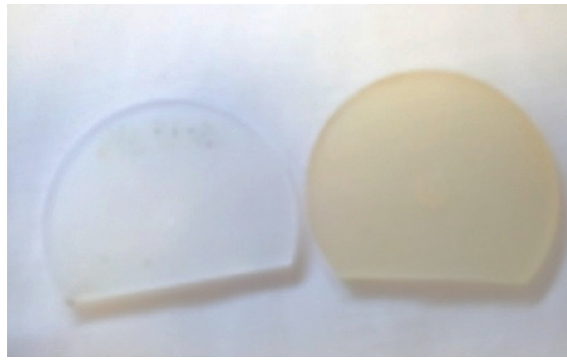

Figure 2.8 Yellowing of the epoxy resin.
Reproduced from M. Yazdan Mehr, W.D. van Driel, G.Q. (Kouchi) Zhang, Progress in understanding color maintenance in solid-state lighting systems, Engineering 1 (2015) 170−178. https://doi.org/10.15302/J-ENG-2015035, under Creative Commons Attribution License.

2.7 Concluding remarks

LEDs have proved itself as the most trustworthy and artificial lighting source that is blessed with loads of advantages. It scores above all when it comes to the matter of environmental safety. The integration of semiconductor light-emitting chips with the insulating/semiconducting phosphors facilitated the production of light of almost any color. Close inspection is necessary to ensure that the quality of the materials used in the LED package is of top class to achieve extended lifespan and better lumen output from the package.

References

[1] N. Holonyak Jr., Is the light emitting diode (LED) an ultimate lamp? Am. J. Phys. 68 (2000) 864−866, https://doi.org/10.1119/1.1301966.
[2] J.I. Pankove, Optical absoption of GaN, Appl. Phys. Lett. 17 (1970) 197, https://doi.org/10.1063/1.1653363.
[3] J.I. Pankove, J.E. Berkeyheiser, E.A. Miller, Properties of Zn-doped GaN. I. Photoluminescence, J. Appl. Phys. 45 (1974) 1280, https://doi.org/10.1063/1.1663402.
[4] Y. Zhao, S. Tanaka, C.C. Pan, K. Fujito, D. Feezell, J.S. Speck, S.P. DenBaars, S. Nakamura, High-power blue-violet semipolar (2021) InGaN/GaN light-emitting diodes with low efficiency droop at 200 A/cm^2, Appl. Phys. Express 4 (2011) 2−5, https://doi.org/10.1143/APEX.4.082104.
[5] H. Masui, H. Yamada, K. Iso, S. Nakamura, S.P. DenBaars, Optical polarization characteristics of *m*-oriented InGaN/GaN light-emitting diodes with various indium compositions in single-quantum-well structure, J. Phys. D Appl. Phys. 41 (2008) 225104, https://doi.org/10.1088/0022-3727/41/22/225104.
[6] S. Nakamura, InGaN/AlGaN blue-light-emitting diodes, J. Vac. Sci. Technol. A 13 (1995) 705, https://doi.org/10.1116/1.579811.

[7] K. Iida, T. Kawashima, A. Miyazaki, H. Kasugai, S. Mishima, A. Honshio, Y. Miyake, M. Iwaya, S. Kamiyama, H. Amano, I. Akasaki, 350.9 nm UV laser diode grown on low-dislocation-density AlGaN, Jpn J. Appl. Phys. 43 (2) (2004) L499−L500, https://doi.org/10.1143/JJAP.43.L499.
[8] A.A. Setlur, Phosphors for LED-based solid-state lighting, Electrochem. Soc. Interfac. 18 (2009) 32−36.
[9] R.J. Keyes, T.M. Quist, Recombination radiation emitted by gallium arsenide, Proc. IRE. 50 (1962) 1822−1823, https://doi.org/10.1016/B978-1-55860-737-8.50028-4.
[10] S. Nakamura, M. Senoh, T. Mukai, P-GaN/N-InGaN/N-GaN double-heterostructure blue-light-emitting diodes, Jpn. J. Appl. Phys. 32 (1993) L8−L11, https://doi.org/10.1143/JJAP.32.L8.
[11] H. Round, A note on carborundum, Electr. World 49 (1907) 309−310.
[12] H.P. Maruska, J.J. Tietjen, The preparation and properties of vapor-deposited single-crystal-line GaN, Appl. Phys. Lett. 15 (1969) 327−329, https://doi.org/10.1063/1.1652845.
[13] W.-J. Liu, X.-L. Hu, Y.-J. Liu, Performance enhancement of GaN-based near-ultraviolet flip-chip light-emitting diodes with two-step insulating layer scheme on patterned sapphire substrate, J. Mater. Sci. Mater. Electron. (2019), https://doi.org/10.1007/s10854-018-00580-7.
[14] C.-Y. Cho, K.-H. Park, S.-J. Park, Enhanced optical output power of blue light-emitting diode grown on sapphire substrate with patterned distributed Bragg reflector, ECS J. Solid State Sci. Technol. 7 (2018) Q66−Q69, https://doi.org/10.1149/2.0161804jss.
[15] Y. Xu, J. Zou, X. Lin, W. Wu, W. Li, B. Yang, M. Shi, Quality-improved GaN epitaxial layers grown on striped patterned sapphire substrates ablated by femtosecond laser, Appl. Sci. 8 (2018) 1842, https://doi.org/10.3390/app8101842.
[16] J.I. Pankove, Properties of Zn-doped GaN. II. Photoconductivity, J. Appl. Phys. 45 (1974) 3892, https://doi.org/10.1063/1.1663881.
[17] J.I. Pankove, E.A. Miller, D. Richman, J.E. Berkeyheiser, Electroluminescence in GaN, J. Lumin. 4 (1971) 63−66, https://doi.org/10.1016/0022-2313(71)90009-3.
[18] J.I. Pankove, E.A. Miller, J.E. Berkeyheiser, GaN blue light-emitting diodes, J. Lumin. 5 (1972) 84−86, https://doi.org/10.1016/0022-2313(72)90038-5.
[19] H.P. Maruska, W.C. Rhines, D.A. Stevenson, Preparation of Mg-doped GaN diodes exhibiting violet electroluminescence, Mater. Res. Bull. 7 (1972) 777−781, https://doi.org/10.1016/0025-5408(72)90127-4.
[20] H. Amano, M. Kito, K. Hiramatsu, I. Akasaki, P-type conduction in Mg-doped GaN treated with low-energy electron beam irradiation (LEEBI), Jpn. J. Appl. Phys. 28 (1989) L2112−L2114, https://doi.org/10.1143/JJAP.28.L2112.
[21] S. Nakamura, T. Mukai, M. Senoh, N. Iwasa, Thermal annealing effects on P-type Mg-doped GaN films, Jpn. J. Appl. Phys. 139 (1992) L139−L142, https://doi.org/10.1143/JJAP.31.L139.
[22] S. Nakamura, N. Iwasa, M. Senoh, T. Mukai, Hole compensation mechanism of p-type GaN films, Jpn. J. Appl. Phys. 31 (1992) 1258−1266, https://doi.org/10.1143/JJAP.31.1258.
[23] K.L. Suk, H.Y. Son, C.K. Chung, J. Do Kim, J.W. Lee, K.W. Paik, Flexible Chip-on-Flex (COF) and embedded Chip-in-Flex (CIF) packages by applying wafer level package (WLP) technology using anisotropic conductive films (ACFs), Microelectron. Reliab. 52 (2012) 225−234, https://doi.org/10.1016/j.microrel.2011.08.003.
[24] J. Brgoch, S.P. Denbaars, R. Seshadri, Proxies from Ab initio calculations for screening efficient Ce^{3+} phosphor hosts, J. Phys. Chem. C 117 (2013) 17955−17959, https://doi.org/10.1021/jp405858e.
[25] J. McKittrick, L.E. Shea-Rohwer, Review: down conversion materials for solid-state lighting, J. Am. Ceram. Soc. 97 (2014) 1327−1352, https://doi.org/10.1111/jace.12943.

[26] L.-B. Chang, K.-W. Pan, C.-Y. Yen, M.-J. Jeng, C.-T. Wu, S.-C. Hu, Y.-K. Kuo, Comparison of silicone and spin-on glass packaging materials for light-emitting diode encapsulation, Thin Solid Films 570 (2014) 496−499, https://doi.org/10.1016/j.tsf.2014.03.033.
[27] Z. Gao, Y. Zhang, Y. Fu, M.M.F. Yuen, J. Liu, Thermal chemical vapor deposition grown graphene heat spreader for thermal management of hot spots, Carbon N. Y. 61 (2013) 342−348, https://doi.org/10.1016/j.carbon.2013.05.014.
[28] Q. Shao, H. Lin, Y. Dong, J. Jiang, Temperature-dependent photoluminescence properties of $(Ba,Sr)_2SiO_4:Eu^{2+}$ phosphors for white LEDs applications, J. Lumin. 151 (2014) 165−169, https://doi.org/10.1016/j.jlumin.2011.01.013.
[29] Z. Xia, X. Wang, Y. Wang, L. Liao, X. Jing, Synthesis, structure, and thermally stable luminescence of Eu^{2+} -doped $Ba_2Ln(BO_3)_2$ Cl (Ln = Y, Gd and Lu) host compounds, Inorg. Chem. 50 (2011) 10134−10142, https://doi.org/10.1021/ic200988w.
[30] T. Pulli, T. Dönsberg, T. Poikonen, F. Manoocheri, P. Kärhä, E. Ikonen, Advantages of white LED lamps and new detector technology in photometry, Light Sci. Appl. 4 (2015) e332, https://doi.org/10.1038/lsa.2015.105.
[31] C. Bois, P. Bodrogi, T. Khanh, H. Winkler, Measuring, simulating and optimizing current LED phosphor systems to enhance the visual quality of lighting, J. Solid State Light. 1 (2014) 5, https://doi.org/10.1186/2196-1107-1-5.
[32] H. Yaguchi, A. David, T. Fuchida, K. Hashimoto, G. Heidel, W. Jordan, S. Jost-Boissard, S. Kobayashi, T. Kotani, R. Luo, Y. Mizokami, Y. Ohno, P. Pardo, K. Richter, K. Smet, K.N. Teunissen, A. Tsukitani, M. Wei, L. Whitehead, T. Yano, CIE 2017 Colour Fidelity Index for Accurate Scientific Use, CIE Central Bureau, Jeju Island, 2017.
[33] W.D. Wright, A re-determination of the trichromatic coefficients of the spectral colours, Trans. Opt. Soc. 30 (1929) 141−164, https://doi.org/10.1088/1475-4878/30/4/301.
[34] J. Guild, The colorimetric properties of the spectrum, Philos. Trans. R. Soc. A Math. Phys. Eng. Sci. 230 (1932) 149−187, https://doi.org/10.1098/rsta.1932.0005.
[35] J. Zhang, Z. Hua, F. Zhang, Warm white-light generation in $Ca_9MgNa(PO_4)_7:Sr^{2+}$, Mn^{2+}, Ln (Ln=Eu^{2+}, Yb^{3+}, Er^{3+}, Ho^{3+}, and Tm^{3+}) under near-ultraviolet and near-infrared excitation, Ceram. Int. 41 (2015) 9910−9915, https://doi.org/10.1016/j.ceramint.2015.04.068.
[36] C.H. Huang, T.M. Chen, W.R. Liu, Y.C. Chiu, Y.T. Yeh, S.M. Jang, A single-phased emission-tunable phosphor $Ca_9Y(PO_4)_7:Eu^{2+},Mn^{2+}$ with efficient energy transfer for white-light-emitting diodes, ACS Appl. Mater. Interface. 2 (2010) 259−264, https://doi.org/10.1021/am900668r.
[37] M. Yazdan Mehr, W.D. van Driel, G.Q. (Kouchi) Zhang, Progress in understanding color maintenance in solid-state lighting systems, Engineering 1 (2015) 170−178, https://doi.org/10.15302/J-ENG-2015035.
[38] G.B. Nair, S.J. Dhoble, A perspective perception on the applications of light-emitting diodes, Luminescence 30 (2015) 1167−1175, https://doi.org/10.1002/bio.2919.
[39] G.B. Nair, H.C. Swart, S.J. Dhoble, A review on the advancements in phosphor-converted lightemitting diodes (pc-LEDs): Phosphor synthesis, device fabrication and characterization, Progress in Materials Science 109 (2020) 100622, https://doi.org/10.1016/j.pmatsci.2019.100622.

Part Two

Materials

Semiconductor LEDs

3

3.1 Introduction

The progress made by the semiconductor physics paved way for the emergence of solid-state lighting (SSL) that brought about a revolution in the lighting industry. SSL devices consists of light-emitting diodes (LEDs) working on the inorganic and the organic materials. The onset of LEDs came with the introduction of certain semiconductor materials that produced luminescence on passing an electric current through it. It was also observed that such phenomenon was observed typically for the semiconductor materials based on group III−V elements. Although LEDs have progressed way ahead, their initial days completely relied on semiconductor materials, and they still form the crux of an LED luminaire that is commercially available for lighting. At present, there are several variants of LEDs available that are based on organic materials, quantum dots, metalorganic perovskites, or inorganic phosphors, but each has their own merits and limitations. Also, the device architecture and the working mechanism for each of these variants are different from the originally proposed semiconductor LEDs. But the dominance of semiconductor LEDs in the commercial market makes it a good deal to discuss the concepts and background of semiconductor materials used for LEDs.

As discussed in the previous chapter, LEDs are constructed from the conjunction of very thin layers of p-type and n-type semiconductor materials. The p-type layer has a deficit of electrons, whereas the n-type layer has an excess of electrons. These layers can be as thin as half a micron or less than that. The p-type and n-type layers are created by intentionally doping a trivalent and a pentavalent impurity, respectively, in an intrinsic semiconductor. This helps in achieving the required hole and electron densities in the two respective layers, thereby enabling the semiconductor material to conduct electricity. The manufacturing of an LED chip can be divided into four stages: (1) preparing semiconductor wafers for substrate, (2) growing epitaxial layers over the wafers, (3) defining metal contacts on the wafer, and (4) mounting and packaging of the semiconductor dies. Depending on the color of the LED being fabricated, the composition of the semiconductor wafer for the substrate is decided. These wafers must have uniform composition and must be free of any imperfections. This is one of the essential conditions to achieve fault-free deposition or growth of epitaxial layers over the wafers and, thereby, ensure a smooth and efficient LED device construction. In the subsequent sections, there shall be discussion over the various growth techniques employed to grow epitaxial layers of semiconductor crystals over the surface of the wafer. We shall also briefly report some of the semiconductor material compositions that are commonly used in LED packages.

The Fundamentals and Applications of Light-Emitting Diodes. https://doi.org/10.1016/B978-0-12-819605-2.00003-3

3.2 Growth techniques

Epitaxial growth techniques are the most widely adopted methods for the growth of layers or thin films of materials for optical, electronic, microelectronics, photonics, magneto-optical, and optoelectronic applications. Epitaxy is a process in which a thin layer of a crystalline material is grown on a crystalline substrate, and the grown layers are known as epitaxial layers or epitaxial films. The epitaxial layers have a well-defined orientation with respect to the crystalline substrate. The orientation of the crystalline substrate controls the orientation of the epitaxial layer. Each of the new epitaxial layers grown over the substrate shall have only single-crystalline orientation and shall not have polycrystalline growth with any random orientation or amorphous growth. Depending on the composition of the substrate and the epitaxial layers, epitaxy can be classified as homoepitaxy, heteroepitaxy, homotopotaxy, heterotopotaxy, and pendeoepitaxy. When the multiple epitaxial layers of the same composition are grown over the substrate, the process is termed as homoepitaxy [1]. If the epitaxial layers of different materials are grown on the substrate, then the process is termed as heteroepitaxy [2]. Homotopotaxy and heterotopotaxy are processes similar to homoepitaxy and heteroepitaxy, respectively, with the exception that the growth of thin films is not restricted to two-dimensional growth [3]. In pendeoepitaxy, the heteroepitaxial growth is allowed to occur simultaneously both laterally and vertically [4].

Epitaxial growth can be achieved by any of the methods such as liquid-phase epitaxy (LPE), vapor-phase epitaxy (VPE), molecular beam epitaxy (MBE), metal−organic chemical vapor deposition (MOCVD), and so on. However, none of the growth techniques can satisfy the requirements of all the materials meant for magnetic devices, magneto-optical devices, optoelectronics, photovoltaics, microelectronics, microelectrochemical systems, electrochemical devices, semiconductor devices, thermoelectrics, or thermophotovoltaics. The selection of epitaxial growth technology is usually made as per the material system, which is to be grown, and the device application, for which the material is required. The choice of growth technique also takes into account the basic principles of chemical kinetics, thermodynamics, surface energies, etc. as well as the practical concerns regarding the infrastructure costs, process control, reproducibility, scalability, and instrumentation safety.

3.2.1 Liquid-phase epitaxy

LPE is a high-temperature solution growth method for growing layers of semiconductor crystals by depositing thin layers of required material from the melt or a solution onto a suitable solid substrate. The very first LPE systems were considered to be developed by Nelson for producing multilayer semiconducting structures for tunnel and laser diodes [5]. Thereafter, the technology extended for the development of semiconductor materials belonging to III−V group for LEDs, lasers, photovoltaic cells, and photodiode applications. This technique found applications in the development of a large number of materials for diverse applications. These include materials for ferroelectric, magnetic, optical, and superconductivity applications.

When compared with other epitaxial techniques involving vapor phase, the growth process in the LPE technique is characterized as a near-equilibrium one [6]. There are several advantages of using LPE technique. LPE is highly favorable for the growth of thick layers of semiconductors owing to their very high growth rates. LPE is 10−100 times faster than other VPE methods. Additionally, the expenses pertaining to the infrastructure setup and operation costs of LPE are much lower than the vapor-phase techniques. The segregation of impurities into the liquid phase is favorably achieved in LPE, which also leads to much lower probability of the residual or background impurities from appearing in the epitaxial layers. The structural perfection of the materials prepared by LPE is highly excellent. The substrates prepared by this method would have very flat surface and lower point defects. There is no involvement of toxic precursors during the growth or formation of toxic by-products in this technique. The material growth can be carried out in a wide range of temperatures after establishing an appropriate phase diagram. This technique also has the advantage of involving a wide range of materials unlike vapor-phase techniques, wherein major precautions must be taken in the growth kinetics while developing materials from volatile precursors. On the other hand, most of the liquids or solids can be incorporated within the layers or added directly to the melt in LPE. However, there are some disadvantages associated with this method. There are complications while attempting for abrupt interfaces between successive layers within the structures. The poor reproducibility of the materials grown by the LPE technique and the difficulty in scaling up the quantity/yield further add to the woes. The difficulties also arise while controlling the doping concentrations, alloy compositions, thickness of the layers, and the smoothness between the interfaces.

LPE involves bringing the substrate in contact with the melt or the growth solution and facilitating the growth of the epitaxial layer over the substrate. After the required amount of growth is achieved, the epitaxial layer grown over the substrate must be cleanly separated from the solution. The deposition of the layer on the substrate is driven by the supersaturation in the growth solution. Two-phase growth, transient growth, constant-temperature growth, step cooling, ramp cooling, supercooled growth, or electroepitaxy can contribute in the occurrence of supersaturation [6]. The composition and requirements of the material to be grown decide the choice of the method among the aforementioned ones to initiate the supersaturation. There are three manifestations of the LPE technique which are realized in the form of tipping, dipping, and sliding boat. A simplified illustration of the three LPE arrangements can be visualized from Fig. 3.1. The dipping method is usually considered to grow structures from Hg-rich melt [7]. More than 90% of the growth solutions comprise Hg, and the vapor pressure of Hg has a significant role in the design and operation of the dipping furnace. The growth solution or the melt is held in a pot carefully installed in a vertical high-pressure furnace. The pot is positioned at the center of the furnace where the temperature is optimum enough to maintain the melt form. These systems can hold about 10−20 kg of melt at 550°C without any degradation of its integrity or purity for several years [6]. In the sliding boat approach, the substrate is positioned in a cavity in a slider [8]. The slider is supported by a base section. In the upper section of the boat, the growth solution is held in the wells. The push rod arrangement can be

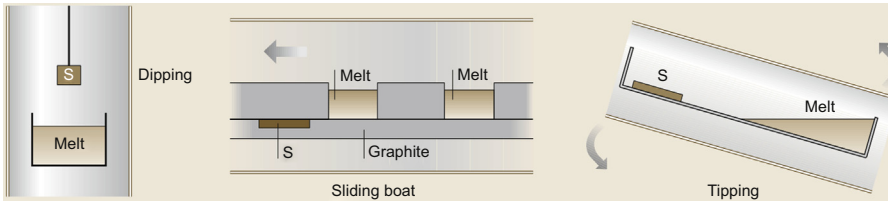

Figure 3.1 The dipping, sliding boat, and tipping arrangements used in the LPE technique. *LPE*, liquid-phase epitaxy.
Reproduced with permission from P. Capper, S. Irvine, T. Joyce, Epitaxial crystal growth: methods and materials, in: Springer Handb. Electron. Photonic Mater., Springer, Berlin, Heidelberg, 2006: pp. 271−301. https://doi.org/10.1007/978-0-387-29185-7_14, Copyright 2017.

used to reposition the wells over the substrate. The gap between the bottom of the top section and the top of the grown layer can be controlled using a wipe-off, which is featured in the critical design of the boat. If the gap is too small, the grown layer will bear scratches. On the other hand, if the gap is too large, the layer will retain some melt over it. If the retention of the melt over the layer is kept minimum, then multilayer growth can be possible using the sliding boat method. When the melt is thin, the edge growth can be constrained due to the suppression of the thermal convection. Scaling-up can also be achieved by incorporating several substrates in a single run. In a tipping arrangement, a boat is placed in a work tube, which is kept in the center of a tilted furnace [5]. The boat is, generally, made from graphite or silica. The boat is arranged in such a way that one end of the boat carries the substrate and the other end carries the growth solution/melt. After the equilibration of the melt, the temperature is gradually decreased, and the furnace is tilted to bring the solution over the substrate. After an appropriate period, the boat is tilted back to the initial position so that the solution flows off from the grown layer over the substrate. The tipping approach is relatively cheap and simple method. However, the technique is suitable only for the growth of single layers due to the difficulty experienced during the removal of solution from the grown layer. Among the three approaches, the sliding boat technique is the most versatile and popular one [8].

3.2.2 Vapor-phase epitaxy

VPE growth method can be considered as a manifestation of the chemical vapor deposition (CVD), which is widely used for the growth of thin films. This method is suitable for even those materials, which cannot be grown using LPE. For instance, silicon cannot be dissolved in some liquid easily, and hence, LPE is not a suitable process for them. But silicon can be considered to be grown using VPE. The working principle of VPE is relatively simple and can handle growth of multiple large wafers. It also allows flexibility during the growth process, which includes the type of doping, concentration levels of dopant, etc. VPE is essentially employed in the microelectronics industry to grow very good-quality epitaxial layers of the III−V semiconductors such as InGaAsP, InP, GaAsP, GaAs, GaP, and so on [9]. Its major advantage is

the scope to achieve higher growth rates (μm/min) for the epitaxial growth, which also forms the reason for its extensive usage in the industry. It is crucial to deploy proper equipment to ensure high-quality yield through the VPE growth.

In VPE, the material transport is in the form of vapors, and hence, the precursors are in the gaseous form. In principle, the gas precursors above the substrate are dissociated by providing them with enough energy, and then, they are deposited onto the substrate with uniform arrangement of atoms on its surface. A general experimental setup consists of a sample holder, wherein the sample is loaded and a gas is allowed to flow over the sample. On certain occasions, a liquid with very high vapor pressure is used that can be easily vaporized. The reactants are carried through this gas flow, which is controlled by the mass flow controllers. When the gas flows over the sample, the reactants are deposited on top of the samples. In the vicinity of the sample, the reactants in the gas may decompose or dissociate to react with the sample. The gas species undergo adsorption on the surface of the sample substrate. The species are, then, diffused into the preferential sites of the substrate. They undergo chemical decomposition to get incorporated into the lattice of the epitaxial film. The secondary products, thus, formed during these processes undergo desorption and are diffused away from the surface. This method can be carried out by various means, and they are classified depending upon the type of reactor equipped for the deposition as well as the energy supplied for the vaporization in the chamber. The major requirements for a basic epitaxial reactor are as follows:

(i) A reactor tube or a chamber: To carry out the epitaxial growth in an isolated environment.
(ii) Distribution system: To initiate a controlled distribution of the chemical species for the epitaxial growth.
(iii) Heating system: To initiate heating of wafers.
(iv) Cleaning system: To diffuse away the secondary products and scrub off the effluent gases from the epitaxial layer.

High-temperature CVD systems are used as epitaxial reactors for VPE. These reactors can either be a hot-walled reactor or a cold-walled reactor. The heating system can be either RF heating or resistance heating. RF heating is preferred for cold-walled reactors, whereas resistance heating gives rise to hot-walled reactors. When the deposition reaction is exothermic in nature, hot-walled reactors are preferred. On the contrary, cold-walled reactors are preferred to carry out depositions that are endothermic in nature. Since the reactor wall is cold, the deposition of the contaminants is more likely to be on the walls of the reactor. On the other hand, if the walls are hot, the contaminants can get deposited on the sample itself. The top layer of the wafer substrate is more prone to contamination, and if the epitaxial layer is grown on this surface, the quality of the grown layer will be inferior. Also, the devices fabricated using such layers will show degraded performance. Consequently, cold-walled reactors are preferred over hot-walled ones for most depositions. There is provision for in situ cleaning in the chamber so that the sample can be cleaned before the epitaxial growth without taking the sample out of the chamber. The growth and the deposition takes place at atmospheric pressure and at low pressure in the atmospheric pressure chemical vapor deposition (APCVD) and the low-pressure chemical vapor deposition (LPCVD),

respectively. The gas filling speed is higher in APCVD than in LPCVD. Yet, heating in both the types of reactors is provided by the magnetic induction or the Joule's heating effect. Another type of VPE is the rapid thermal chemical vapor deposition (RTCVD), wherein the heating is provided by halogen lamps. There is another type of reactor that operates at low temperatures by providing energy through a plasma discharge. This type is known as plasma enhancement CVD (PECVD). In all these manifestations of VPE, there are several stages of the growth kinetics that consists of two categories: (1) transportation of the chemicals and (2) surface chemical reactions [9].

The configuration of the reactor can be either, horizontal, vertical, or barrel-shaped. The horizontal reactor, as illustrated in Fig. 3.2, is the simplest among them [10]. The costs surrounding the construction of this reactor are very less. It consists of a horizontal quartz tube in which wafers are horizontally positioned on a graphite susceptor. The susceptor is coupled with RF coil to provide heating to the wafer. There is a gas inlet at one end of the tube to allow the gases necessary for the epitaxial growth to flow in the tube. The gas exhausts from the outlet provided at the other end of the tube. The gas is allowed to flow parallel to the substrate surface, and the necessary reactants are carried by the gas. The gas flow supplies the reactant species to the growth interface of the wafer. However, there are difficulties faced in controlling the growth over the entire susceptor. Some other limitations experienced in this reactor are the difficulties in achieving appropriate temperature, layer thickness, and uniformity in the doping levels within the wafer [9]. The horizontal reactor got its name due to the horizontal flow of the gas through the tube. Similarly, vertical reactor got its name due to the fact that the gas flow is in a direction normal to the surface of the sample. But the design of a vertical reactor is more complex than the horizontal reactor. Also, not many samples can be loaded at a time in this type of reactor. A schematic representation of the vertical VPE reactor is shown in Fig. 3.3.

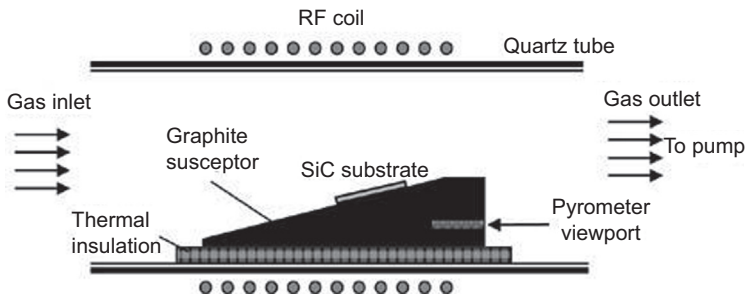

Figure 3.2 Schematic representation of the cold-walled horizontal VPE reactor for the epitaxial growth of SiC. *VPE*, vapor-phase epitaxy.
Reproduced with permission from A. Schöner, New development in hot wall vapor phase epitaxial growth of silicon carbide, in: W.J. Choyke, H. Matsunami, G. Pensl (Eds.), Silicon Carbide. Adv. Texts Phys., Springer, Berlin, Heidelberg, 2004: pp. 229−250. doi:10.1007/978-3-642-18870-1_10, Copyright 2004.

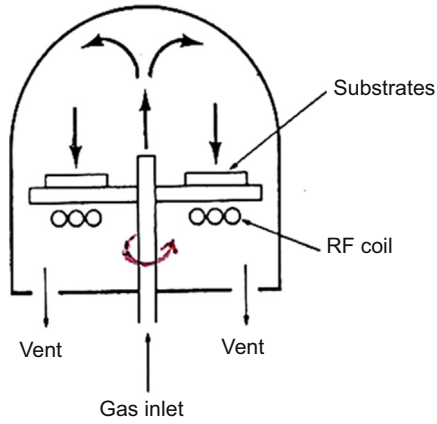

Figure 3.3 Schematic representation of a vertical VPE reactor. *VPE*, vapor-phase epitaxy.

A vertical VPE reactor working at atmospheric pressure consists of the SiC-coated graphite susceptor on which the wafers are positioned. Similar to horizontal reactor, the susceptor is coupled with RF coils to provide heating. Frequencies ranging from few kHz to few hundreds of kHz are used for achieving temperatures between 1000 and 1200 $^{\circ}$C by RF heating. The gas containing the reactant species is entered through the center of the circular susceptor. The gases rise towards the top of the reactor and spread downward. The gases flow evenly across the wafers and then proceed to exit from the outlet at the bottom. Any nonuniformity in the gas flow is smoothened by the rotation of the susceptor. This aids in achieving uniformity in the doping and good thickness of the grown layer. Vertical reactors can operate at both atmospheric pressures and low pressures. The third type of the reactor is the barrel-shaped reactor that is preferably used for mass-production and better throughput. In this type, the reactor is shaped like a barrel or a drum on which several small grooves are carved out to position the samples in them. Each of the grooves can hold a single whole wafer. Such type of system is suitable to support the mass-production. The barrel can be rotated for achieving better and uniform deposition. Similar to horizontal reactor, the gas flows parallel to the sample-surface in the barrel reactor. A barrel reactor can accommodate large quantities of samples at the same time, as opposed to the other two versions of the VPE reactor. A schematic representation of the barrel-shaped reactor is shown in Fig. 3.4.

3.2.3 Molecular beam epitaxy

MBE is a popularly used epitaxy method for the thin-film deposition of semiconductor materials. This method was first observed by Arthur and LePore in 1969 while growing the epitaxial films of GaAs, GaP, and $GaAs_xP_{1-x}$ in the Bell Telephone Laboratories [11]. Subsequently, this method caught the attention of Cho, who then closely studied and described it in detail [12]. The foundation for this method was laid down

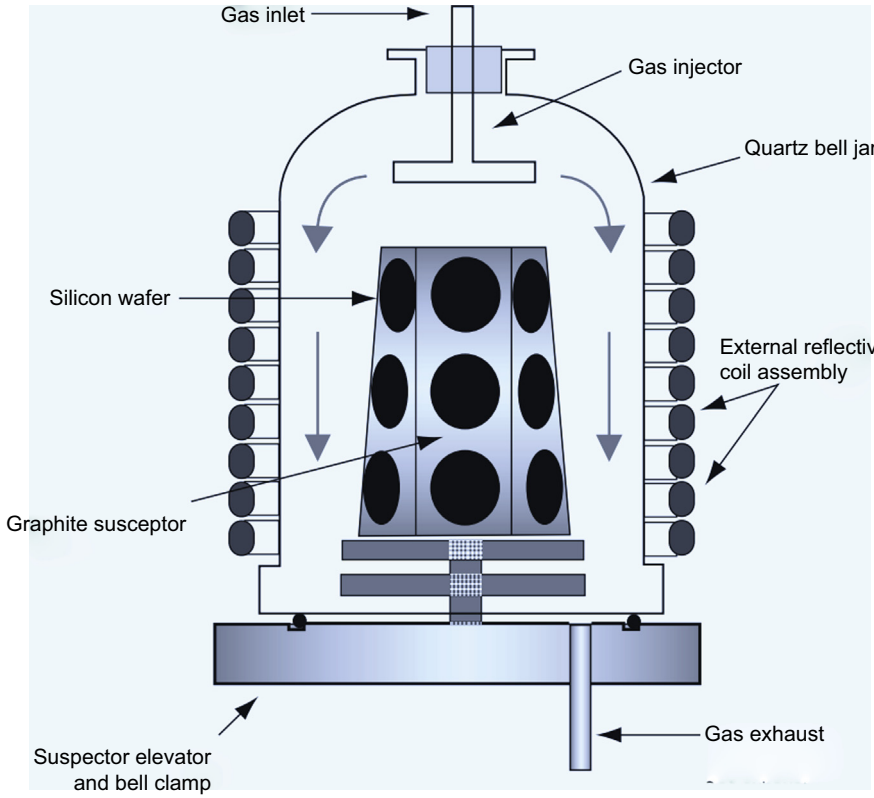

Figure 3.4 Schematic representation of a barrel-shaped VPE reactor. *VPE*, vapor-phase epitaxy. Reproduced with permission from M. Lemiti, Vapor phase epitaxy, in: K. Nakajima, N. Usami (Eds.), Cryst. Growth Si Sol. Cells. Adv. Mater. Res., Berlin, Heidelberg, 2009: pp. 159−175. https://doi.org/10.1007/978-3-642-02044-5_10, Copyright 2009.

on the basis of the studies conducted on the surface kinetics of silane (SiH_4) beam with the silicon substrate [13], as well as Ga and As_2 beam with GaAs substrate [14]. The earlier versions of MBE took long periods of system pumpdown between the growths. This is particularly because the system consisted of only a single vacuum chamber for the loading, deposition, and analysis. This put a bar on the growth of very high-quality thin film using MBE. In 1971, Cho reported the growth of p- and n-type GaAs thin films for devices using MBE method [15]. For this purpose, he provided thermal insulation to the system by surrounding the effusion cells with a liquid nitrogen cryopanel. MBE can be used to achieve atomic (or molecular) layer-by-layer deposition with controlled thickness. The epitaxial layers are grown by the reaction of neutral atomic or molecular beam with the heated crystalline substrate in an ultrahigh-vacuum (UHV) environment. Due to unidirectional nature, the beams do not show any interaction between or within them. Hence, the growth is only influenced by the beam fluxes and the surface reactions. This forms the reason that the structures grown by this method grant

reproducibility and unrivalled control over the layer thickness, alloy compositions, and uniformity in the doping levels. The beams directly interact with the substrate giving rise to the desired epitaxial layers. The reaction of the molecular beam with the substrate follows the reaction kinetics such as incorporation, adsorption, dissociation, and migration. MBE shares some similarities with the vapor deposition technique, but it shows some advanced and superior features such as the use of UHV environment [16]. UHV environment provides highly pure and dust-free epitaxial layers. Heterostructured semiconductors with high purity and precise control of doping (particle size in the nanometre scale) can be achieved by this method, as it relies on the reaction kinetics that can be controlled accurately. This also leads to bandgap engineering of the semiconductor materials. Though the method seems to be very beneficial over other methods, experimental setup for MBE is very challenging, especially when achieving the UHV environment is a major task. Yet, majority of the semiconductor LED chips are grown using the MBE method and this includes the III-nitride materials such as AlGaN. AlGaN LED emits light in UV region in the wavelengths ranging from 280 to 400 nm [17]. The UV-emitting AlGaN chips are technologically very important class of LED materials. MBE techniques can be used for the growth of LED materials belonging to the II−IV group such as MgZnSSe/ZnSSe/CdZnSe [18].

Fig. 3.5 shows a schematic representation of an MBE system. [19] The system consists of a growth chamber with UHV environment, a gas handling system, Knudsen

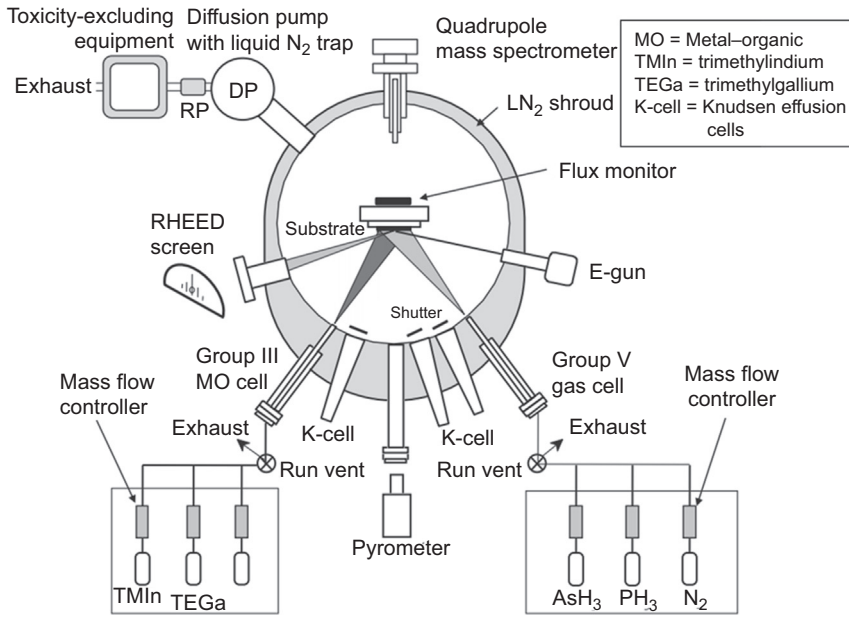

Figure 3.5 Schematic representation of a molecular beam epitaxy system with gaseous sources. Reproduced with permission from H. Asahi, Molecular beam epitaxy with gaseous sources, in: Handb. Cryst. Growth, Elsevier, 2015: pp. 193−224. https://doi.org/10.1016/B978-0-444-63304-0.00005-6, Copyright 2015.

effusion cells, a sample holding chamber, and RHEED (reflection high-energy electron diffraction) system. Knudsen effusion cells are specially designed for the MBE method. They are endowed with the heating system and a fast action refractory metal shutter for each of the cells. The operation of the shutters is either pneumatic or solenoid. They evaporate the material (Ga, As_2, etc.), which is to be deposited as a thin film, by converting it to a molecular beam, and allow the beam to fall on the crystalline substrate (Si, Ge, or GaAs). The amount of material deposition can be controlled with the help of shutter. The substrate can be positioned in the substrate holder, which can rotate and heat the substrate. The RHEED system consists of a RHEED gun and a RHEED screen. It performs the in-situ characterization of the thin film deposited on the substrate. The RHEED gun emits an electron beam at a very low angle with respect to the substrate. This electron beam, after diffraction from the substrate, falls on the RHEED screen. The diffracted pattern reveals the information about the surface of the film and the thickness down the single layer. The growth of the thin film is continuously monitored by the RHEED system by which the growth of the layer can be controlled. Prior to growth, the cleanliness of the surface is confirmed through the RHEED system. In this method, formation of the epitaxial layer is done very slowly and gradually. Although this method is having merits of developing high-purity, thin, and complex epitaxial layers, it is very slow and laborious method. The operational setup is expensive as it requires UHV environment, and hence, the method is suitable for laboratory research only. The UHV system is generally constructed by stainless steel. The ultimate vacuum of the system is less than 5×10^{-11} torr, which is achievable with the filled liquid-nitrogen cryopanels and a clean system after baking [6]. Another limitation is the complications experienced during the substrate temperature measurements, which is normally faced while rotating the substrate. There is no direct contact between the substrate and the thermocouple, and hence, the actual temperature of the substrate will always be different than the one indicated by the thermocouple. The rotation of the substrate is essential to achieve uniformity in their growth rate. But the mechanical requirements are quite demanding for setting up the rotating substrate stage in the system. One such challenge is achieving a prolonged lifetime of the rotating stage to make it rotate several million times. This challenge is mainly because no conventional lubricants can be used to lubricate the bearings or feedthroughs. Inspite of these issues, MBE method is still popular due to their several pronounced benefits. One such advantage is their growth-control precision to less than a monolayer, which has granted unparalleled ability to grow high-quality nanostructures and quantum dots using this method.

3.2.4 Metal–organic chemical vapor deposition

MOCVD, which is also known as the metal–organic vapor-phase epitaxy (MOVPE) or organometalic vapor-phase epitaxy (OMVPE), is a well-established technique for the growth of III–V group semiconductor materials on the silicon substrate. MOCVD is a technique that has also shown industrial applicability for the solid-state lighting. It is important in both research field as well as large-scale production of semiconductor wafers. It has the advantage of being flexible and faster in growth-rate as compared

with other growth techniques. It can also be used to fabricate materials for photovoltaic cells, lasers, photodetectors, and transistors. This technique enables deposition of very thin layers of atoms of semiconductor compounds onto a semiconductor wafer of silicon or sapphire. It is mostly used for making III−V semiconductor, especially GaN-based LEDs. GaN-based LEDs are very important, as they emit in the visible region. This method provides controlled growth of layers leading to uniformity of crystals and controlled doping. Different layers can be grown in the same system. In MOCVD, deposition of the layer is achieved from the vapor phase. Manasevit *and* Simpson invented this method in 1969 to develop optoelectronic semiconductors such as GaAs [20]. In this method, for the deposition of III−V layer on various substrates, alkyl organometallic (trimethyl or triethyl species) of the group III element and hydride of the group V element (AsH_3/PH_3) are used as precursors. These precursors are generally volatile in gas stream, and they are chemically stable at appropriate temperature. Carrier gases such as H_2 and N_2 are used to carry out the growth process. Precursors, in the vapor form, are mixed with each other in the gas stream. After mixing, precursor vapors are injected into the reaction chamber so that they get deposited on the hot substrate after the surface chemical reaction. Flow of the gas in the reaction container is controlled by the valve and mass flow controller.

Fig. 3.6 gives the schematic representation of GaAs layer formation by MOCVD. Chemical reaction that would take place in the reaction chamber for GaAs is as follows:

$$(CH_3)_3Ga + AsH_3 \rightarrow GaAs + 3\ CH_4$$

Although this reaction looks very simple, there are complex processes occurring during each step of the reaction. Firstly, trimethylgallium (organometallic compound—$(CH_3)_3Ga$) is converted to dimethylgallium and methyl radical (CH_3) by gas-phase homolysis. Then, this methyl radical reacts with hydrogen gas and produces stable methane (CH_4) gas and hydrogen radical. Also, methyl radicals react with arsine (AsH_3) to produce AsH_2 and stable methane gas. In this way, the methyl group is removed step by step from Ga, and the hydrogen is removed from arsine to yield GaAs. Carrier hydrogen gas

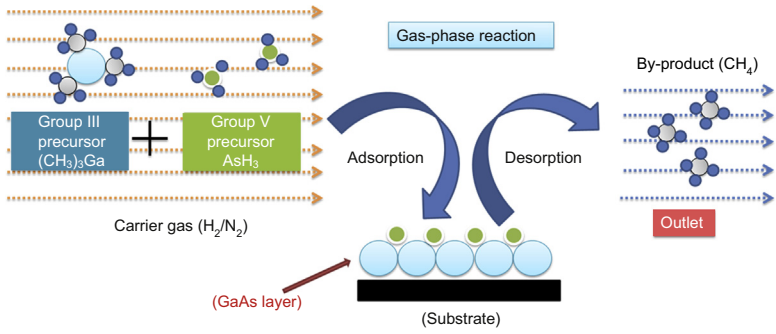

Figure 3.6 Schematic representation of the epitaxial layer formation of GaAs in MOCVD. *MOCVD*, metal−organic chemical vapor deposition.

plays an important role in the decomposition reaction of precursors. Temperature for the decomposition of $(CH_3)_3Ga$ is 500 °C, whereas for AsH_3, it is 700 °C. Radicals initiate the reaction in the system; hence, different decomposition temperatures of the precursors do not affect the reaction kinetics. Gases that are produced in the reaction such as methane, trimethyl gallium, and arsine are highly explosive, so special care is taken to avoid the danger. Growth of epitaxial layers is determined by three different temperature regimes that are evaporation-limited, transport-limited, and kinetic-limited. At lower-temperature kinetic-limited, growth will be dominated, as growth rate will depend on the temperature of the substrate. As the temperature increases, growth rate will become a function of the supply of precursors to the substrate and, hence, called as transport−limited growth. In this regime, the growth of layer will be controlled by the precursor concentration, and the temperature will have less influence. In this region, depletion layer is formed above the surface; diffusion through this depletion region to the surface will govern the growth rate. There will be some dependence of growth on the temperature in this region also as the diffusion rate increases with temperature. At very high temperature, precursors become highly volatile and will get expelled from the reactor without reacting, and hence, growth will be evaporation-limited in this regime [6]. There are two types of design for MOCVD reactors. One is the horizontal reactor and another is the vertical reactor, which are illustrated in Fig. 3.7 and Fig. 3.8, respectively. [21][22] In the horizontal reactor, gases are supplied laterally with respect to the substrate placed on a graphite suspector plate. Suspector plate is rotated and heated by RF oscillator. The reactor wall is coiled by water circulation to minimize the deposition on the walls. In the vertical reactor, gas enters from the top of the reactor and is directed onto the substrate mounted on the suspector plate.

MOCVD has experienced a major evolution in the past five decades. It has evolved from a basic research tool to a sophisticated manufacturing technology for large-scale

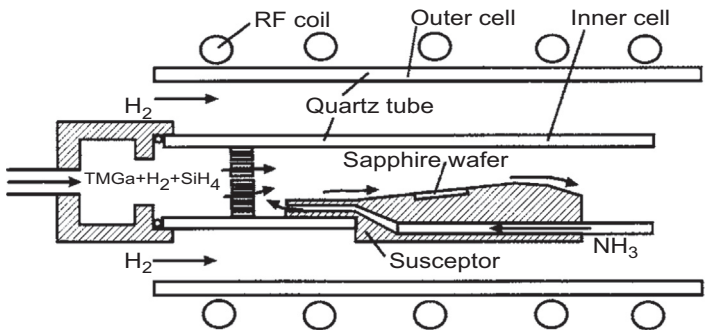

Figure 3.7 A schematic representation of the horizontal MOCVD reactor used for the epitaxial growth of GaN film. *MOCVD*, metal−organic chemical vapor deposition.
Reproduced with permission from K. Kim, S.K. Noh, Reactor design rules for GaN epitaxial layer growths on sapphire in metal-organic chemical vapour deposition, Semicond. Sci. Technol. 15 (2000) 868−874. https://doi.org/10.1088/0268-1242/15/8/314, Copyright 2000, IOP Publishing.

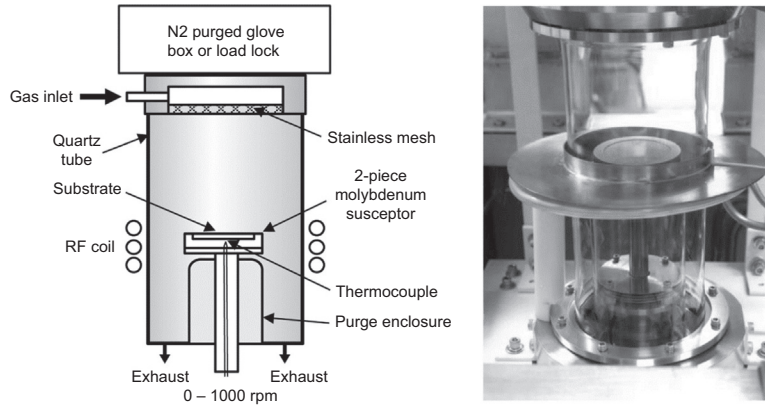

Figure 3.8 Schematic representation and photograph of the vertical MOCVD reactor. *MOCVD*, metal−organic chemical vapor deposition.
Reproduced with permission from C.A. Wang, Early history of MOVPE reactor development, J. Cryst. Growth 506 (2019) 190−200. https://doi.org/10.1016/j.jcrysgro.2018.10.004, Copyright 2018, Elsevier B.V.

production of semiconductor materials for optoelectronic applications. Advances in MOCVD led to better gas handling systems, in-situ monitoring, safety assurance, and precursor purification [21]. It also underwent significant improvements in the reactor designs that led to its massive adoption in the semiconductor-manufacturing industry.

3.3 Semiconductor materials for light-emitting diodes

The III−V compound semiconductors have brought out a revolution in the semiconductor industry and paved way for the rapid commercialization of optoelectronic materials. The III−V semiconductors formed a new class of materials, especially known for their light-emitting properties. This class of semiconductors were obtained by combining the group III elements (B, Al, Ga, In) with the group V elements (N. P, As, Sb). There were 12 possible combinations with these eight elements, viz., BN, BP, BAs, BSb, AlN, AlP, AlAs, AlSb, GaN, GaP, GaAs, GaSb, InN, InP, InAs, and InSb. However, only few of them were successful as light-emitting semiconductor materials. Among these, the most prominent semiconductors were GaAs, InP, GaN, AlN, and GaP as well as their ternary and quaternary compounds. While all other III-semiconductors stably exist in sphalerite (zinc blende or ZnS) structure, the stable crystal structure of III-nitrides at standard temperature and atmospheric pressure is hexagonal wurtzite. The III-nitrides were the first to be reported and explored for their properties. Fitcher reported about the AlN and later about InN in 1907 and 1910, respectively [23,24]. It took almost a couple of decades for the first report on GaN semiconductors [25]. Furthermore, it took another couple of decades for the first report

on the III-phosphides and III-arsenides [26]. But III-arsenides and III-phosphides garnered more momentum as they were easily grown over native substrates. On the other hand, III-nitrides were grown over nonnative substrates such as Si or sapphire. In this section, we shall discuss some of the semiconductors that established their presence in the light-emitting devices.

3.3.1 III-arsenides

Among the III-arsenides, the gallium arsenide (GaAs) and its ternary compounds with Al and In were found to be the most popular in the optoelectronic industry for LEDs. GaAs is a direct bandgap material with energy bandgap equal to 1.424 eV. They exhibit higher thermal conductivity, chemical resistance, mechanical strength, and hardness. Although GaAs have shown potential applications in infrared (IR)-emitting LEDs and laser diodes, they are more often considered as substrates for the epitaxial growth of other semiconductors belonging to the group III−V. Indium gallium arsenide (InGaAs) and aluminum gallium arsenide (AlGaAs) are also grown using GaAs as substrates. Sometimes, indium arsenide (InAs) is also used as a substrate for growing materials for mid-IR LEDs [27]. Aluminum gallium arsenide ($Al_xGa_{1-x}As$ or more commonly known as, AlGaAs) covers a wide range of spectra from red to IR emission. AlGaAs is a ternary compound formed between GaAs and AlAs. AlAs is a semiconductor with an indirect bandgap of 2.168 eV [28]. There is a large difference between the energy gaps of AlAs and GaAs. In their ternary compound, the energy gap of $Al_xGa_{1-x}As$ increases from that of AlAs to GaAs with the increasing composition of Al. When the composition of Al reaches 0.45, the $Al_xGa_{1-x}As$ starts showing transition from the direct bandgap to indirect bandgap. At this point, the bandgap of the compound is 1.98 eV, and hence, the emission wavelength of $Al_xGa_{1-x}As$ is limited to about 650 nm [29]. As a result, $Al_xGa_{1-x}As$ is suitable only for red and IR LEDs and not for obtaining orange or yellow emission from LEDs. Yet, the LEDs fabricated from AlGaAs materials showed very high efficiency [30]. One of the factors that contributed in the large-scale adoption of the fabrication of AlGaAs devices is the close matching in the lattice constants of AlAs and GaAs. The lattice mismatch between these two materials is just 0.2% at normal room temperature. As a result, very high-quality films of AlGaAs materials can be grown on GaAs substrates. Also, there is very low interface defect densities created during the deposition of such heterostructures [31,32]. The device performance can be, thus, optimized by growing such complex device structures. Although AlGaAs material system was conceived in the late 1960s, it took more than a decade for the LEDs based on this system to become commercially available [33]. One of the reasons behind this delay was the lack of proper LPE reactors that could support large-volume production of high-quality multilayer device structures [34]. Interestingly, AlGaAs-based red LEDs were the first LEDs to surpass the luminous efficiency of incandescent bulbs [28].

AlGaAs have been grown by several crystal growth methods such as LPE, MBE, and MOCVD. But there were always difficulties while growing high-quality layers of AlGaAs with high Al content by techniques other than LPE. One of the issues faced is the sensitivity of aluminum to oxygen that leads to contamination in the AlGaAs

phase [35]. To ensure the removal of moisture during the growth, ultrahigh-purity hydrogen carrier gas is used in MOCVD as a precaution to avoid oxygen contamination. Hashimoto et al. achieved growth of 700 nm emitting AlGaAs heterojunction on Si substrates using MOCVD technique [36]. An outstanding resistivity of 0.018 Ω/cm was observed for AlGaAs grown on the sapphire substrate by MOCVD [37]. The LPE technique has provided an added advantage of growing thick epitaxial layers. Hence, LPE emerged as the most commonly used technique to grow these crystal layers. There are many benefits of employing LPE technique while growing III-arsenides. The materials grown by LPE have shown higher luminescence efficiency. This is mainly attributed to the low concentration of nonradiative centers and deep trap levels in the materials grown by LPE. Also, the layers grown by LPE showed uniformity and controlled doping of n-type and p-type impurities as well as good reproducibility [38]. In MBE growth, the net flux of the group III (Ga or Al) atoms decides the growth rate. A flux of 6.25×10^{14} atoms cm^{-2} s^{-1} of Ga or Al can lead to a growth rate of 1 μm per hour [6]. At low-growth temperatures, there is minimum loss of group III atoms, and almost all of them are incorporated into the growing film. The stoichiometry is also maintained, as sufficient amount of arsenic atoms are incorporated along with the group III atoms and the excess of As atoms are desorbed. However, the desorption of As atoms becomes more prominent at temperatures above 600 K [39]. As a result, excess flux of As atoms is required to retain the stoichiometry. When the growth temperature is high, there is a significant loss of group III atoms and the growth rate falls below the expected rate. Typically, AlGaAs exhibits best optical properties when the growth temperatures are above 923 K [40]. To ensure that the composition of the compound is maintained even at high temperatures, the Ga flux is considerably increased than that used at lower temperatures.

3.3.2 III-phosphides

Since the discovery of the first red-emitting GaAsP LED in 1962, phosphide materials such as GaP and InP gained attention as light-emitting semiconductors [41]. Also, their ternary compounds gallium arsenide phosphide ($GaAs_{1-x}P_x$ or GaAsP), indium gallium phosphide ($In_xGa_{1-x}P$ or InGaP), and aluminum gallium indium phosphide ($(Al_xGa_{1-x})_yIn_{1-y}P$ or AlGaInP) were found suitable for fabrication of LEDs.

GaP is a semiconductor that possesses an indirect bandgap of 2.26 eV at 300 K [42]. In polycrystalline form, it has a pale orange appearance. On the other hand, it shows clear orange appearance in its undoped single crystal form. When they are strongly doped, they show darker appearance as a result of the free-carrier absorption. Since GaP is transparent to yellow and red wavelengths, they prove to be better substrates than GaAs to grow GaAsP. Also, they are transparent to wavelengths from visible to long-wavelength infrared spectrum. GaP shows higher refractive index than most of the materials (even greater than diamond). GaP is known to produce pure green electroluminescence emission with the peak at 556 nm [43]. Due to its indirect bandgap, the efficiency of the emission is difficult to exceed 0.12% in its undoped state [43]. Hence, GaP is often doped with some other elements (such as oxygen, zinc, or nitrogen) to increase the efficiency of the green emission. Still, the

doping has allowed to improve the efficiency to only 3% [42]. Similar to GaAs, GaP is also used as a substrate material for growing several semiconductor crystals. Both of them exhibit similar mechanical properties, but they have different spectral properties. While GaAs emits in the infrared region (~1150 nm), GaP emits in the visible region (~556 nm). In 1981, Yamaguchi and Niina developed a multicolor-emitting GaP LED [44]. They developed such LEDs by epitaxially growing a double junction of red- and green-emitting wafers on one side of a GaP substrate. The multicolor GaP LED could emit red, orange, yellow and green color. Indium phosphides are another binary compound in the III-phosphide family. Unlike GaP, they have a direct bandgap of 1.35 eV [45]. However, they are considered more appropriate for lasers than LEDs. Yet they have found important position as substrate materials for several LED device structures and as multishell colloidal quantum dots [46].

In the ternary compounds, GaAsP was first reported semiconductor to emit in the visible spectrum [41]. $GaAs_{0.6}P_{0.4}$, which was grown on the GaAs substrate, emitted in the red region of the spectrum. Unlike AlGaAs, there is a lattice mismatch between GaAsP and GaAs, and hence, there is a limitation in fabricating efficient heterostructures and, that too with low defect densities. Similar to GaP, the external quantum efficiency of GaAsP associated with the radiative combination processes is low [47]. GaAsP wafers are preferred to be grown on GaAs and GaP substrates. The performance of GaAsP diodes was found to be better on doping them with nitrogen [48]. A p^+/p-layer structure of GaAsP:N led to the optimization of the carrier concentration at the junction and decreased the light absorption [49]. The doping of nitrogen also helps in tuning the color emission of GaAsP. Thus, GaAsP diodes can emit throughout the range from 700 nm (red) to 550 nm (green) [50]. Another ternary compound is the indium gallium phosphide (InGaP), which is formed by the solid solution of InP and GaP. InP and GaP are semiconductors with direct and indirect bandgap, respectively. Hence, the crossover point from the indirect to direct bandgap for $In_{1-x}Ga_xP$ occurs when the value of x is between 0.63 and 0.74 [51–53]. InGaPs are generally grown on Si, GaAs, and GaP substrates [54–58]. InGaP can be used to fabricate red, orange, yellow, and green-emitting LEDs [58]. Since InGaP/GaAs systems exhibit better thermal conductivity and shorter wavelength than the AlGaAs/GaAs system, the former is preferred for the fabrication of high-brightness LEDs (HB-LEDs) [54].

Among the quaternary compounds of III-phosphides, AlGaInP is commercially used for LEDs and laser applications. This quaternary compound was introduced in 1990 by Kuo et al. [59]. At that time, the AlGaInP exhibited a 20 lm/A luminous efficiency in the yellow (590 nm) region of the spectrum and external quantum efficiency (EQE) $> 2\%$. In addition, its performance was 10 times better than the then existing yellow LEDs. With the exception of nitrogen-based materials, AlGaInP system possesses largest direct bandgap among the group III–V semiconductors [60]. AlGaInP is the solid solution of AlInP and GaInP. The optical properties of $(Al_xGa_{1-x})_yIn_{1-y}P$ were found to be optimum for $y = 0.5$ [61]. The bandgap of $Ga_{0.5}In_{0.5}P$ and $Al_{0.5}In_{0.5}P$ are 1.91 and 2.28 eV, respectively. Consequently, the bandgap of $(Al_xGa_{1-x})_{0.5}In_{0.5}P$ can be tuned from 1.91 to 2.28 eV by varying the value of x from 0 to 1. This quaternary compound experiences a crossover from the direct bandgap to indirect bandgap when the composition of Al is 0.53 [59,61]. Due to the

large direct bandgap, the emission wavelength of the AlGaInP LED is limited to wavelengths longer than 560 nm [29]. Thus, AlGaInP can emit from the yellowish-green to red region of the spectrum. AlGaInP is commercially used to fabricate red, orange, and yellow LEDs. Similar to AlGaAs, the AlGaInP wafers are suitably grown on GaAs substrates due to good lattice-match between them. In fact, GaAs is the only lattice-matching substrate among the binary compound semiconductors. In addition, the thermal expansion coefficients of GaAs and AlGaInP are similar. This facilitates their thermal recycling without producing any damaging crystalline defects in them [62]. For the growth of AlGaInP LEDs, the most preferred technique is the MOCVD. The MOCVD technique has helped in the realization of commercial AlGaInP LEDs. Also, the AlGaInP materials have shown highest efficiency when they were grown by MOCVD technique. LPE technique is not suitable for its growth as the Al-aggregation occurs in the melt [60]. MOCVD technique has allowed to grow high-quality, lattice-matched AlGaInP semiconductors over GaAs substrate. The requirement of large-chamber crystal growth reactors to achieve high-volume production of AlGaInP for optoelectronic devices has been satisfied by MOCVD [60]. This technique has also allowed better growth control at lower costs for designing a number of sophisticated structures of AlGaInP.

3.3.3 III-nitrides

There has been significant progress in the nitride-based semiconductor industry over the last three decades. HB-LEDs have benefited from the progress made in the growth, processing, fabrication, and doping of III-nitride LEDs. Gallium nitride (GaN), aluminum nitride (AlN), indium nitride (InN), and their ternary as well as the quaternary compounds such as indium gallium nitride ($In_xGa_{1-x}N$ or InGaN), aluminum gallium nitride ($Al_xGa_{1-x}N$ or AlGaN), and aluminum gallium indium nitride ($Al_xGa_yIn_{1-x-y}N$ or AlGaInN) are the commercially most popular nitrides considered for LED devices. The binary nitride semiconductors of group-III, such as GaN, AlN, and InN, show direct bandgap. At room temperature, the bandgap of GaN, AlN, and InN are 3.4 eV, 6.2 eV and 1.95 eV, respectively [63]. Among the ceramic materials, aluminum nitride has the highest thermal conductivity [64]. However, there is difficulty in controlling the electrical conductivity of wide-bandgap materials such as AlN. Taniyasu et al. successfully controlled the p-type and n-type doping in AlN [65]. They developed a homojunction LED from the AlN (p-type/intrinsic/n-type) PIN structure that was able to successfully demonstrate emission at 210 nm. This deep-UV emission was attributed to the exciton transition. InN belongs to the family of group III-nitrides, wherein other binary semiconductors have proved their worth as efficient light emitters. Although InN semiconductors are poor light emitters, they have a noteworthy role in the LED industry, especially because of their significance in the formation of ternary and quaternary compounds with AlN and GaN. Since InN has narrow bandgap as compared with the other two binary nitrides, they can be alloyed with GaN and AlN to cover the light emission spectrum from UV to IR. InN is, however, the least investigated compound due to the difficulty in obtaining high structural

quality. Since there is weak bonding between In and N, the growth of InN is more difficult than GaN and AlN [66].

The development of LEDs based on gallium nitride was pioneered by Nakamura et al. [67]. Due to their excellent thermal and chemical stability, GaNs are considered for high-power devices. Hence, GaN has found applications as laser diodes, photodetectors, LEDs, etc. They exist in two crystal structures, viz., wurtzite and zinc blende structures. Since bulk GaN substrates are expensive and not easily available, homoepitaxial growth of GaN is very rarely performed. As a result, majority of the GaN production involves heteroepitaxial growth on different materials. For the selection of substrate, there are several requirements that need to be satisfied. It is essential that the substrates are in the single-crystalline form with high quality, which offers a large surface area for the growth. Also, the substrate materials should show lattice matching, similarity in thermal and chemical stability at higher temperatures, and crystalline structure with GaN [68]. Other factors considered during the selection of substrates are its manufacturability and scalability, price, wafer size, etc. There are a wide choice of substrates for growing GaN wafers, and these include sapphire, Si, SiC, MgO, $MgAl_2O_4$, GaAs, GaN, $LiGaO_2$, and ZnO [63]. Sapphire substrates are predominantly used to manufacture the GaN buffer layers [69]. GaN is a key factor for the production of blue LEDs. Prior to this, blue LEDs remained as the missing piece from the red–green–blue (RGB) combination in white LEDs. The growth of crystalline GaN on the known substrates with controlled surface roughness seemed to be a herculean task. It was further difficult to dope GaN to prepare p-type GaN as the doping created defects in them [70]. Isamu Akasaki, Hiroshi Amano, and Shuji Nakamura were the pioneers who paved way for the production of blue LEDs by effectively doping GaN and growing uniform and highly crystalline doped- GaN [71–73]. Subsequently, they were awarded the 2014 Nobel Prize in physics for their outstanding achievement. Although the idea of blue LEDs based on GaN was conceived from the late 1950s, it was not brought to practicality due to the difficulty in growing high-quality GaN due to certain challenging issues. It was inevitable to grow GaN layers with uniformity and free of any defects or dislocations. In the 1970s, MOCVD and MBE techniques were employed to grow GaN crystals. GaN thin films, which were grown on the sapphire substrate using AlN buffer by MOCVD, showed crack-free optically flat surfaces [74]. Nakamura replaced the AlN layer with a thin layer of GaN and produced high-quality GaN with clean interfaces using MOCVD technique at low temperature [75]. This low-temperature GaN buffer growth by MOCVD technique did not require the replacement of the AlN during the growth, and hence, it gained recognition for the volume production of GaN. Another challenge was to develop p-type GaN by introducing suitable dopants such as Mg. Many unsuccessful attempts were made for this purpose. H. Amano, I. Akasaki, and their coworkers discovered that the blue luminescence from Zn-doped GaN significantly improved when irradiated with 9–30 kV electron beam [76]. This motivated them to proceed with their experiments on Mg-doped GaN too. They treated the Mg-doped GaN with low-energy electron-beam irradiation and discovered distinct p-type conduction in them accompanied by the drastic lowering of its resistivity [73]. The p-n junction LED fabricated using such p-type Mg-doped GaN demonstrated strong near-band-edge emission at room temperature. Nakamura et al. noticed the inactivity of Mg-doped GaN due to the formation of Mg–H complexes. They introduced the concept of thermal annealing in N_2-ambient atmosphere

to enable p-type doping in GaN by freeing up the Mg from the Mg−H complexes [77]. These innovative ideas enabled massive production of p-type GaN and also acted as milestones in the development of blue LEDs. The p−n junction GaN LEDs were reported to exhibit blue emission that has 10 times higher luminous intensity than the then commercially available SiC LEDs [78].

A major revolution in the LED industry came with the invention of the InGaN ternary compounds that led to the development of commercial blue LEDs. The indium mole fraction can be varied to tune the bandgap of InGaN from 1.95 to 3.4 eV [79]. The bandgap of InGaN is inversely proportional to the concentration of In. When the In-concentration is high, there is an increase in the lattice mismatch that results in dislocations [29]. InGaN was also introduced with several doping elements to improve the blue emission. Nakamura et al. introduced Cd-doping in InGaN films and observed that the blue emission peaks lowered by 0.5 eV as compared to undoped InGaN [80]. However, the emission intensity of Cd-doped films looked similar to the band-edge emission of the Si-doped InGaN films. HB-LEDs fabricated using InGaN/AlGaN double heterostructures demonstrated blue light with luminous intensity over 1 cd [71]. By codoping Zn and Si into the InGaN active layer, the EQE of the double heterostructure LED was increased to 5.4% [81]. By increasing the In-concentration, the emission peak was successfully shifted from the blue region to green and yellow regions too [81,82]. Superbright green emission with a luminous intensity of 12 cd was also achieved by fabricating a single quantum well−structured LED of p-AlGaN/InGaN/n-GaN using MOCVD [83].

AlGaN is a direct bandgap ternary compound that can be used for developing light-emitting devices in the deep-UV (DUV) to near-UV (NUV) region. Generally, AlGaN LEDs emit in the wavelength range between 200 and 365 nm, thus making them suitable alternative to mercury-based lamps for UV applications. The bandgap of AlGaN can be tuned between 3.43 and 6.11 eV [84]. AlGaN crystals are mainly grown on sapphire or AlN substrates. AlN substrates provided the advantage of growing high-crystalline AlGaN crystals with the threading dislocation density lower than 10^4 cm^{-2} that could possible increase the internal quantum efficiency due to lesser nonradiative recombination centers [85,86]. However, the extraction of UV emission from AlGaN LEDs is a bit challenging due to the difficulty faced in the suppression of the electron overflow [87]. AlGaInN, which is the quaternary compound among the group III-nitrides, has gained huge popularity for their efficient emission in the DUV and NUV region. Depending on the composition, the bandgap of AlGaInN can be tuned from 1.95 to 6.2 eV at room temperature [79]. Unlike AlGaN, the emission intensity from the AlGaInN is not much sensitive to the threading dislocation density. Kim et al. fabricated a 340 nm emitting LED by growing AlGaInN using MOCVD [88]. The LED structural quality and the emission efficiency were enhanced by incorporating the δ-doping in the Si-doped n-type and Mg-doped p-type layers of AlGaInN. The growth conditions such as temperature, pressure, and V/III ratio are also significant for optimizing the quality of the AlGaInN crystals [89]. The quality of the quaternary compound was also optimized by suppressing the vapour-phase reactions of trimethylaluminum, trimethylgallium, and NH_3 by introducing the alternating gas supply in the MOCVD [90,91].

3.4 Conclusions

With the advent of new and better processing technologies, the optoelectronic industry has blossomed. This has enabled the production of semiconductor wafers with higher purity and uniformity, which has further helped in boosting the LED market. The progressive developments in the growth, doping, and processing of semiconductor wafers have improved the brightness and efficiency of LEDs. This improvement has also been reflected in the applications such as light-based digital communications and data transfer systems. The identification and adoption of growth techniques appropriate for each of the semiconductors has been a key factor in the rapid expansion of the optoelectronic industry. Each of the growth techniques has their own merits and limitations. The first epitaxial technique to be used for the growth of materials for optoelectronic devices was LPE. LPE still continue to be pursued in conditions where vapour-phase techniques are found unsuitable. The advantages of LPE technique comprise the use of nontoxic materials, high growth rates, cheaper costs, lesser defects, etc. Vapour-phase techniques also have their own advantages and are more prominently used for the materials that are insoluble in liquids, which make LPE technique futile. MBE also has shown advantage when it comes to utilize UHV systems for the growth of semiconductor films with precise control. MOCVD offers a high degree of uniformity, reproducibility, efficiency, and control over the growth of multicomponent heterostructures. In addition, the choice of substrates is of great importance to determine the quality of the grown semiconductor wafers. Sapphire, silicon, GaN, GaAs, and so on were the substrates used for the growth of group III−V semiconductors, which are notable for the LED applications. The most prominently used semiconductor materials for LEDs are summarized in Table 3.1.

Table 3.1 Semiconductor materials used for light-emitting diodes and their emission in the electromagnetic spectrum.

Semiconductor material	Emission region
AlGaAs	Red to infrared
GaP	Red, yellow, green
GaAsP	Red, orange, yellow
InGaP	Red, orange, yellow, green
AlGaInP	Red, orange, yellow, yellowish-green
GaN	Ultraviolet
AlN	Far ultraviolet
InGaN	Near ultraviolet, blue, cyan, green
AlGaN	Deep ultraviolet, near ultraviolet
AlGaInN	Deep ultraviolet, near ultraviolet, blue

References

[1] R. Dwilinski, R. Doradzinski, J. Garczynski, L.P. Sierzputowski, M. Zajac, M. Rudzinski, Homoepitaxy on bulk ammonothermal GaN, J. Cryst. Growth (2009), https://doi.org/10.1016/j.jcrysgro.2009.01.078.

[2] S. Lourdudoss, Heteroepitaxy and selective area heteroepitaxy for silicon photonics, Curr. Opin. Solid State Mater. Sci. 16 (2012) 91−99, https://doi.org/10.1016/j.cossms.2012.01.003.

[3] R.D. Shannon, R.C. Rossi, Definition of topotaxy, Nature 202 (1964) 1000−1001, https://doi.org/10.1038/2021000a0.

[4] T.S. Zheleva, S.A. Smith, D.B. Thomson, T. Gehrke, K.J. Linthicum, P. Rajagopal, E. Carlson, W.M. Ashmawi, R.F. Davis, Pendeo-epitaxy - a new approach for lateral growth of gallium nitride structures, Mater. Res. Soc. Symp. Proc. (1999), https://doi.org/10.1557/s1092578300002581.

[5] H. Nelson, Epitaxial growth from the liquid state and its application to the fabrication of tunnel and laser diodes, RCA Rev. 24 (1963) 603−615.

[6] P. Capper, S. Irvine, T. Joyce, Epitaxial crystal growth: methods and materials, in: Springer Handb. Electron. Photonic Mater., Springer, Berlin, Heidelberg, 2006, pp. 271−301, https://doi.org/10.1007/978-0-387-29185-7_14.

[7] M. Winkler, T. Teubner, Liquid-phase epitaxy of (Hg, Cd)Te on CdTe substrates by a vertical dipping technique, Cryst. Res. Technol. 26 (1991) 283−288, https://doi.org/10.1002/crat.2170260307.

[8] M.B. Panish, I. Hayashi, S. Sumski, Double-heterostructure injection lasers with room-temperature thresholds as low as 2300 A/cm 2, Appl. Phys. Lett. 16 (1970) 326−327, https://doi.org/10.1063/1.1653213.

[9] M. Lemiti, Vapor phase epitaxy, in: K. Nakajima, N. Usami (Eds.), Cryst. Growth Si Sol. Cells, Adv. Mater. Res., Berlin, Heidelberg, 2009, pp. 159−175, https://doi.org/10.1007/978-3-642-02044-5_10.

[10] A. Schöner, New development in hot wall vapor phase epitaxial growth of silicon carbide, in: W.J. Choyke, H. Matsunami, G. Pensl (Eds.), Silicon Carbide. Adv. Texts Phys., Springer, Berlin, Heidelberg, 2004, pp. 229−250, https://doi.org/10.1007/978-3-642-18870-1_10.

[11] J.R. Arthur, J.J. LePore, GaAs, GaP, and $GaAs_xP_{1-x}$ epitaxial films grown by molecular beam deposition, J. Vac. Sci. Technol. 6 (1969) 545−548, https://doi.org/10.1116/1.1315677.

[12] A.Y. Cho, GaAs epitaxy by a molecular beam method: observations of surface structure on the (001) face, J. Appl. Phys. 42 (1971) 2074−2081, https://doi.org/10.1063/1.1660490.

[13] B.A. Joyce, R.R. Bradley, A study of nucleation in chemically grown epitaxial silicon films using molecular beam techniques I.—experimental methods, Philos. Mag. A 14 (1966) 289−299, https://doi.org/10.1080/14786436608219012.

[14] J.R. Arthur Jr. Interaction of Ga and As_2 molecular beams with GaAs surfaces, J. Appl. Phys. 39 (1968) 4032−4034.

[15] A.Y. Cho, Film deposition by molecular-beam techniques, J. Vac. Sci. Technol. 8 (1971) S31−S38, https://doi.org/10.1116/1.1316387.

[16] K. Alavi, Molecular beam epitaxy, Encycl. Mater. Sci. Technol. (2001) 5765−5780, https://doi.org/10.1016/C2010-0-68986-3, second ed.

[17] R.T. Velpula, B. Jain, M.R. Philip, H.D. Nguyen, R. Wang, H.P.T. Nguyen, Epitaxial growth and characterization of AlInN-based core-shell nanowire light emitting diodes operating in the ultraviolet spectrum, Sci. Rep. 10 (2020), https://doi.org/10.1038/s41598-020-59442-0.

[18] P. Uusimaa, P. Sipilä, M. Saarinen, L. Toikkanen, A. Rinta-Möykky, M. Pessa, Molecular beam epitaxy growth of MgZnSSe/ZnSSe/CdZnSe microcavity light-emitting diodes using in situ reflectance monitoring, J. Cryst. Growth 201 (1999) 1032−1035, https://doi.org/10.1016/S0022-0248(98)01516-4.
[19] H. Asahi, Molecular beam epitaxy with gaseous sources, in: Handb. Cryst. Growth, Elsevier, 2015, pp. 193−224, https://doi.org/10.1016/B978-0-444-63304-0.00005-6.
[20] H.M. Manasevit, W.I. Simpson, The use of metal-organics in the preparation of semiconductor materials: I . Epitaxial gallium- V compounds, J. Electrochem. Soc. 116 (1969) 1725, https://doi.org/10.1149/1.2411685.
[21] K. Kim, S.K. Noh, Reactor design rules for GaN epitaxial layer growths on sapphire in metal-organic chemical vapour deposition, Semicond. Sci. Technol. 15 (2000) 868−874, https://doi.org/10.1088/0268-1242/15/8/314.
[22] C.A. Wang, Early history of MOVPE reactor development, J. Cryst. Growth 506 (2019) 190−200, https://doi.org/10.1016/j.jcrysgro.2018.10.004.
[23] F. Fichter, Ü. Aluminiumnitrid, Z. Anorg. Chem. 54 (1907) 322−327, https://doi.org/10.1002/zaac.19070540128.
[24] F. Fischer, F. Schröter, Über neue Metall-Stickstoff-Verbindungen und ihre Stabilität an der Hand des periodischen Systems, Berichte Der Dtsch. Chem. Gesellschaft. 43 (1910) 1465−1479, https://doi.org/10.1002/cber.19100430249.
[25] W.C. Johnson, J.B. Parson, M.C. Crew, Nitrogen compounds of gallium. III, J. Phys. Chem. 36 (1932) 2651−2654, https://doi.org/10.1021/j150340a015.
[26] H. Welker, Über neue halbleitende Verbindungen, Z. Naturforsch. 7 (1952), https://doi.org/10.1515/zna-1952-1110.
[27] I.R. Grant, V. III−, Compound semiconductors: growth, in: Encycl. Mater. Sci. Technol., Elsevier, 2001, pp. 1441−1452, https://doi.org/10.1016/B0-08-043152-6/00264-3.
[28] F.M. Steranka, Chapter 3 AlGaAs red light-emitting diodes, in: Semicond. Semimetals, Elsevier B.V, 1997, pp. 65−96, https://doi.org/10.1016/S0080-8784(08)62404-7.
[29] S.M. Sze, K.K. Ng, Physics of Semiconductor Devices, John Wiley & Sons, Inc., Hoboken, NJ, USA, 2006, https://doi.org/10.1002/0470068329.
[30] P. Dalapati, N.B. Manik, A.N. Basu, Effect of temperature on the intensity and carrier lifetime of an AlGaAs based red light emitting diode, J. Semiconduct. 34 (2013) 092001, https://doi.org/10.1088/1674-4926/34/9/092001.
[31] T. Egawa, Y. Niwano, K. Fujita, K. Nitatori, T. Watanabe, T. Jimbo, M. Umeno, First fabrication of AlGaAs/GaAs double-heterostructure light-emitting diodes grown on GaAs(111)A substrates using only silicon dopant, Jpn. J. Appl. Phys. 34 (1995) 1270−1272, https://doi.org/10.1143/JJAP.34.1270.
[32] M.A. Ladugin, I.V. Yarotskaya, T.A. Bagaev, K.Y. Telegin, A.Y. Andreev, I.I. Zasavitskii, A.A. Padalitsa, A.A. Marmalyuk, Advanced AlGaAs/GaAs heterostructures grown by MOVPE, Crystals 9 (2019) 305, https://doi.org/10.3390/cryst9060305.
[33] H. Rupprecht, J.M. Woodall, G.D. Pettit, Efficient visible electroluminescence at 300°K from $Ga_{1-x}Al_xAs$ p-n Junctions grown by liquid-phase epitaxy, Appl. Phys. Lett. 11 (1967) 81−83, https://doi.org/10.1063/1.1755045.
[34] J. Nishizawa, K. Suto, T. Teshima, Minority-carrier lifetime measurements of efficient GaAlAs p - n heterojunctions, J. Appl. Phys. 48 (1977) 3484−3495, https://doi.org/10.1063/1.324198.
[35] E.S. Tok, J.H. Neave, J. Zhang, B.A. Joyce, T.S. Jones, Arsenic incorporation kinetics in GaAs(001) homoepitaxy revisited, Surf. Sci. 374 (1997) 397−405, https://doi.org/10.1016/S0039-6028(97)01241-7.

[36] A. Hashimoto, Y. Kawarada, T. Kamijoh, M. Akiyama, N. Watanabe, M. Sakuta, AlGaAs heterojunction visible (700 nm) light-emitting diodes on Si substrates fabricated by metalorganic chemical vapor deposition, Appl. Phys. Lett. 48 (1986) 1617−1619, https://doi.org/10.1063/1.96835.
[37] J.H. Kim, H.J. Lee, Study of p-type AlGaAs film grown on sapphire substrate using GaAs buffer layer, Mater. Lett. 123 (2014) 1−5, https://doi.org/10.1016/j.matlet.2014.02.070.
[38] Z.I. Alferov, Electroluminescence of heavily-doped heterojunctions $pAl_xGa_{1-x}As$-nGaAs, J. Lumin. 1−2 (1970) 869−884, https://doi.org/10.1016/0022-2313(70)90099-2.
[39] C.T. Foxon, B.A. Joyce, Interaction kinetics of As4 and Ga on {100} GaAs surfaces using a modulated molecular beam technique, Surf. Sci. 50 (1975) 434−450, https://doi.org/10.1016/0039-6028(75)90035-7.
[40] T. Fujii, S. Hiyamizu, O. Wada, T. Sugahara, S. Yamakoshi, T. Sakurai, H. Hashimoto, Extremely uniform GaAs-AlGaAs heterostructure layers with high optical quality by molecular beam epitaxy, J. Cryst. Growth 61 (1983) 393−396, https://doi.org/10.1016/0022-0248(83)90377-9.
[41] N. Holonyak, S.F. Bevacqua, Coherent (visible) light emission from $Ga(As_{1-x}P_x)$ junctions, Appl. Phys. Lett. 1 (1962) 82−83, https://doi.org/10.1063/1.1753706.
[42] J. Václavík, D. Vápenka, Gallium Phosphide as a material for visible and infrared optics, EPJ Web Conf. 48 (2013) 00028, https://doi.org/10.1051/epjconf/20134800028.
[43] J. Nishizawa, Y. Okuno, M. Koike, F. Sakurai, Bright pure green emission from N-free GaP LED's, Jpn. J. Appl. Phys. 19 (1980) 377, https://doi.org/10.7567/JJAPS.19S1.377.
[44] T. Yamaguchi, T. Niina, A high brightness GaP multicolor LED, IEEE Trans. Electron. Dev. 28 (1981) 588−592, https://doi.org/10.1109/T-ED.1981.20387.
[45] R. Toufanian, A. Piryatinski, A.H. Mahler, R. Iyer, J.A. Hollingsworth, A.M. Dennis, Bandgap engineering of indium phosphide-based core/shell heterostructures through shell composition and thickness, Front. Chem. 6 (2018), https://doi.org/10.3389/fchem.2018.00567.
[46] J.P. Park, J.J. Lee, S.W. Kim, Highly luminescent InP/GaP/ZnS QDs emitting in the entire color range via a heating up process, Sci. Rep. (2016), https://doi.org/10.1038/srep30094.
[47] L. Forbes, C.K. Vaughn, Deep-level defects in red GaAs 1-x P x light-emitting diodes, Proc. IEEE 62 (1974) 534−535, https://doi.org/10.1109/PROC.1974.9468.
[48] C. Robert, A. Bondi, T.N. Thanh, J. Even, C. Cornet, O. Durand, J.P. Burin, J.M. Jancu, W. Guo, A. Létoublon, H. Folliot, S. Boyer-Richard, M. Perrin, N. Chevalier, O. Dehaese, K. Tavernier, S. Loualiche, A. Le Corre, Room temperature operation of GaAsP(N)/GaP(N) quantum well based light-emitting diodes: effect of the incorporation of nitrogen, Appl. Phys. Lett. 98 (2011) 251110, https://doi.org/10.1063/1.3601857.
[49] T. Sato, M. Imai, Nitrogen-doped GaAsP light-emitting diodes with junctions grown by hydride vapor-phase epitaxy, Appl. Phys. Lett. 80 (2002) 2875−2877, https://doi.org/10.1063/1.1473693.
[50] M.G. Craford, D.L. Keune, W.O. Groves, A.H. Herzog, The luminescent properties of nitrogen doped GaAsP light emitting diodes, J. Electron. Mater. 2 (1973) 137−158, https://doi.org/10.1007/BF02658108.
[51] A.M. Joullie, C. Alibert, On the Γ-Γ and Γ- X transitions of the $Ga_xIn_{1-x}P$ alloys, J. Appl. Phys. 45 (1974) 5472−5474, https://doi.org/10.1063/1.1663265.
[52] J. Novák, S. Hasenöhrl, R. Kúdela, M. Kučera, Growth and characterisation of layers with composition close to crossover from direct to indirect band gap, J. Cryst. Growth 275 (2005) e1281−e1286, https://doi.org/10.1016/j.jcrysgro.2004.11.076.
[53] A. Onton, R.J. Chicotka, Photoluminescence processes in $In_{1-x}Ga_xP$ at 2°K, Phys. Rev. B 4 (1971) 1847−1853, https://doi.org/10.1103/PhysRevB.4.1847.

[54] C.C. Hu, C.S. Sheu, M.K. Lee, The fabrication of InGaP/Si light emitting diode by metalorganic chemical vapor deposition, Mater. Chem. Phys. 48 (1997) 17−20, https://doi.org/10.1016/S0254-0584(97)80070-3.

[55] C. Wang, B. Wang, K.E.K. Lee, S.F. Yoon, J. Michel, A yellow InGaP light emitting diode epitaxially grown on Si substrate, in: Asia Commun. Photonics Conf. ACPC, vol. 2015, 2015, https://doi.org/10.1364/acpc.2015.as3a.3.

[56] A. Myllynen, T. Sadi, J. Oksanen, Diffusion-driven GaInP/GaAs light-emitting diodes enhanced by modulation doping, Opt. Quant. Electron. 51 (2019) 90, https://doi.org/10.1007/s11082-019-1806-z.

[57] J.G. Neff, M.R. Islam, R.V. Chelakara, K.G. Fertitta, F.J. Ciuba, R.D. Dupuis, Characterization of GaP/InGaP and GaP/GaAsP strained-layer quantum wells grown by metal-organic chemical vapor deposition, J. Cryst. Growth 145 (1994) 746−751, https://doi.org/10.1016/0022-0248(94)91137-1.

[58] L.J. Stinson, J.G. Yu, S.D. Lester, M.J. Peanasky, K. Park, High-efficiency InGaP light-emitting diodes on GaP substrates, Appl. Phys. Lett. 58 (1991) 2012−2014, https://doi.org/10.1063/1.105024.

[59] C.P. Kuo, R.M. Fletcher, T.D. Osentowski, M.C. Lardizabal, M.G. Craford, V.M. Robbins, High performance AlGaInP visible light-emitting diodes, Appl. Phys. Lett. 57 (1990) 2937−2939, https://doi.org/10.1063/1.103736.

[60] F.A. Kish, R.M. Fletcher, Chapter 5 AlGalnP light-emitting diodes, in: Semicond. Semimetals, Elsevier B.V., 1997, https://doi.org/10.1016/S0080-8784(08)62406-0, pp. 149-C3.

[61] H. Chui, N.F. Gardner, P.N. Grillot, J.W. Huang, M.R. Krames, S.A. Maranowski, Chapter 2 high-efficiency AlGalnP light-emitting diodes, in: Semicond. Semimetals, 1999, pp. 49−128, https://doi.org/10.1016/S0080-8784(08)62488-6.

[62] D.P. Bour, J.R. Shealy, Organometallic vapor phase epitaxial growth of $(Al_xGa_{1-x})_{0.5}In_{0.5}P$ and its heterostructures, IEEE J. Quant. Electron. 24 (1988) 1856−1863. https://doi.org/10.1109/3.7127.

[63] R.S. Kern, W. Götz, C.H. Chen, H. Liu, R.M. Fletcher, C.P. Kuo, Chapter 3 high-brightness nitride-based visible-light-emitting diodes, in: Semicond. Semimetals, 1999, pp. 129−207, https://doi.org/10.1016/S0080-8784(08)62489-8.

[64] Y. Zhou, H. Wang, L. Wang, K. Yu, Z. Lin, L. He, Y. Bai, Fabrication and characterization of aluminum nitride polymer matrix composites with high thermal conductivity and low dielectric constant for electronic packaging, Mater. Sci. Eng., B 177 (2012) 892−896, https://doi.org/10.1016/j.mseb.2012.03.056.

[65] Y. Taniyasu, M. Kasu, T. Makimoto, An aluminium nitride light-emitting diode with a wavelength of 210 nanometres, Nature 441 (2006) 325−328, https://doi.org/10.1038/nature04760.

[66] Z. Liliental-Weber, Structure of InN and InGaN: transmission electron microscopy studies, in: W.J.S.C.F. McConville (Ed.), Indium Nitride Relat. Alloy, CRC Press Taylor and Francis group, 2009, https://doi.org/10.1201/9781420078107.

[67] S. Nakamura, G. Fasol, The Blue Laser Diode: GaN Based Light Emitters and Lasers, 1997. Berlin, http://link.springer.com/content/pdf/10.1007/978-3-642-57032-2.pdf%5Cnhttp://scholar.google.com/scholar?hl=en&btnG=Search&q=intitle:The+Blue+Laser+Diode+GaN+Based+Light+Emitters+and+Lasers#4%5Cnhttp://scholar.google.com/scholar?hl=en&btnG=Search&q=intitle.

[68] J.-H. Ryou, W. Lee, GaN on sapphire substrates for visible light-emitting diodes, in: Nitride Semicond. Light. Diodes, Elsevier, 2018, pp. 43−78, https://doi.org/10.1016/B978-0-08-101942-9.00003-4.

[69] O. Abdullaev, M. Mezhenny, A. Chelny, A. Savchuk, Y. Ahmerov, O. Rabinovich, V. Murashev, S. Didenko, Y. Osipov, S. Sizov, M. Orlova, A. Aluyev, MOCVD growth GaN on sapphire, IOP Conf. Ser. Mater. Sci. Eng. 617 (2019) 012015, https://doi.org/10.1088/1757-899X/617/1/012015.
[70] J.I. Pankove, Luminescence in GaN, J. Lumin. 7 (1973) 114−126, https://doi.org/10.1016/0022-2313(73)90062-8.
[71] S. Nakamura, T. Mukai, M. Senoh, Candela-class high-brightness InGaN/AlGaN double-heterostructure blue-light-emitting diodes, Appl. Phys. Lett. 64 (1994) 1687−1689, https://doi.org/10.1063/1.111832.
[72] H. Search, C. Journals, A. Contact, M. Iopscience, I.P. Address, S. Nakamura, N. Iwasa, M. Senoh, T. Mukai, Hole compensation mechanism of p-type GaN films, Jpn. J. Appl. Phys. 31 (1992) 1258−1266, https://doi.org/10.1143/JJAP.31.1258.
[73] H. Amano, M. Kito, K. Hiramatsu, I. Akasaki, P-type conduction in Mg-doped GaN treated with low-energy electron beam irradiation (LEEBI), Jpn. J. Appl. Phys. 28 (1989) L2112−L2114, https://doi.org/10.1143/JJAP.28.L2112.
[74] H. Amano, N. Sawaki, I. Akasaki, Y. Toyoda, Metalorganic vapor phase epitaxial growth of a high quality GaN film using an AlN buffer layer, Appl. Phys. Lett. 48 (1986) 353−355, https://doi.org/10.1063/1.96549.
[75] S. Nakamura, GaN growth using GaN buffer layer, Jpn. J. Appl. Phys. 30 (1991) L1705−L1707, https://doi.org/10.1143/JJAP.30.L1705.
[76] H. Amano, I. Akasaki, T. Kozawa, K. Hiramatsu, N. Sawaki, K. Ikeda, Y. Ishii, Electron beam effects on blue luminescence of zinc-doped GaN, J. Lumin. 40−41 (1988) 121−122, https://doi.org/10.1016/0022-2313(88)90117-2.
[77] S. Nakamura, T. Mukai, M. Senoh, N. Iwasa, Thermal annealing effects on P-type Mg-doped GaN films, Jpn. J. Appl. Phys. 139 (1992) L139−L142, https://doi.org/10.1143/JJAP.31.L139.
[78] S. Nakamura, M.R. Krames, History of gallium−nitride-based light-emitting diodes for illumination, Proc. IEEE 101 (2013) 2211−2220, https://doi.org/10.1109/JPROC.2013.2274929.
[79] S. Nakamura, III-V nitride based light-emitting devices, Solid State Commun. 102 (1997) 237−243, https://doi.org/10.1016/S0038-1098(96)00722-3.
[80] S. Nakamura, N. Iwasa, S. Nagahama, Cd-doped InGaN films grown on GaN films, Jpn. J. Appl. Phys. 32 (1993) L338−L341, https://doi.org/10.1143/JJAP.32.L338.
[81] S. Nakamura, InGaN/AlGaN blue-light-emitting diodes, J. Vac. Sci. Technol. A Vacuum, Surfaces, Film. 13 (1995) 705−710, https://doi.org/10.1116/1.579811.
[82] S. Nakamura, M. Senoh, N. Iwasa, S. Nagahama, High-brightness InGaN blue, green and yellow light-emitting diodes with quantum well structures, Jpn. J. Appl. Phys. 34 (1995) L797−L799, https://doi.org/10.1143/JJAP.34.L797.
[83] S. Nakamura, M. Senoh, N. Iwasa, S. Nagahama, T. Yamada, T. Mukai, Superbright green InGaN single-quantum-well-structure light-emitting diodes, Jpn. J. Appl. Phys. 34 (1995) L1332−L1335, https://doi.org/10.1143/JJAP.34.L1332.
[84] Y. Nagasawa, A. Hirano, A review of AlGaN-based deep-ultraviolet light-emitting diodes on sapphire, Appl. Sci. 8 (2018) 1264, https://doi.org/10.3390/app8081264.
[85] R.T. Bondokov, S.G. Mueller, K.E. Morgan, G.A. Slack, S. Schujman, M.C. Wood, J.A. Smart, L.J. Schowalter, Large-area AlN substrates for electronic applications: an industrial perspective, J. Cryst. Growth 310 (2008) 4020−4026, https://doi.org/10.1016/j.jcrysgro.2008.06.032.
[86] T. Zhou, B. Raghothamachar, F. Wu, R. Dalmau, B. Moody, S. Craft, R. Schlesser, M. Dudley, Z. Sitar, Characterization of threading dislocations in PVT-grown AlN

substrates via x-ray topography and ray tracing simulation, J. Electron. Mater. 43 (2014) 838−842, https://doi.org/10.1007/s11664-013-2968-2.

[87] H. Hirayama, S. Fujikawa, Quaternary InAlGaN quantum-dot ultraviolet light-emitting diode emitting at 335 nm fabricated by anti-surfactant method, Phys. Status Solidi 5 (2008) 2312−2315, https://doi.org/10.1002/pssc.200778732.

[88] K.H. Kim, J. Li, S.X. Jin, J.Y. Lin, H.X. Jiang, III-nitride ultraviolet light-emitting diodes with delta doping, Appl. Phys. Lett. 83 (2003) 566−568, https://doi.org/10.1063/1.1593212.

[89] H. Hirayama, Quaternary InAlGaN-based high-efficiency ultraviolet light-emitting diodes, J. Appl. Phys. 97 (2005) 091101, https://doi.org/10.1063/1.1899760.

[90] C. Chen, J. Yang, M.-Y. Ryu, J. Zhang, E. Kuokstis, G. Simin, M.A. Khan, Pulsed metalorganic chemical vapor deposition of quaternary AlInGaN layers and multiple quantum wells for ultraviolet light emission, Jpn. J. Appl. Phys. 41 (2002) 1924−1928, https://doi.org/10.1143/JJAP.41.1924.

[91] J. Zhang, E. Kuokstis, Q. Fareed, H. Wang, J. Yang, G. Simin, M.A. Khan, R. Gaska, M. Shur, Pulsed atomic layer epitaxy of quaternary AlInGaN layers, Appl. Phys. Lett. 79 (2001) 925−927, https://doi.org/10.1063/1.1392301.

Phosphor-converted LEDs

4

4.1 Phosphor

Phosphor is a term coined by Vincentinus Casciarolo, an Italian alchemist in the 17th century. The term came into existence after the discovery of phosphorous, which glowed after coming in contact with air. Soon, all the materials that glowed were called as phosphors. A prototype of artificially prepared phosphor was introduced by Théodore Sidot in 1886 when he unintentionally prepared ZnS-type material. Soon, many new luminescent materials were discovered or artificially prepared and they found wide-scale applications in different sectors. All inorganic materials that can show luminescence are now classified as phosphors. Phosphors, which can be either semiconducting or insulating, comprise an imperfect host lattice that is intentionally doped with an impurity ion that can act as luminescence centers in the lattice. In some cases, the host matrix itself can exhibit luminescence without any external doping.

Phosphors found their use in light-emitting diodes (LEDs) when it was realized that semiconductor chips failed to produce a full-color spectrum essentially required to obtain the white emission. The gaps left out by the RGB-emitting semiconductor chips can be filled by combining them with a suitable phosphor. Instead of incorporating three highly expensive semiconductor chips, the idea was to design a package with a single chip that can provide the pump power required for exciting the phosphor. Most of the phosphors showed absorption in the ultraviolet (UV), near-ultraviolet (NUV), and blue region of the electromagnetic spectrum. Consequently, NUV-LEDs and blue-LEDs became more popular owing to their suitability for exciting these phosphors. Soon, phosphor-converted LEDs (pc-LEDs) were successful in the extermination of several other light sources that performed inefficiently. The quest for more efficient and advanced phosphors led to the discovery of several novel phosphors that were able to emit different colors such as red, orange, yellow, green, blue, and white. The major revolution in the lighting industry was brought out by the white-LED (WLED) that comprised of the combination of YAG:Ce with a blue-LED chip. The physical properties of phosphors play a major role while defining the LED characteristics such as luminous efficacy, correlated color temperature, color-rendering index (CRI), and lifespan. In turn, these characteristics are strongly influenced by the synthetic conditions and precision during LED device fabrication. Even the selection of synthesis methods must be wisely made depending on the composition of the phosphor, the raw materials available, and the climatic conditions in which the synthesis is to be performed.

The Fundamentals and Applications of Light-Emitting Diodes. https://doi.org/10.1016/B978-0-12-819605-2.00004-5

4.2 Dopant and its types

Materials having an energy bandgap equivalent to the energy of a visible light photon can emit in the visible region of the spectrum. But, the number of such materials is very few. However, materials having a wider bandgap can also be compelled to provide luminescence emission in the visible region by introducing an external agent into the host lattice of the material. The external agent can be either an ion or a crystal defect. The additionally introduced ions have an electron orbital structure different from that of the host lattice, and these ions are called dopants. The energy levels of dopant ions try to accommodate themselves within the forbidden energy gap of the host lattice. These levels can be close to the conduction band (in such case, the dopant is called a donor) or close to the valence band (in such a case, it is called an acceptor). Electronic transitions between these levels can give rise to a photon emission resulting in luminescence, and the energy difference between the excited and ground states decides the wavelength of the emitted light. Depending upon the electronic configuration, solubility, and structure of the host lattices, different roles are played by the dopant in the host matrix. Besides, dopants have been classified into different classes on the basis of their function in host lattices.

4.2.1 Activator

When a dopant ion absorbs the excitation energy, an electron jumps from the ground state to the excited state of the ion and then emits the energy in the form of radiation while returning to the ground state. Such dopant ions are known as activators (A) or luminescent centers. Generally, the concentration of activators is very less in the host matrix, and their concentrations can range from as much as one dopant atom in 5000 host atoms down to as little as one dopant atom in 1 million host atoms. Some of the commonly used activators are the rare-earth ions, especially lanthanides with trivalent or divalent oxidation states, and the transition metal ions such as Mn^{4+}, Mn^{2+}, Cu^{+}, and Cr^{3+}.

4.2.2 Coactivator

The dopant ions that do not produce luminescence on their own but support the activator ions in the luminescence processes by acting as charge compensators or by creating hole/electron traps are known as coactivators. For example, Li^{+}, Na^{+}, and K^{+} are some of the commonly used coactivators [1].

4.2.3 Sensitizer

In some cases, the activator ions are not capable enough to efficiently absorb the excitation energy provided by the external source. In this scenario, there must be a mediator that can act as a bridge to transfer energy from the excitation source to the activator. The dopant ions playing such a role are known as sensitizers (S). A sensitizer

absorbs the excitation energy provided by the external source and emits an energy, which overlaps with the excitation of the activator. The energy transfer process from the sensitizer to the activator is known as sensitization. Ce^{3+} and Eu^{2+} form the most effective sensitizers to a number of activators.

4.3 Synthesis of inorganic phosphors

4.3.1 Solid-state diffusion

The solid-state diffusion method is the most commonly used synthesis method for phosphors. It is also referred as a solid-state reaction in many literatures. This is a straightforward method, which is suitable for large-scale production of oxides, chlorides, oxychlorides, fluorides, oxyfluorides, and nitrides. This method involves the pulverization and sintering of the precursors at high temperatures for the formation of the desired compound. The precursors are ground and mixed well to break the grain boundaries and facilitate better diffusion of atoms in the chemical reaction. The grain-boundary contacts and the temperature of the reaction have a significant influence on the diffusion of atoms. The defects and impurities present at the grain boundaries also affect the transport of atoms across the boundaries. The presence of grain boundaries ceases the diffusion of atoms and the reaction stops at midway. The mixture of precursors must be ground and mixed repeatedly to break the grain boundaries and create fresh surfaces to initiate further reaction through diffusion between the heat treatments [2,3]. The precursors are mostly used in the form of oxides, which needs to be mixed in stoichiometric proportion in a suitable medium (for example, acetone). Eventually, the well-crushed powder is fired at high temperatures to obtain the desired product. This method is best suitable for the synthesis of polycrystalline ceramic materials, and hence, solid-state diffusion is sometimes referred to as a conventional ceramic route method.

In general, solid-state diffusion method involves the following steps:

1. Mixing and crushing of the reactants or precursors uniformly.
2. Heat treatment of the crushed reactants at a moderate temperature (200−450 °C) to remove unwanted residual gases.
3. Recrushing of the mixture followed by reheating at very high temperatures (1000−1500 °C) in an appropriate atmosphere desirable for the product formation.
4. Repetition of the crushing and heating cycles until the homogenous formation of the desired product with high crystallinity is achieved.

The rate of reaction is often limited due to the poor diffusion of ions through the newly formed grain boundaries and the nucleation of the product phase. The reaction rate can be promoted by increasing the surface area of the grains, for which it is essential to adopt repeated grinding and mixing followed by sintering at high temperatures. Another version of this method is the modified solid-state reaction method wherein the precursors are not subjected to multiple heat treatments, but instead, a single heat treatment at a very high temperature is sufficient to form the final product. The reactant and

the product oxides have very low vapor pressures, and hence, the loss of material experienced during the synthesis is the least. Yet, it is essential to be aware of the shortcomings and drawbacks suffered in the quality of the product before adopting this method for synthesis. The distribution of the grain size and the homogeneity in the phase formation are often compromised unless certain rigorous measures are adopted to control them. Another drawback is the requirement of expensive high-temperature furnaces for firing the phosphors. There is also a possibility of the precursors remaining unreacted to form intermediates or impurity phases, thereby hampering the overall luminescence yield. This can be avoided if they are subjected to repeated pulverization in between heat treatments. In some cases, the non-stoichiometric amount of precursors must be used to adjust for the losses occurring from their volatility.

4.3.2 Sol–gel/Pechini

The sol–gel method is one of the best methods for the synthesis of nano/micron-sized phosphors with uniform particle size distribution. The precursors are mainly in the form of nitrates, which are mixed homogeneously along with a chelating agent and a surfactant in a suitable solvent. In general, citric acid and polyethylene glycol are the most widely used chelating agent and surfactant, respectively, for the sol–gel synthesis of phosphors. The homogenous solution of the precursors along with the chelating agent and the surfactant is kept for continuous stirring and heating at about 80 °C. After some time, the solution undergoes condensation to form a polymeric network that leads to the formation of sol and further stirring leads to the formation of a gel. The solution starts to yield an elastic viscous form due to sudden loss of fluidity and this results in the gelation of the solution [4]. The gel, thus obtained, is subjected to an appropriate heat treatment for removing the organic contaminants from the phosphor. Sometimes, the organic molecules that are trapped deep within the interstitials of the phosphor lattice are not easily removed and may require annealing at temperatures above 500 °C for removing them. The morphology and dimensions of the final product can be varied by monitoring the ratio of metal ions, surfactants, and the chelating agent. In case, the lanthanide precursors are available only in the oxide form, then they must be transformed into the nitrate form. This can be achieved by dissolving the oxides of lanthanides in conc. HNO_3. This solution must be then heated and stirred well before diluting it with a few drops of distilled water. However, some of the oxides, like Ce_2O_3, are difficult to get transformed into nitrate form by adopting this procedure. Even though the sol–gel method involves lengthy procedures, it is known to produce a high-quality final product with excellent phase-purity and morphology. A modified version of the sol–gel method is Pechini's method. The materials lacking favorable hydrolysis equilibria are not easily synthesized by the sol–gel method but can be prepared by Pechini's method. In the sol–gel synthesis, the materials undergo controlled hydrolysis to form a cryogel, an aerogel, or a xerogel, which is decided by the drying process involved for the removal of the solvent. On the contrary, Pechini's method involves the formation of citrate gel that undergoes combustion to remove the solvent.

4.3.3 Combustion synthesis

The combustion method is one of the easiest and cost-effective methods for synthesizing phosphors. This method requires less efforts and minimal time than other synthesis routes. This method involves an exothermic reaction accompanied by the emission of light and heat. The end products obtained are chemically homogenous with higher surface areas and lesser impurities as compared to those obtained from the solid-state diffusion method. The prerequisites for this method are oxidizers and fuel. Generally, metal nitrates are considered as the oxidizing reactants, and fuel may be chosen from the list of available organic reducing agents such as urea, glycine, thiourea, and carbohydrazide in this method, and the aqueous solution of oxidizing reactants and the fuel are ignited at a low temperature ($\sim$400−600 °C), thereby leading to a redox, exothermic reaction accompanied by a flame, as shown in Fig. 4.1 [5,6]. The reaction temperature can rise as high as 1200 °C but will not last for more than 10 minutes. Due to the short duration at high temperatures, nanocrystalline powders may also be yielded from this reaction. In most cases, the end products are weakly agglomerated into submicron-sized powders that can be pulverized easily into a fine powder. However, the stoichiometric balance between the oxidizer and the fuel proportions plays an important role in the redox reaction to occur, and the maximum heat is generated during the synthesis only if both the proportions are balanced well.

4.3.4 Precipitation method

Precipitation method is a type of wet-chemical method that yields the end products in the form of precipitate in an aqueous solution. The procedures involved in both precipitation and wet-chemical methods are similar, but the major difference is that the end product formed in the former precipitates out from the solution and that formed in the

Figure 4.1 Combustion synthesis.

latter remains dissolved in the solution. The final product of the precipitation method can be obtained by several washing in distilled water and other organic solvents followed by drying. In the wet-chemical method, the solution needs to be dried completely to get the final product. Precipitation method is the most appropriate technique for producing fluoride, oxide, or oxyfluoride-based phosphors. Typically, chloride, acetate, or nitrate precursors are chosen for carrying out the synthesis. The precursors are dissolved in a solvent (preferably distilled water, ethanol, cyclohexane, or *N*-*N*-dimethylformaldehyde), which are then mixed together. A precipitating agent is kept on adding slowly to this solution along with constant stirring. This results in the formation of hydroxide, fluoride, or carbonate compounds in the form of a precipitate. The precipitated phosphor particles are washed several times in distilled water and other suitable organic solvents such as ethanol and cyclohexane to remove any water-soluble and organic impurity content present in the yield. This can be done either by filtering or by the centrifuging process. The final product must then be dried in an oven to decompose the hydroxides or carbonates and then subjected to high-temperature annealing to crystallize the powder. The condition for the success of this method is that the final product must precipitate out from the solution and must not be soluble in the solvent. Hence, the solubility of the precursors and the final product must be confirmed beforehand. This method can produce uniform-sized particles with narrow size distribution with proper selection of the precursors, precipitating agent, and solvent, by controlling the pH of the solution, deciding the stirring and heating rate of the solution and the order of addition of the precursors. It was observed that the coprecipitation method induces a better reaction in acidic conditions. On the other hand, the formation of larger crystallites with less surface defects is possible in alkali conditions. Hence, the photoluminescence intensity is more pronounced in the alkali or acidic conditions, while the moderate pH values do not support such intense emissions [7].

4.3.5 Solvothermal method

Solvothermal synthesis route is a process taking place in a closed system that requires high temperatures and pressures to induce a chemical reaction or decomposition of the precursor materials to form the desired compound directly from a solution. The solvothermal method is applicable to both the aqueous and nonaqueous forms of solvents. Few of the solvents preferred in this method are water, ethanol, methanol, ammonia, carbon dioxide, hydrochloric acid, and hydrofluoric acid. The term "solvothermal" changes to "hydrothermal" when the solvent used is water. The process involves the mixing of the precursors in the solvent and then sealing them in an autoclave. The autoclave is then heated at temperatures above the boiling point of the solvent. The autoclave acts as a closed system that elevates the temperature and pressure of the solution and subsequently crystallizes the dissolved material. With proper selection of the precursor composition and the reaction conditions, it is possible to achieve high purity and homogeneously dispersed nanoparticles with a very narrow size distribution. This method requires no high-temperature treatments. Despite being a low-temperature synthesis, this method yields phosphors with high crystallinity. The size, morphology, and phase

formation of the phosphors greatly depend on the reaction temperatures, pH, solvent, and the precursor compositions. A major disadvantage of this method lies in its inability to produce bulk quantity of phosphors in a single run. The small-sized autoclaves limit the mass production of phosphors.

4.3.6 Microwave-assisted method

Microwave-assisted synthesis techniques have now emerged as a valuable substitute for many other conventional methods used for the synthesis of inorganic phosphors, organic compounds, or polymers. This technique is highly effective for the synthesis of well-defined nanomaterials. Microwaves are used to heat the precursors to induce chemical reactions between them to form a final product. The difference from the conventional heating lies on the fact that microwaves can produce very high temperatures at ambient conditions. Microwaves target a molecule with dipole nature (mostly water molecules) to induce heat. A dipolar molecule tends to efficiently absorb microwaves and convert them into heat. When the dipoles get excited by microwaves, they start to align themselves in the direction of the external field. The reorientation of the molecules in phase with the externally applied field causes strong agitation resulting in strong internal heating. Hence, it is highly essential to dissolve the precursors in a polar solvent to effectively produce phosphors by this method. However, every solvent will absorb the microwave radiations differently as they have a different degree of polarity within their molecules. More the strength of polarity of the solvent more will be the heat generated. Sometimes, microwave methods are combined with some other methods to produce phosphors with higher quality. To name a few, microwave-modified sol−gel method [8], microwave-assisted hydrothermal method [9], microwave solid-state synthesis [10], etc. have been performed.

4.3.7 Sonochemical synthesis

To avoid the complications in attaining high temperatures, high pressures, and longer duration of synthesis, a novel method for the preparation of nano- to bulk-sized phosphors have originated by employing high-intensity ultrasound. This method, which is more commonly termed as sonochemical synthesis, involves an acoustic cavitation process that involves the formation, growth, and implosive collapse of bubbles [11]. The physical and the chemical effects of ultrasound facilitate the production of nanophosphors in a room-temperature liquid, without subjecting itself to any high-temperature/pressure treatments. An added advantage of this method is that it can promote the diffusion of dopant ion into spherical nanoparticles. Sonochemical synthesis employs a powerful tool in the form of ultrasonic sound waves, which when irradiated to a solution of metal precursors result in wondrous effects. The physical and chemical effects of ultrasound irradiation prove fruitful when the aim is to develop nanomaterials. Most of the time, the sonochemical synthesis method can be assumed to be a type of precipitation method that uses an additional tool in the form of ultrasonic waves. The solution of precursors is maintained at a specific pH value and then subjected to ultrasonic radiation. Simultaneously, a precipitating agent is added drop by drop

to the solution. The frequency and duration of the ultrasonic radiation depend on the synthesis requirements. During the process, the temperature of the solution is maintained at about 80 °C using a water bath. Sonochemical methods offer a wide range of options to develop phosphors with controlled morphologies and dimensions by simply monitoring the reaction conditions and precursor compositions.

4.3.8 Template-assisted method

Template-assisted methods are adopted to synthesize phosphors in the nanoscale with controlled morphology and size. These are one of those novel methods that give a good yield of products with improved particle size distribution. This method involves three stages: (1) preparation of template materials; (2) deposition of target materials on the template, and (3) removal of the template from the target without any tension between them. On the basis of the template employed, template-assisted methods can be categorized into hard templates and soft templates. The templates are meant to act as physical platforms to support the growth of material and to confine its shape and size. They are inert and do not diffuse into the target material that is deposited over them. After synthesis, the fully developed nanophosphors are subjected to several washing and cleaning procedures to remove the templates. The hard-template method is preferred for the fabrication of a large number of materials with controllable structures, morphologies, and sizes. The templates used are generally nonflexible, and the materials preferred to form hard templates can be carbon nanotubes, silica spheres, polystyrene spheres, carbonaceous microspheres, or metal oxide particles [12]. The soft-template method involves the deposition of target materials on a flexible and soft material such as surfactants, organic macromolecules, and biomolecules. This method has some shortcomings as compared to a hard-template method such as low yield and instability of the prepared template, inefficiency in material processing, and rigorous conditions required during the synthesis. The earlier mentioned methods required predeveloped templates for depositing the target material. Apart from these categories, a third-type of template-assisted method can be listed in the form of in-situ template method that rules out the need for an already prepared template. Contrary to the previous two methods, the in-situ template method itself develops a template during the synthesis of the target material.

4.3.9 Laser ablation

Laser ablation cannot be considered as a method to synthesis a phosphor from individual raw materials. Yet, the readily available bulk phosphors can be used to form their thin films or nanoparticles with the aid of high-power lasers. Laser ablation is a physical vapor deposition method. The prerequisites are the solid target of the phosphor (which can be developed by pelletizing the phosphor powders) and a high-power UV-emitting laser. The solid target is placed in a vacuum tube and irradiated with a focused laser beam. The heat generated on the irradiated zone of the target by the laser

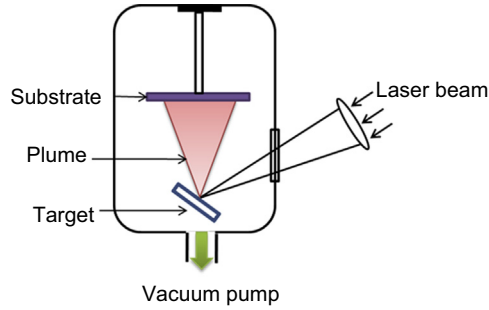

Figure 4.2 Laser ablation.

compels the target material to sublime or evaporate and form a plume. The plume of phosphor deposits on the substrate to form a thin film. If the laser flux is very high, then the target stands a chance to get converted into plasma. A schematic representation of laser ablation is shown in Fig. 4.2. Laser ablation has other nomenclatures such as laser deposition and laser evaporation. Generally, laser ablation is performed using a pulsed laser, and hence, it is also termed as a pulsed-laser deposition. If the laser intensity is high enough, then a continuous-wave laser can also be used to ablate the target.

4.3.10 Spray pyrolysis

Spray pyrolysis is an effective and lost-cost method for the synthesis of submicron and nano-sized phosphors, especially oxides. It can produce porous films with high-density packaging. This method is also important for the preparation of ultrafine phosphor powder with highly uniform particles, narrow size distribution, and high purity. In this method, the solution of precursors is sprayed or injected on a heated substrate where the precursors react to form a thin film of the desired compound. A general setup consists of an atomizer, a solution consisting of all the precursors, a temperature controller, and a substrate heater. The procedure involves the generation of droplets of the precursor solution using an atomizer. The droplets are then carried through a tube furnace onto a hot substrate by a carrier gas. The droplets are, then, vaporized vigorously, and the precipitate is subjected to thermolysis. The size and morphology of the particles are dependent on the concentration of reactants in the precursor solution, nature of additives, flow rate of droplets, and other preparatory conditions [13]. In ultrasonic spray pyrolysis, an ultrasonic atomizer is used to generate droplets of precursor solution. A schematic representation of the ultrasonic spray pyrolysis setup can be seen in Fig. 4.3 [13].

There are some disadvantages, too, which are linked with this method [13]. It is not suitable for the synthesis of nonoxide-based materials like sulfides, if they are processed in a normal air atmosphere. In addition, there is difficulty in recording the accurate growth temperatures during the deposition. The biggest concern is the low yield obtained and the difficulty in scaling up the overall yield.

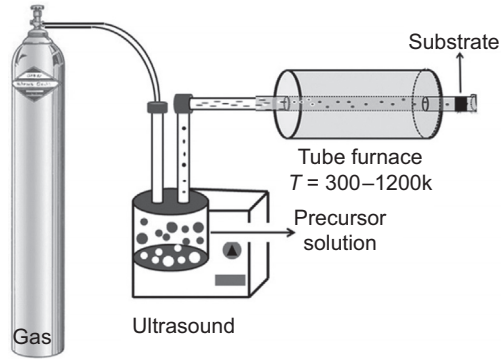

Figure 4.3 Schematic representation of ultrasonic spray pyrolysis technique.
Reproduced with permission from T.V. Gavrilović, D.J. Jovanović, M.D. Dramićanin, Synthesis of multifunctional inorganic materials: from micrometer to nanometer dimensions, in: Nanomaterials for Green Energy, Elsevier, 2018 55−81. Copyright 2018 Elsevier.

4.3.11 Microemulsions

When two immiscible liquids are compelled to mix together by stirring or mechanical agitation, they form an emulsion. The liquid in lesser proportion tends to form layers, droplets, or coagulated droplets to separate itself from the other liquid. The sizes of the droplets are generally larger than 100 nm up to few millimeters. These droplets form macroemulsions. There is another class of immiscible liquids, known as microemulsions, in which the droplets are usually in the range of 1−100 nm. Microemulsions are stabilized using a surfactant and a cosurfactant. One of the liquids used in microemulsion synthesis is water and the other is oil, which is usually a complex mixture of hydrocarbons with olefins. When hydrocarbons are introduced into an aqueous solution, it starts floating on the aqueous solution. When a sufficient quantity of surfactant is introduced into this mixture, they try to form an entity known as micelles. In other words, micelles are aggregates of the surfactant molecules dispersed in a colloidal solution. Micelles are formed when the organic solvents or oil is in lesser proportion than water. Hence, micelles can be called as oil-in-water (o/w) microemulsions. The head groups of micelles float in water, while the tail group remains inside the oil. Thus, the head group is hydrophilic, while the tail group is hydrophobic. When the water is in lesser proportion than oil, the microemulsions are called water-in-oil (w/o) microemulsions or reverse micelles. Micelles and reverse micelles are formed depending on the concentration of the water and the organic solvent, as shown in Fig. 4.4.

The shape and size of a micelle or reverse micelle are strongly dependent on the solution conditions such as pH, temperature, ionic strength, and surfactant concentration. Reverse micelles are more profoundly used for the synthesis of nanophosphors. There are two techniques of synthesizing nanophosphors from reverse micelles. The first method involves the mixing of two different reverse micelles with different precursors. In the second method, all the precursors are mixed in the same reverse micelles. The mixing of reverse micelles leads to intermicellar exchange, which is

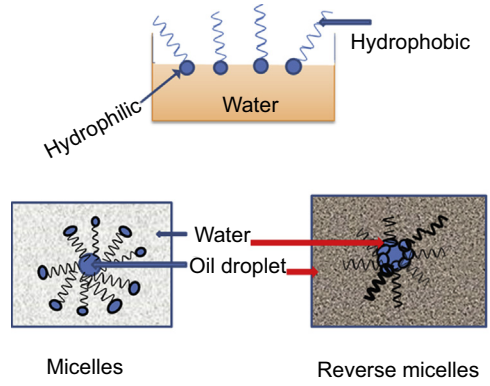

Figure 4.4 Formation of micelles and reverse micelles.

followed by the chemical reaction between the reactants to precipitate the desired product in water droplets of reverse micelles. This method too suffers from some disadvantages. This method requires those organic solvents that can result in microemulsion and a very high quantity of surfactants. It also results in low yield and can incorporate defects or impurities in the yield.

4.3.12 Vapor deposition

Nano-sized or submicron-sized phosphors in the form of particles, thin films, or multilayer films can be synthesized by evaporating the precursors and depositing them onto a suitable substrate. In vapor deposition, materials can be evaporated either by physical methods or by chemical methods. Consequently, they are categorized into two classes, viz. physical vapor deposition (PVD) and chemical vapor deposition (CVD). In physical vapor deposition, the evaporation of materials is achieved by laser heating, resistive heating, sputtering, or electron-beam heating. A properly designed vacuum system is essential to evaporate and deposit the vapors on the substrate by avoiding the uncontrolled oxidation of materials. PVD methods are less commonly implemented due to numerous demerits and sophisticated requirements. The CVD process uses the reactant chemicals in the vapor phase, which are then transported by a carrier gas towards a substrate placed at a high temperature in a reaction chamber. When the reactant vapors come in contact with the substrate, they diffuse into the substrate surface and undergo chemical reactions at suitable sites to nucleate and grow into a thin film of the desired material. This is also accompanied by the formation of some by-products, which are then transported back to the gaseous phase and removed from the substrate. CVD methods are preferred for the synthesis of inorganic phosphors over PVD techniques owing to numerous advantages. Some of the advantages of CVD techniques can be listed as follows:

- Facile techniques.
- Requires much less temperature for the synthesis ($<350\ ^{\circ}C$).

- Large amount of yield can be obtained.
- Cost-effective and requires less instrumentation as compared to many physical deposition methods.
- Possibility to dope foreign ions (or atoms) during the synthesis.
- Doping of foreign atoms (ions) possible during the synthesis.
- Possible to control the sizes and shapes of phosphor particles.
- Higher growth rates and better quality of deposition.

4.3.13 Colloidal route

Colloidal synthesis is best noted for the synthesis of nanophosphors and quantum dots. It can also be employed for preparing core−shell structures with good control over its shape and size. Generally, a three-necked flask is preferred to carry out the reaction between the precursors, as shown in Fig. 4.5. The precursors are either inorganic salts or organometallic compounds of the constituent elements, which are added to a suitable reaction media already containing a surfactant. The injection of the precursors can be made at room temperature, but it is a common practice to inject the precursors at relatively high temperatures ranging between 100 and 300 °C. As a result, the colloidal route is often known as the hot-injection method. On immediately increasing the temperature after injection, the nucleation period and the particle growth can be arrested. The precursors undergo thermal decomposition to release large concentrations of the constituents in a small duration. This leads to a small period of nucleation, and the developed nuclei grow very slowly. The surfactants present in the reaction media control the nucleation and further growth of nuclei. The entire reaction must be carried out in an inert atmosphere to avoid any contamination or oxidation of the desired product. The end products need to be washed several times in water or suitable organic solvents like ethanol and cyclohexane. It can then, be dried to obtain nanophosphors or dispersed in a solvent to form quantum dots. It is also possible to prepare

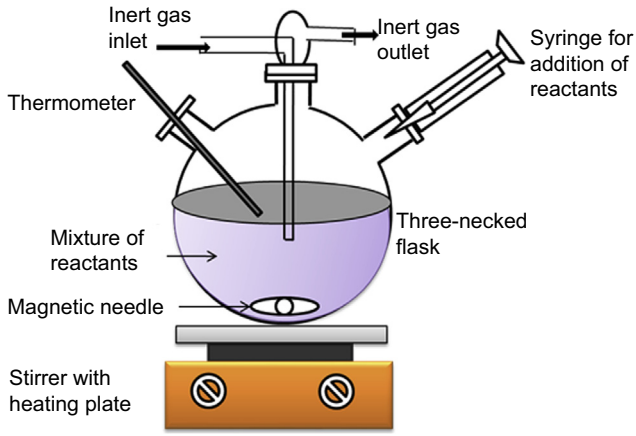

Figure 4.5 Colloidal synthesis of nanophosphors.

core−shell structures of the same or different compositions by repeating this procedure. For this, a suitable core material needs to be introduced before injecting the precursors in the reaction media.

4.4 Red/orange-emitting phosphors

Eu^{3+}-doped phosphors are the most sought red-emitting phosphors due to their deep red emissions from 593 to 650 nm [14]. A perfect red component with pure color purity is obtained by the $^5D_0 \rightarrow {}^7F_2$ transition of Eu^{3+}, corresponding to the emission wavelength ~615 nm [14,15]. There is a general belief that Eu^{3+} ions will show their characteristic emission even if they are doped in mere sand. However, not all the Eu^{3+}-doped phosphors are suitable for lighting purposes. While considering phosphors for lighting, the major priority must be given to those materials that have a broad excitation band. Although Eu^{3+} ions are known for their characteristic excitation and emission peaks corresponding to forbidden f−f transitions, they have a useful charge transfer band in the UV region that could be utilized to sensitize the red emission [16]. The charge transfer band acts as a sensitizer that absorbs light in the UV region and transfers it to Eu^{3+} ions, thereby reducing them to Eu^{2+} formally. In some cases, the charge transfer band is more intense than the characteristic excitation peaks of Eu^{3+} [17]. Yet, this characteristic has no advantage in NUV-excited red-emitting LEDs, as the charge transfer band of Eu^{3+} seldom covers the NUV region [18]. The only possible way to employ Eu^{3+}-doped phosphor for red-emitting NUV-LEDs is by selecting a host in which Eu^{3+} ions shall occupy a site with lower symmetry [19]. When Eu^{3+} ions occupy noncentrosymmetric site in a host lattice, there is a relaxation in the parity-forbidden 4f−4f transition and the efficiency of the 4f−4f excitation band is improved. A vast number of Eu^{3+}-doped phosphors have been reported till date and to name a few, these include Y_2O_3:Eu^{3+} [20], YVO_4:Eu^{3+} [21], $CaTiO_3$:Eu^{3+} [22], Ca_2ZnWO_6:Eu^{3+} [23], $LaPO_4$:Eu^{3+} [24], and $GdAlO_3$:Eu^{3+} [25]. Except for the 396-nm excitation peak, no other excitation band of Eu^{3+} lies in the NUV region. This peak cannot be intense unless Eu^{3+} ions occupy a site with lower symmetry and partially permit the parity-forbidden 4f−4f transitions to occur. Hence, we must rethink the possibility of using Eu^{3+}-doped phosphors in the pc-LEDs. A similar case goes for the phosphors doped with Sm^{3+}: Sm^{3+}-doped phosphors give a characteristic excitation peak at 405 nm, which is a forbidden 4f−4f transition [5,14,26−29]. In addition, there are very few cases in which Sm^{3+}-doped phosphors turned out to give bright red luminescence [26,30,31]. Otherwise, in most cases, Sm^{3+} is commonly known to give orange-red luminescence [27,28,32−36].

Another approach for developing red-emitting phosphors is to find Eu^{2+}-doped nitride or oxynitride phosphors [37]. Nitride-based phosphors are known to exhibit outstanding stability, both thermally and chemically, accompanied by excellent luminescence properties [38,39]. Besides, nitride hosts provide highly covalent surroundings for the Eu^{2+} ions to experience a strong crystal field effect and shift its emission band towards longer wavelengths. Sialon type of hosts has attracted huge attention due to their ability to absorb strongly in the UV to the blue region [40,41]. However, not all

sialon materials are known to bring about red luminescence with Eu^{2+} doping [42,43]. Although nitride-based phosphors activated with Eu^{2+} provide excellent red luminescence combined with good thermal and chemical stability, there is a big matter of concern regarding the complexity of its synthesis. This justifies the fact that comparatively very few nitride phosphors are available for discussion. Eu^{2+} ions have also triggered red luminescence in some of the borate phosphors, which is a rare occurrence. Zhang et al. [44] have reported red luminescence in $LiSrBO_3$:Eu^{2+} phosphors, but with the coexistence of a small amount of $LiSr_4(BO_3)_3$ phase. The phosphors were prepared by adding 40 and 60 mol% excess of boric acid, and it was inferred that more the amount of boric acid was added, the percentage of $LiSrBO_3$ phase increased in the sample. Irrespective of the percentage of $LiSrBO_3$ phase and $LiSr_4(BO_3)_3$ phase in the sample, a broad emission band was obtained with the peak centered at 618 nm. However, this is in contrast to the report published by Wang et al., wherein $LiSrBO_3$:Eu^{2+} phosphors were endowed with a yellowish-green light emission peak at 565 nm [45]. On the other hand, Wang et al. and Wu et al. independently reported that $LiSr_4(BO_3)_3$:Eu^{2+} phosphors produced a broad emission band in the red region of the visible spectrum [46,47]. From this, we may infer that the $LiSr_4(BO_3)_3$ phase is responsible for the red luminescence, whereas $LiSrBO_3$ phase produces yellowish-green emission. $Ba_2Mg(BO_3)_2$:Eu^{2+} phosphors have also exhibited orange-yellow luminescence under 365 nm UV excitation [48]. However, the addition of Mn^{2+} ions to this phosphor has shifted the emission peak to a longer wavelength. $Ba_2Mg(BO_3)_2$:Eu^{2+}, Mn^{2+} phosphors depict a broad excitation ranging from 250 to 450 nm and the red emission is intensified as well as purified until the Mn^{2+} concentration increased up to 0.05 mol. Some halophosphates like $K_2Ca(PO_4)F$:Eu^{2+} phosphor has also shown broad red emission bands [49]. Alkali earth sulfides also dictate red luminescence with Eu^{2+} ions, but their thermal instability and sensitivity to moisture do not promote their application as red-emitting phosphor materials in LEDs [50].

Yet another approach is to develop phosphor materials that are doped with Mn^{4+} ions [51−54]. Mn^{4+} ions show a distinct $^2E_g \rightarrow {}^4A_{2g}$ transition in the crystal field that is octahedrally symmetric and this transition corresponds to deep red luminescence with narrow-band emission peaks in the range 600−750 nm with high quantum efficiency [55−60]. Although the emission peaks corresponding to $^2E_g \rightarrow {}^4A_{2g}$ transition is spin-forbidden, their excitation peaks lying in the NUV region and blue region correspond to the spin-allowed $^4A_{2g} \rightarrow {}^4T_{2g}$ and $^4A_{2g} \rightarrow {}^4T_{1g}$ transitions, respectively. The excitation peaks are broad and can be easily excited by InGaN chips [58]. This is a noteworthy feature required for a phosphor to be used in pc-LEDs. However, the main difficulty lies in controlling the valence state of Mn ions that are doped in the host material. Mn can exist in 2+, 3+, 4+, 6+, and 7+ oxidation states, and the synthesis temperature has a huge effect on the occurrence of a particular valence state of Mn ions [61]. Mn^{4+} emission is tuned depending on the host material in which it is doped. When the host material is highly ionic, as in the case of fluorides, the prominent emission peak is obtained in the range 600−630 nm [56,60,62−66]. A number of complex alkaline metal fluorides have been reported to be excellent host materials for Mn^{4+} doping. Jiang et al. [62] have synthesized the hexagonal phase of $BaSiF_6$:Mn^{4+} phosphors by the hydrothermal method. Its room-temperature emission

spectrum consists of narrow-band peaks at 615 nm, 632 nm and 648 nm, with an exceptionally intense and prominent peak at 632 nm. The peak at 615 nm gradually disappears when the emission spectrum is measured at 78 K, and this peak has been associated with the anti-Stokes vibronic sidebands related to the excited state ^2E of Mn^{4+} ions [62]. On the other hand, the prominent emission band is obtained in the range 630−700 nm when the host material is covalent, as in the case of oxides [58−60,67−69]. The crystal field effect is found to strongly affect the luminescence of Mn^{4+} ions doped in oxides such as $Sr_4Al_{14}O_{25}$, Ba_2GdNbO_6, and $Mg_7Ga_2GeO_{12}$ [58,59,67,69,70]. Mn^{2+} is also likely to show red luminescence in some cases. Unlike Mn^{4+}, a broad emission band is obtained for Mn^{2+}-doped phosphors [71,72].

4.5 Yellow-emitting phosphors

Whenever there is a discussion about the yellow-emitting phosphors, the first thing that comes to our mind is about $Y_3Al_5O_{12}:Ce^{3+}$ phosphors. Cerium-doped yttrium aluminum garnet phosphors (more commonly known as $Y_3Al_5O_{12}:Ce^{3+}$ or YAG:Ce) is the most commercially successful yellow-emitting phosphor that were combined with the blue-emitting InGaN chips for the production of WLEDs. YAG:Ce has dominated all other phosphors in the yellow region of the visible light spectrum for long and perhaps, we may even feel if there is any necessity to look for some other alternative yellow phosphors in the magnificent presence of YAG:Ce. YAG:Ce has acceptable values of phonon energies and other electron-vibrational interaction parameters, thereby providing a convenient environment for the Ce^{3+} emission to take place [73−75]. It is also possible to increase the intensity of Ce^{3+} emission by converting the remnant Ce^{4+} ions in YAG into Ce^{3+} using a suitable reduction atmosphere [76]. It is also possible to increase the luminescence intensity by optimizing the calcination temperature and duration, thereby enabling a homogenous distribution of Ce^{3+} ions in the YAG host [77]. Furthermore, Ga^{3+}-ion doping can be done to improve its thermal stability [78]. Despite this fact, there certainly is an urgency to research for new yellow phosphors when we come to know that YAG:Ce-based WLEDs deliver CRI values ~70 and high correlated color temperatures (CCT) [79,80]. In addition, their use in high-power LEDs shall be limited citing their inefficiency to provide the same spectral energy distribution at higher temperatures [81]. To modify its emission spectrum, different synthesis methods have been adopted and the structural modifications were made by doping Tb^{3+}, Gd^{3+}, Mg^{2+}, or Ti^{4+} in the Y^{3+} site, Ga^{3+} or In^{3+} in the Al^{3+} site, and codoping Sm^{3+}, Eu^{3+}, Tb^{3+}, or Pr^{3+} ions along with Ce^{3+} [82−91]. Researchers have also tried to replace the Y^{3+} ion with Gd^{3+}, La^{3+}, or Lu^{3+} ions, but their color emissions failed to optimize at the desired level [92−95]. Aboulaich et al. [96] devised a method to increase its CRI by preparing YAG:Ce nanophosphors and $CuInS_2/ZnS$ quantum dots individually and then piling them up as bilayered YAG:Ce—$CuInS_2/ZnS$ structure. The WLEDs fabricated using this bilayered structure delivered a higher CRI (>80) and lower CCT.

In the meantime, several new yellow-emitting phosphors have emerged as suitable candidates for WLEDs. Nitride-based host materials have provided a good platform for Eu^{2+} and Ce^{3+} ions to luminesce in the yellow region. $Ba_2Si_5N_8:Eu^{2+}$ [97], $SrSi_2O_2N_2:Eu^{2+}$ [98], $CaAlSiN_3:Ce^{3+}$ [99], Eu^{2+}-doped Ca-α-SiAlON [100–102], $La_3Si_6N_{11}:Ce^{3+}$ [81], $CaSi_2O_2N_2:Eu^{2+}$ [103], and Mg-α/β-SiAlON [104] are some examples of yellow-emitting nitride phosphors that are activated with Ce^{3+} and Eu^{2+} ions. The strong nephelauxetic effect found in nitride hosts provides a suitable environment for the Ce^{3+} and Eu^{2+} ions to tune their emission in the yellow–orange–red region of the visible light spectrum. Besides nitrides, there are quite a number of oxide-based host compounds that have also shown yellow luminescence with these ions. Garnets such as $Lu_{3-x}Y_xMgAl_3SiO_{12}:Ce^{3+}$ and $CaY_2Al_4SiO_{12}:Ce^{3+}$ have also shown promises as efficient yellow-emitting phosphor [105,106]. $Lu_{3-x}Y_xMgAl_3SiO_{12}:Ce^{3+}$ has shown high yellow luminescence with good thermal stability and quantum efficiency. However, the emission peak wavelength shows a redshift with the increasing substitution of larger Y^{3+} ions in relatively smaller Lu^{3+} sites. This substitution causes shrinkage of CeO_8 polyhedron and provides a more varied local environment around the Ce^{3+} ions. Yellow–orange-emitting $Lu_{2-x}CaMg_2Si_{2.9}Ti_{0.1}O_{12}:xCe^{3+}$ garnets also showed a redshift in the emission spectrum, but with the increasing substitution of Ce^{3+} ions in the Lu^{3+} sites [107]. On the other hand, $Lu_3MgAl_3SiO_{12}:Ce^{3+}$ garnets gave a stable yellow emission that did not shift its peak position with the variation in Ce concentration [108]. Another garnet with superior luminescence properties was identified to be $Gd_3Sc_2Al_3O_{12}:Ce^{3+}$ that could incorporate six times more Ce^{3+} ions than YAG and exhibit 30% more external quantum yield than YAG:Ce [109]. However, its applicability gets limited due to lower temperature quenching as compared to YAG:Ce. Apart from garnets, other oxide compounds such as silicates, phosphates, and borates have also shown yellow luminescence with Ce^{3+} and Eu^{2+} ions. Phosphates are high-bandgap materials and their Ce^{3+}- or Eu^{2+}-emissions are often limited to the NUV or blue region. However, some special class of Eu^{2+}-doped phosphates has shown broadband yellow emission. Phosphates such as $Sr_9Mg_{1.5}(PO_4)_7:Eu^{2+}$ [110], $Sr_8MgGd(PO_4)_7:Eu^{2+}$ [111], $Sr_8MgY(PO_4)_7:Eu^{2+}$ [112], $Sr_8MgLa(PO_4)_7:Eu^{2+}$ [112], $Sr_8CaBi(PO_4)_7:Eu^{2+}$ [113], $Ca_{10}Na(PO_4)_7:Eu^{2+}$ [114], and $Ba_4Gd_3Na_3(PO_4)_6F_2:Eu^{2+}$ [115] have shown yellow luminescence but with much lower quantum yields. Unlike garnets, phosphates cannot be excited by blue-LEDs and the majority of their excitation spectra covers the NUV region. A similar trend goes for Eu^{2+}-activated borates such as $Sr_3B_2O_6:Eu^{2+}$ [79] and $Ca_2BO_3Cl:Eu^{2+}$ [116,117], wherein their excitation spectra are mainly covered in the NUV region with a slight extension in the blue region. However, we can consider that these borates can be excited by both blue-LED chips and more efficiently by NUV chips. On the other hand, Eu^{2+}-doped silicates can be efficiently excited with blue-LEDs and produce yellow luminescence. Some examples of yellow-emitting silicate phosphors are $Sr_3SiO_5:Eu^{2+}$ [118], $(Ca,Sr)_7(SiO_3)_6Cl_2:Eu^{2+}$ [119], $M_2MgSi_2O_7:Eu^{2+}$ [120], $Na_3K(Si_{1-x}Al_x)_8O_{16\pm\delta}:Eu^{2+}$ [121], $Sr_{1.44}Ba_{0.46}SiO_4:0.1Eu^{2+}$ [122], and $CaSrSiO_4:Eu^{2+}$ [123].

4.6 Green-emitting phosphors

Among the tricolor phosphors, a relatively lesser quantity of literature is available on the green-emitting phosphors than the other color-emitting phosphors. However, this available literature itself is enormously vast to provide a sound discussion and review the developments made by the green-emitting phosphors in the LED technology. Tb^{3+} and Mn^{2+} ions are, generally, found to produce green emission in numerous host materials [124–128]. An adequate amount of Mn^{2+} ions can produce luminescence with greater intensity if they are sensitized with Ce^{3+} or Eu^{2+} ions. At times, even Ce^{3+} and Eu^{2+} ions themselves are capable of producing green luminescence due to their tunable 4f ↔ 5d transitions. The crystal field strength allows the Mn^{2+} emission to vary from green to red. However, their low absorption in the UV region due to forbidden $^4T_1-^6A_1$ transition is a disappointing factor from the perspective of LED manufacturers.

Tb^{3+} ions are known to produce only green luminescence, and hence, they are often doped in host materials with a suitable local environment for the Tb^{3+} ions to luminesce. These ions are not yet reported to produce any color other than green. Hence, it is a sure shot that Tb^{3+} ions will either produce green light emission or no emission at all, depending on the conditions of the crystal local environment in which it is doped. However, there is a chance that Tb ions, which are introduced into the host, may take up +4 charge state and in this case, no luminescence will be observed. In such a situation, it becomes essential to subject the phosphor to heating under the reducing conditions and convert the Tb^{4+} ions into Tb^{3+} ions. Generally, the peak wavelength positions of Tb^{3+} ions can be located at 490 nm, 540 nm, 580 nm and 620 nm corresponding to the transitions $^5D_4 \rightarrow {}^7F_6$, $^5D_4 \rightarrow {}^7F_5$, $^5D_4 \rightarrow {}^7F_4$, and $^5D_4 \rightarrow {}^7F_3$, respectively [129]. These emission peaks are narrow-band emissions arising due to the spin-forbidden 4f–4f transitions, and hence, their peak positions will show variations of only ±5 nm from host to host. Among these, the $^5D_4 \rightarrow {}^7F_5$ transition often gives a prominent intensity and contributes to the overall green emission of the phosphor. The excitation spectrum of Tb^{3+} consists of spin-allowed 4f–5d transition that towers a broadband in the range of 200–270 nm and numerous spin-forbidden 4f–4f transitions lying in the NUV range. In most cases, the most intense excitation peak is found to be occurring due to the spin-allowed transitions that are not suitable for LEDs. So, most of the Tb^{3+}-doped phosphors fail to meet the criterion for LEDs even though they exhibit strong green luminescence [10,129–138]. There are very few cases wherein a Tb^{3+} ion exhibits a prominent excitation peak at ~380 nm [139–143]. However, this excitation peak corresponds to spin-forbidden 4f–4f transitions, and it becomes essential to sensitize it with Eu^{2+} or Ce^{3+} ions. Even the use of such sensitizers do not guarantee a pure green color emission as Eu^{2+} and Ce^{3+} ions will produce their emission colors and blend with the green color emission of Tb^{3+} to form an entirely different color [144]. In most cases, the excitation spectrum of Ce^{3+} ions falls in the UV region, and this rules out its applicability for NUV convertible LEDs [145]. It is still a matter of concern to identify suitable Tb^{3+}-based phosphors for green-emitting LEDs. Phosphors that are singly doped

with Tb^{3+} are best used as green-emitting phosphors for display devices or mercury-excited lamps. On the other hand, phosphors codoped with Tb^{3+} and Eu^{2+}/Ce^{3+} offer color-tunable properties in most cases. With proper selection of the dopant combination, it is possible to obtain green luminescence with Ce−Tb or Eu−Tb pairs that have its excitation spectra overlapping with the emission of NUV or blue-LED chips. For example, $BaY_2Si_3O_{10}:Ce^{3+},Tb^{3+}$ shows color tuning from blue to green with a fixed concentration of Ce and varying concentration of Tb ions [146]. $BaY_2Si_3O_{10}:0.05Ce^{3+},1.00Tb^{3+}$ phosphor gives greenish-yellow luminescence with CIE coordinates located at (0.294, 0.562) and its excitation spectrum covers a broad region from 250 to 400 nm. Nevertheless, it still has a drawback that the excitation spectrum peaks at 337 nm and fails to efficiently get excited by NUV chips. $Sr_3Y(PO_4)_3:Eu^{2+},Tb^{3+}$ phosphor is an example of green luminescence arising from the Eu−Tb pair that can be excited by NUV chips [147].

Eu^{2+} ions have proved to provide green luminescence when they are singly doped in some host materials. Eu^{2+}-based phosphors are most sought for their excellent excitation band that broadly covers the NUV to blue region and their intense broadband emission. The parity-allowed 4f−5d transitions of Eu^{2+} are tunable from UV to red luminescence by changing the host environment in which these ions are introduced. Silicate materials are privileged with high chemical and physical stability, and these materials provide a favorable host environment for Eu^{2+} to luminesce in the green to yellow region. Some examples of green-emitting Eu^{2+}-doped silicates are $Ca_{2-x}Sr_xSiO_4:Eu^{2+}$ [148], $SrBaSiO_4:Eu^{2+}$ [149], $Ca_{15}(PO_4)_2(SiO_4)_6:Eu^{2+}$ [150], $M_2SiO_4:Eu^{2+}$ (M = Ca, Sr, Ba) [151], $Ba_2CaZn_2Si_6O_{17}:Eu^{2+}$ [152], and $Sr_{3.5}Mg_{0.5}Si_3O_8Cl_4:Eu^{2+}$ [153]. $Ca_3SiO_4Cl_2:Eu^{2+}$ has shown green luminescence under 400 nm blue excitation [154]. Its thermal stability was found to be exceptionally higher than the commercially used green-emitting $Ba_2SiO_4:Eu^{2+}$ phosphor. In some cases, the hosts provide two or more types of cation sites for the Eu^{2+} ions to occupy. For example, $Ca_6Sr_4(Si_2O_7)_3Cl_2$ provides two types of luminescence centers due to the presence of two crystallographically different Sr-sites, and this gives rise to two Eu^{2+} emission bands that are centered at 508 nm and 560 nm, respectively [155]. $Sr_2LiSiO_4F:Eu^{2+}$ also shows such dual emission bands at 475 nm and 505 nm due to the occupancy of Eu ions in dissimilar Sr-sites [156]. Exceptional chemical, thermal, and mechanical stability in addition to outstanding luminescence properties were demonstrated by nitridosilicates as well. Eu^{2+}-doped nitridosilicates such as $Ba_3Si_6O_9N_4:Eu^{2+}$ [157], $Ba_3Si_6O_{12}N_2:Eu^{2+}$ [158], $Ba_2LiSi_7AlN_{12}:Eu^{2+}$ [159], and $SrSi_2O_2N_2:Eu^{2+}$ [160] have shown promises for green-emitting LEDs.

4.7 Blue-emitting phosphors

The advent of InGaN LED chips in 1994 has paved the way for several advancements in the field of lighting [161]. The combination of a blue-LED chip with a yellow phosphor coating, especially yellow-emitting $YAG:Ce^{3+}$ phosphor, is known to produce white light emission. Meanwhile, the poor CRI of blue LED + yellow phosphor

combination has been disapproved by many researchers, and to overcome this problem a new combination has been suggested wherein a NUV-LED chip shall excite the tricolor red, green, blue phosphors (RGB phosphors). This approach is considered as one of the best approaches to produce white light with high CRI and higher luminous efficiency [162]. Blue-emitting phosphors, thus, gained enough significance in the context of white-light-emitting NUV LED + RGB phosphors' combination. Blue-emitting phosphors have noteworthy applications in plasma display panels, backlight for liquid crystal displays, and tricolor lamps. One of the most commercially used blue phosphor is $BaMgAl_{10}O_{17}:Eu^{2+}$ phosphor (more commonly known as BAM phosphor) [163,164]. The popularity of BAM:Eu^{2+} phosphor has inspired several researchers to investigate its optical and structural properties to a further depth and also design new methods for the preparation [165−171]. Its excitation spectrum covers a wide range from 225 nm to 410 nm. However, the excitation band shows prominent absorption in the 250−300-nm range and relatively much lesser absorption in the 360−410-nm range, which is quite unsuitable for the LED fabrication. Consequently, this led to the search for newer blue-emitting phosphors that comply with the requirements of an LED.

A vast number of Eu^{2+}-doped phosphors have shown excellent blue luminescence under NUV excitation. Phosphates are one of the best-known families that provide favorable conditions for Eu^{2+} ions to luminesce in the blue region. Phosphates have very high bandgap, moderate phonon energy values, and high chemical and thermal stability. $KMg_4(PO_4)_3:Eu^{2+}$ [172], $SrZnP_2O_7:Eu^{2+}$ [173], $RbBaPO_4:Eu^{2+}$ [174], $SrCaP_2O_7:Eu^{2+}$ [175], $Ca_3Mg_3(PO_4)_4:Eu^{2+}$ [176], $NaMgPO_4:Eu^{2+}$ [177], $LiCaPO_4:Eu^{2+}$ [178], etc. are some of the known phosphate-based phosphors producing blue luminescence. Kim et al. [179] demonstrated a novel zero-thermal-quenching $Na_{3-2x}Sc_2(PO_4)_3:xEu^{2+}$ phosphor that retains its PL emission intensity up to 200 °C without exhibiting thermal quenching. At higher temperatures, the excess amount of thermal energy contributes to the formation of electron-trapping defect levels due to the structural transformation related to Na^+ disordering in this phosphor. This initiates an energy transfer from the traps to Eu^{2+} ions, thereby countering the thermal quenching phenomenon. Some Ce^{3+}-activated phosphors such as $NaCaBO_3:Ce^{3+}$ [180], $Na_4CaSi_3O_9:Ce^{3+}$ [181], $Ba_{1.2}Ca_{0.8}SiO_4:Ce^{3+}$ [182], $Li_4SrCa(SiO_4)_2:Ce^{3+}$ [183], and $Gd_5Si_3O_{12}N:Ce^{3+}$ [184] have also exhibited blue luminescence. Cerium oxides are less expensive and relatively abundant than Europium. Hence, it is worthy to approach Ce^{3+}-doped phosphors against the ones doped with Eu^{2+} to bring down the overall cost of blue-emitting phosphor-converted LEDs.

4.8 White-emitting phosphors

White light-emitting diodes are, undoubtedly, the new generation of solid-state lighting sources because of their excellent properties, such as high luminous efficiency, energy-saving properties, long lifetime, and absence of toxic mercury. There are three different strategies to fabricate WLEDs. The first way is to achieve a perfect blend of

the red, green, and blue phosphors that could be excited by NUV LEDs to create white light. However, each of these phosphors will degrade differently and the overall emission color will also change with time. The instability in the color temperature and the excessive loss of energy faced in this approach compelled the technologists to think of a new way. It is also possible to combine the red, green, and blue-emitting LEDs to produce white light, but the same problem of instability in the color persists here too. The second and the most popular approach, in the present scenario, is the combination of a blue-emitting LED with a yellow-emitting phosphor [80,185]. At present, all the commercial WLEDs employ a YAG:Ce^{3+} phosphor pumped with a blue-emitting LED [80,162,186]. Although this approach resulted in an energy loss lower than that in the tricolor phosphor blending approach, it has some other issues that need to be solved. One such issue is the low CRI of the emitted white light that arises due to the lack of red component in the blend. To overcome the failures of these two approaches, a third approach has been proposed to produce white light from a single-phased host lattice. The use of such single-phased materials will enable easy fabrication of NUV-convertible WLEDs without compromising in the color reproducibility and stability. Till date, a huge number of publications have come up in the support of white light-emitting single-phased host materials, but none of them succeeded to reach the commercial scale. In this section, we will briefly discuss single-phased host materials capable of producing white light emission.

A host material cannot produce white light on its own. For this purpose, it is essential to identify a dopant ion that could luminesce in the host matrix. Numerous efforts were taken to develop white light-emitting single-phased host materials that operate under ultraviolet or NUV excitation. One of the commonly exercised methods is doping a single activator ion into a host matrix. Doping a Dy^{3+} ion in a host is the most common way to obtain white light emission that results from the combination of its characteristic line emissions in the blue and yellow regions. The Dy^{3+} emissions in the blue region (470−500 nm) and the yellow region (570−590 nm) correspond to the transitions $^4F_{9/2} \rightarrow {}^6H_{15/2}$ and $^4F_{9/2} \rightarrow {}^6H_{13/2}$, respectively. The yellow emission in Dy^{3+} is a hypersensitive one and the ratio of yellow to blue emission must be tuned to obtain the white light with desired color temperature. When Dy^{3+} ion occupies a site with inversion symmetry, the blue emission becomes dominant whereas the yellow emission becomes dominant if the ion occupies a noninversion symmetry center in a host matrix. Plenty of Dy^{3+}-doped phosphors have been reported to be potential candidates for WLEDs. To name a few: $NaLa(PO_3)_4:Dy^{3+}$ [187], $Ca_8MgBi(PO_4)_7:Dy^{3+}$ [188], $CaZr_4(PO_4)_6:Dy^{3+}$ [189,190], $Ca_3B_2O_6:Dy^{3+}$ [191], $Sr_3Gd(PO_4)_3:Dy^{3+}$ [192], $Ca_3Mg_3(PO_4)_4:Dy^{3+}$ [193], etc. However, the transitions arising from the Dy^{3+} ions are mainly due to the 4f−4f transitions, which are forbidden as per the selection rules. Hence, the luminescence arising from the phosphors doped with Dy^{3+} ions are bound to exhibit less efficiency unless there is some host sensitization or an energy transfer from some other dopant ion to the Dy^{3+} ions [193]. Apart from Dy^{3+}, it is also feasible to produce white light by singly doping Eu^{2+} or Eu^{3+} ions in a host. Eu^{3+} ions are mostly known for their red emissions; however, in some rare cases, they have also shown their ability to give numerous narrow-band emission peaks extending from blue to red region of the visible light spectrum and their combination, thus, result in

white light appearance [194,195]. An example of this is $Ba_5Zn_4Y_{7.92}O_{21}$:0.08Eu^{3+} nanophosphor that gives full-color emission at 274 nm and 395 nm excitation, as shown in Fig. 4.6 [195]. This special tuning of emission bands of Eu^{3+} ions requires the lowering of multiphonon-relaxation and cross-relaxation phenomena that occurs among its energy levels. This can be effectively done by selecting host materials with lower vibrational energies (phonon frequencies) and preferring lower values of Eu^{3+} concentration.

Eu^{2+} ions present a broadband emission due to their spectroscopically allowed 5d → 4f transition. As the outermost electrons of Eu^{2+} lie in the 5d state, their energies are strongly influenced by the coordination environment of the host in which Eu^{2+} ions are incorporated. In some cases, Eu^{2+} ions are capable of demonstrating full-color emission. $Ba_{0.97}Sr_{0.99}Mg(PO_4)_2$:0.04$Eu^{2+}$ phosphor can be excited at 350 nm to give a full-color emission band that peaks at 447 nm and 536 nm [196]. As shown in Fig. 4.7, a WLED fabricated by coating the mixture of $Ba_{0.97}Sr_{0.99}Mg(PO_4)_2$:0.04$Eu^{2+}$ phosphor with epoxy resin on the 380 nm-emitting InGaN chip demonstrated white light emission with CIE-1931 color coordinates located at (0.3287, 0.3638) and CRI of 87. There is a rare possibility to obtain an Eu^{2+} emission spectrum that covers the entire visible light region [197,198]. However, by selecting a suitable codopant, it is possible to generate white light in almost every type of host material. Dramatic experimentations have been carried out and finally, Mn^{2+} was hailed as the best choice to support Eu^{2+} ions in generating white light [199−203]. Red emission from Mn^{2+} ions forms an ideal pair with the blue emission

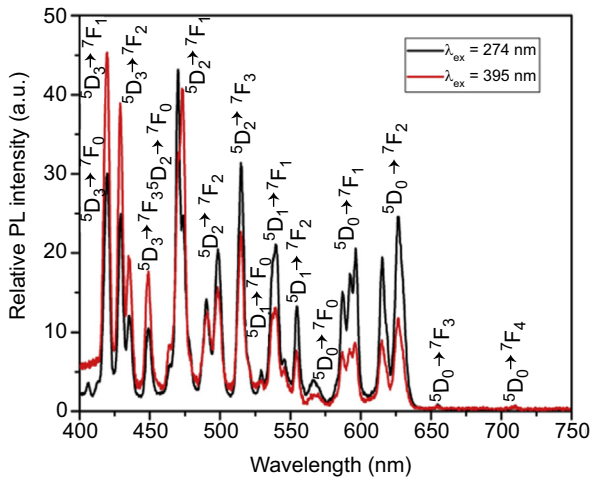

Figure 4.6 Emission spectra of $Ba_5Zn_4Y_{7.92}Eu_{0.08}O_{21}$ nanophosphor, excited at 274and 395 nm, respectively.

Reproduced with permission from M. Dalal, V.B. Taxak, J. Dalal, A. Khatkar, S. Chahar, R. Devi, S.P. Khatkar, Crystal structure and Judd-Ofelt properties of a novel color tunable blue-white-red $Ba_5Zn_4Y_8O_{21}$:Eu3+ nanophosphor for near-ultraviolet based WLEDs, J. Alloys Compd. 698 (2017) 662−672. https://doi.org/10.1016/j.jallcom.2016.12.257. Copyright 2016, Elsevier.

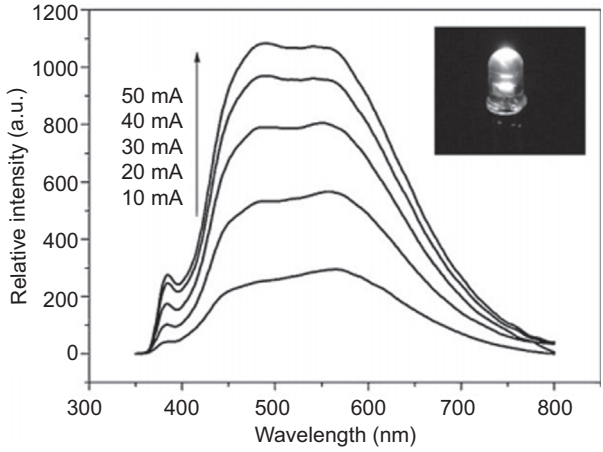

Figure 4.7 The emission spectra of the WLED fabricated with $Ba_{0.97}Sr_{0.99}Mg(PO_4)_2$:0.04$Eu^{2+}$ phosphor coated on a 380-nm-emitting InGaN chip with increasing forward-bias current. The inset shows the photograph of the WLED under 20-mA current excitation.
Reproduced with permission from Z.C. Wu, J. Liu, W.G. Hou, J. Xu, M.L. Gong, A new single-host white-light-emitting $BaSrMg(PO_4)_2$: Eu^{2+} phosphor for white-light-emitting diodes, J. Alloys Compd. 498 (2010) 139−142. https://doi.org/10.1016/j.jallcom.2010.03.136. Copyright 2010, Elsevier.

from Eu^{2+} ions in several compounds. Ironically, Mn^{2+} ions do not show strong red luminescence when they are singly doped; the $^4T_1-^6A_1$ transition of Mn^{2+} is forbidden and is quite inefficient unless a sensitizer like Eu^{2+} or Ce^{3+} is involved. A number of phosphors have been reported to give white luminescence with the combination of Eu−Mn pair of ions. Although such phosphors show a commendable combination of blue + red emission, their excitation band does not match well with the commercial NUV-LED chips that are needed to pump these phosphors. Barring a few exceptions like $NaSrPO_4$ [204], most of the phosphate hosts bear the Eu^{2+} excitation peak at about 330−350 nm [205].

Recently, achieving the co-existence of Eu^{2+} and Eu^{3+} ionic states in the same host lattice has provided a wide opportunity to tune the color emission and achieve a white color point with the desired chromaticity coordinates [206]. $LiMgPO_4$ [207], $KCaBO_3$ [208], β-Ca_2SiO_4 [209], $Sr_5(PO_4)_3Cl$ [210], and $Ca_3Y_2Si_3O_{12}$ [211] are some of those special hosts that can contain Eu in both its oxidation states simultaneously. $Ca_3Y_2Si_3O_{12}$ possesses three different sites that are occupied by divalent Ca^{2+} and trivalent Y^{3+} ions. These sites are seven-coordinated, eight-coordinated, and nine-coordinated and can be occupied by europium ions [211]. However, only the nine-coordinated site shows some distinct feature and greater Y−O bond length, while the other two sites resemble each other on several fronts. Hence, it was inferred that the bigger Eu^{2+} ions can occupy the nine-coordinated site quite easily, whereas the other two sites can be preferentially filled by smaller Eu^{3+} ions. It was further suggested that Eu^{2+} luminescence was a consequence of its anomalous character with the neighboring

oxygen vacancies. When Eu^{2+} is forced to occupy the Y^{3+} site, it leaves a hole that started acting as a defect at that site. It was also assumed that O^{2-} vacancies (with positive net charge) are created under reducing conditions and they tend to move near Eu^{2+} ions in the host. The O^{2-} vacancies can effectively trap the electrons that are excited in the 5d states of Eu^{2+}. This leads to the formation of an exciton-like excited state that consists of a hole localized to Eu^{2+} and an electron bound to the O^{2-} vacancy by Coulomb's force of attraction. The annihilation of this state leads to the broadening of the emission band with a large Stokes shift. Upon exciting the phosphor with 395 nm, it showed a color emission close to white but with a yellowish hue. This indicated a lack of blue component in the overall color emission of the phosphor. Chen et al. [210] have introduced an abnormal reduction of Eu^{3+} into Eu^{2+} in the $Sr_5(PO_4)_3Cl$ host. On exciting this phosphor, the emission peaks consisted of the red emission peaks corresponding to the 4f−4f transitions of Eu^{3+} as well as the broad emission band centered at 446 nm corresponding to the 4f−5d transition of Eu^{2+}. The overall color emission can be tuned from blue to white by adjusting the doping concentration levels of Eu in the phosphor. On introducing the charge-compensators into this composition, the Eu^{3+} emissions intensified to a significant level, but the intensity of the Eu^{2+}-emission band decreased. There are several other materials too that have shown simultaneous emission of Eu^{3+} and Eu^{2+}, but they do not satisfy the conditions required for LEDs and hence, have been omitted from this discussion [212].

4.9 Color-tunable phosphors

To meet the requirements of modern lighting technology, efforts are being made to acquire phosphors capable of spectral tuning that could probably improve the luminous efficiency, CRI, and color gamut of pc-LEDs. The changing light generations will witness a huge revolution in the lighting industry that shall be brought about by these color-tunable phosphors. Li et al. [213] have elaborately discussed, in their review, several strategies that may be employed to successfully tune the photoluminescence spectra, to achieve the properties desirable for efficient working of pc-LEDs. Yet, their discussion is mostly limited to the spectral tuning of Eu^{2+}- and Ce^{3+}-doped phosphors only. There are vast avenues that have been explored during the quest to achieve color-tunable phosphors. A compilation of all these research work can form an independent study that will tarnish the present concepts known to us and give a deeper understanding of the methodology and genuine mechanisms involved in these new types of luminescent materials. Though our review is not specifically dedicated to the color-tunable phosphors, we strongly believe that this topic shall also be included as an integral part of this review. There are plenty of color-tunable phosphors reported, but we shall briefly limit our discussion only on those applicable for pc-LEDs.

One of the most commonly practiced methods for color tuning is the appropriate selection of luminescent ions/dopants wherein the excitation spectrum of one type of ion will overlap with the emission spectrum of the other. The pair of Ce^{3+}−Eu^{2+} ions forms a fabulous duo of luminescent ions that could tune the color from yellow−

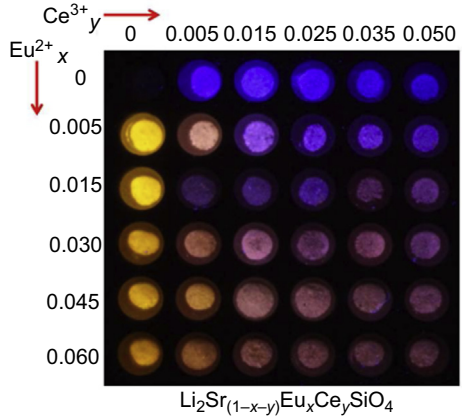

Figure 4.8 Composition map and luminescence photograph of the $Li_2(Sr_{1-x-y}Eu_xCe_y)SiO_4$ phosphor with varying Ce^{3+} and Eu^{2+} concentration.
Reproduced with permission from L. Chen, A. Luo, Y. Zhang, F. Liu, Y. Jiang, Q. Xu, X. Chen, Q. Hu, S.F. Chen, K.J. Chen, H.C. Kuo, Optimization of the single-phased white phosphor of Li_2SrSiO_4: Eu^{2+}, Ce^{3+} for light-emitting diodes by using the combinatorial approach assisted with the Taguchi method, ACS Comb. Sci. 14 (2012) 636−644. https://doi.org/10.1021/co300058x. Copyright 2012, American Chemical Society.

white−blue in most host materials that are experiencing strong crystal field splitting and nephelauxetic effect [214−217]. A better understanding of this sort of color tuning can be derived from the compositional map drawn for $Li_2(Sr_{1-x-y}Eu_xCe_y)SiO_4$ phosphor with varying Ce^{3+} and Eu^{2+} concentration, as shown in Fig. 4.8 [218]. There are several possibilities to obtain color tuning with Ce^{3+} along with Eu^{2+}, Tb^{3+}, Eu^{3+}, etc. [219]. However, most of their excitation spectra do not overlap with the emission spectra of InGaN or GaN chips. Hence, most of the Ce-doped phosphors are not considerable for pc-LEDs [220,221]. Still, there are a few exceptions like Y_2SiO_5: Ce^{3+},Tb^{3+},Eu^{3+} [222] that satisfy the conditions required by a phosphor for LEDs. The triad of Ce^{3+}, Tb^{3+}, and Eu^{3+} ions play together to tune the color emission from blue → white → orange/red. For pc-LEDs, this set of triple dopants is found to be more effective when doped in host materials based on silicates, nitrides, and some borates [222−224]. The excitation energy is often absorbed by Ce^{3+} ions, part of which gets nonradiatively transferred to both Tb^{3+} and Eu^{3+} ions.

Another known pair of Eu^{2+}−Mn^{2+} ions also have shown fascinating luminescence properties with color tuning in numerous host materials [199,201,205,225−232]. Mn^{2+} ions show broadband emission with color varying from 500 to 700 nm (green to red), depending on the crystal-field splitting of its d-orbitals. For a strong crystal field around the Mn^{2+} ion, the spitting will be large and the emission occurs in the lower energy side (probably red) [205]. For a weak field, the splitting will be small and emission occurs in the higher energy side (green) owing to $^4T_1 \rightarrow {}^6A_1$ transition. As their excitation bands corresponding to d−d transitions are both parity and spin forbidden, it becomes difficult to pump Mn^{2+} ions to produce

luminescence with significant efficiency. Hence, the use of sensitizer ions like Eu^{2+} or Ce^{3+} is often required to efficiently pump Mn^{2+} ions. Eu^{2+} ions produce emission from blue to red depending on the crystal field environment around it and a number of various other factors, while Ce^{3+} ions produce luminescence in the NUV region for most cases. By adjusting the ratio of Eu^{2+} and Mn^{2+} ions, a single-phased host phosphor can tune its emission color.

4.10 Conclusions

The technological advancements exhibited by LEDs have honored it with the tag of the most recommended and admired lighting technology. It has expanded its applications to numerous fields and the rising demands for more efficient and flexible lighting have promoted its growth from the traditional semiconductors to the phosphor incorporated versions. Incorporation of the phosphors have helped to fill the gaps left out in the visible light emission spectrum by the RGB semiconductor chips and now, it is possible to produce any color emission by blending a suitable phosphor with a blue-emitting or NUV-emitting LED chip. This motivated the researchers around the globe to come up with several novel phosphors that could be embedded within the LED package and pumped by GaN/InGaN chips. The suitability of the phosphors for LEDs is determined by various factors such as its lifespan, CRI, quantum efficiency, and thermal and chemical stability. These parameters can be strongly affected by the synthesis methods adopted to prepare the phosphors. To achieve a successful synthesis, it should be made sure that the atmospheric conditions and the raw materials are suitable for producing the desired phosphor. In addition, the purity of the raw materials play an important role in achieving the desired composition of the phosphor.

References

[1] G.B. Nair, A. Kumar, H.C. Swart, S.J. Dhoble, Improved steady-state photoluminescence derived from the compensation of the charge-imbalance in $Ca_3Mg_3(PO_4)_4:Eu^{3+}$ phosphor, Ceram. Int. 45 (2019) 21709−21715, https://doi.org/10.1016/j.ceramint.2019.07.171.

[2] G.-M. Chow, L.K. Kurihara, Synthesis and processing of nanostructured powders and films, Nanostructured Mater. Process. Prop. Appl. (2006) 784.

[3] G.B. Nair, S.J. Dhoble, White light emitting $MZr_4(PO_4)_6:Dy^{3+}$ (M = Ca, Sr, Ba) phosphors for WLEDs, J. Fluoresc. 27 (2017) 575−585, https://doi.org/10.1007/s10895-016-1985-y.

[4] C.J. Brinker, G.W. Scherer, Sol−Gel Science: the Physics and Chemistry of Sol−Gel Processing, Academic Press INC, UK, London, 1990.

[5] G.B. Nair, S.J. Dhoble, Orange light-emitting $Ca_3Mg_3(PO_4)_4:Sm^{3+}$ phosphors, Luminescence 32 (2017) 125−128, https://doi.org/10.1002/bio.3194.

[6] S.A. Pardhi, G.B. Nair, R. Sharma, S.J. Dhoble, Investigation of thermoluminescence and electron-vibrational interaction parameters in $SrAl_2O_4:Eu^{2+}$, Dy^{3+} phosphors, J. Lumin. 187 (2017) 492−498, https://doi.org/10.1016/j.jlumin.2017.03.028.
[7] X. Li, H. Wang, L. Guan, Y. Fu, Z. Guo, K. Yuan, L. Tie, Z. Yang, F. Teng, Influence of pH value on properties of $YPO_4:Tb^{3+}$ phosphor by co-precipitation method, J. Rare Earths 33 (2015) 346−349, https://doi.org/10.1016/S1002-0721(14)60424-5.
[8] C. Sung Lim, Microwave-modified sol-gel process of $NaY(WO_4)_2:Ho^{3+}/Yb^{3+}$ phosphors and the upconversion of their photoluminescence properties, Ceram. Int. 41 (2015) 2616−2621, https://doi.org/10.1016/j.ceramint.2014.10.042.
[9] J. Prado-Gonjal, R. Schmidt, J. Espíndola-Canuto, P. Ramos-Alvarez, E. Morán, Increased ionic conductivity in microwave hydrothermally synthesized rare-earth doped ceria $Ce_{1-x}RE_xO_{2-(x/2)}$, J. Power Sources 209 (2012) 163−171, https://doi.org/10.1016/j.jpowsour.2012.02.082.
[10] C. He, Z. Xia, Q. Liu, Microwave solid state synthesis and luminescence properties of green-emitting $Gd_2O_2S:Tb^{3+}$ phosphor, Opt. Mater. 42 (2015) 11−16, https://doi.org/10.1016/j.optmat.2014.12.012.
[11] H. Xu, B.W. Zeiger, K.S. Suslick, Sonochemical synthesis of nanomaterials, Chem. Soc. Rev. 42 (2013) 2555−2567, https://doi.org/10.1039/C2CS35282F.
[12] Z. Wang, R. Yu, Hollow micro/nanostructured ceria-based materials: synthetic strategies and versatile applications, Adv. Mater. 31 (2019) 1800592, https://doi.org/10.1002/adma.201800592.
[13] T.V. Gavrilović, D.J. Jovanović, M.D. Dramićanin, Synthesis of multifunctional inorganic materials:from micrometer to nanometer dimensions, in: Nanomaterials for Green Energy, Elsevier, 2018, pp. 55−81, https://doi.org/10.1016/B978-0-12-813731-4.00002-3.
[14] G.B. Nair, S.J. Dhoble, Photoluminescence properties of Eu^{3+}/Sm^{3+} activated $CaZr_4(PO_4)_6$ phosphors, J. Fluoresc. 26 (2016) 1865−1873, https://doi.org/10.1007/s10895-016-1880-6.
[15] M.M. Yawalkar, G.B. Nair, G.D. Zade, S.J. Dhoble, Effect of the synthesis route on the luminescence properties of Eu^{3+} activated $Li_6M(BO_3)_3$ (M = Y, Gd) phosphors, Mater. Chem. Phys. 189 (2017) 136−145, https://doi.org/10.1016/j.matchemphys.2016.12.006.
[16] S. Ray, G.B. Nair, P. Tadge, N. Malvia, V. Rajput, V. Chopra, S.J. Dhoble, Size and shape-tailored hydrothermal synthesis and characterization of nanocrystalline $LaPO_4:Eu^{3+}$ phosphor, J. Lumin. 194 (2018) 64−71, https://doi.org/10.1016/j.jlumin.2017.10.015.
[17] W. Jiang, R. Fu, X. Gu, P. Zhang, A. Coşgun, A red-emitting phosphor $LaSr_2AlO_5:Eu^{3+}/Eu^{2+}$ prepared under oxidative and reductive atmospheres, J. Lumin. 157 (2015) 46−52, https://doi.org/10.1016/j.jlumin.2014.07.018.
[18] P. Dorenbos, The Eu^{3+} charge transfer energy and the relation with the band gap of compounds, J. Lumin. 111 (2005) 89−104, https://doi.org/10.1016/j.jlumin.2004.07.003.
[19] N. Zhang, C. Guo, L. Yin, J. Zhang, M. Wu, Red emitting phosphors of Eu^{3+} doped $Na_2Ln_2Ti_3O_{10}$ (Ln=Gd, Y) for white light emitting diodes, J. Alloys Compd. 635 (2015) 66−72, https://doi.org/10.1016/j.jallcom.2015.02.014.
[20] M.G. Ivanov, U. Kynast, M. Leznina, Eu^{3+} doped yttrium oxide nano-luminophores from laser synthesis, J. Lumin. 169 (2016) 744−748, https://doi.org/10.1016/j.jlumin.2015.05.036.
[21] Z. Cheng, R. Xing, Z. Hou, S. Huang, J. Lin, Patterning of light-emitting $YVO_4:Eu^{3+}$ thin films via inkjet printing, J. Phys. Chem. C 114 (2010) 9883−9888, https://doi.org/10.1021/jp101941y.

[22] S. Som, A.K. Kunti, V. Kumar, V. Kumar, S. Dutta, M. Chowdhury, S.K. Sharma, J.J. Terblans, H.C. Swart, Defect correlated fluorescent quenching and electron phonon coupling in the spectral transition of Eu^{3+} in $CaTiO_3$ for red emission in display application, J. Appl. Phys. 115 (2014), https://doi.org/10.1063/1.4876316.
[23] K.V. Dabre, S.J. Dhoble, Synthesis and photoluminescence properties of Eu^{3+}, Sm^{3+} and Pr^{3+} doped Ca_2ZnWO_6 phosphors for phosphor converted LED, J. Lumin. 150 (2014) 55−58, https://doi.org/10.1016/j.jlumin.2014.01.045.
[24] Y. Xia, Y. Huang, Q. Long, S. Liao, Y. Gao, J. Liang, J. Cai, Near-UV light excited Eu^{3+}, Tb^{3+}, Bi^{3+} co-doped $LaPO_4$ phosphors: synthesis and enhancement of red emission for WLEDs, Ceram. Int. 41 (2015) 5525−5530, https://doi.org/10.1016/j.ceramint.2014.12.128.
[25] V. Lojpur, S. Ćulubrk, M. Medić, M. Dramicanin, Luminescence thermometry with Eu^{3+} doped $GdAlO_3$, J. Lumin. 170 (2015) 467−471, https://doi.org/10.1016/j.jlumin.2015.06.032.
[26] P. Li, Z. Wang, Z. Yang, Q. Guo, X. Li, Emission features of $LiBaBO_3$:Sm^{3+} red phosphor for white LED, Mater. Lett. 63 (2009) 751−753, https://doi.org/10.1016/j.matlet.2008.12.041.
[27] V.R. Prasad, S. Damodaraiah, S. Babu, Y.C. Ratnakaram, Structural, optical and luminescence properties of Sm^{3+} and Eu^{3+} doped calcium borophosphate phosphors for reddish-orange and red emitting light applications, J. Lumin. 187 (2017) 360−367, https://doi.org/10.1016/j.jlumin.2017.03.050.
[28] N. Kiran, A.P. Baker, G.-G. Wang, Synthesis and luminescence properties of MgO:Sm^{3+} phosphor for white light-emitting diodes, J. Mol. Struct. 1129 (2017) 211−215, https://doi.org/10.1016/j.molstruc.2016.09.046.
[29] B. Ramesh, G.R. Dillip, G.R. Reddy, B.D.P. Raju, S.W. Joo, N.J. Sushma, B. Rambabu, Luminescence properties of $CaZn_2(PO_4)_2$:Sm^{3+} phosphor for lighting application, Optik 156 (2018) 906−913, https://doi.org/10.1016/j.ijleo.2017.12.023.
[30] X. He, J. Zhou, N. Lian, J. Sun, M. Guan, Sm^{3+}-activated gadolinium molybdate: an intense red-emitting phosphor for solid-state lighting based on InGaN LEDs, J. Lumin. 130 (2010) 743−747, https://doi.org/10.1016/j.jlumin.2009.11.016.
[31] B. Bondzior, D. Stefańska, A. Kubiak, P.J. Dereń, Spectroscopic properties of $K_4SrSi_3O_9$ doped with Sm^{3+}, J. Lumin. 173 (2016) 38−43, https://doi.org/10.1016/j.jlumin.2015.12.031.
[32] Z. Ju, R. Wei, J. Zheng, X. Gao, S. Zhang, W. Liu, Synthesis and phosphorescence mechanism of a reddish orange emissive long afterglow phosphor Sm^{3+}-doped Ca_2SnO_4, Appl. Phys. Lett. 98 (2011) 121906, https://doi.org/10.1063/1.3567511.
[33] H.N. Luitel, T. Watari, R. Chand, T. Torikai, M. Yada, Photoluminescence properties of a novel orange red emitting $Sr_4Al_{14}O_{25}$:Sm^{3+} phosphor and PL enhancement by Bi^{3+} co-doping, Opt. Mater. 34 (2012) 1375−1380, https://doi.org/10.1016/j.optmat.2012.02.025.
[34] X. Min, M. Fang, Z. Huang, Y. Liu, C. Tang, H. Zhu, X. Wu, Preparation and luminescent properties of orange reddish emitting phosphor $LaMgAl_{11}O_{19}$:Sm^{3+}, Opt. Mater. (2014) 3−8, https://doi.org/10.1016/j.optmat.2014.05.008.
[35] R. Zhou, L. Wang, M. Xu, D. Jia, Photoluminescence characteristics of Sm^{3+} doped $Sr_2P_2O_7$ as new orange-red emitting phosphor, J. Alloys Compd. 647 (2015) 136−140, https://doi.org/10.1016/j.jallcom.2015.06.081.
[36] R. Yu, H. Mi Noh, B. Kee Moon, B. Chun Choi, J. Hyun Jeong, H. Sueb Lee, K. Jang, S. Soo Yi, Photoluminescence characteristics of Sm^{3+} doped $Ba_3La(PO_4)_3$ as new

orange-red emitting phosphors, J. Lumin. 145 (2014) 717−722, https://doi.org/10.1016/j.jlumin.2013.08.049.
[37] H. Watanabe, N. Kijima, Crystal structure and luminescence properties of $Sr_xCa_{1-x}AlSiN_3:Eu^{2+}$ mixed nitride phosphors, J. Alloys Compd. 475 (2009) 434−439, https://doi.org/10.1016/j.jallcom.2008.07.054.
[38] X. Teng, Y. Liu, Y. Liu, Y. Hu, H. He, W. Zhuang, Luminescence properties of Tm^{3+} co-doped $Sr_2Si_5N_8:Eu^{2+}$ red phosphor, J. Lumin. 130 (2010) 851−854, https://doi.org/10.1016/j.jlumin.2009.12.012.
[39] Q. Wu, J. Ding, X. Wang, Y. Li, Y. Wang, Structure modification and covalence variation induced by cation substitution in pure nitride Ca-α-sialon phosphor, Mater. Res. Bull. 83 (2016) 649−656, https://doi.org/10.1016/j.materresbull.2016.07.018.
[40] V. Bachmann, A. Meijerink, C. Ronda, Luminescence properties of $SrSi_2AlO_2N_3$ doped with divalent rare-earth ions, J. Lumin. 129 (2009) 1341−1346, https://doi.org/10.1016/j.jlumin.2009.06.023.
[41] R.-J. Xie, N. Hirosaki, Silicon-based oxynitride and nitride phosphors for white LEDs-A review, Sci. Technol. Adv. Mater. 8 (2007) 588−600, https://doi.org/10.1016/j.stam.2007.08.005.
[42] J.H. Ryu, H.S. Won, Y.G. Park, S.H. Kim, W.Y. Song, H. Suzuki, C. Yoon, Synthesis of $Eu_xSi_{6-z}Al_zO_zN_{8-z}$ green phosphor and its luminescent properties, Appl. Phys. Mater. Sci. Process 95 (2009) 747−752, https://doi.org/10.1007/s00339-008-5044-7.
[43] Y.Q. Li, C.M. Fang, Y. Fang, A.C.A. Delsing, G. de With, H.T. Hintzen, Electronic structure and photoluminescence properties of Eu^{2+}-activated Ca_2BN_2F, J. Solid State Chem. 182 (2009) 3299−3304, https://doi.org/10.1016/j.jssc.2009.09.028.
[44] J. Zhang, X. Zhang, M. Gong, J. Shi, L. Yu, C. Rong, S. Lian, $LiSrBO_3:Eu^{2+}$: a novel broad-band red phosphor under the excitation of a blue light, Mater. Lett. 79 (2012) 100−102, https://doi.org/10.1016/j.matlet.2012.04.011.
[45] W. Zhi-Jun, L. Pan-Lai, Y. Zhi-Ping, G. Qing-Lin, F. Guang-Sheng, Energy transfer from Ce^{3+} to Eu^{2+} in $LiSrBO_3$ and its potential application in UV-LED-Based white LEDs, Chin. Phys. Lett. 26 (2009) 117802, https://doi.org/10.1088/0256-307X/26/11/117802.
[46] Q. Wang, D. Deng, Y. Hua, L. Huang, H. Wang, S. Zhao, G. Jia, C. Li, S. Xu, Potential tunable white-emitting phosphor $LiSr_4(BO_3)_3:Ce^{3+}$, Eu^{2+} for ultraviolet light-emitting diodes, J. Lumin. 132 (2012) 434−438, https://doi.org/10.1016/j.jlumin.2011.09.003.
[47] L. Wu, X.L. Chen, H. Li, M. He, Y.P. Xu, X.Z. Li, Structure determination and relative properties of novel cubic borates $MM'_4(BO_3)_3$ (M=Li, M′=Sr; M=Na, M′=Sr, Ba), Inorg. Chem. 44 (2005) 6409−6414, https://doi.org/10.1021/ic050299s.
[48] S. Yuan, Y. Yang, X. Zhang, F. Tessier, F. Cheviré, J.-L. Adam, B. Moine, G. Chen, Eu^{2+} and Mn^{2+} codoped $Ba_2Mg(BO_3)_2$—new red phosphor for white LEDs, Opt. Lett. 33 (2008) 2865, https://doi.org/10.1364/OL.33.002865.
[49] H. Daicho, Y. Shinomiya, K. Enomoto, A. Nakano, H. Sawa, S. Matsuishi, H. Hosono, A novel red-emitting $K_2Ca(PO_4)F:Eu^{2+}$ phosphor with a large Stokes shift, Chem. Commun. 54 (2018) 884−887, https://doi.org/10.1039/C7CC08202A.
[50] D. Jia, X.J. Wang, Alkali earth sulfide phosphors doped with Eu^{2+} and Ce^{3+} for LEDs, Opt. Mater. 30 (2007) 375−379, https://doi.org/10.1016/j.optmat.2006.11.061.
[51] T. Senden, E.J. van Harten, A. Meijerink, Synthesis and narrow red luminescence of $Cs_2HfF_6:Mn^{4+}$, a new phosphor for warm white LEDs, J. Lumin. 194 (2018) 131−138, https://doi.org/10.1016/j.jlumin.2017.10.006.
[52] A. Fu, L. Zhou, S. Wang, Y. Li, Preparation, structural and optical characteristics of a deep red-emitting $Mg_2Al_4Si_5O_{18}:Mn^{4+}$ phosphor for warm w-LEDs, Dye. Pigment. 148 (2018) 9−15, https://doi.org/10.1016/J.DYEPIG.2017.08.050.

[53] S. Zhang, Y. Hu, H. Duan, Y. Fu, M. He, An efficient, broad-band red-emitting $Li_2MgTi_3O_8:Mn^{4+}$ phosphor for blue-converted white LEDs, J. Alloys Compd. 693 (2017) 315–325, https://doi.org/10.1016/j.jallcom.2016.09.203.

[54] T. Sasaki, J. Fukushima, Y. Hayashi, H. Takizawa, Synthesis and photoluminescence properties of a novel $Sr_2Al_6O_{11}:Mn^{4+}$ red phosphor prepared with a B_2O_3 flux, J. Lumin. 194 (2018) 446–451, https://doi.org/10.1016/j.jlumin.2017.10.076.

[55] A.M. Srivastava, M.G. Brik, Crystal field studies of the Mn^{4+} energy levels in the perovskite, $LaAlO_3$, Opt. Mater. 35 (2013) 1544–1548, https://doi.org/10.1016/j.optmat.2013.03.021.

[56] Y.K. Xu, S. Adachi, Properties of $Na_2SiF_6:Mn^{4+}$ and $Na_2GeF_6:Mn^{4+}$ red phosphors synthesized by wet chemical etching, J. Appl. Phys. 105 (2009) 013525, https://doi.org/10.1063/1.3056375.

[57] R. Hoshino, S. Adachi, Optical spectroscopy and degradation behavior of $ZnGeF_6 \cdot 6H_2O:Mn^{4+}$ red-emitting phosphor, J. Lumin. 162 (2015) 63–71, https://doi.org/10.1016/j.jlumin.2015.02.011.

[58] S.J. Kim, H.S. Jang, S. Unithrattil, Y.H. Kim, W. Bin Im, Structural and luminescent properties of red-emitting $SrGe_4O_9:Mn^{4+}$ phosphors for white light-emitting diodes with high color rendering index, J. Lumin. 172 (2016) 99–104, https://doi.org/10.1016/j.jlumin.2015.11.042.

[59] A. Fu, C. Zhou, Q. Chen, Z. Lu, T. Huang, H. Wang, L. Zhou, Preparation and optical properties of a novel double-perovskite phosphor, $Ba_2GdNbO_6:Mn^{4+}$, for light-emitting diodes, Ceram. Int. 43 (2017) 6353–6362, https://doi.org/10.1016/j.ceramint.2017.02.044.

[60] M.G. Brik, S.J. Camardello, A.M. Srivastava, Influence of covalency on the Mn^{4+} $^2E_g \rightarrow {}^4A_{2g}$ emission energy in crystals, ECS J. Solid State Sci. Technol. 4 (2015) R39–R43, https://doi.org/10.1149/2.0031503jss.

[61] H.-D. Nguyen, C.C. Lin, M.-H. Fang, R. Liu, Synthesis of $Na_2SiF_6:Mn^{4+}$ red phosphors for white LED applications by co-precipitation, J. Mater. Chem. C 2 (2014) 10268–10272, https://doi.org/10.1039/C4TC02062F.

[62] X. Jiang, Y. Pan, S. Huang, X. Chen, J. Wang, G. Liu, Hydrothermal synthesis and photoluminescence properties of red phosphor $BaSiF_6:Mn^{4+}$ for LED applications, J. Mater. Chem. C 2 (2014) 2301, https://doi.org/10.1039/c3tc31878h.

[63] L. Lv, X. Jiang, S. Huang, X. Chen, Y. Pan, The formation mechanism, improved photoluminescence and LED applications of red phosphor $K_2SiF_6:Mn^{4+}$, J. Mater. Chem. C 2 (2014) 3879, https://doi.org/10.1039/c4tc00087k.

[64] S. Adachi, T. Takahashi, Direct synthesis of $K_2SiF_6:Mn^{4+}$ red phosphor from crushed quartz schist by wet chemical etching, Electrochem. Solid State Lett. 12 (2009) J20, https://doi.org/10.1149/1.3039192.

[65] D. Sekiguchi, S. Adachi, Synthesis and photoluminescence spectroscopy of $BaGeF_6:Mn^{4+}$ red phosphor, Opt. Mater. 42 (2015) 417–422, https://doi.org/10.1016/j.optmat.2015.01.039.

[66] J. Long, X. Yuan, C. Ma, M. Du, X. Ma, Z. Wen, R. Ma, Y. Wang, Y. Cao, Strongly enhanced luminescence of $Sr_4Al_{14}O_{25}:Mn^{4+}$ phosphor by co-doping B^{3+} and Na^+ ions with red emission for plant growth LEDs, RSC Adv. 8 (2018) 1469–1476, https://doi.org/10.1039/C7RA11967D.

[67] Y.D. Xu, D. Wang, L. Wang, N. Ding, M. Shi, J.G. Zhong, S. Qi, Preparation and luminescent properties of a new red phosphor ($Sr_4Al_{14}O_{25}:Mn^{4+}$) for white LEDs, J. Alloys Compd. 550 (2013) 226–230, https://doi.org/10.1016/j.jallcom.2012.09.139.

[68] Z. Qiu, T. Luo, J. Zhang, W. Zhou, L. Yu, S. Lian, Effectively enhancing blue excitation of red phosphor $Mg_2TiO_4:Mn^{4+}$ by Bi^{3+} sensitization, J. Lumin. 158 (2015) 130−135, https://doi.org/10.1016/j.jlumin.2014.09.032.

[69] C. Wu, J. Li, H. Xu, J. Wu, J. Zhang, Z. Ci, L. Feng, C. Cao, Z. Zhang, Y. Wang, Preparation, structural and photoluminescence characteristics of novel red emitting $Mg_7Ga_2GeO_{12}:Mn^{4+}$ phosphor, J. Alloys Compd. 646 (2015) 734−740, https://doi.org/10.1016/j.jallcom.2015.06.166.

[70] L. Meng, L. Liang, Y. Wen, A novel red phosphor Na^+, Mn^{4+} co-doped $Sr_4Al_{14}O_{25}$ for warm white light emitting diodes, Mater. Chem. Phys. 153 (2015) 1−4, https://doi.org/10.1016/j.matchemphys.2014.12.041.

[71] R. Cao, Z. Shi, G. Quan, Z. Hu, G. Zheng, T. Chen, S. Guo, H. Ao, Rare-earth free broadband $Ca_3Mg_3P_4O_{16}:Mn^{2+}$ red phosphor: synthesis and luminescence properties, J. Lumin. 194 (2018) 542−546, https://doi.org/10.1016/j.jlumin.2017.10.079.

[72] R. Kasahara, K. Tezuka, Y.J. Shan, Preparation and luminescence properties of a red phosphor $Ba_5Ta_4O_{15}:Mn^{2+}$, Optik 158 (2018) 1170−1178, https://doi.org/10.1016/j.ijleo.2017.12.175.

[73] G.B. Nair, S.J. Dhoble, Assessment of electron-vibrational interaction (EVI) parameters of YAG:Ce^{3+}, TAG:Ce^{3+} and LuAG:Ce^{3+} garnet phosphors by spectrum fitting method, Spectrochim. Acta Part A Mol. Biomol. Spectrosc. 173 (2017) 822−826, https://doi.org/10.1016/j.saa.2016.10.049.

[74] V. Bachmann, C. Ronda, A. Meijerink, Temperature quenching of yellow Ce^{3+} luminescence in YAG:Ce, Chem. Mater. 21 (2009) 2077−2084, https://doi.org/10.1021/cm8030768.

[75] D. Valiev, T. Han, V. Vaganov, S. Stepanov, The effect of Ce^{3+} concentration and heat treatment on the luminescence efficiency of YAG phosphor, J. Phys. Chem. Solid. 116 (2018) 1−6, https://doi.org/10.1016/j.jpcs.2018.01.007.

[76] L. Wang, L. Zhuang, H. Xin, Y. Huang, D. Wang, Semi-quantitative estimation of Ce^{3+}/Ce^{4+} ratio in YAG:Ce^{3+} phosphor under different sintering atmosphere, Open J. Inorg. Chem. 05 (2015) 12−18, https://doi.org/10.4236/ojic.2015.51003.

[77] X. He, X. Liu, R. Li, B. Yang, K. Yu, M. Zeng, R. Yu, Effects of local structure of Ce^{3+} ions on luminescent properties of $Y_3Al_5O_{12}$:Ce nanoparticles, Sci. Rep. 6 (2016) 22238, https://doi.org/10.1038/srep22238.

[78] Y. Liu, J. Zou, M. Shi, B. Yang, Y. Han, W. Li, Z. Wang, H. Zhou, M. Li, N. Jiang, Effect of gallium ion content on thermal stability and reliability of YAG:Ce phosphor films for white LEDs, Ceram. Int. 44 (2018) 1091−1098, https://doi.org/10.1016/j.ceramint.2017.10.056.

[79] W.-S. Song, Y.-S. Kim, H. Yang, Yellow-emitting phosphor of $Sr_3B_2O_6:Eu^{2+}$ for application to white light-emitting diodes, Mater. Chem. Phys. 117 (2009) 500−503, https://doi.org/10.1016/j.matchemphys.2009.06.042.

[80] Y. Zhao, H. Xu, X. Zhang, G. Zhu, D. Yan, A. Yu, Facile synthesis of YAG:Ce^{3+} thick films for phosphor converted white light emitting diodes, J. Eur. Ceram. Soc. 35 (2015) 3761−3764, https://doi.org/10.1016/j.jeurceramsoc.2015.05.017.

[81] Z. Chen, Q. Zhang, Y. Li, H. Wang, R. Xie, A promising orange-yellow-emitting phosphor for high power warm-light white LEDs: pure-phase synthesis and photoluminescence properties, J. Alloys Compd. 715 (2017) 184−191, https://doi.org/10.1016/j.jallcom.2017.04.270.

[82] Y. Pan, M. Wu, Q. Su, Tailored photoluminescence of YAG:Ce phosphor through various methods, J. Phys. Chem. Solid. 65 (2004) 845−850, https://doi.org/10.1016/j.jpcs.2003.08.018.

[83] M. Gong, W. Xiang, X. Liang, J. Zhong, D. Chen, J. Huang, G. Gu, C. Yang, R. Xiang, Growth and characterization of air annealing Tb-doped YAG:Ce single crystal for white-light-emitting diode, J. Alloys Compd. 639 (2015) 611−616, https://doi.org/10.1016/j.jallcom.2015.03.162.
[84] Y. Matsui, H. Horikawa, M. Iwasaki, W. Park, Preparation of YAG: Ce nanocrystals by an environmentally friendly wet process effect of Ce^{3+} concentration on photo-luminescent property, J. Ceram. Process. Res. 12 (2011) 348−351.
[85] Y. Zorenko, E. Zych, a. Voloshinovskii, Intrinsic and Ce^{3+}-related luminescence of YAG and YAG:Ce single crystals, single crystalline films and nanopowders, Opt. Mater. 31 (2009) 1845−1848, https://doi.org/10.1016/j.optmat.2008.11.026.
[86] M. Upasani, B. Butey, S.V. Moharil, Luminescence studies on lanthanide ions (Gd^{3+}, Tb^{3+}) doped YAG:Ce phosphors by combustion synthesis, J. Appl. Phys. 6 (2014) 28−33.
[87] S. Mukherjee, V. Sudarsan, R.K. Vatsa, A.K. Tyagi, Luminescence studies on lanthanide ions (Eu^{3+}, Dy^{3+} and Tb^{3+}) doped YAG:Ce nano-phosphors, J. Lumin. 129 (2009) 69−72, https://doi.org/10.1016/j.jlumin.2008.08.003.
[88] W. Gao, Y. Hu, W. Zhuang, S. Zhang, Y. Liu, H. He, A novel method for the synthesis of YAG:Ce phosphor, J. Rare Earths 27 (2009) 886−890, https://doi.org/10.1016/S1002-0721(08)60355-5.
[89] Y. Pan, M. Wu, Q. Su, Comparative investigation on synthesis and photoluminescence of YAG:Ce phosphor, Mater. Sci. Eng. B Solid-State Mater. Adv. Technol. 106 (2004) 251−256, https://doi.org/10.1016/j.mseb.2003.09.031.
[90] Y.C. Chen, Y.T. Nien, Microstructure and photoluminescence properties of laser sintered YAG:Ce phosphor ceramics, J. Eur. Ceram. Soc. 37 (2017) 223−227, https://doi.org/10.1016/j.jeurceramsoc.2016.07.032.
[91] M.J. Yoon, S.H. Son, J.H. Lee, J.W. Lee, C.H. Lee, Synthesis of YAG:Ce phosphor particles using continuous supercritical water system, Ind. Eng. Chem. Res. 47 (16) (2006) 5994−6000.
[92] J. Li, J.-G. Li, S. Liu, X. Li, X. Sun, Y. Sakka, The development of Ce^{3+} -activated $(Gd,Lu)_3Al_5O_{12}$ garnet solid solutions as efficient yellow-emitting phosphors, Sci. Technol. Adv. Mater. 14 (2013) 054201, https://doi.org/10.1088/1468-6996/14/5/054201.
[93] W. Zhou, X. Ma, M. Zhang, Y. Luo, Z. Xia, Synthesis and photoluminescence properties of green-emitting $Lu_3(Al,Sc)_5O_{12}:Ce^{3+}$ phosphor, Ceram. Int. 41 (2015) 7140−7145, https://doi.org/10.1016/j.ceramint.2015.02.030.
[94] H.T. Kim, J.H. Kim, J.-K. Lee, Y.C. Kang, Green light-emitting $Lu_3Al_5O_{12}$:Ce phosphor powders prepared by spray pyrolysis, Mater. Res. Bull. 47 (2012) 1428−1431, https://doi.org/10.1016/j.materresbull.2012.02.050.
[95] K. Zhang, W. Hu, Y. Wu, H. Liu, Photoluminescence investigations of $(Y_{1-x}Ln_x)_3Al_5O_{12}$:Ce ($Ln^{3+}$=$Gd^{3+}$, La^{3+}) nanophosphors, Phys. B Condens. Matter 403 (2008) 1678−1681, https://doi.org/10.1016/j.physb.2007.09.084.
[96] A. Aboulaich, M. Michalska, R. Schneider, A. Potdevin, J. Deschamps, R. Deloncle, G. Chadeyron, R. Mahiou, Ce-doped YAG nanophosphor and red emitting $CuInS_2$/ZnS core/shell quantum dots for warm white light-emitting diode with high color rendering index, ACS Appl. Mater. Interfaces 6 (2014) 252−258, https://doi.org/10.1021/am404108n.
[97] X. Piao, K.I. Machida, T. Horikawa, H. Hanzawa, Self-propagating high temperature synthesis of yellow-emitting $Ba_2Si_5N_8:Eu^{2+}$ phosphors for white light-emitting diodes, Appl. Phys. Lett. 91 (2007) 041908, https://doi.org/10.1063/1.2760038.

[98] Q.N. Fei, Y.H. Liu, T.C. Gu, D.J. Wang, Color improvement of white-light through Mn-enhancing yellow-green emission of $SrSi_2O_2N_2$:Eu phosphor for white light emitting diodes, J. Lumin. 131 (2011) 960−964, https://doi.org/10.1016/j.jlumin.2011.01.001.

[99] J. Chen, Y. Zhao, G. Li, Z. Mao, D. Wang, L. Bie, Facile synthesis of yellow-emitting $CaAlSiN_3:Ce^{3+}$ phosphors and the enhancement of red-component by co-doping Eu^{2+} ions, Solid State Commun. 256 (2017) 1−4, https://doi.org/10.1016/j.ssc.2017.02.010.

[100] Y. Chen, J. Xu, Y. Yu, W. Chen, R. Zeng, Preparation Eu-doped ca-α-SiAlON phosphor by heterogeneous precipitation: an orange−yellow phosphor for white light-emitting diodes, Ceram. Int. 41 (2015) 11086−11090, https://doi.org/10.1016/j.ceramint.2015.05.055.

[101] Y. Ge, S. Sun, M. Zhou, Y. Chen, Z. Tian, J. Zhang, Z. Xie, Impacts of Si particle size and nitrogen pressure on combustion synthesis of Eu^{2+}-doped α-SiAlON yellow phosphors, Powder Technol. 305 (2017) 141−146, https://doi.org/10.1016/j.powtec.2016.09.066.

[102] R.J. Xie, N. Hirosaki, K. Sakuma, Y. Yamamoto, M. Mitomo, Eu^{2+} -doped Ca - α - SiAlON: a yellow phosphor for white light-emitting diodes, Appl. Phys. Lett. 84 (2004) 5404−5406, https://doi.org/10.1063/1.1767596.

[103] J. Huo, W. Lü, B. Shao, Y. Song, Y. Feng, S. Zhao, H. You, Enhanced luminescence intensity of $CaSi_2O_2N_2:Eu^{2+}$ phosphor by using flux in the preparation process and incorporating Gd^{3+} ions, J. Lumin. 180 (2016) 46−50, https://doi.org/10.1016/j.jlumin.2016.08.014.

[104] B. Joshi, Y.K. Kshetri, G. Gyawali, S.W. Lee, Transparent Mg−α/β-Sialon:Eu^{2+} ceramics as a yellow phosphor for pc-WLED, J. Alloys Compd. 631 (2015) 38−45, https://doi.org/10.1016/j.jallcom.2015.01.081.

[105] A. Katelnikovas, S. Sakirzanovas, D. Dutczak, J. Plewa, D. Enseling, H. Winkler, A. Kareiva, T. Jüstel, Synthesis and optical properties of yellow emitting garnet phosphors for pcLEDs, J. Lumin. 136 (2013) 17−25, https://doi.org/10.1016/j.jlumin.2012.11.012.

[106] H. Ji, L. Wang, M.S. Molokeev, N. Hirosaki, Z. Huang, Z. Xia, O.M. Ten Kate, L. Liu, R. Xie, New garnet structure phosphors, $Lu_{3-x}Y_xMgAl_3SiO_{12}:Ce^{3+}$ (x=0−3), developed by solid solution design, J. Mater. Chem. C 4 (2016), https://doi.org/10.1039/c6tc00089d.

[107] Y. Chu, Q. Zhang, J. Xu, Y. Li, H. Wang, An orange emitting phosphor $Lu_{2-x}CaMg_2Si_{2.9}Ti_{0.1}O_{12}$:xCe with pure garnet phase for warm white LEDs, J. Solid State Chem. 229 (2015) 213−218, https://doi.org/10.1016/j.jssc.2015.06.002.

[108] Y. Shi, G. Zhu, M. Mikami, Y. Shimomura, Y. Wang, A novel Ce^{3+} activated $Lu_3MgAl_3SiO_{12}$ garnet phosphor for blue chip light-emitting diodes with excellent performance, Dalt. Trans. 44 (2015) 1775−1781, https://doi.org/10.1039/C4DT03144J.

[109] L. Devys, G. Dantelle, G. Laurita, E. Homeyer, I. Gautier-Luneau, C. Dujardin, R. Seshadri, T. Gacoin, A strategy to increase phosphor brightness: application with Ce^{3+} -doped $Gd_3Sc_2Al_3O_{12}$, J. Lumin. 190 (2017) 62−68, https://doi.org/10.1016/j.jlumin.2017.05.035.

[110] W. Sun, Y. Jia, R. Pang, H. Li, T. Ma, D. Li, J. Fu, S. Zhang, L. Jiang, C. Li, $Sr_9Mg_{1.5}(PO_4)_7:Eu^{2+}$: a novel broadband orange-yellow-emitting phosphor for blue light-excited warm white LEDs, ACS Appl. Mater. Interfaces 7 (2015) 25219−25226, https://doi.org/10.1021/acsami.5b06961.

[111] C.-H. Huang, D.-Y. Wang, Y.-C. Chiu, Y.-T. Yeh, T.-M. Chen, $Sr_8MgGd(PO_4)_7:Eu^{2+}$: yellow-emitting phosphor for application in near-ultraviolet-emitting diode based white-light LEDs, RSC Adv. 2 (2012) 9130, https://doi.org/10.1039/c2ra20646c.

[112] C.H. Huang, T.M. Chen, Novel yellow-emitting $Sr_8MgLn(PO_4)_7:Eu^{2+}$ (Ln=Y, La) phosphors for applications in white LEDs with excellent color rendering index, Inorg. Chem. 50 (2011) 5725−5730, https://doi.org/10.1021/ic200515w.

[113] Q. Zhang, X. Wang, X. Ding, Y. Wang, A broad band yellow-emitting $Sr_8CaBi(PO_4)_7:Eu^{2+}$ phosphor for n-UV pumped white light emitting devices, Dye. Pigment. 149 (2018) 268−275, https://doi.org/10.1016/J.DYEPIG.2017.10.004.

[114] H. Yu, D. Deng, Y. Li, S. Xu, Y. Li, C. Yu, Y. Ding, H. Lu, H. Yin, Q. Nie, Electronic structure and photoluminescence properties of yellow-emitting $Ca_{10}Na(PO_4)_7:Eu^{2+}$ phosphor for white light-emitting diodes, J. Lumin. 143 (2013) 132−136, https://doi.org/10.1016/j.jlumin.2013.04.036.

[115] X. Fu, W. Lü, M. Jiao, H. You, Broadband yellowish-green emitting $Ba_4Gd_3Na_3(PO_4)_6F_2:Eu^{2+}$ phosphor: structure refinement, energy transfer, and thermal stability, Inorg. Chem. 55 (2016) 6107−6113, https://doi.org/10.1021/acs.inorgchem.6b00648.

[116] X. Zhang, J. Zhang, Z. Dong, J. Shi, M. Gong, Concentration quenching of Eu^{2+} in a thermal-stable yellow phosphor $Ca_2BO_3Cl:Eu^{2+}$ for LED application, J. Lumin. 132 (2012) 914−918, https://doi.org/10.1016/j.jlumin.2011.11.001.

[117] Z. Xia, L. Liao, Z. Zhang, Y. Wang, Combustion synthesis and luminescence properties of yellow-emitting phosphors $Ca_2BO_3Cl:Eu^{2+}$, Mater. Res. Bull. 47 (2012) 405−408, https://doi.org/10.1016/j.materresbull.2011.11.006.

[118] C. Shen, Y. Yang, S. Jin, J. Ming, H. Feng, Z. Xu, White light-emitting diodes using blue and yellow-orange-emitting phosphors, Optik 121 (2010) 1487−1491, https://doi.org/10.1016/j.ijleo.2009.02.003.

[119] F. Liu, Y. Fang, N. Zhang, J. Hou, L. Zhang, S. Yu, S. Liu, Eu^{2+} and Dy^{3+} codoped $(Ca,Sr)_7(SiO_3)_6Cl_2$ highly efficient yellow phosphor, J. Rare Earths 32 (2014) 812−816, https://doi.org/10.1016/S1002-0721(14)60146-0.

[120] M. Zhang, J. Wang, W. Ding, Q. Zhang, Q. Su, Luminescence properties of $M_2MgSi_2O_7:Eu^{2+}$ (M=Ca, Sr) phosphors and their effects on yellow and blue LEDs for solid-state lighting, Opt. Mater. 30 (2007) 571−578, https://doi.org/10.1016/j.optmat.2007.01.008.

[121] J.Y. Han, W. Bin Im, G. Lee, D.Y. Jeon, Near UV-pumped yellow-emitting Eu^{2+}-doped $Na_3K(Si_{1-x}Al_x)_8O_{16\pm\delta}$ phosphor for white-emitting LEDs, J. Mater. Chem. 22 (2012) 8793, https://doi.org/10.1039/c2jm16739e.

[122] U. Bin Humayoun, Y.H. Song, S. Bin Kwon, K. Masato, K. Toda, Y. Sato, T. Masaki, D.H. Yoon, Exquisite morphology, highly emissive yellow $Sr_{1.44}Ba_{0.46}SiO_4:0.1Eu^{2+}$ phosphor synthesized by a liquid phase precursor process, Dye. Pigment. 142 (2017) 147−152, https://doi.org/10.1016/j.dyepig.2017.03.029.

[123] H.-J.J. Woo, S. Gandhi, B.-J.J. Kwon, D.-S.S. Shin, S.S. Yi, J.H. Jeong, K. Jang, Soluble silica assisted synthesis and luminescent characteristics of yellow emitting $CaSrSiO_4:Eu^{2+}$ phosphors for warm white light production, Ceram. Int. 41 (2015) 5547−5553, https://doi.org/10.1016/j.ceramint.2014.12.131.

[124] R. Naik, S.C. Prashantha, H. Nagabhushana, H.P. Nagaswarupa, K.S. Anantharaju, S.C. Sharma, B.M. Nagabhushana, H.B. Premkumar, K.M. Girish, $Mg_2SiO_4:Tb^{3+}$ nanophosphor: auto ignition route and near UV excited photoluminescence properties for WLEDs, J. Alloys Compd. 617 (2014) 69−75, https://doi.org/10.1016/j.jallcom.2014.07.100.

[125] Z.J. Zhang, O.M. ten Kate, A. Delsing, P. Dorenbos, J.T. Zhao, H.T. Hintzen, Photoluminescence properties of Pr^{3+}, Sm^{3+} and Tb^{3+} doped $SrAlSi_4N_7$ and energy level locations of rare-earth ions in $SrAlSi_4N_7$, J. Mater. Chem. C Mater. Opt. Electron. Devices. 2 (2014) 7952−7959, https://doi.org/10.1039/c4tc00538d.

[126] V. Singh, R.P.S. Chakradhar, J.L. Rao, D.-K. Kim, Mn^{2+} activated $MgSrAl_{10}O_{17}$ green-emitting phosphor—a luminescence and EPR study, J. Lumin. 128 (2008) 1474−1478, https://doi.org/10.1016/j.jlumin.2008.02.001.

[127] J.S. Kim, J.S. Kim, T.W. Kim, H.L. Park, Y.G. Kim, S.K. Chang, S. Do Han, Energy transfer among three luminescent centers in full-color emitting $ZnGa_2O_4$:Mn^{2+}, Cr^{3+} phosphors, Solid State Commun. 131 (2004) 493−497, https://doi.org/10.1016/j.ssc.2004.06.023.

[128] V.R. Panse, N.S. Kokode, K.N. Shinde, S.J. Dhoble, Luminescence in microcrystalline green emitting $Li_2Mg_{1-x}ZrO_4$:xTb^{3+}($0.1 \leq x \leq 2.0$) phosphor, Results Phys 8 (2018) 99−103, https://doi.org/10.1016/j.rinp.2017.10.025.

[129] X. Liu, L. Yan, J. Lin, Synthesis and luminescent properties of $LaAlO_3$:RE^{3+} (RE=Tm, Tb) nanocrystalline phosphors via a sol-gel process, J. Phys. Chem. C 113 (2009) 8478−8483, https://doi.org/10.1021/jp9013724.

[130] R.K. Tamrakar, K. Upadhyay, Combustion synthesis and luminescence behaviour of the Tb^{3+} doped SrY_2O_4 phosphor, J. Electron. Mater. 47 (2018), https://doi.org/10.1007/s11664-017-5825-x.

[131] X. Sun, P. Jiang, W. Gao, R. Cong, T. Yang, Effect of vacancy and activator concentrations on the luminescence of $Sr_{1-1.5x}Tb_x\square_{0.5x}WO_4$ and Tb^{3+}/Li^+ co-doped phosphors, J. Alloys Compd. 645 (2015) 517−524, https://doi.org/10.1016/j.jallcom.2015.05.007.

[132] J. Liao, B. Qiu, H. Lai, Synthesis and luminescence properties of Tb^{3+}:$NaGd(WO_4)_2$ novel green phosphors, J. Lumin. 129 (2009) 668−671, https://doi.org/10.1016/j.jlumin.2009.01.016.

[133] J.Y. Park, H.C. Jung, G. Seeta Rama Raju, B.K. Moon, J.H. Jeong, S.-M.M. Son, J.H. Kim, Enhanced green emission from Tb^{3+}−Bi^{3+} co-doped $GdAlO_3$ nanophosphors, Mater. Res. Bull. 45 (2010) 572−575, https://doi.org/10.1016/j.materresbull.2010.01.016.

[134] K. Park, M.H. Heo, S.J. Dhoble, VUV photoluminescence of green-emitting $GdPO_4$: Tb,M (M:Al, Zn) synthesized by ultrasonic spray pyrolysis, Mater. Chem. Phys. 140 (2013) 108−112, https://doi.org/10.1016/j.matchemphys.2013.03.007.

[135] S.J.J. Yoon, K. Park, Photoluminescence properties of a novel green-emitting phosphor $Zr_{1-x}O_2$:xTb^{3+}, Int. J. Hydrogen Energy 40 (2015) 825−832, https://doi.org/10.1016/j.ijhydene.2014.09.048.

[136] Z. Ren, C. Tao, H. Yang, S. Feng, A novel green emitting phosphor $SrAl_2B_2O_7$:Tb^{3+}, Mater. Lett. 61 (2007) 1654−1657, https://doi.org/10.1016/j.matlet.2006.07.161.

[137] J. Zhang, T. Zhao, B. Wang, L. Li, L. Zou, S. Gan, PEG-assisted hydrothermal synthesis and photoluminescence of $CdMoO_4$:Tb^{3+} green phosphor, J. Phys. Chem. Solid. 79 (2015) 14−22, https://doi.org/10.1016/j.jpcs.2014.11.003.

[138] D.R. Taikar, S. Tamboli, S.J. Dhoble, Synthesis and photoluminescence properties of red, green and blue emitting $LaYO_3$:M (M=Eu^{3+}, Tb^{3+}, Sm^{3+},Bi^{3+}, Pb^{2+}) phosphors, Opt. Int. J. Light Electron Opt. 142 (2017) 183−190, https://doi.org/10.1016/j.ijleo.2017.05.095.

[139] F. Yang, Y. Liang, Y. Lan, W. Gao, M. Liu, X. Li, W. Huang, Y. Li, Z. Xia, A novel green-emitting phosphor $NaSrBO_3$:Tb^{3+}, Li^+, Mater. Lett. 83 (2012) 59−61, https://doi.org/10.1016/j.matlet.2012.05.105.

[140] R. Wang, J. Xu, C. Chen, Luminescent characteristics of $Sr_2B_2O_5$:Tb^{3+}, Li^+ green phosphor, Mater. Lett. 68 (2012) 307−309, https://doi.org/10.1016/j.matlet.2011.10.005.

[141] X. Huang, B. Li, H. Guo, Synthesis, photoluminescence, cathodoluminescence, and thermal properties of novel Tb^{3+}-doped BiOCl green-emitting phosphors, J. Alloys Compd. 695 (2017) 2773−2780, https://doi.org/10.1016/j.jallcom.2016.11.224.

[142] D. Alexander, K. Thomas, S. Sisira, G. Vimal, K.P. Mani, P.R. Biju, N.V. Unnikrishnan, M.A. Ittyachen, C. Joseph, Photoluminescence properties of fully concentrated terbium oxalate: a novel efficient green emitting phosphor, Mater. Lett. 189 (2017) 160−163, https://doi.org/10.1016/j.matlet.2016.12.002.

[143] B. Ramesh, G.R. Dillip, B. Rambabu, S.W. Joo, B.D.P. Raju, Structural studies of a green-emitting terbium doped calcium zinc phosphate phosphor, J. Mol. Struct. 1155 (2018) 568−572, https://doi.org/10.1016/j.molstruc.2017.11.044.

[144] M. Xin, D. Tu, H. Zhu, W. Luo, Z. Liu, P. Huang, R. Li, Y. Cao, X. Chen, Single-composition white-emitting $NaSrBO_3$:Ce^{3+},Sm^{3+},Tb^{3+} phosphors for NUV light-emitting diodes, J. Mater. Chem. C 3 (2015) 7286−7293, https://doi.org/10.1039/C5TC00832H.

[145] B.P. Kore, S. Tamboli, N.S. Dhoble, A.K. Sinha, M.N. Singh, S.J. Dhoble, H.C. Swart, Efficient resonance energy transfer study from Ce^{3+} to Tb^{3+} in $BaMgF_4$, Mater. Chem. Phys. 187 (2017) 233−244, https://doi.org/10.1016/j.matchemphys.2016.12.005.

[146] Z. Xia, Y. Liang, D. Yu, M. Zhang, W. Huang, M. Tong, J. Wu, J. Zhao, Photoluminescence properties and energy transfer in color tunable $BaY_2Si_3O_{10}$:Ce,Tb phosphors, Optic Laser. Technol. 56 (2014) 387−392, https://doi.org/10.1016/j.optlastec.2013.09.014.

[147] A. Guan, Z. Lu, F. Gao, X. Zhang, H. Wang, T. Huang, L. Zhou, Synthesis and optical characterization of Eu^{2+},Tb^{3+} -codoped $Sr_3Y(PO_4)_3$ green phosphors, J. Rare Earths (2017) 6−10, https://doi.org/10.1016/j.jre.2017.06.013.

[148] W.J. Park, Y.H. Song, D.H. Yoon, Synthesis and luminescent characteristics of $Ca_{2-x}Sr_xSiO_4$:Eu^{2+} as a potential green-emitting phosphor for near UV-white LED applications, Mater. Sci. Eng. B Solid-State Mater. Adv. Technol. (2010) 76−79, https://doi.org/10.1016/j.mseb.2010.01.041. Elsevier B.V.

[149] X. Zhang, X. Tang, J. Zhang, M. Gong, An efficient and stable green phosphor $SrBaSiO_4$:Eu^{2+} for light-emitting diodes, J. Lumin. 130 (2010) 2288−2292, https://doi.org/10.1016/j.jlumin.2010.07.006.

[150] S. Hur, H.J. Song, H.S. Roh, D.W. Kim, K.S. Hong, A novel green-emitting $Ca_{15}(PO_4)_2(SiO_4)_6$:Eu^{2+} phosphor for applications in n-UV based w-LEDs, Mater. Chem. Phys. 139 (2013) 350−354, https://doi.org/10.1016/j.matchemphys.2013.02.009.

[151] J.S. Kim, Y.H. Park, S.M. Kim, J.C. Choi, H.L. Park, Temperature-dependent emission spectra of M_2SiO_4: Eu^{2+} (M=Ca, Sr, Ba) phosphors for green and greenish white LEDs, Solid State Commun. 133 (2005) 445−448, https://doi.org/10.1016/j.ssc.2004.12.002.

[152] G. Annadurai, S.M.M. Kennedy, V. Sivakumar, Luminescence properties of a novel green emitting $Ba_2CaZn_2Si_6O_{17}$:Eu^{2+} phosphor for white light − emitting diodes applications, Superlattice. Microst. 93 (2016) 57−66, https://doi.org/10.1016/j.spmi.2016.02.045.

[153] X. Zhang, F. Zhou, J. Shi, M. Gong, $Sr_{3.5}Mg_{0.5}Si_3O_8Cl_4$:$Eu^{2+}$ bluish-green-emitting phosphor for NUV-based LED, Mater. Lett. 63 (2009) 852−854, https://doi.org/10.1016/j.matlet.2009.01.024.

[154] I. Baginskiy, R.S. Liu, Significant improved luminescence intensity of Eu^{2+}-doped $Ca_3SiO_4Cl_2$ green phosphor for white LEDs synthesized through two-stage method, J. Electrochem. Soc. 156 (2009) G29, https://doi.org/10.1149/1.3089366.

[155] Z. Li, S. Gao, X. Chen, Q. Yu, Synthesis and luminescence properties of green phosphors $Ca_6Sr_4(Si_2O_7)_3Cl_2$:Eu^{2+} for white light emitting diodes, J. Lumin. 132 (2012) 1497−1500, https://doi.org/10.1016/j.jlumin.2012.01.043.

[156] V. Sivakumar, U.V. Varadaraju, Eu^{2+}, Ce^{3+} luminescence and Ce^{3+}/Eu^{2+} energy-transfer studies on Sr_2LiSiO_4F: a white light-emitting phosphor, J. Electrochem. Soc. 156 (2009) J179, https://doi.org/10.1149/1.3122663.

[157] L. Yu, Y. Hua, H. Chen, D. Deng, H. Wang, H. Ma, S. Xu, Luminescence properties of $Ba_3Si_6O_9N_4$:Eu^{2+} green-emitting phosphors for white LEDs, Opt. Commun. 315 (2014) 83−86, https://doi.org/10.1016/j.optcom.2013.10.091.

[158] C. Li, H. Chen, S. Xu, $Ba_3Si_6O_{12}N_2$:Eu^{2+} green-emitting phosphor for white light emitting diodes: luminescent properties optimization and crystal structure analysis, Optik 126 (2015) 499−502, https://doi.org/10.1016/j.ijleo.2015.01.008.

[159] T. Takeda, N. Hirosaki, S. Funahshi, R.J. Xie, Narrow-band green-emitting phosphor $Ba_2LiSi_7AlN_{12}$:Eu^{2+} with high thermal stability discovered by a single particle diagnosis approach, Chem. Mater. 27 (2015) 5892−5898, https://doi.org/10.1021/acs.chemmater.5b01464.

[160] C.-Y. Wang, R.-J. Xie, F. Li, X. Xu, Thermal degradation of the green-emitting $SrSi_2O_2N_2$:Eu^{2+} phosphor for solid state lighting, J. Mater. Chem. C 2 (2014) 2735−2742, https://doi.org/10.1039/C3TC32582B.

[161] S. Nakamura, InGaN/AlGaN blue-light-emitting diodes, J. Vac. Sci. Technol. A Vacuum Surfaces Film. 13 (1995) 705−710, https://doi.org/10.1116/1.579811.

[162] S. Ye, F. Xiao, Y.X. Pan, Y.Y. Ma, Q.Y. Zhang, Phosphors in phosphor-converted white light-emitting diodes: recent advances in materials, techniques and properties, Mater. Sci. Eng. R Rep. 71 (2010) 1−34, https://doi.org/10.1016/j.mser.2010.07.001.

[163] S.-S. Lee, H.J. Kim, S.-H. Byeon, J.-C. Park, D.-K. Kim, Thermal-shock-assisted solid-state process for the production of $BaMgAl_{10}O_{17}$:Eu phosphor, Ind. Eng. Chem. Res. 44 (2005) 4300−4303, https://doi.org/10.1021/ie048953j.

[164] K.-B. Kim, Y.-I. Kim, H.-G. Chun, T.-Y. Cho, J.-S. Jung, J.-G. Kang, Structural and optical properties of $BaMgAl_{10}O_{17}$:Eu^{2+} phosphor, Chem. Mater. 14 (2002) 5045−5052, https://doi.org/10.1021/cm020592f.

[165] Y. Liu, S. Zhang, D. Pan, J. Tian, H. Liu, M. Wu, A.A. Volinsky, Mechanism and kinetics of the $BaMgAl_{10}O_{17}$:Eu^{2+} alkaline fusion reaction, J. Rare Earths 33 (2015) 664−670, https://doi.org/10.1016/S1002-0721(14)60468-3.

[166] C.W.W. Won, H.H.H. Nersisyan, H.I.I. Won, S.J.J. Kwon, H.Y.Y. Kim, S.Y.Y. Seo, Synthesis of nano-size $BaMgAl_{10}O_{17}$:Eu^{2+} blue phosphor by a rapid exothermic reaction, J. Lumin. 130 (2010) 678−681, https://doi.org/10.1016/j.jlumin.2009.11.017.

[167] Z.H. Zhang, Y.H. Wang, X.X. Li, Y.K. Du, W.J. Liu, Photoluminescence degradation and color shift studies of annealed $BaMgAl_{10}O_{17}$:Eu^{2+} phosphor, J. Lumin. 122−123 (2007) 1003−1005, https://doi.org/10.1016/j.jlumin.2006.01.351.

[168] S. Zhang, T. Kono, A. Ito, T. Yasaka, H. Uchiike, Degradation mechanisms of the blue-emitting phosphor $BaMgAl_{10}O_{17}$:Eu^{2+} under baking and VUV-irradiating treatments, J. Lumin. 106 (2004) 39−46, https://doi.org/10.1016/S0022-2313(03)00132-7.

[169] Z. Zhang, J. Feng, Z. Huang, Synthesis and characterization of $BaMgAl_{10}O_{17}$:Eu^{2+} phosphor prepared by homogeneous precipitation, Particuology 8 (2010) 473−476, https://doi.org/10.1016/j.partic.2010.04.001.

[170] Á. Yáñez-González, E. Ruiz-Trejo, B. van Wachem, S. Skinner, F. Beyrau, A. Heyes, A detailed characterization of $BaMgAl_{10}O_{17}$:Eu phosphor as a thermal history sensor for harsh environments, Sens. Actuators A Phys. 234 (2015) 339−345, https://doi.org/10.1016/j.sna.2015.09.020.

[171] X. Wang, J. Li, P. Shi, W. Guan, H. Zhang, High dispersibility and enhanced luminescence properties of $BaMgAl_{10}O_{17}:Eu^{2+}$ phosphors derived from molten salt synthesis, Opt. Mater. 46 (2015) 432−437, https://doi.org/10.1016/j.optmat.2015.04.060.
[172] X. Lan, Q. Wei, Y. Chen, W. Tang, Luminescence properties of Eu^{2+}-activated $KMg_4(PO_4)_3$ for blue-emitting phosphor, Opt. Mater. 34 (2012) 1330−1332, https://doi.org/10.1016/j.optmat.2012.02.013.
[173] J.L. Yuan, X.Y. Zeng, J.T. Zhao, Z.J. Zhang, H.H. Chen, G. Bin Zhang, Rietveld refinement and photoluminescent properties of a new blue-emitting material: Eu^{2+} activated $SrZnP_2O_7$, J. Solid State Chem. 180 (2007) 3310−3316, https://doi.org/10.1016/j.jssc.2007.09.023.
[174] H.J. Song, D.K. Yim, H.-S. Roh, I.S. Cho, S.-J. Kim, Y.-H. Jin, H.-W. Shim, D.-W. Kim, K.S. Hong, $RbBaPO_4:Eu^{2+}$: a new alternative blue-emitting phosphor for UV-based white light-emitting diodes, J. Mater. Chem. C 1 (2013) 500, https://doi.org/10.1039/c2tc00162d.
[175] R.L. Kohale, S.J. Dhoble, Eu^{2+} luminescence in $SrCaP_2O_7$ pyrophosphate phosphor, Luminescence 28 (2012) 656−661, https://doi.org/10.1002/bio.2411.
[176] G. Ju, Y. Hu, L. Chen, X. Wang, Z. Mu, Blue persistent luminescence in Eu^{2+} doped $Ca_3Mg_3(PO_4)_4$, Opt. Mater. 36 (2014) 1183−1188, https://doi.org/10.1016/j.optmat.2014.02.024.
[177] S.W. Kim, T. Hasegawa, T. Ishigaki, K. Uematsu, K. Toda, M. Sato, Efficient red emission of blue-light excitable new structure type $NaMgPO_4:Eu^{2+}$ phosphor, ECS Solid State Lett. 2 (2013) R49, https://doi.org/10.1149/2.004312ssl.
[178] X. Zhang, F. Mo, L. Zhou, M. Gong, Properties−structure relationship research on $LiCaPO_4:Eu^{2+}$ as blue phosphor for NUV LED application, J. Alloys Compd. 575 (2013) 314−318, https://doi.org/10.1016/j.jallcom.2013.05.188.
[179] Y.H. Kim, P. Arunkumar, B.Y. Kim, S. Unithrattil, E. Kim, S.H. Moon, J.Y. Hyun, K.H. Kim, D. Lee, J.S. Lee, W. Bin Im, A zero-thermal-quenching phosphor, Nat. Mater. 16 (2017) 543−550, https://doi.org/10.1038/nmat4843.
[180] X. Zhang, J. Song, C. Zhou, L. Zhou, M. Gong, High efficiency and broadband blue-emitting $NaCaBO_3:Ce^{3+}$ phosphor for NUV light-emitting diodes, J. Lumin. 149 (2014) 69−74, https://doi.org/10.1016/j.jlumin.2014.01.012.
[181] H. Ju, B. Wang, Y. Ma, S. Chen, H. Wang, S. Yang, Preparation and luminescence properties of $Na_4CaSi_3O_9:Ce^{3+}$ phosphors for solid state lighting, Ceram. Int. 40 (2014) 11085−11088, https://doi.org/10.1016/j.ceramint.2014.03.126.
[182] K. Park, J. Kim, P. Kung, S.M. Kim, Thermally stable deep-blue $Ba_{1.2}Ca_{0.8}SiO_4:Ce^{3+}$ phosphor for white-light-emitting diode, J. Lumin. 130 (2010) 1292−1294, https://doi.org/10.1016/j.jlumin.2010.02.041.
[183] J. Zhang, W. Zhang, Z. Qiu, W. Zhou, L. Yu, Z. Li, S. Lian, $Li_4SrCa(SiO_4)_2:Ce^{3+}$, a highly efficient near-UV and blue emitting orthosilicate phosphor, J. Alloys Compd. 646 (2015) 315−320, https://doi.org/10.1016/j.jallcom.2015.05.280.
[184] F. Lu, L. Bai, Z. Yang, X. Han, Synthesis and photoluminescence of a novel blue-emitting $Gd_5Si_3O_{12}N:Ce^{3+}$ phosphor, Mater. Lett. 151 (2015) 9−11, https://doi.org/10.1016/j.matlet.2015.03.031.
[185] G.B. Nair, S.J. Dhoble, A perspective perception on the applications of light-emitting diodes, Luminescence 30 (2015) 1167−1175, https://doi.org/10.1002/bio.2919.
[186] R. Kasuya, T. Isobe, H. Kuma, J. Katano, Photoluminescence enhancement of PEG-modified $YAG:Ce^{3+}$ nanocrystal phosphor prepared by glycothermal method, J. Phys. Chem. B 109 (2005) 22126−22130, https://doi.org/10.1021/jp052753j.

[187] F. Liu, Q. Liu, Y. Fang, N. Zhang, B. Yang, G. Zhao, White light emission from $NaLa(PO_3)_4$: Dy^{3+} single-phase phosphors for light-emitting diodes, Ceram. Int. 41 (2015) 1917−1920, https://doi.org/10.1016/j.ceramint.2014.09.078.

[188] Z.W. Zhang, A.J. Song, M.Z. Ma, X.Y. Zhang, Y. Yue, R.P. Liu, A novel white emission in $Ca_8MgBi(PO_4)_7$:Dy^{3+} single-phase full-color phosphor, J. Alloys Compd. 601 (2014) 231−233, https://doi.org/10.1016/j.jallcom.2014.02.165.

[189] W. Geng, G. Zhu, Y. Shi, Y. Wang, Luminescent characteristics of Dy^{3+} doped calcium zirconium phosphate $CaZr_4(PO_4)_6$ (CZP) phosphor for warm-white LEDs, J. Lumin. 155 (2014) 205−209, https://doi.org/10.1016/j.jlumin.2014.06.044.

[190] Z. Zhang, L. Liu, X. Zhang, J. Zhang, W. Zhang, D. Wang, Preparation and investigation of $CaZr_4(PO_4)_6$:Dy^{3+} single-phase full-color phosphor, Spectrochim. Acta Part A Mol. Biomol. Spectrosc. 137 (2015) 1−6, https://doi.org/10.1016/j.saa.2014.07.052.

[191] X.-Y. Sun, J.-C. Zhang, X.-G. Liu, L.-W. Lin, Enhanced luminescence of novel $Ca_3B_2O_6$: Dy^{3+} phosphors by Li^+-codoping for LED applications, Ceram. Int. 38 (2012) 1065−1070, https://doi.org/10.1016/j.ceramint.2011.08.032.

[192] Q. Xu, J. Sun, D. Cui, Q. Di, J. Zeng, Synthesis and luminescence properties of novel $Sr_3Gd(PO_4)_3$:Dy^{3+} phosphor, J. Lumin. 158 (2015) 301−305, https://doi.org/10.1016/j.jlumin.2014.10.034.

[193] G.B. Nair, S.J. Dhoble, White light emission through efficient energy transfer from Ce^{3+} to Dy^{3+} ions in $Ca_3Mg_3(PO_4)_4$ matrix aided by Li^+ charge compensator, J. Lumin. 192 (2017) 1157−1166, https://doi.org/10.1016/j.jlumin.2017.08.047.

[194] L. Chunxia, Z. Cuimiao, H. Zhiyao, W. Lili, Q. Zewei, L. Hongzhou, L. Jun, β-$NaYF_4$ and β-$NaYF_4$:Eu^{3+} microstructures: morphology control and tunable luminescence properties, J. Phys. Chem. C 113 (2009) 2332−2339, https://doi.org/10.1021/jp8101628.

[195] M. Dalal, V.B. Taxak, J. Dalal, A. Khatkar, S. Chahar, R. Devi, S.P. Khatkar, Crystal structure and Judd-Ofelt properties of a novel color tunable blue-white-red $Ba_5Zn_4Y_8O_{21}$: Eu^{3+} nanophosphor for near-ultraviolet based WLEDs, J. Alloys Compd. 698 (2017) 662−672, https://doi.org/10.1016/j.jallcom.2016.12.257.

[196] Z.C. Wu, J. Liu, W.G. Hou, J. Xu, M.L. Gong, A new single-host white-light-emitting $BaSrMg(PO_4)_2$:Eu^{2+} phosphor for white-light-emitting diodes, J. Alloys Compd. 498 (2010) 139−142, https://doi.org/10.1016/j.jallcom.2010.03.136.

[197] M. Shang, C. Li, J. Lin, How to produce white light in a single-phase host? Chem. Soc. Rev. 43 (2014) 1372−1386, https://doi.org/10.1039/c3cs60314h.

[198] J.Y. Han, W. Bin Im, D. Kim, S.H. Cheong, G. Lee, D.Y. Jeon, New full-color-emitting phosphor, Eu^{2+}-doped $Na_{2-x}Al_{2-x}Si_xO_4$ ($0 \leq x \leq 1$), obtained using phase transitions for solid-state white lighting, J. Mater. Chem. 22 (2012) 5374, https://doi.org/10.1039/c2jm15501j.

[199] Y. Liu, A. Lan, Y. Jin, G. Chen, X. Zhang, $Sr_3Bi(PO_4)_3$:Eu^{2+}, Mn^{2+}: single-phase and color-tunable phosphors for white-light LEDs, Opt. Mater. 40 (2015) 122−126, https://doi.org/10.1016/j.optmat.2014.12.007.

[200] X.M. Zhang, W.L. Li, H.J. Seo, Luminescence and energy transfer in Eu^{2+}, Mn^{2+} co-doped $Li_4SrCa(SiO_4)_2$ for white light-emitting-diodes, Phys. Lett. Sect. A Gen. At. Solid State Phys. 373 (2009) 3486−3489, https://doi.org/10.1016/j.physleta.2009.07.052.

[201] W. Wu, Z. Xia, Synthesis and color-tunable luminescence properties of Eu^{2+} and Mn^{2+}-activated $Ca_3Mg_3(PO_4)_4$ phosphor for solid state lighting, RSC Adv. 3 (2013) 6051−6057, https://doi.org/10.1039/c3ra40313k.

[202] C. Shen, Y. Yang, S. Jin, H. Feng, Synthesis and luminous characteristics of $Ba_2MgSi_{2-x}Al_xO_7$:0.1Eu^{2+}, 0.1Mn^{2+} phosphor for WLED, Optik 121 (2010) 29−32, https://doi.org/10.1016/j.ijleo.2008.05.009.

[203] N. Guo, H. You, C. Jia, R. Ouyang, D. Wu, A Eu^{2+} and Mn^{2+}-coactivated fluoro-apatite-structure $Ca_6Y_2Na_2(PO_4)_6F_2$ as a standard white-emitting phosphor via energy transfer, Dalt. Trans. 43 (2014) 12373−12379, https://doi.org/10.1039/c4dt01021c.
[204] S. Choi, Y.J. Yun, H.-K. Jung, Eu^{2+} and Mn^{2+} activated single phase white emitting phosphor Na(Sr,Ba)PO_4 for phosphor converted-LEDs, Mater. Lett. 75 (2012) 186−188, https://doi.org/10.1016/j.matlet.2012.02.019.
[205] N. Guo, Y. Zheng, Y. Jia, H. Qiao, H. You, Warm-white-emitting from Eu^{2+}/Mn^{2+}-codoped $Sr_3Lu(PO_4)_3$ phosphor with tunable color tone and correlated color temperature, J. Phys. Chem. C Deriv. 116 (2012) 1329−1334.
[206] A. Baran, S. Mahlik, M. Grinberg, P. Cai, S.I. Kim, H.J. Seo, Luminescence properties of different Eu sites in $LiMgPO_4$:Eu^{2+},Eu^{3+}, J. Phys. Condens. Matter 26 (2014) 385401, https://doi.org/10.1088/0953-8984/26/38/385401.
[207] A. Baran, S. Mahlik, M. Grinberg, P. Cai, S.I. Kim, H.J. Seo, Luminescence properties of different Eu sites in $LiMgPO_4$:Eu^{2+}, Eu^{3+}, J. Phys. Condens. Matter 26 (2014) 385401, https://doi.org/10.1088/0953-8984/26/38/385401.
[208] A.A. Reddy, S. Das, S. Ahmad, S.S. Babu, J.M.F. Ferreira, G.V. Prakash, Influence of the annealing temperatures on the photoluminescence of $KCaBO_3$:Eu^{3+} phosphor, RSC Adv. 2 (2012) 8768, https://doi.org/10.1039/c2ra20866k.
[209] A. Baran, J. Barzowska, M. Grinberg, S. Mahlik, K. Szczodrowski, Y. Zorenko, Binding energies of Eu^{2+} and Eu^{3+} ions in β-Ca_2SiO_4 doped with europium, Opt. Mater. 35 (2013) 2107−2114, https://doi.org/10.1016/j.optmat.2013.05.030.
[210] J. Chen, Y. Liang, Y. Zhu, S. Liu, H. Li, W. Lei, Abnormal reduction of Eu^{3+} to Eu^{2+} in $Sr_5(PO_4)_3Cl$:Eu phosphor and its enhanced red emission by the charge compensation, J. Lumin. 214 (2019) 116569, https://doi.org/10.1016/j.jlumin.2019.116569.
[211] A. Dobrowolska, E. Zych, Spectroscopic characterization of $Ca_3Y_2Si_3O_{12}$:Eu^{2+},Eu^{3+} powders in VUV-UV−vis region, J. Phys. Chem. C 116 (2012) 25493−25503, https://doi.org/10.1021/jp306764f.
[212] K. Biswas, A.D. Sontakke, K. Annapurna, Synthesis and structural probing of Eu^{3+} doped $BaYF_5$ nano-crystals in transparent oxyfluoride glass-ceramics, Int. J. Appl. Glass Sci. 3 (2012) 154−162, https://doi.org/10.1111/j.2041-1294.2012.00087.x.
[213] G. Li, Y. Tian, Y. Zhao, J. Lin, Recent progress in luminescence tuning of Ce^{3+} and Eu^{2+}-activated phosphors for pc-WLEDs, Chem. Soc. Rev. 44 (2015) 8688−8713, https://doi.org/10.1039/C4CS00446A.
[214] F. Xiao, Y.N.N. Xue, Q.Y.Y. Zhang, Ca_2BO_3Cl:Ce^{3+},Eu^{2+}: a potential tunable yellow−white−blue-emitting phosphors for white light-emitting diodes, Phys. B Condens. Matter 404 (2009) 3743−3747, https://doi.org/10.1016/j.physb.2009.06.122.
[215] Z. Zheng, T. Wanjun, Tunable luminescence and energy transfer of Ce^{3+}/Eu^{2+}/Mn^{2+}-tridoped $Sr_8MgLa(PO_4)_7$ phosphor for white light LEDs, J. Alloys Compd. 663 (2016) 731−737, https://doi.org/10.1016/j.jallcom.2015.12.184.
[216] Y. Song, G. Jia, M. Yang, Y. Huang, H. You, H. Zhang, $Sr_3Al_2O_5Cl_2$:Ce^{3+},Eu^{2+}: a potential tunable yellow-to-white-emitting phosphor for ultraviolet light emitting diodes, Appl. Phys. Lett. 94 (2009) 091902, https://doi.org/10.1063/1.3094753.
[217] Q. Wang, D. Deng, Y. Hua, L. Huang, H. Wang, S. Zhao, G. Jia, C. Li, S. Xu, Potential tunable white-emitting phosphor $LiSr_4(BO_3)_3$:Ce^{3+}, Eu^{2+} for ultraviolet light-emitting diodes, J. Lumin. 132 (2012) 434−438, https://doi.org/10.1016/j.jlumin.2011.09.003.
[218] L. Chen, A. Luo, Y. Zhang, F. Liu, Y. Jiang, Q. Xu, X. Chen, Q. Hu, S.F. Chen, K.J. Chen, H.C. Kuo, Optimization of the single-phased white phosphor of Li_2SrSiO_4:Eu^{2+}, Ce^{3+} for light-emitting diodes by using the combinatorial approach assisted with the Taguchi method, ACS Comb. Sci. 14 (2012) 636−644, https://doi.org/10.1021/co300058x.

[219] C. Lv, X. Min, S. Li, Z. Huang, Y. Liu, X. Wu, M. Fang, Luminescence properties of emission tunable single-phased phosphor $La_7O_6(BO_3)(PO_4)_2$:Ce^{3+}, Tb^{3+}, Eu^{3+}, Mater. Res. Bull. 97 (2018) 506−511, https://doi.org/10.1016/j.materresbull.2017.09.030.

[220] M. Zhao, Z. Zhao, L. Yang, L. Dong, A. Xia, S. Chang, Y. Wei, Z. Liu, The generation of energy transfer from Ce^{3+} to Eu^{3+} in $LaPO_4$:Ce^{3+}/Tb^{3+}/Eu^{3+} phosphors, J. Lumin. 194 (2018) 297−302, https://doi.org/10.1016/j.jlumin.2017.10.041.

[221] X. Zhang, X. Fu, J. Song, M. Gong, Luminescent properties and energy transfer studies of color-tunable $LuBO_3$: Ce^{3+}/Tb^{3+}/Eu^{3+} phosphors, Mater. Res. Bull. 80 (2016) 177−185, https://doi.org/10.1016/j.materresbull.2016.03.023.

[222] X. Zhang, L. Zhou, Q. Pang, J. Shi, M. Gong, Tunable luminescence and $Ce^{3+} \rightarrow Tb^{3+} \rightarrow Eu^{3+}$ energy transfer of broadband-excited and narrow line red emitting Y_2SiO_5:Ce^{3+}, Tb^{3+}, Eu^{3+} phosphor, J. Phys. Chem. C 118 (2014) 7591−7598, https://doi.org/10.1021/jp412702g.

[223] J. Zhou, Z. Xia, Luminescence color tuning of Ce^{3+} , Tb^{3+} and Eu^{3+} codoped and tri-doped $BaY_2Si_3O_{10}$ phosphors via energy transfer, J. Mater. Chem. C 3 (2015) 7552−7560, https://doi.org/10.1039/C5TC00962F.

[224] X. Zhang, L. Zhou, Q. Pang, M. Gong, A broadband-excited and narrow-line $GdBO_3$: Ce^{3+}, Tb^{3+}, Eu^{3+} red phosphor with efficient $Ce^{3+} \rightarrow (Tb^{3+})_n \rightarrow Eu^{3+}$ energy transfer for NUV LEDs, Opt. Mater. 36 (2014) 1112−1118, https://doi.org/10.1016/j.optmat.2014.02.009.

[225] J. Zhang, Z. Hua, S. Wen, Luminescence of emission-tunable $Ca_{10}Li(PO_4)_7$:Eu^{2+}, Sr^{2+}, Mn^{2+} phosphors with various Eu^{2+} centers for LED applications, J. Alloys Compd. 637 (2015) 70−76, https://doi.org/10.1016/j.jallcom.2015.02.117.

[226] C.H. Huang, T.M. Chen, W.R. Liu, Y.C. Chiu, Y.T. Yeh, S.M. Jang, A single-phased emission-tunable phosphor $Ca_9Y(PO_4)_7$:Eu^{2+},Mn^{2+} with efficient energy transfer for white-light-emitting diodes, ACS Appl. Mater. Interfaces 2 (2010) 259−264, https://doi.org/10.1021/am900668r.

[227] G. Ju, Y. Hu, L. Chen, X. Wang, Photoluminescence properties of color-tunable $SrMgAl_{10}O_{17}$:Eu^{2+},Mn^{2+} phosphors for UV LEDs, J. Lumin. 132 (2012) 1792−1797, https://doi.org/10.1016/j.jlumin.2012.02.036.

[228] J. Chen, Y. Liu, L. Mei, Z. Wang, M. Fang, Z. Huang, Emission red shift and energy transfer behavior of color-tunable $KMg_4(PO_4)_3$:Eu^{2+},Mn^{2+} phosphors, J. Mater. Chem. C 3 (2015) 5516−5523, https://doi.org/10.1039/C5TC00636H.

[229] M. Jiao, Y. Jia, W. Lü, W. Lv, Q. Zhao, B. Shao, H. You, $Sr_3GdNa(PO_4)_3F$:Eu^{2+},Mn^{2+}: a potential color tunable phosphor for white LEDs, J. Mater. Chem. C 2 (2014) 90−97, https://doi.org/10.1039/C3TC31837K.

[230] Y. Tian, N. Feng, M. Wierzbicka-Wieczorek, P. Huang, L. Wang, Q. Shi, C. Cui, Energy transfer-induced tunable emission color and thermal quenching of $Ca_3Y(PO_4)_3$: Eu^{2+}, Mn^{2+} phosphor for NUV-pumped white LEDs, Dye. Pigment. 131 (2016) 91−99, https://doi.org/10.1016/j.dyepig.2016.04.010.

[231] Y. Chen, Y. Li, J. Wang, M. Wu, C. Wang, Color-tunable phosphor of Eu^{2+} and Mn^{2+} codoped $Ca_2Sr(PO_4)_2$ for UV light-emitting diodes, J. Phys. Chem. C 118 (2014) 12494−12499, https://doi.org/10.1021/jp502571c.

[232] K. Li, D. Geng, M. Shang, Y. Zhang, H. Lian, J. Lin, Color-tunable luminescence and energy transfer properties of $Ca_9Mg(PO_4)_6F_2$:Eu^{2+}, Mn^{2+} phosphors for UV-LEDs, J. Phys. Chem. C 118 (2014) 11026−11034, https://doi.org/10.1021/jp501949m.

Advanced variants of LEDs

5

5.1 Introduction

The swift progression in light-emitting diode (LED) technology has flagged way to countless innovations in the lighting sector. This has also promoted the application of LEDs in fields beyond lighting. LEDs have garnered huge admiration owing to their efficiency, durability, and ease of use. However, the LED structure has undergone several modifications to meet the requirements that are varying from time to time. The journey of LEDs started with the semiconductor diodes, mainly based on nitrides, arsenides, and phosphides of the group-III elements. These diodes were capable of emitting red, green, or blue color, depending on the composition of the semiconducting material. The semiconducting chips, however, were unable to cover the entire wavelength range and often suffered from several pitfalls in their color emission. A single chip is unable to give multiple color emissions. The blending of several chips to produce a desired color emission could have been a solution, unless all the chips have a similar pattern of degradation. The lacunas faced in the color composition of these diodes were later on solved by incorporating phosphors with the LED package. A phosphor can be prepared at a much cheaper way with less sophisticated equipment as compared to the production of a semiconductor chip. It also can be combined with a single chip that is able to provide the pump power required for the phosphor's optical excitation. LEDs soon expanded their applications beyond the household lighting needs. It started dominating the display industry, biomedical field, digital communications, and horticulture. The need for more efficient and durable materials for LEDs started intensifying to satisfy the needs of diverse fields. Researchers started experimenting with alternative materials and found success.

Although phosphor-converted LEDs (pc-LEDs) are still a dominating element in the LED industry, newer variants of LEDs started showing promising results. Organic materials soon gained recognition for their self-emissive properties and started replacing inorganic phosphors. This gave rise to a new version called organic light-emitting diodes (OLEDs). Quantum dots (QDs) too came into the picture with exceptional quantum yield (QY) values and gave birth to quantum dot LEDs (QLEDs). Apart from these, there are several other versions of LEDs that are still under development and are yet to face the commercial market. In this chapter, there will be discussion on some of the newest versions of LEDs that have shown exceptional characteristics and higher efficiency than the pc-LEDs. The topics highlighted here will be biased on microLEDs, OLEDs, QLEDs, perovskite LEDs (Pe-LEDs), and bioLEDs.

The Fundamentals and Applications of Light-Emitting Diodes. https://doi.org/10.1016/B978-0-12-819605-2.00005-7

5.2 MicroLEDs

With the advancement of InGaN/GaN-based LEDs, many research groups have started focusing on improving the efficiency and fabrication of high-power LEDs. Attempts were made by these research groups to extract higher power output by adopting several strategies. Some of them successfully accomplished this objective by adopting the strategies such as optimization of epitaxy and processing, designing of resonant cavity structures, or improved current spreading [1−3]. However, there are instances of total internal reflections occurring within the LED interface, which can confine a significant amount of emitted light within the device [4]. A noteworthy enhancement in the external quantum efficiency can be achieved if the conventional LEDs are replaced with microLEDs [5]. MicroLEDs are a form of new LED structures that are benefited with superior light extraction efficiency. They are microscopic versions of LEDs devoid of a package. They are also known as mLED or μLED. The size of a microLED is 1/100th of a conventional LED and often measures less than 50 μm, as shown in Fig. 5.1.

MicroLEDs have exhibited a display luminance about 1000 times more than the normal commercial displays [6]. Their exceptional luminescence features have found promising results in the display devices and as a tool for manipulation or stimulation in life sciences [7]. On paper, mircoLEDs are proposed to provide higher brightness and color than the existing display devices and that too at a much lower power. Additionally, they are self-emissive. Unlike conventional LEDs that are mostly used as backlights for liquid crystal displays (LCDs), microLEDs do not require backlights. They are scaled-down versions of traditional LEDs that provide better and brighter displays. It can also withstand high current densities and produce high power densities [8]. It has showed improved light extraction and better thermal management than the conventional LEDs [8,9].

The fabrication of microLEDs also follows a pattern similar to conventional LEDs and mini-LEDs. Since the ability of the μLEDs to tolerate the defects at the micron-level decreases, it is essential to manufacture them with virtually no defects. Much sophisticated equipment and clean environment are required to achieve a defect-free microLED. The type of display decides the process flow for the fabrication using μLEDs. The device performance, productivity, and reliability of the display devices are highly influenced by the structure and packing of the microLEDs. Several strategies have been explored to enhance the performance of microLEDs, which also includes altering their device structure into lateral structured, vertical structured, and flip-chip lateral structured microLEDs [10−13]. The very first step involves the manufacturing of microLEDs, which is similar to that of conventional LEDs to some extent. Thin layers of GaN are deposited on a wafer epitaxially [14]. Generally, metal−organic chemical vapor deposition (MOCVD) method is preferred for depositing the III-nitride layers over a sapphire or a silicon substrate. The first layer is the n-type layer of GaN/InGaN/AlGaN materials. This is followed by deposition of a thin layer of MQWs. Again a p-type layer of GaN/InGaN/AlGaN is deposited over the MQW layer. The individual microLED chips, then, must be tested and transferred

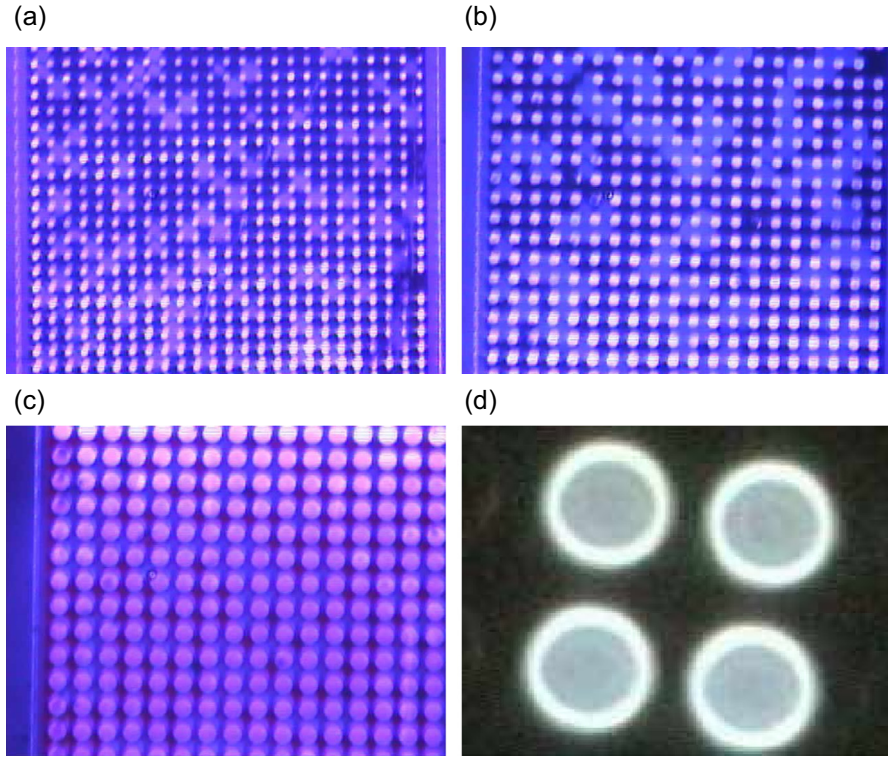

Figure 5.1 Optical microscope images of operating arrays of (a) 8-μm, (b) 12-μm, and (c) 20-μm element diameter and (d) optical image of cathodoluminescence under broad-beam excitation of a cluster of four 12-μm microLED elements.
Reprinted with permission from H.W. Choi, C.W. Jeon, M.D. Dawson, P.R. Edwards, R.W. Martin, Efficient GaN-based micro-LED arrays, Mater. Res. Soc. Symp. Proc. 743 (2002) 433−438. Copyright 2003, Materials Research Society.

to a backplane to form an array. Transferring millions of such microLEDs is a daunting process. This can be solved by adopting the fabrication of thin films based on microLEDs. Thin films can be transferred in a more cost-effective way by facilitating mass transfer of microLEDs at one go. Depending on the device structure, thin-film microLEDs are classified into lateral microLEDs (LLEDs) and vertical microLEDs (VLEDs) [15]. LLEDs suffer from high heat generation and low optical power, whereas VLEDs have high stability and exceptionally good output efficiency. Some of the methods to transfer microLEDs from the mother substrate to a target substrate are listed as laser-assisted transfer, electrostatic transfer, electromagnetic transfer, elastomer stamping, ACF adhesive transfer, and pressure-based transfer [15]. Another critical step for preparing the microLEDs for optoelectronic applications is their packaging. Technologies such as flip-chip, wire bonding, and wafer bonding have been developed to enable interconnection of peripheral and core electronics.

At present, two different technologies have dominated the display market to a great extent. The first one is the LCD that consists of thin-film transistors (TFTs) and is backlit by LEDs. The other one is the OLEDs, which are more efficient than LCDs and are self-emissive. However, most of the devices such as cell phones and low-cost televisions are still equipped with LCDs. On the other hand, OLEDs are slowly conquering the cell phone industry, and by 2023, it is expected to be found in more than 50% of the cell phones manufactured all over the world. OLED displays are ultrathin and are easily foldable too. In addition to these two technologies, miniLEDs and microLEDs are also building inroads to the display market. Although they are not yet unveiled in the display market commercially, they have displayed promising results with greater luminance and higher resolution than OLEDs. MicroLEDs are still in their development phase and are expected to be very expensive in the initial days of their business trade in the market.

MicroLEDs are also GaN-based semiconductor LEDs and operate on the same principle as that of conventional LEDs. MiniLEDs are bigger versions of microLEDs with a size of 100 μm or more but smaller than conventional LEDs. Conventional LEDs are available as monochromes or multicolor-emitting diodes. A popular version of LEDs is the RGB LEDs (red, green, blue LEDs) that can be tuned to meet the requirements of a display or lighting device. Similarly, microLEDs can also offer RGB tuning, wherein each color will be represented as a subpixel in the display. The combination of these three colors will ultimately produce a pixel. However, making a display panel using microLEDs is still a costly and tedious affair. A horde of microLEDs will be required to develop a display panel. On the other hand, OLEDs can be deposited and processed over a wide area, thus, making it easy to develop large display panels relatively with ease. However, microLEDs show a much better life span, as they are made of inorganic materials, and unlike OLEDs, they will not be fading away so easily. OLEDs have maximum pixels per inch (PPI) of 3500 with 2×10^3 nits, whereas microLEDs have 5000 PPI with 10^5 nits. A nit is a unit of measuring the luminance, and it is equal to a candela per unit area (cd/m^2). This superior luminance and resolution of microLED over OLEDs has motivated the display industries to work and find a solution to overcome the challenging fabrication issues and bring microLEDs as frontline materials for displays. The major technical issue in fabrication of microLED displays is their transfer and assembly on to a substrate. Display devices such as smartphones and televisions require microLED dies ranging from 3 to 10 μm to be assembled on the substrate. If the displays are made for high-resolution devices, such as 8K televisions, then there must be a 100 million microLED dies assembled on the substrate with a placement accuracy of 1 μm. This makes the fabrication of microLED display a daunting process. Sony, a giant in electronics-manufacturing, developed a 55-inch prototype of microLED display by incorporating 6 million microLEDs in them and demonstrated the display in 2012. They branded this prototype as crystal LED. The challenge is to assemble such huge number of microLEDs on the substrate without a single error. Another challenge was to obtain high external quantum efficiency (EQE) from the microLEDs to prove their worth as an appropriate replacement for OLED displays. The initial versions of microLEDs provided a limited EQE of 1%−5%, and this was never going to be sufficient to challenge the rising dominance of OLEDs in the display

market. To deliver better efficiency and live up to the expectations of the display industry, it must have demonstrated a much higher EQE. However, dramatic progress has been made to increase their efficiency, and close to 50% EQE has been achieved [14]. A research group characterized the functioning efficiency of AlGaN-based LEDs on the basis of their size, p-cladding layer, and the number of multiquantum wells (MQWs) [16]. Although EQE decreased with the decreasing size of the LEDs, the EQE values were found to be higher for microLEDs with less number of MQWs. A thicker layer of p-cladding layer also produced more efficient microLEDs.

Application-wise, microLEDs are suitable for both microdisplays as well as large displays. An example of microdisplays is the augmented reality (AR) glass, which is considered as the future of cell phones. MicroLEDs are the best choice for microdisplays. MicroLEDs can provide 100,000 pixels at a size of 10 mm × 10 mm size, which is 100 times more than the existing OLED technology. The requirements for microdisplays to be used in AR glasses can be fulfilled only using microLEDs. MicroLEDs have also found way into the midsized displays such as smartphones and smartwatches as well as large-sized displays such as high-resolution televisions. They do not need any color filter and, hence, can brightly display with less effort and energy. They can also provide much thinner displays than OLEDs and provide perfect viewing angles for televisions. Samsung demonstrated its 75- and 146-inch versions of the microLED TV "The Wall." They also demonstrated an even bigger version of "The Wall" with a 219-inch display. Sony, TCL, and Hisense also demonstrated their respective versions of microLED TV.

5.3 Organic light-emitting diodes

OLEDs have made rapid progress in the lighting industry, since the discovery of electroluminescence in organic crystals in 1963 [17]. The technologies prior to OLEDs suffered from several shortcomings, which were essentially rectified by the LEDs based on organic materials. OLEDs operate in a fashion similar to normal LEDs, except that the organic compounds are responsible for producing the negative and positive charges instead of a semiconductor or an inorganic material. The display devices made from OLEDs showed better contrast and brightness, high-resolution, ultrathin, and flexible displays with low power consumption. Also, it is much economical to construct a display using OLEDs than LCDs or plasma displays. OLED displays are self-emissive and do not require any backlights or chemical shutters. This makes OLEDs thinner and lighter than other displays. OLEDs can be directly printed on a substrate using screen-print or ink-print technology. Also, large-sized displays can also be realized using OLEDs. OLED displays provide consistency in the image quality and screen clarity along with incomparable efficiency. The visuals displayed on OLED screens can be viewed from any angle [18]. OLEDs provide tough and durable screens for portable devices such as digital cameras, cell phones, personal digital assistant, and so on.

OLEDs are known to generate nonglaring, diffuse lighting with high color rendering index (CRI). They are semiconductors with some properties of plastics

that can emit light by electroluminescence phenomenon. The basic structure of an OLED comprises four major parts: a substrate, a cathode, an anode, and one or more organic layers. The substrate forms the base for all OLED structures, and different layers are deposited one by one on the substrate. It is essential for OLEDs to have a flexible and transparent substrate with high work-function (4.7−4.9 eV), scratch resistance, high stability, and low roughness [19]. Generally, transparent metal foils, glass, or plastics are considered as suitable substrates for OLEDs. A layer of indium tin oxide (ITO) or graphene is then coated to act as anode. Anodes are meant to serve as the positive electrode to OLEDs and, hence, must possess high work-function as well as low roughness. Next comes the organic layers, which are coated above the anode. Above the organic layers, the cathode layer is coated for which alloys of magnesium with silver (Mg:Ag) or aluminum with lithium (Al:Li) are used. The cathode must be transparent and have low work-function. The organic layers that are sandwiched between the two electrodes enable the OLEDs to give out much brighter light than conventional LEDs, but these thin organic layers form a complicated system. Depending upon the number of organic layers fused between the electrodes, an OLED can be single-layered, double-layered, triple-layered, or multi-layered, as shown in Fig. 5.2 [20]. The organic layers are divided into hole-injection layer (HIL), hole-transport layer (HTL), emissive layer (EML), hole-blocking layer (HBL), and electron-transport layer (ETL). A single-layered OLED consists of only the emissive layer sandwiched between the two electrodes. The emissive layer in single-layered structure includes the electron transport, hole transport, and emissive properties. The electrons and holes must be injected in same proportion, or else there will be no recombination of the excess charge carrier, and this will result in lower efficiency of the device. In double-layered structure, there are two organic layers. One layer acts as the ETL, whereas the other acts as the HTL. Emission can take place from either of the two layers due to the recombination of the electron−hole pairs. In triple-layered structure, an emissive layer is sandwiched between the HTL and ETL.

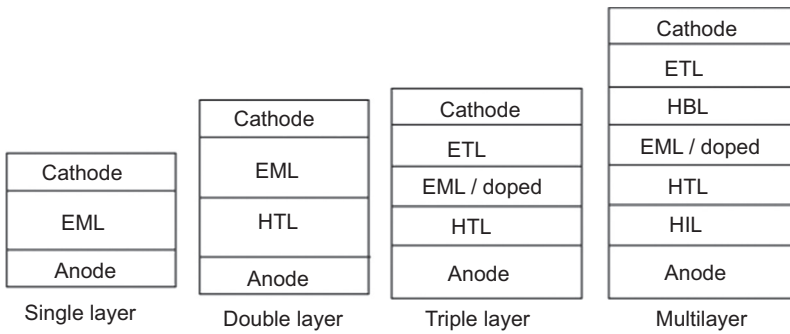

Figure 5.2 Different anatomies of OLEDs. *EML*, emissive layer; *ETL*, electron transport layer; *HBL*, hole-blocking layer; *HTL*, hole transport layer; *OLEDs*, organic light-emitting diodes. Reprinted with permission from N. Thejo Kalyani, S.J. Dhoble, Novel materials for fabrication and encapsulation of OLEDs, Renew. Sustain. Energy Rev. 44 (2015) 319−347. https://doi.org/10.1016/j.rser.2014.11.070. Copyright 2014 Elsevier.

Since all these layers have their distinct functions, they can be individually optimized. In multilayered structure, there are additional organic layers that improve the overall efficiency of the device. An HIL coated above the anode injects holes into the emissive layer from the anode and blocks the electrons for recombination to occur. Copper (II) phthalocyanine (CuPC), 4,4′,4″-tris[phenyl(m-tolyl)amino]triphenylamine (m-MTDATA), N,N,N′,N′-tetrakis(4-methoxy-phenyl)benzidine (MeO-TPD), phthalocyanine, and platinum complex (PtPC) are the organic complexes that are generally considered as HIL. The complexes used for HIL must have high glass temperature, high mobility, and electron-blocking capacity [19]. The role of HTL is to transport holes and block the electrons. Thus, HTL materials must have good hole-transporting capacity, low electron affinity, and low ionization potential. N,N′-Bis(naphthalen-1-yl)-N,N′-bis(phenyl)-benzidine (NPB), N,N′-bis(naphthalen-1-yl)-N,N′-bis(phenyl)-2,2′-dimethylbenzidine (α-NPD), and N,N′-bis(3-methy lphenyl)-N,N′-diphenylbenzidine (TPD) are generally used as HTL. EML is sandwiched between the HTL and HBL. EML is normally fabricated using organic molecules, dendrimers, or polymers that have high luminescence efficiency, color purity, and longer lifetime. They are very good emitter of photons in the visible light range and can tune the emission color of the device by selecting appropriate organic complexes. The electrons from the cathode and the holes from the anode are forced to recombine in the EML by the electrostatic forces to form an exciton, which then leads to the emission of light. The energy separation between the highest occupied molecular orbit (HOMO) and lowest unoccupied molecular orbit (LUMO) as well as the energy gap of the organic compound decides the color of the emitted light. The role of HBL is to inject the holes and block the electrons. ETL has an inverse functioning as that of the HTL. The role of ETL is to transport the electrons and block the holes. The ionization potential and electron affinity of the materials functioning as ETL must be high. The electrons injected by the cathode are directed towards the EML by the ETL without any leakage of charges. It also prevents the accumulation of charges at the ETL and cathode interfaces. An advantage enjoyed by multilayered structure is that it eliminates the leakage of electrons and holes and prevents the exciton quenching at the metal and organic layer interface [19]. Proper selection of materials for each organic layer, controlling their thickness, use of high purity organic compounds, and doping strategies are all essential to optimize the performance of the OLED device. The mechanism of light emission from an OLED is shown in Fig. 5.3 [21].

An OLED device can be fabricated in any of the architectures, viz., top-emitting OLEDs, bottom-emitting OLEDs, transparent OLEDs, stacked OLEDs, etc. In top-emitting OLEDs, a transparent or a semitransparent cathode is placed at the top and the conductive layer of anode is placed at the bottom. The emissive layer is sandwiched between the two electrodes. During their operation, top-emitting OLEDs emit light from the top, and hence, it is essential to have a transparent cathode. In bottom-emitting OLEDs, the light is emitted from the bottom, and the transparent cathode is placed at the bottom, whereas the conducting layer of anode is placed at the top. Bottom-emitting OLEDs can be integrated easily with nontransparent transistor backplane and, hence, are better suited for active matrix applications. In transparent OLEDs (TOLEDs), both sides of the device comprise transparent or semitransparent electrode

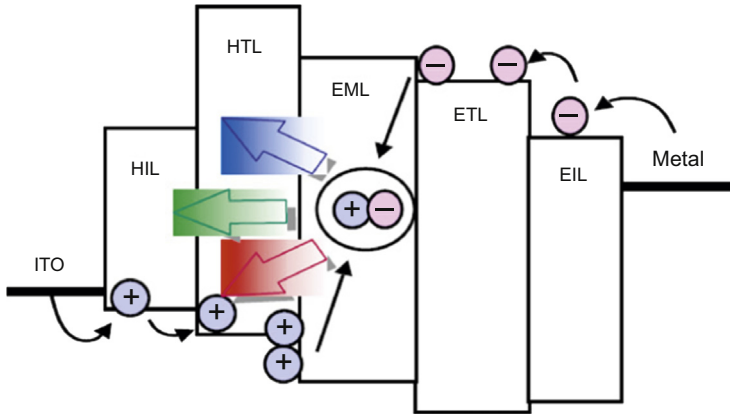

Figure 5.3 Mechanism of light emission from OLEDs. *EIL*, electron injection layer; *EML*, emissive layer; *ETL*, electron transport layer; *HIL*, hole injection layer; *HTL*, hole transport layer; *ITO*, indium tin oxide; *OLEDs*, organic light-emitting diodes.
Reprinted with permission from N. Thejo Kalyani, S.J.J. Dhoble, N.T. Kalyani, S.J.J. Dhoble, N. Thejo Kalyani, S.J.J. Dhoble, N.T. Kalyani, S.J.J. Dhoble, N. Thejo Kalyani, S.J.J. Dhoble, Organic light emitting diodes: energy saving lighting technology - a review, Renew. Sustain. Energy Rev. 16 (2012) 2696−2723. https://doi.org/10.1016/j.rser.2012.02.021. Copyright 2012 Elsevier.

contacts. Displays made from TOLEDs enjoy improved contrast and better visibility in sunlight. Graded heterojunction OLEDs take care of the stabilization of charge injection and concurrently minimizes the distance to be traveled by an electron to reach the hole. This modification enables them to operate with longer device lifetimes and less power consumption. This feature also reduces the complexity of the structure by combining the double-emissive layer with the mixed-emissive layer to form a single layer and, thereby, lower the production costs. The quantum efficiency of the graded heterojunction OLEDs is almost double than that of the existing OLEDs available commercially. Stacked OLEDs (SOLEDs) consists of a pixel architecture, wherein the red, green, and blue subpixels are placed in a vertical stack and separated by conducting, transparent electrodes [22]. Such type of architecture is found to reduce the pixel gap but significantly enhance the color depth and gamut. Another design of OLEDs is the inverted OLEDs. In conventional OLEDs, it is essential to have at least one of the electrodes to be transparent and conductive, to extract light efficiently from the device. The best choice is ITO, which can act as both transparent and conductive anode. But deposition of ITO on the substrate will require the device to be exposed to harsh conditions, which can destroy the organic layers. The chemical integrity of these organic layers can be preserved if the ITO is deposited prior to organic layer deposition. Thus, the OLED device gets fabricated in the reverse order and hence, the name inverted OLED [23].

OLEDs have showcased exceptional benefits in the lighting and display industries and have compelled the manufacturers to opt for OLEDs over other lighting sources. OLEDs can be directly printed onto a substrate by traditional inkjet method and,

thereby, lower the costs incurred in the device fabrication. Another advantage is that displays prepared from OLEDs have a wide viewing angle of up to 170 degrees. These displays do not require any backlights and exhibit immense brightness, good contrast, high clarity, high luminescence efficiency, and consistent image quality. They provide full range of colors with high resolution with thinner, flexible, and lighter screens. They use lesser power consumption ($\sim$3−4 V), but operate at wider temperatures. In spite of several such benefits, there are many hurdles that need to be addressed to make OLEDs more reliable and efficient in the long run. The very first issue is their degradation caused due to the deposition of dust particles or other pollutants during the device fabrication. During operation, OLEDs can get exposed to water vapors or oxidative atmospheres that can delaminate the electrodes and also produce dark spots on the device. Nonemissive spots appear on the device mainly due to the oxidation and delamination of cathode [24]. Some of the mechanisms that lead to the degradation of the device can be listed as migration of ionic species, electrochemical reactions at the electrode/organic layer interface, and crystallization of organic molecules. Organic molecules can get damaged easily when they get in contact with water. Hence, the devices must be sealed well during fabrication to provide more longevity to OLED displays. The stability of an OLED device can be classified into short-term degradation and long-term degradation, on the basis of the time scale required to degrade the device. The former is found to occur in the initial stage of operation, whereas the latter ensues gradually during the subsequent operation. Short-term degradation can be either recoverable or unrecoverable. Recoverable degradation can arise without any trace of dark spots or crystallization. The device performance of OLEDs can be improved by protecting the devices from the atmosphere. Another issue is the limited life span of the organic layers that need to be resolved to elongate the lifetime of an OLED device. The life span of the device is measured as the time taken for the emission of a device to degrade to half its initial intensity. The life span of OLEDs is found to decrease when they are operated at higher temperatures. Blue OLEDs are found to have the least life span in contrast to their red and green counterparts. Hence, it is a challenge to prepare efficient blue organic materials that can stand against the test of time. The power consumption of OLED displays also needs to be consistent for all types of images. Although OLEDs consume only 40% of the power as that required for LCDs, it does not show the same efficiency levels consistently. Depending on the color of the image, OLEDs can consume about 80% of the power as that of LCDs. On the other hand, OLEDs can consume almost thrice the power required by an LCD if the image shows a white background. This will considerably reduce the battery life that powers the OLED devices. If these issues are addressed, then OLEDs can definitely dominate the lighting and display industry.

5.4 Quantum dot light-emitting diodes

In the recent years, LEDs based on QDs have witnessed a huge progress in the commercial industry. QDs are semiconductor nanocrystals that can emit any color by varying their size [25]. By altering the size of the QDs, their absorption and emission

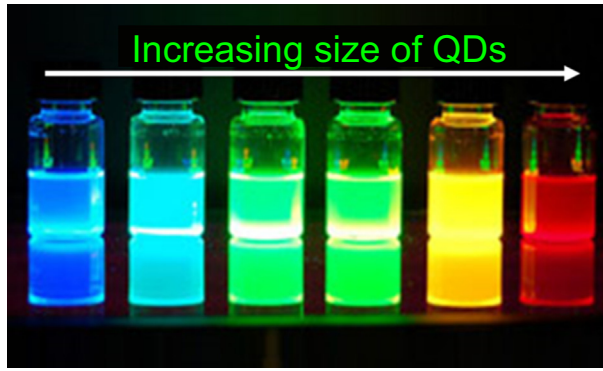

Figure 5.4 Color shift in the emission from blue to red with increasing size of quantum dots (QDs).

bands can be tuned accordingly from ultraviolet to infrared region. With the decreasing size of QDs, the emission shows a hypsochromic shift, as shown in Fig. 5.4. On the other hand, the lifetime becomes longer when the size of QDs increases. QDs are even tinier than a virus. A strong quantum confinement effect is exhibited by QDs whose radius is less than the Bohr radius.

Colloidal QDs have found immense demand for industrial applications owing to their high quantum efficiency, narrow full-width at half maxima (FWHM), ease of color tunability, higher stability, etc. [26]. QDs are preferred to be grown as a core/shell structure. This will help avert the luminescence quenching due to the recombination of the delocalized charge carriers at the surface by passivation of the surface [27]. Thus, a defect-sensitive core can be passivated by coating a bare QD with single or multiple shells. Based on the relative position of the electronic energy levels and the bandgap of the core/shells, the core/shell nanocrystals can be classified as type I, reverse type I, and type II [28]. In type I, the bandgap of the core material is smaller than that of the shell and both the holes and electrons are confined within the core. In reverse type I, the bandgap of the core material is larger than that of the shell material. The electrons and holes are partially or completely confined within the shell, depending on the thickness of the shell. In type II, either the conduction band edge or the valence band edge of the shell material is located in the bandgap of the core. It shows a staggered band alignment due to which the wave functions of electrons and holes are located in different regimes. Primarily, there are three types of coating in the synthesis of core/shell semiconductors, [26]. The coating can be either a single-shell, multishell, or a graded alloyed structure. The type I, reverse type I, and type II core/shell structures are included in the single-shell coating. Some examples of single-shell coating are CdSe/ZnSe [29,30] and CdSe/ZnS [31−33]. The most common examples of multishell coating are CdSe/CdS/ZnS [34,35], CdSe/ZnSe/ZnS [36], CdTe/CdS/ZnS [37], CdTe/CdSe/CdS/ZnS [38], and CdSe/CdS/ZnS/CdS/ZnS [39]. The lattice stress of QDs can be decreased, and the tuning of lattice mismatch can be achieved by using the interfacial alloyed layer of $CSe_{0.5}S_{0.5}$ [28]. The bandgap of graded alloyed QDs is engineered either by employing single pot methods of core/shell synthesis or by

high-temperature annealing of QD core/shell structures. The examples of graded alloyed QDs are ZnCdSeS [40], ZnCdSe [41], ZnCdS [42], CdSeTe [43], CdSe// ZnS [44], and CdSeS [45].

QDs have the ability to exhibit both electroluminescence and photoluminescence by receiving the electrical and optical excitations, respectively. The LEDs based on QDs can be used either as a backlight for LCDs or as a QLED. Generally, the photoluminescence property of QDs is considered for backlights, whereas the electroluminescence property is utilized for QLEDs. For LCD backlights, QDs are used as nanophosphors and a combination of different QDs with different color emissions are employed. For QLEDs, the QDs are directly injected with holes and electrons to bring out the radiative recombination of these charge carriers accompanied by the emission of photons of desired color. QDs can be realized as backlights for LCDs by any of the three possible configurations. The first one is the edge configuration consisting of a fragile QD tube and is seldom used for LCD backlights. The second one is the film configuration, wherein the QDs are arranged over a light guide plate. This configuration suffers from the drawback that QDs can be damaged due to excessive heat liberated from the chip, and hence, the film must be kept at a distance away from the high-intensity flux-generating chips. The third one is the on-chip configuration, which requires very few numbers of QDs. In this case, QDs are directly sprayed on to the blue-emitting InGaN chip. Here, QDs must be capable enough to withstand the heat and flux generated by the chip.

QLEDs based on the principle of electroluminescence have witnessed drastic developments in their fabrication technology. With the enhancement in their EQE, QLEDs have started giving a tough competition to the existing OLED technology and are soon expected to rule the display industry with their flexible and thin displays. However, there are some hindrances that limit the efficiency of OLEDs. Although QY of QDs have been enhanced up to 100% by novel synthetic methods, their efficiencies were found to drop when incorporated in devices. The EQE of QLEDs is still less than that of OLEDs. Due to their high surface-to-volume ratio, QDs are very sensitive to their environment. Factors such as Auger recombination, field-induced quenching (FIQ), and Förster resonance energy transfer (FRET) limit the QLED performance. These factors lead to increased exciton nonradiative recombination rates that ultimately decrease the QY of QDs. Auger recombination is also associated with blinking, wherein a random switching occurs between the emitting states and the dark states. This phenomenon is also known as fluorescence intermittency. The blinking behavior can be suppressed by coating multiple monolayer shells over the QDs to form a giant QD (g-QD) with ultrathick shell [46]. The device performance of g-QDs has shown improved performances owing to interfacial engineering. The introduction of an intermediate alloyed layer in between the core and shell of the QD structure can significantly suppress the Auger decay and enhance the performance of QLEDs [47]. Similarly, coating the QDs with a suitable bipolar organic matrix or a material having high dielectric constant can reduce the effects of field-induced quenching. Such an encapsulation can protect the QDs from the direct exposure to electric fields that form the main reason behind the occurrence of FIQ. The optimization of the device architecture and QD engineering can significantly reduce the problems that limit the

QD efficiency. Also, in the regions where QDs are located in the architecture, there must be low operating fields. Such measures can effectively suppress the nonradiative recombinations and field-induced quenching in the QD-based devices and improve their performance considerably.

To display sharp images with vivid colors, QDs must exhibit very narrow band emissions with high QY and long-term stability. It is also essential that QDs are prepared from nontoxic precursors, thereby, making them eco-friendly. Currently, cadmium-based QDs are known to produce the best color emissions with incomparable narrow FWHMs. However, it is essential to find alternatives to toxic elements such as Cd and introduce a more environment-friendly QD for LEDs and display devices. Graphene is one such material that, being organic, can operate without damaging the ecosystem. Graphene is a 2D material that consists of monolayers of carbon atoms bonded together in a honeycomb-like pattern. Although graphene is not suitable for optical applications due to lack of an electronic bandgap, graphene quantum dots (GQDs) possess a bandgap due to effect of quantum confinement and can be readily used for optoelectronic applications. GQDs are infinitesimal domains that have less than 100 layers of graphene. GQDs are known to be chemically stable and nontoxic materials that can produce stable luminance in excess of 1000 cd/m^2 with distinct quantum confinement effect, making it suitable for several biological, environmental, and optoelectronic applications [48−50]. GQDs can also be used to realize ultrathin displays that can be folded just like a paper. For a given energy level, GQDs have four quantum states against the two quantum states of a semiconductor QD. The additional two quantum states prove GQDs valuable for quantum computing. Nevertheless, the understanding of GQD mechanism is limited, and more deep investigations must be carried out to reap huge benefits from GQDs. The quest for Cd-free QDs also led to a class of perovskite QDs having high QYs (>95%) and narrow FWHMs (<9 nm). The most attractive among the perovskite QDs are $CsPbX_3$ (X = Br, Cl, I) [51,52]. The anion exchange between Br^-, Cl^-, and I^- ions at the X-site in $CsPbX_3$ can facilitate the tuning of color emission from blue to red, as shown in Fig. 5.5 [52]. But these QDs are based on lead, which is also toxic and can pose a threat to human health and the environment. However, alternatives to Pb were found, and less-toxic or nontoxic elements such as Sn, Sb, and Bi started gaining attention [53]. $Cs_3Bi_2X_9$ (X = Cl, Br or I) perovskite QDs have shown great potential as a lead-free composition that exhibited excellent air stability [54]. However, lead-free perovskites were not found to be as efficient and often displayed much less photoluminescence quantum yield (PLQY) than that of lead-based perovskite QDs. Particularly, Sn-based QDs showed worst stability and efficiency than those based on Bi and Sb [53]. Double perovskites such as Cs_2InAgX_6 and Cs_2AgBiX_6 have also found their way into the race but bowed out soon due to their lower efficiency.

High PLQY is a necessity for QDs to be used in devices, but it is not the only sufficient criterion for the fabrication of QLEDs. Many QDs with high PLQY exhibit very less EQE after being incorporated in a device. Even the best inorganic perovskite QDs have failed to raise the EQE above 4%. This is mainly due to the indulgence of nonradiative Auger recombination and FRET with the heterostructural details of QDs such as the shape and dimensions of the core/shell. It is essential to pursue the

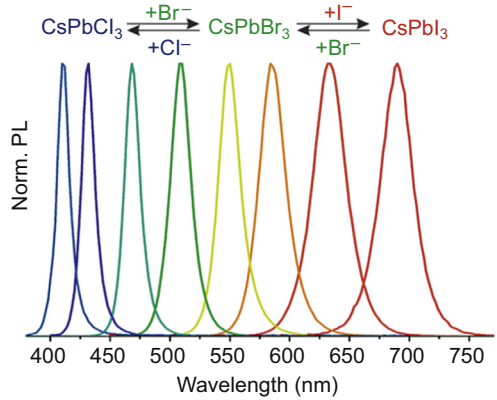

Figure 5.5 PL emission spectra of $CsPbBr_3$ achieved by ion exchange between Br^-, Cl^-, and I^- ions. *PL*, photoluminescence.
Reprinted with permission from G. Nedelcu, L. Protesescu, S. Yakunin, M.I. Bodnarchuk, M.J. Grotevent, M. V. Kovalenko, Fast anion-exchange in highly luminescent nanocrystals of cesium lead halide perovskites (CsPbX 3 , X = Cl, Br, I), Nano Lett. 15 (2015) 5635−5640. https://doi.org/10.1021/acs.nanolett.5b02404. Copyright 2015, American Chemical Society.

heterostructural tailoring of QDs in a more advanced way to suppress the nonradiative Auger recombination and FRET. Auger recombination and FRET are also responsible for limited brightness and lifetimes of QLEDs. Furthermore, the woes are added up by the PL quenching and roll-off of efficiency at high driving currents. These effects can be minimized by adopting strategic designing of QDs and their device architecture in addition to passivation of QDs, proper engineering of interface, and encapsulation, as well as control over the interdots distance between the QDs. Also, the performance of QLEDs can be significantly enhanced by coupling the QDs with surface plasmons [55]. Additionally, the rapid commercialization of QLEDs requires that the cost of their production and device fabrication be decreased. Implementing the large-scale synthesis of QDs using a reactor can help in reducing the production costs to a certain level [56].

5.5 Perovskite light-emitting diodes

Whenever steps were undertaken to enhance certain characteristics, some other drawbacks always accompanied in the fabrication of phosphor-free LEDs. Yet, there is lot of scope to research and find solutions to these glitches, and one may even imagine receiving a Nobel Prize if he or she succeeds in bringing out a truly potential phosphor-free LED with exceptional characteristics at a competitive price. Most LEDs, including pc-LEDs, rely on III−V semiconductors that require expensive rigid substrates, very clean epitaxial growth, and vacuum-based processing at high temperatures. OLEDs and QLEDs have shown the potential to replace the existing

semiconductor-based LEDs to a great extent. The former has even become a popular candidate for commercial applications, whereas QLEDs have just entered to compete in the market. However, OLEDs still face issues with their stability and their synthesis processes. There is still a matter of concern over the large-scale production of OLEDs, especially using the vacuum-based sublimation [57]. Another issue is the limited intrinsic emission from conjugate polymers due to their forbidden (triplet exciton) radiative recombinations that pose hurdles in the efficient use of light-emitting polymers [57]. QLEDs also suffer from surface-defect concentrations that lead to a large number of nonradiative recombinations. Similarly, the display technologies too faced issues in finding an appropriate material that could exhibit high color purity in addition to high efficiency. To obtain higher color purity, it is essential to obtain a material that could emit with least FWHM. Organic materials were the best choice for fabricating displays, as their FWHM was near to 40 nm. Soon, inorganic QDs displayed much better color purity with FWHM less than 30 nm, and this slowly resulted in the marching over of QDs into the display technology. However, the stability issues, difficulty in the particle size control, and high production costs retarded their progress and stood as an obstacle for wide use of QD-based displays. The quest for new materials for display devices with high color purity led to the discovery of metal−halide perovskites that demonstrated emission bands with FWHM less than 20 nm [58]. Concurrently, researchers are now focusing on developing novel perovskite materials that are also known to produce photovoltaic devices with high efficiency [58,59]. The recent advances in perovskite-structured hybrid organic−inorganic materials in photovoltaic cells have brought such materials to the limelight. It is foreseen that perovskite hybrid organic−inorganic materials will rule the LED market in the near future.

Perovskite derived its name from the Russian Count and mineralogist, Lev Perovski. The term was coined by the German mineralogist, Gustav Rose, to describe the structure of $CaTiO_3$ mineral, which was discovered in the Ural Mountains. Soon, the term became a generic nomenclature to describe the category of materials that have structure similar to that of $CaTiO_3$. Perovskites are categorized by the general formula ABX_3, where the A is a monovalent cation, B is an inorganic metal cation, and X is the anion (generally oxygen ions). B-cations are octahedrally bonded with six X-anions, and these octahedrons form a three-dimensional (3D) network through corner sharing of atoms. A-cations are usually larger than the B-cations and are located within the cavities of octahedrons. Hybrid organic−inorganic perovskites have a different composition than their classical counterpart. Here, the A-site is introduced with monovalent organic moieties, whereas the X-site is introduced with halides (X = Cl, Br, I) instead of oxygen. The B-sites are, generally, occupied by the divalent metal cations such as Pb^{2+}, Sn^{2+}, Bi^{2+}, Cu^{2+}, Sb^{2+}, Ge^{2+}, Eu^{2+}, Co^{2+}, and so on. Using the Goldschmidt tolerance factor (t) and the octahedral factor (μ), it is possible to find the probability of the formation of a perovskite crystal structure [60,61]. These relations are given by

$$\text{Goldschmidt tolerance factor, } t = \frac{(r_A + r_X)}{\sqrt{2}(r_B + r_X)}$$

$$\text{Octahedral factor, } \mu = \frac{r_B}{r_X}$$

where, r_A, r_B, and r_X are the effective ionic radii of the A-cation, B-cation, and X-anion, respectively. The value of t should be approximately unity to form a perovskite structure. Perovskite materials rose to popularity with the advancement in solar technology and were earlier investigated for photovoltaic devices. These materials made it possible to enhance the solar energy conversion efficiency of photovoltaic devices from 3.8% to 22% in a period spanning half a decade [62–69]. Gradually, the research on these materials gained momentum, and their applications expanded in the field of LEDs. These materials have proven to be potential alternatives for the existing LED materials and that too, at a lower cost. Perovskites prove more advantageous in the sense that they exhibit direct bandgap and have low defect densities; thus, the issues observed in OLEDs and QLEDs will not be found in Pe-LEDs. Although perovskite materials for LED were investigated in the early 1990s, those failed to gain attention due to inferior optical and luminescence properties [70–73]. During this period, many unsuccessful attempts were made to develop highly efficient 2D perovskites incorporated with long chains of organic dye molecules. In those days, LEDs built from inorganic QDs and organic materials exhibited better photoluminescence and electroluminescence properties, respectively, and this shook away the interest from 2D perovskites to OLEDs and inorganic QDs [58,74–77]. But once again, the interest in perovskite emitters was rediscovered with the development of novel hybrid organic–inorganic perovskites that displayed the advantages of both organic and inorganic materials [78]. The advent of 3D perovskites such as organometal halide perovskites paved way to a more systematic and recognized approach to perovskite-based LEDs [78]. Pe-LEDs made rapid progress and was able to achieve relatively rapid enhancement in their EQE and brightness than OLEDs and QLEDs, as shown in Fig. 5.6. The display industries have also started demanding more from the perovskite light emitters for vivid display and high color purity.

The structure of a Pe-LED is similar to that of an OLED. The perovskite emitter is sandwiched between the HTL and the ETL, as shown in Fig. 5.7. The perovskite emitter can be either an inorganic perovskite or a hybrid metalorganic perovskite. Metal–halide perovskites satisfy the requirements for better injection and transport of charges due to their high diffusion lengths and optimized formation of interfaces with most of the contacts. The injection and transport of the charges across the interfaces must be efficient to reduce the energy losses. To reduce the nonradiative recombinations across the interfaces, it is also essential to have energetically matched contacts [57]. The balance between the hole and electron injection must be maintained to maximize the radiative recombinations, which can be achieved by tailoring the interfaces. For this, the selection of materials for the ETL and HTL must be judiciously made to ensure compatibility with the emitting perovskite layer. Some of the materials used for the ETL, HTL, and perovskite emitters as well as their energy bandgaps are shown in Fig. 5.8.

Although perovskites boast of excellent luminescence properties and the capability to rule the LED industry in the near future, they are still not free of all the adversaries

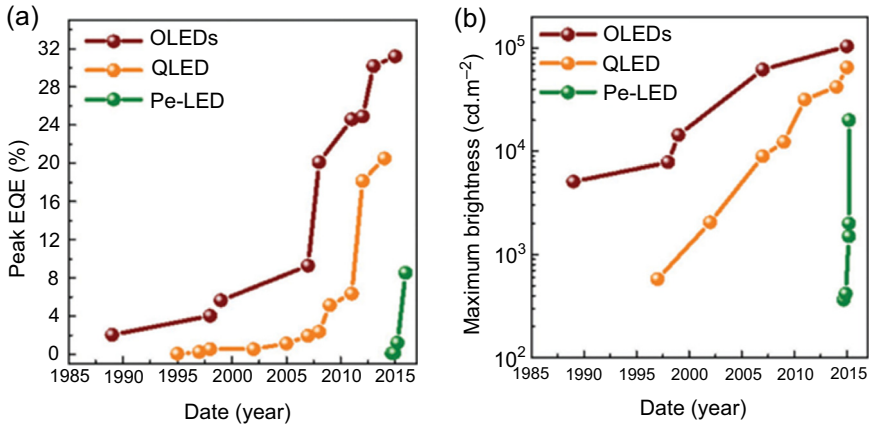

Figure 5.6 Progress made in the (a) external quantum efficiency (EQE) and (b) maximum brightness by OLEDs, QLEDs, and Pe-LEDs. *OLED*, organic light-emitting diode; *Pe-LED*, perovskite light-emitting diode; *QLED*, quantum dot light-emitting diode.
Reprinted with permission from S.A. Veldhuis, P.P. Boix, N. Yantara, M. Li, T.C. Sum, N. Mathews, S.G. Mhaisalkar, Perovskite materials for light-emitting diodes and lasers, Adv. Mater. 28 (2016) 6804−6834. https://doi.org/10.1002/adma.201600669. Copyright 2016, Wiley-VCH Verlag.

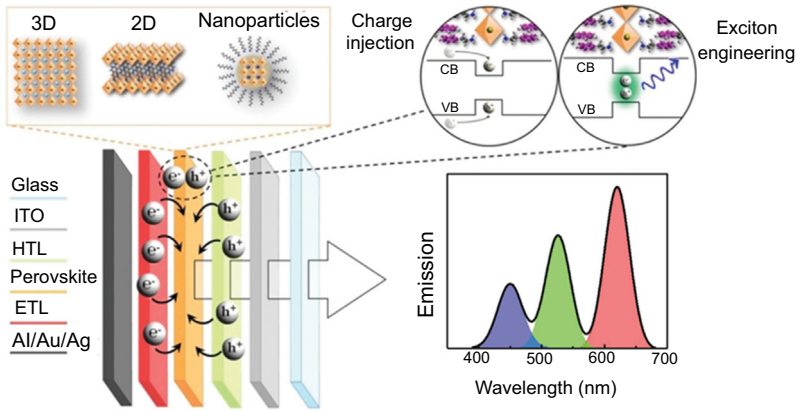

Figure 5.7 Schematic representation of a Pe-LED. *CB*, conduction band; *ETL*, electron-transport layer; *HTL*, hole-transport layer; *ITO*, indium tin oxide; *Pe-LED*, perovskite light-emitting diode; *VB*, valence band.
Reprinted with permission from S.A. Veldhuis, P.P. Boix, N. Yantara, M. Li, T.C. Sum, N. Mathews, S.G. Mhaisalkar, Perovskite materials for light-emitting diodes and lasers, Adv. Mater. 28 (2016) 6804−6834. https://doi.org/10.1002/adma.201600669. Copyright 2016, Wiley-VCH Verlag.

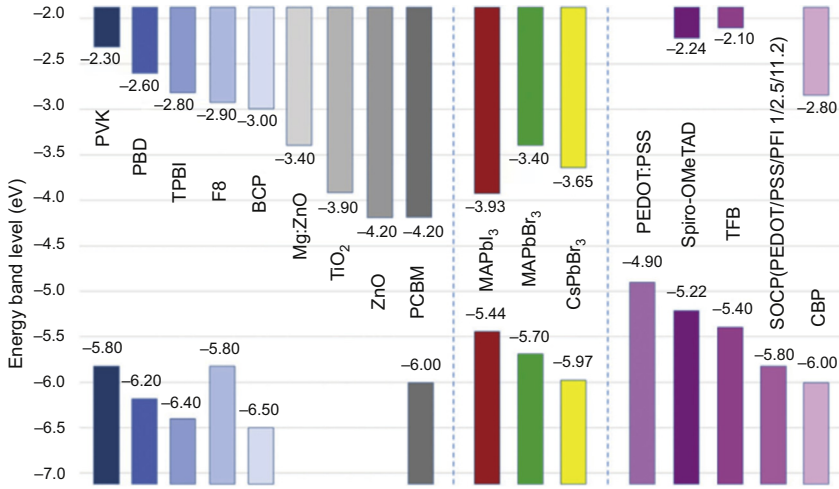

Figure 5.8 Energy levels for different materials acting as ETL (left), thin-film 3D perovskite emitter (middle) and HTL (right) in Pe-LEDs. *ETL*, electron transport layer; *HTL*, hole transport layer; *Pe-LED*, perovskite light-emitting diode.
Reprinted with permission from S.A. Veldhuis, P.P. Boix, N. Yantara, M. Li, T.C. Sum, N. Mathews, S.G. Mhaisalkar, Perovskite materials for light-emitting diodes and lasers, Adv. Mater. 28 (2016) 6804−6834. https://doi.org/10.1002/adma.201600669. Copyright 2016, Wiley-VCH Verlag.

that hamper their efficiency. Most of the efficient perovskites are prepared from the lead metal, which is infamous for their toxicity. The alternative elements for lead in the perovskite structure often faced issues such as low stability, less efficiency, and so on. If the metallic lead from the stoichiometric amount of precursors remains unreacted due to incomplete perovskite formation, it can act as defect trap centers and initiates nonradiative decay pathways. One way to neutralize the excess Pb from the stoichiometry is to introduce excess amount of CH_3NH_3Br into the solution during the film deposition. This will ensure to suppress the formation of metallic Pb and improve the luminescence efficiency. Nonradiative losses can also occur from the shunt paths, which originate from the pinhole defects or incomplete coverage of the surface. The light emission from the perovskite thin films can be optimized if smooth morphology and high surface coverage of the perovskites are achieved [57]. Pinhole-free thin films can be realized by embedding the perovskite emitters in polymer matrix such as poly(ethylene oxide), polyimide, and so on. Recently, Xiao et al. made an advancement in Pe-LEDs and took it to a new level by introducing a technique to produce more efficient, durable, and stable Pe-LEDs from self-assembled nanosized crystallites of perovskite materials [79]. The grain growth of three-dimensional perovskite grains in the film was inhibited by adding long-chain organic ammonium halides such as n-butylammonium halide (BaX; X = I, Br) crystals in the precursor solution, consequently resulting in nanocrystalline, ultraflat thin films.

These nanosized perovskite crystallites produced a blueshift in the photoluminescence and electroluminescence emission. LEDs fabricated by incorporating the BaX layers exhibited highly enhanced performance and stability.

Although Pe-LEDs boast of excellent luminescence efficiency suitable for LEDs, they still have concerns with their stability issues that haunt their journey to the device fabrication. There are apprehensions regarding the long-term stability of the perovskite materials as well, which need to be confirmed before implementing them in LEDs. Several nanostructured perovskites have shown noteworthy luminescence QY almost approaching 100% and notably high color purity. In spite of these, the devices fabricated from the perovskites QDs failed to deliver expected brightness and efficiencies, and the results were inferior to the devices fabricated from thin films [80]. Perovskites can be formed as thin films too, but it is a bigger challenge to obtain pinhole-free, smooth thin films out of these perovskites due to their wettability that pose adverse effects. Also, the measures taken to curb the kinetics of nucleation and crystallization by capping ligands can pose hurdles in obtaining smooth thin films. At times, the device efficiencies are adversely affected due to the remnant surface ligands that often result in photoluminescence quenching and poor electrical charge injection. There is a need to address the challenges faced in improving the device efficiency of nanostructured perovskites by getting a deeper understanding of their charge transport mechanisms and intrinsic material characteristics.

5.6 BioLEDs

LEDs are emerging towards bringing in the green revolution in the lighting industry. Already they have started replacing the traditional lamps in most parts of the world and are progressively becoming the prime source for both household and street lighting. The move to adapt the green technology has resulted in dumping of the hazardous mercury-based lighting, and this has paved way for the LED luminaires to spread their existence as the prime lighting system. The green technology has granted innovation in the form of bioLEDs, which was introduced by Costa and his coworkers, and these new variants of LEDs could offer the same efficiency offered by inorganic LEDs [81]. These bioLEDs are hybrid devices that utilize the blue LEDs to excite the protein rubbers to emit red/green/white light. The luminescent proteins are introduced into a polymer matrix to produce luminescent rubber, which is then packaged with a UV-LED or a blue LED. A schematic representation of the bioLEDs and the appearance of fluorescent proteins (FPs) under normal light and 310 nm excitation are shown in Fig. 5.9. The bioLEDs are low-cost and biodegradable devices that are simple to manufacture. This means that they can be definitely recycled, replaced, and disposed without causing any adverse effects on the environment.

FPs, which were discovered in 1962, found several applications such as protein labeling, environmental biosensors, live-cell imaging, and finally light-emitting devices. They are known to exhibit noteworthy luminescence properties with excellent photostability, narrow emission line width, and exceptional photon flux saturation [82]. However, FPs cannot be directly used in white LED package due to their poor thermal

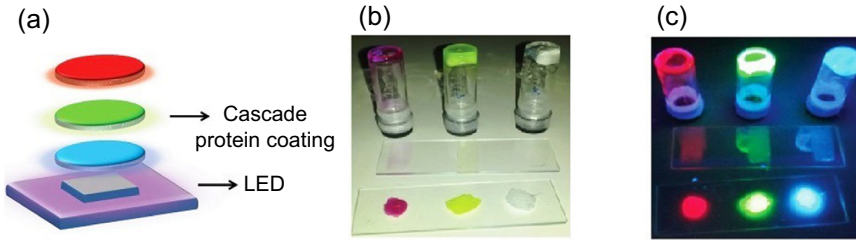

Figure 5.9 (a) Schematic representation of a hybrid bioLED with a cascade coating based on blue, green, and red fluorescent proteins, (b) protein-based gels and rubberlike materials under room light conditions, and (c) protein-based gels and rubberlike materials upon excitation at 310 nm. *LED*, light-emitting diode.
Reproduced with permission from M.D. Weber, L. Niklaus, M. Pröschel, P.B. Coto, U. Sonnewald, R.D. Costa, Bioinspired hybrid white light-emitting diodes, Adv. Mater. 27 (2015) 5493−5498. https://doi.org/10.1002/adma.201502349. Copyright 2015 WILEY-VCH Verlag GmbH & Co. KGaA, Weinheim.

stability, as a result of which they may degrade soon in the harsh temperature conditions arising during the LED operation. But embedding these FPs in the polymer matrix ensured that these issues were resolved [81]. The matrix plays a great role in deciding the overall thermal stability and optical performance of bioLEDs. They themselves must show good optical transparency to visible light so that the light emitted by the FPs does not get absorbed by the matrix. Additionally, they must be good enough to allow FPs to be uniformly dispersed in them and also show high thermal stability. Recently, metal−organic frameworks (MOFs) have found popularity as ideal encapsulants for fluorescent proteins due to their porous structures. MOFs show several diverse properties among which their permanent porosity and tunable structures are of great advantage for protein encapsulation. They are hybrid organic−inorganic materials formed by the self-assembly of organic ligands and metal ions. Zeolitic imidazolate frameworks (ZIFs) are a class of MOFs that stand out as an excellent encapsulant to support fluorescent proteins. Among ZIFs, the ZIF-8 has a thermally and chemically stable structure with well-defined cavities [83]. They are highly transparent to visible light that ensures maximum yield of the light emitted from the FPs embedded in the ZIF structure.

BioLEDs prepared from the FPs promise a high PLQY and good photostability. Yet, the color temperatures of these bioLEDs were reported with contrasting results by different research groups. While Costa and his research group claimed of obtaining the CIE color coordinates of (0.33, 0.33) with color temperature of 5500 K [84], another research group headed by Nizamoglu obtained a CCT of 8400 K after integrating the green and red FPs on a blue LED chip [85]. Also, there were issues such as random spatial distribution of different fluorescent proteins that led to low luminous efficiency and complex procedures for fabricating two or more FPs. Wang et al. developed a single-component fluorescent protein, R-phycoerythrin (R-PE), that consists of two types of chromophores comprising phycourobilin (PUB) and phycoerythrobilin (PEB) as downconversion materials [86]. R-PE shows absorption

peaks in the blue (498 nm), green (540 nm), and yellow (560 nm) regions. The blue peak can be attributed to the PUB chromophore, whereas the green and yellow peaks can be attributed to the PEB chromophore. Due to the energy transfer occurring between these two chromophores, the overall emission is focused at 578 nm, which is in the orange region. Hence, it is highly essential to block the energy transfer between the PUB and PEB in R-PE for obtaining two- or three-color emissions that can blend to give out white light. A possible way to block this energy transfer was found by preparing denatured R-PE encapsulated within HSB-W1 (where HSB = hydrogenated Schiff base). HSB-W1 is a novel MOF developed by Wu and his coworkers [87]. When excited by 365 nm UV light, it can give out blue emissions centered at 454 nm. HSB-W1 can be encapsulated on R-PE proteins by a facile solid confinement conversion process to form R-PE@HSB-W1 composites. This process involves the use of zinc hydroxide nanostrands as a precursor that leads to the formation of PEB−Zn and PUB−Zn complexes, which aid in the suppression of 578 nm emission from the R-PE protein. Also, the PEB and PUB derived from denatured R-PE proteins also block the energy transfer process between them and further boost the suppression of the 578 nm emission. As a result, R-PE encapsulated within HSB-W1 gives out dual emissions at green (518 nm) and red (600 nm, 647 nm) regions. These emissions blend together with the blue (454 nm) emission of HSB-W1 to give an overall emission of white light having CIE coordinates of (0.33, 0.34), a moderate CCT value of 5740 K and a high CRI of 85 [86].

5.7 Conclusions

Although many new variants of LEDs have come into picture, they are not yet in their prime, and hence, pc-LEDs still rule the LED industry. The newer variants such as microLEDs are not completely viable to buy owing to their high initial costs. However, they will soon hit the markets with a much cheaper price tag after the recovery of the expenses incurred during their research and development by the companies. Currently, major LED manufacturers are trying to improve the yield at each stage of microLED production with a view to reduce the overall expenditure. Most of the issues with the yield are arising due to quality of the substrate, lack of precision with the epitaxial growth processes, chances of errors during the deposition of epilayers on the substrate, and their transfer on arrays during microLED fabrication. Without any doubt, microLEDs can be foreseen as the future of display industry. But this will require the overcoming of numerous hurdles and challenges that come in the way of making affordable and efficient microLED devices. MicroLEDs possess the capability to turn the display market upside down. But for now, the LED display market is reigned by OLEDs and to some extent by QLEDs. OLEDs have reached to greater heights of progress with an unmatchable lifetime for their blue-, red-, and green-emitting organic layers. Their rival QLEDs are still far behind in terms of the lifetime, especially for the blue-emitting QDs that have the worst operating lifetime. Inkjet-printed OLEDs have greatly overshadowed QLEDs particularly with relatively more consistency of the operating lifetime of their different emissive layers (red, green, and blue). On the other

hand, QLEDs can knock down OLEDs from their current spot if the operating lifetimes of their blue-, green-, and red-emitting layers become consistent with each other. For LEDs based on perovskites and biomaterials, lots of work need to be done. They are assumed to be more efficient, especially bioLEDs whose fluorescent proteins are biodegradable and eco-friendly for use. Pe-LEDs are fighting with their stability issues and a suitable replacement for Pb in their composition. Although several Pb-free perovskites have come into picture, they have raised certain new challenges such as formation of p-type defects or lower conductivity. But these materials are still in their early stages of development and will require more results before putting a final verdict on the future of these materials.

References

[1] S. Nakamura, M. Senoh, S. Nagahama, N. Iwasa, T. Yamada, T. Matsushita, H. Kiyoku, Y. Sugimoto, InGaN-based multi-quantum-well-structure laser diodes, Jpn. J. Appl. Phys. 35 (1996) L74–L76, https://doi.org/10.1143/JJAP.35.L74.

[2] M. Diagne, Y. He, H. Zhou, E. Makarona, A.V. Nurmikko, J. Han, K.E. Waldrip, J.J. Figiel, T. Takeuchi, M. Krames, Vertical cavity violet light emitting diode incorporating an aluminum gallium nitride distributed Bragg mirror and a tunnel junction, Appl. Phys. Lett. 79 (2001) 3720–3722, https://doi.org/10.1063/1.1415405.

[3] S.-R. Jeon, Y.-H. Song, H.-J. Jang, G.M. Yang, S.W. Hwang, S.J. Son, Lateral current spreading in GaN-based light-emitting diodes utilizing tunnel contact junctions, Appl. Phys. Lett. 78 (2001) 3265–3267, https://doi.org/10.1063/1.1374483.

[4] H.W. Choi, C.W. Jeon, M.D. Dawson, P.R. Edwards, R.W. Martin, Efficient GaN-based micro-LED arrays, Mater. Res. Soc. Symp. Proc. 743 (2002) 433–438.

[5] S.X. Jin, J. Li, J.Y. Lin, H.X. Jiang, InGaN/GaN quantum well interconnected microdisk light emitting diodes, Appl. Phys. Lett. 77 (2000) 3236–3238, https://doi.org/10.1063/1.1326479.

[6] J. Herrnsdorf, J.J.D. McKendry, S. Zhang, E. Xie, R. Ferreira, D. Massoubre, A.M. Zuhdi, R.K. Henderson, I. Underwood, S. Watson, A.E. Kelly, E. Gu, M.D. Dawson, Active-matrix GaN micro light-emitting diode display with unprecedented brightness, IEEE Trans. Electron. Dev. 62 (2015) 1918–1925, https://doi.org/10.1109/TED.2015.2416915.

[7] V. Poher, N. Grossman, G.T. Kennedy, K. Nikolic, H.X. Zhang, Z. Gong, E.M. Drakakis, E. Gu, M.D. Dawson, P.M.W. French, P. Degenaar, M.A.A. Neil, Micro-LED arrays: a tool for two-dimensional neuron stimulation, J. Phys. D Appl. Phys. 41 (2008) 094014, https://doi.org/10.1088/0022-3727/41/9/094014.

[8] Z. Gong, S. Jin, Y. Chen, J. McKendry, D. Massoubre, I.M. Watson, E. Gu, M.D. Dawson, Size-dependent light output, spectral shift, and self-heating of 400 nm InGaN light-emitting diodes, J. Appl. Phys. 107 (2010), https://doi.org/10.1063/1.3276156.

[9] H.W. Choi, C.W. Jeon, M.D. Dawson, P.R. Edwards, R.W. Martin, S. Tripathy, Mechanism of enhanced light output efficiency in InGaN-based microlight emitting diodes, J. Appl. Phys. 93 (2003) 5978–5982, https://doi.org/10.1063/1.1567803.

[10] P. Tian, J.J.D. McKendry, Z. Gong, S. Zhang, S. Watson, D. Zhu, I.M. Watson, E. Gu, A.E. Kelly, C.J. Humphreys, M.D. Dawson, Characteristics and applications of micro-pixelated GaN-based light emitting diodes on Si substrates, J. Appl. Phys. 115 (2014) 033112, https://doi.org/10.1063/1.4862298.

[11] C.K. Jeong, K.-I. Park, J.H. Son, G.-T. Hwang, S.H. Lee, D.Y. Park, H.E. Lee, H.K. Lee, M. Byun, K.J. Lee, Self-powered fully-flexible light-emitting system enabled by flexible energy harvester, Energy Environ. Sci. 7 (2014) 4035−4043, https://doi.org/10.1039/C4EE02435D.

[12] H.E. Lee, J. Choi, S.H. Lee, M. Jeong, J.H. Shin, D.J. Joe, D. Kim, C.W. Kim, J.H. Park, J.H. Lee, D. Kim, C.-S. Shin, K.J. Lee, Monolithic flexible vertical GaN light-emitting diodes for a transparent wireless brain optical stimulator, Adv. Mater. 30 (2018) 1800649, https://doi.org/10.1002/adma.201800649.

[13] H.E. Lee, S.H. Lee, M. Jeong, J.H. Shin, Y. Ahn, D. Kim, S.H. Oh, S.H. Yun, K.J. Lee, Trichogenic photostimulation using monolithic flexible vertical AlGaInP light-emitting diodes, ACS Nano 12 (2018) 9587−9595, https://doi.org/10.1021/acsnano.8b05568.

[14] D. Hwang, A. Mughal, C.D. Pynn, S. Nakamura, S.P. DenBaars, Sustained high external quantum efficiency in ultrasmall blue III−nitride micro-LEDs, Appl. Phys. Express. 10 (2017) 032101, https://doi.org/10.7567/APEX.10.032101.

[15] H.E. Lee, J.H. Shin, J.H. Park, S.K. Hong, S.H. Park, S.H. Lee, J.H. Lee, I. Kang, K.J. Lee, Micro light-emitting diodes for display and flexible biomedical applications, Adv. Funct. Mater. 29 (2019) 1808075, https://doi.org/10.1002/adfm.201808075.

[16] J.-T. Oh, S.-Y. Lee, Y.-T. Moon, J.H. Moon, S. Park, K.Y. Hong, K.Y. Song, C. Oh, J.-I. Shim, H.-H. Jeong, J.-O. Song, H. Amano, T.-Y. Seong, Light output performance of red AlGaInP-based light emitting diodes with different chip geometries and structures, Opt. Express 26 (2018) 11194, https://doi.org/10.1364/oe.26.011194.

[17] M. Pope, H.P. Kallmann, P. Magnante, Electroluminescence in organic crystals, J. Chem. Phys. 38 (1963) 2042−2043, https://doi.org/10.1063/1.1733929.

[18] N. Thejokalyani, S.J. Dhoble, Novel approaches for energy efficient solid state lighting by RGB organic light emitting diodes - a review, Renew. Sustain. Energy Rev. 32 (2014) 448−467, https://doi.org/10.1016/j.rser.2014.01.013.

[19] D. Chitnis, N. Thejo kalyani, H.C. Swart, S.J. Dhoble, Escalating opportunities in the field of lighting, Renew. Sustain. Energy Rev. 64 (2016) 727−748, https://doi.org/10.1016/j.rser.2016.06.041.

[20] N. Thejo Kalyani, S.J. Dhoble, Novel materials for fabrication and encapsulation of OLEDs, Renew. Sustain. Energy Rev. 44 (2015) 319−347, https://doi.org/10.1016/j.rser.2014.11.070.

[21] N. Thejo Kalyani, S.J.J. Dhoble, N.T. Kalyani, S.J.J. Dhoble, N. Thejo Kalyani, S.J.J. Dhoble, N.T. Kalyani, S.J.J. Dhoble, N. Thejo Kalyani, S.J.J. Dhoble, Organic light emitting diodes: energy saving lighting technology - a review, Renew. Sustain. Energy Rev. 16 (2012) 2696−2723, https://doi.org/10.1016/j.rser.2012.02.021.

[22] S.R. Forrest, P.E. Burrows, Z. Shen, G. Gu, V. Bulovic, M.E. Thompson, The stacked OLED (SOLED): a new type of organic device for achieving high-resolution full-color displays, Synth. Met. 91 (1997) 9−13, https://doi.org/10.1016/S0379-6779(97)03966-0.

[23] G. Shi, X. Zhang, M. Wan, S. Wang, H. Lian, R. Xu, W. Zhu, High-performance inverted organic light-emitting diodes with extremely low efficiency roll-off using solution-processed ZnS quantum dots as the electron injection layer, RSC Adv. 9 (2019) 6042−6047, https://doi.org/10.1039/C8RA10290B.

[24] L.M. Do, E.M. Han, Y. Niidome, M. Fujihira, T. Kanno, S. Yoshida, A. Maeda, A.J. Ikushima, Observation of degradation processes of Al electrodes in organic electroluminescence devices by electroluminescence microscopy, atomic force microscopy, scanning electron microscopy, and Auger electron spectroscopy, J. Appl. Phys. 76 (1994) 5118−5121, https://doi.org/10.1063/1.357224.

[25] J. McKittrick, L.E. Shea-Rohwer, Review: down conversion materials for solid-state lighting, J. Am. Ceram. Soc. 97 (2014) 1327−1352, https://doi.org/10.1111/jace.12943.
[26] Z. Yang, M. Gao, W. Wu, X. Yang, X.W. Sun, J. Zhang, H.-C. Wang, R.-S. Liu, C.-Y. Han, H. Yang, W. Li, Recent advances in quantum dot-based light-emitting devices: challenges and possible solutions, Mater. Today 24 (2019) 69−93, https://doi.org/10.1016/j.mattod.2018.09.002.
[27] J.J. Li, Y.A. Wang, W. Guo, J.C. Keay, T.D. Mishima, M.B. Johnson, X. Peng, Large-scale synthesis of nearly monodisperse CdSe/CdS core/shell nanocrystals using air-stable reagents via successive ion layer adsorption and reaction, J. Am. Chem. Soc. 125 (2003) 12567−12575, https://doi.org/10.1021/ja0363563.
[28] P. Reiss, M. Protière, L. Li, Core/shell semiconductor nanocrystals, Small 5 (2009) 154−168, https://doi.org/10.1002/smll.200800841.
[29] Y.-M. Sung, K.-S. Park, Y.-J. Lee, T.-G. Kim, Ripening kinetics of CdSe/ZnSe core/shell nanocrystals, J. Phys. Chem. C 111 (2007) 1239−1242, https://doi.org/10.1021/jp066203c.
[30] K.G. Sonawane, K.S. Agarwal, C. Phadnis, D.K. Sharma, A. Layek, A. Chowdhury, S. Mahamuni, Manifestations of varying grading level in CdSe/ZnSe core−shell nanocrystals, J. Phys. Chem. C 120 (2016) 5257−5264, https://doi.org/10.1021/acs.jpcc.6b01247.
[31] M. Hamada, N. Takenokoshi, K. Matozaki, Q. Feng, N. Murase, S. Wakida, S. Nakanishi, V. Biju, In situ photochemical surface passivation of CdSe/ZnS quantum dots for quantitative light emission and enhanced photocurrent response in solar cells, J. Phys. Chem. C 118 (2014) 2178−2186, https://doi.org/10.1021/jp4083882.
[32] J.B. Sambur, B.A. Parkinson, CdSe/ZnS core/shell quantum dot sensitization of low index TiO2 single crystal surfaces, J. Am. Chem. Soc. 132 (2010) 2130−2131, https://doi.org/10.1021/ja9098577.
[33] E. Zenkevich, A. Stupak, C. Göhler, C. Krasselt, C. von Borczyskowski, Tuning electronic states of a CdSe/ZnS quantum dot by only one functional dye molecule, ACS Nano 9 (2015) 2886−2903, https://doi.org/10.1021/nn506941c.
[34] J. Lim, S. Jun, E. Jang, H. Baik, H. Kim, J. Cho, Preparation of highly luminescent nanocrystals and their application to light-emitting diodes, Adv. Mater. 19 (2007) 1927−1932, https://doi.org/10.1002/adma.200602642.
[35] X. Wang, W. Li, K. Sun, Stable efficient CdSe/CdS/ZnS core/multi-shell nanophosphors fabricated through a phosphine-free route for white light-emitting-diodes with high color rendering properties, J. Mater. Chem. 21 (2011) 8558, https://doi.org/10.1039/c1jm00061f.
[36] D.V. Talapin, I. Mekis, S. Götzinger, A. Kornowski, O. Benson, H. Weller, CdSe/CdS/ZnS and CdSe/ZnSe/ZnS Core−Shell−Shell nanocrystals, J. Phys. Chem. B 108 (2004) 18826−18831, https://doi.org/10.1021/jp046481g.
[37] A. Samanta, Z. Deng, Y. Liu, Aqueous synthesis of glutathione-capped CdTe/CdS/ZnS and CdTe/CdSe/ZnS core/shell/shell nanocrystal heterostructures, Langmuir 28 (2012) 8205−8215, https://doi.org/10.1021/la300515a.
[38] M.D. Regulacio, M.-Y. Han, Composition-tunable alloyed semiconductor nanocrystals, Acc. Chem. Res. 43 (2010) 621−630, https://doi.org/10.1021/ar900242r.
[39] E. Jang, S. Jun, H. Jang, J. Lim, B. Kim, Y. Kim, White-light-emitting diodes with quantum dot color converters for display backlights, Adv. Mater. 22 (2010) 3076−3080, https://doi.org/10.1002/adma.201000525.
[40] W.K. Bae, K. Char, H. Hur, S. Lee, Single-step synthesis of quantum dots with chemical composition gradients, Chem. Mater. 20 (2008) 531−539, https://doi.org/10.1021/cm070754d.

[41] Y. Zheng, Z. Yang, J.Y. Ying, Aqueous synthesis of glutathione-capped ZnSe and $Zn_{1-x}Cd_xSe$ alloyed quantum dots, Adv. Mater. 19 (2007) 1475−1479, https://doi.org/10.1002/adma.200601939.
[42] X. Zhong, Y. Feng, W. Knoll, M. Han, Alloyed $Zn_xCd_{1-x}S$ nanocrystals with highly narrow luminescence spectral width, J. Am. Chem. Soc. 125 (2003) 13559−13563, https://doi.org/10.1021/ja036683a.
[43] L.E. Shea-Rohwer, J.E. Martin, X. Cai, D.F. Kelley, Red-emitting quantum dots for solid-state lighting, ECS J. Solid State Sci. Technol. 2 (2013) R3112−R3118, https://doi.org/10.1149/2.015302jss.
[44] S. Jun, E. Jang, Interfused semiconductor nanocrystals: brilliant blue photoluminescence and electroluminescence, Chem. Commun. (2005) 4616, https://doi.org/10.1039/b509196a.
[45] R.E. Bailey, S. Nie, Alloyed semiconductor quantum dots: tuning the optical properties without changing the particle size, J. Am. Chem. Soc. 125 (2003) 7100−7106, https://doi.org/10.1021/ja035000o.
[46] F. Garcia-Santamaria, Y. Chen, J. Vela, R.D. Schaller, J.A. Hollingsworth, V.I. Klimov, Suppressed auger recombination in "giant" nanocrystals boosts optical gain performance, Nano Lett. 9 (2009) 3482−3488, https://doi.org/10.1021/nl901681d.
[47] W.K. Bae, Y.-S. Park, J. Lim, D. Lee, L.A. Padilha, H. McDaniel, I. Robel, C. Lee, J.M. Pietryga, V.I. Klimov, Controlling the influence of Auger recombination on the performance of quantum-dot light-emitting diodes, Nat. Commun. 4 (2013) 2661, https://doi.org/10.1038/ncomms3661.
[48] S. Tachi, H. Morita, M. Takahashi, Y. Okabayashi, T. Hosokai, T. Sugai, S. Kuwahara, Quantum yield enhancement in graphene quantum dots via esterification with benzyl alcohol, Sci. Rep. 9 (2019) 14115, https://doi.org/10.1038/s41598-019-50666-3.
[49] Y. Dong, H. Pang, S. Ren, C. Chen, Y. Chi, T. Yu, Etching single-wall carbon nanotubes into green and yellow single-layer graphene quantum dots, Carbon N. Y. 64 (2013) 245−251, https://doi.org/10.1016/j.carbon.2013.07.059.
[50] P. Tian, L. Tang, K.S. Teng, S.P. Lau, Graphene quantum dots from chemistry to applications, Mater. Today Chem. 10 (2018) 221−258, https://doi.org/10.1016/j.mtchem.2018.09.007.
[51] J. Zhang, L. Fan, J. Li, X. Liu, R. Wang, L. Wang, G. Tu, Growth mechanism of $CsPbBr_3$ perovskite nanocrystals by a co-precipitation method in a CSTR system, Nano Res. 12 (2019) 121−127, https://doi.org/10.1007/s12274-018-2190-x.
[52] G. Nedelcu, L. Protesescu, S. Yakunin, M.I. Bodnarchuk, M.J. Grotevent, M.V. Kovalenko, Fast anion-exchange in highly luminescent nanocrystals of cesium lead halide perovskites ($CsPbX_3$, X = Cl, Br, I), Nano Lett. 15 (2015) 5635−5640, https://doi.org/10.1021/acs.nanolett.5b02404.
[53] Q. Zhang, Y. Yin, All-inorganic metal halide perovskite nanocrystals: opportunities and challenges, ACS Cent. Sci. 4 (2018) 668−679, https://doi.org/10.1021/acscentsci.8b00201.
[54] R.D. Nelson, K. Santra, Y. Wang, A. Hadi, J.W. Petrich, M.G. Panthani, Synthesis and optical properties of ordered-vacancy perovskite cesium bismuth halide nanocrystals, Chem. Commun. 54 (2018) 3640−3643, https://doi.org/10.1039/C7CC07223F.
[55] I. Gryczynski, J. Malicka, W. Jiang, H. Fischer, W.C.W. Chan, Z. Gryczynski, W. Grudzinski, J.R. Lakowicz, Surface-plasmon-coupled emission of quantum dots, J. Phys. Chem. B 109 (2005) 1088−1093, https://doi.org/10.1021/jp046173i.
[56] J. Park, K. An, Y. Hwang, J.-G. Park, H.-J. Noh, J.-Y. Kim, J.-H. Park, N.-M. Hwang, T. Hyeon, Ultra-large-scale syntheses of monodisperse nanocrystals, Nat. Mater. 3 (2004) 891−895, https://doi.org/10.1038/nmat1251.

[57] S.A. Veldhuis, P.P. Boix, N. Yantara, M. Li, T.C. Sum, N. Mathews, S.G. Mhaisalkar, Perovskite materials for light-emitting diodes and lasers, Adv. Mater. 28 (2016) 6804−6834, https://doi.org/10.1002/adma.201600669.
[58] Y.-H. Kim, H. Cho, T.-W. Lee, Metal halide perovskite light emitters, Proc. Natl. Acad. Sci. U.S.A. 113 (2016) 11694−11702, https://doi.org/10.1073/pnas.1607471113.
[59] N. Wang, L. Cheng, R. Ge, S. Zhang, Y. Miao, W. Zou, C. Yi, Y. Sun, Y. Cao, R. Yang, Y. Wei, Q. Guo, Y. Ke, M. Yu, Y. Jin, Y. Liu, Q. Ding, D. Di, L. Yang, G. Xing, H. Tian, C. Jin, F. Gao, R.H. Friend, J. Wang, W. Huang, Perovskite light-emitting diodes based on solution-processed self-organized multiple quantum wells, Nat. Photon. 10 (2016) 699−704, https://doi.org/10.1038/nphoton.2016.185.
[60] V.M. Goldschmidt, Die Gesetze der Krystallochemie, Naturwissenschaften 14 (1926) 477−485, https://doi.org/10.1007/BF01507527.
[61] M.A. Green, A. Ho-Baillie, H.J. Snaith, The emergence of perovskite solar cells, Nat. Photon. 8 (2014) 506−514, https://doi.org/10.1038/nphoton.2014.134.
[62] A. Kojima, K. Teshima, Y. Shirai, T. Miyasaka, Organometal halide perovskites as visible-light sensitizers for photovoltaic cells, J. Am. Chem. Soc. 131 (2009) 6050−6051, https://doi.org/10.1021/ja809598r.
[63] S.P. Singh, P. Nagarjuna, Organometal halide perovskites as useful materials in sensitized solar cells, Dalton Trans. 43 (2014) 5247−5251, https://doi.org/10.1039/c3dt53503g.
[64] X. Li, M. Ibrahim Dar, C. Yi, J. Luo, M. Tschumi, S.M. Zakeeruddin, M.K. Nazeeruddin, H. Han, M. Grätzel, Improved performance and stability of perovskite solar cells by crystal crosslinking with alkylphosphonic acid ω-ammonium chlorides, Nat. Chem. 7 (2015) 703−711, https://doi.org/10.1038/nchem.2324.
[65] W.S. Yang, J.H. Noh, N.J. Jeon, Y.C. Kim, S. Ryu, J. Seo, S.I. Seok, High-performance photovoltaic perovskite layers fabricated through intramolecular exchange, Science 348 (2015) 1234−1237, https://doi.org/10.1126/science.aaa9272.
[66] S. Li, B. Yang, R. Wu, C. Zhang, C. Zhang, X.F. Tang, G. Liu, P. Liu, C. Zhou, Y. Gao, J.Q. Meng, J. Yang, High-quality $CH_3NH_3PbI_3$ thin film fabricated via intramolecular exchange for efficient planar heterojunction perovskite solar cells, Org. Electron. Phys. Mater. Appl. 39 (2016) 304−310, https://doi.org/10.1016/j.orgel.2016.10.017.
[67] Y. Chen, X. Wan, G. Long, High performance photovoltaic applications using solution-processed small molecules, Acc. Chem. Res. 46 (2013) 2645−2655, https://doi.org/10.1021/ar400088c.
[68] Y. Jo, K.S. Oh, M. Kim, K.H. Kim, H. Lee, C.W. Lee, D.S. Kim, High performance of planar perovskite solar cells produced from PbI_2(DMSO) and PbI_2(NMP) complexes by intramolecular exchange, Adv. Mater. Interfaces 3 (2016), https://doi.org/10.1002/admi.201500768.
[69] M.I. Asghar, J. Zhang, H. Wang, P.D. Lund, Device stability of perovskite solar cells − a review, Renew. Sustain. Energy Rev. 77 (2017) 131−146, https://doi.org/10.1016/j.rser.2017.04.003.
[70] T. Ishihara, X. Hong, J. Ding, A.V. Nurmikko, Dielectric confinement effect for exciton and biexciton states in PbI_4-based two-dimensional semiconductor structures, Surf. Sci. 267 (1992) 323−326, https://doi.org/10.1016/0039-6028(92)91147-4.
[71] X. Hong, T. Ishihara, A.V. Nurmikko, Photoconductivity and electroluminescence in lead iodide based natural quantum well structures, Solid State Commun. 84 (1992) 657−661, https://doi.org/10.1016/0038-1098(92)90210-Z.
[72] M. Era, S. Morimoto, T. Tsutsui, S. Saito, Organic-inorganic heterostructure electroluminescent device using a layered perovskite semiconductor $(C_6H_5C_2H_4NH_3)_2PbI_4$, Appl. Phys. Lett. 65 (1994) 676−678, https://doi.org/10.1063/1.112265.

[73] T. Hattori, T. Taira, M. Era, T. Tsutsui, S. Saito, Highly efficient electroluminescence from a heterostructure device combined with emissive layered-perovskite and an electron-transporting organic compound, Chem. Phys. Lett. 254 (1996) 103−108, https://doi.org/10.1016/0009-2614(96)00310-7.

[74] K. Chondroudis, D.B. Mitzi, Electroluminescence from an Organic−Inorganic perovskite incorporating a quaterthiophene dye within lead halide perovskite layers, Chem. Mater. 11 (1999) 3028−3030, https://doi.org/10.1021/cm990561t.

[75] H. Mattoussi, L.H. Radzilowski, B.O. Dabbousi, E.L. Thomas, M.G. Bawendi, M.F. Rubner, Electroluminescence from heterostructures of poly(phenylene vinylene) and inorganic CdSe nanocrystals, J. Appl. Phys. 83 (1998) 7965−7974, https://doi.org/10.1063/1.367978.

[76] C.W. Tang, S.A. Vanslyke, C.H. Chen, Electroluminescence of doped organic thin films, Appl. Phys. Lett. 65 (1989) 3610−3616, https://doi.org/10.1063/1.343409.

[77] M.A. Baldo, D.F. O'Brien, Y. You, A. Shoustikov, S. Sibley, M.E. Thompson, S.R. Forrest, Highly efficient phosphorescent emission from organic electroluminescent devices, Nature 395 (1998) 151−154, https://doi.org/10.1038/25954.

[78] A. Kojima, M. Ikegami, K. Teshima, T. Miyasaka, Highly luminescent lead bromide perovskite nanoparticles synthesized with porous alumina media, Chem. Lett. 41 (2012) 397−399, https://doi.org/10.1246/cl.2012.397.

[79] Z. Xiao, R.A. Kerner, L. Zhao, N.L. Tran, K.M. Lee, T.-W. Koh, G.D. Scholes, B.P. Rand, Efficient perovskite light-emitting diodes featuring nanometre-sized crystallites, Nat. Photon. 11 (2017) 108−115, https://doi.org/10.1038/nphoton.2016.269.

[80] J. Song, J. Li, X. Li, L. Xu, Y. Dong, H. Zeng, Quantum dot light-emitting diodes based on inorganic perovskite cesium lead halides ($CsPbX_3$), Adv. Mater. 27 (2015) 7162−7167, https://doi.org/10.1002/adma.201502567.

[81] M.D. Weber, L. Niklaus, M. Pröschel, P.B. Coto, U. Sonnewald, R.D. Costa, Bioinspired hybrid white light-emitting diodes, Adv. Mater. 27 (2015) 5493−5498, https://doi.org/10.1002/adma.201502349.

[82] X. Wang, Y. Guo, Z. Li, W. Ying, D. Chen, Z. Deng, X. Peng, Dual emission from nanoconfined R-phycoerythrin fluorescent proteins for white light emission diodes, RSC Adv. 9 (2019) 9777−9782, https://doi.org/10.1039/C9RA00161A.

[83] Y. Guo, X. Wang, P. Hu, X. Peng, ZIF-8 coated polyvinylidenefluoride (PVDF) hollow fiber for highly efficient separation of small dye molecules, Appl. Mater. Today. 5 (2016) 103−110, https://doi.org/10.1016/j.apmt.2016.07.007.

[84] L. Niklaus, S. Tansaz, H. Dakhil, K.T. Weber, M. Pröschel, M. Lang, M. Kostrzewa, P.B. Coto, R. Detsch, U. Sonnewald, A. Wierschem, A.R. Boccaccini, R.D. Costa, Micropatterned down-converting coating for white bio-hybrid light-emitting diodes, Adv. Funct. Mater. 27 (2017) 1601792, https://doi.org/10.1002/adfm.201601792.

[85] D.A. Press, R. Melikov, D. Conkar, E.N. Firat-Karalar, S. Nizamoglu, Fluorescent protein integrated white LEDs for displays, Nanotechnology 27 (2016), https://doi.org/10.1088/0957-4484/27/45/45LT01, 45LT01.

[86] X. Wang, Z. Li, W. Ying, D. Chen, P. Li, Z. Deng, X. Peng, Blue metal−organic framework encapsulated denatured R-phycoerythrin proteins for a white-light-emitting thin film, J. Mater. Chem. C. 8 (2020) 240−246, https://doi.org/10.1039/C9TC05342E.

[87] Y. Wen, T. Sheng, X. Zhu, C. Zhuo, S. Su, H. Li, S. Hu, Q.-L. Zhu, X. Wu, Introduction of red-green-blue fluorescent dyes into a metal-organic framework for tunable white light emission, Adv. Mater. 29 (2017) 1700778, https://doi.org/10.1002/adma.201700778.

Part Three

Applications

General lighting

6

6.1 Introduction

With its appearance in the late 19th century, incandescent lamps became the prime source of lighting with significant progress in the global urbanization. With the advances in technology, different light sources replaced their preceding ones with an immediate effect. Starting with the sunlight, humankind utilized different sources of light at different time periods, and each light source dominated the corresponding period in which it was developed. Incandescent lamps were subsequently replaced by compact fluorescent lamps (CFLs), which in turn paved way for a more pronounced solid-state lighting (SSL). Recently, the interests in SSL-based research has surged tremendously owing to its immense demand in the global market. Efforts have been taken to undertake device packaging and manufacturing with significant amount of concentration on novel material design. Currently, many researchers around the world are focusing on the production of white light-emitting diodes (WLEDs). LEDs are blessed with a long life of about 50,000 to 100,000 hours as compared to their preceeding light sources such as incandescent bulbs and CFLs each with a life time of 1000 and 10,000 hours, respectively. In addition to this, other advantages of LEDs include their small size, specific wavelength, low thermal output, adjustable light intensity, and quality, as well as high photoelectric conversion efficiency [1,2].

To achieve sustainable life for a luminaire, it is essential to protect it from the pollutants and other environmental threats that can hamper the overall luminous efficiency and output. The immunity of a luminaire against the pollutants are described by ingress protection (IP) codes. IP ratings are international codes that are generally marked on the lighting products or on their package to help the consumer understand the level of protection possessed by the product against solid or liquid intrusions. These ratings are much simpler than the complicated specifications described by the manufacturers. Each of these codes has a specific meaning and defines different protection levels of the luminaire. These ratings are not just limited to luminaires but also applied for other electrical enclosures and mechanical casings. The manufacturers are supposed to print these codes on the product to make the consumers aware of the intrusions by solid or liquid particles that may affect the product's performance. This alphanumeric rating provides better opportunity to consumers in taking appropriate care of their products. For luminaires, it is of utmost importance to know their protection levels against intrusion for the luminaires to sustain in their surrounding. A luminaire that may be used for street lighting may not be durable if it is fixed in a bathroom and vice versa. Thus, IP ratings form a transparent tool that avoids the jargon and unclear specifications to understand the quality and durability of the product. IP codes are expressed in four digits that consist of alphanumeric values: the first two digits are "IP" followed

The Fundamentals and Applications of Light-Emitting Diodes. https://doi.org/10.1016/B978-0-12-819605-2.00006-9

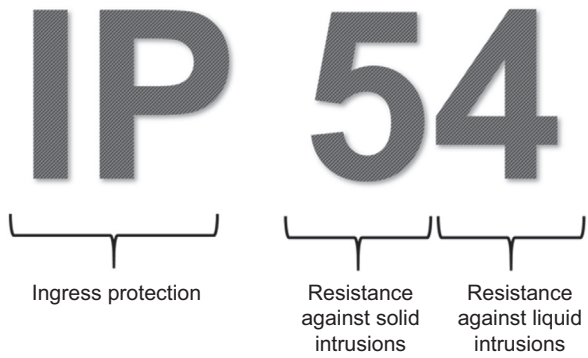

Figure 6.1 Example of an IP rating. *IP*, ingress protection.

by two other numeric values or the letter X in the third and the fourth digits, as shown in Fig. 6.1. The third digit signifies the resistance of the product against solid intrusions, whereas the fourth digit is for liquid intrusions. If the letter "X" is used in place of a numeric value in the third or fourth digit, then the product must have not been tested for its resistance against the solid and liquid intrusions, respectively. The solid IP values goes from 0 to 6, and each of the values has a specific information associated with the protection levels against solid objects or dust particles. Similarly, the liquid IP values are ranked from 0 to 8. Additionally, there is another code 9K added to denote the liquid protection. The protection levels associated with each of the codes for electronic equipments against solid and liquid intrusions are given in Table 6.1.

In the present scenario, the lighting market is flooded with numerous designs of LED lights. These range from retrofitted bulbs, strip lights, and tube lights to a number of downlights and spotlights. Some of them bear a commercial brand tag that granted them with a higher price label, whereas some others are deprived of a promising brand label and, hence, are available in a much cheaper price. Yet, the quality of an LED product cannot be confirmed just by their brand label. It is highly recommended for the consumers to analyze the IP ratings while purchasing the LED luminaire. Apart from that, a consumer must assess the requirements and choose the right product to avoid confusion during the purchase. This can be achieved if the consumers exhibit some interest in gaining the basic awareness about the LED technology and the manufacturers. There are several big and small players offering LED luminaires targeted for specific applications, and each of them offers a different characteristic, technology, and specifications that suit the application for which it is made. These many characteristics are difficult to be remembered and can easily confuse the consumer if he or she is ignorant about the basics of LED. This situation demands the consumers to make queries to themselves and put the reasoning in support of the purchase of commercial LED products. The foremost concern for any consumer is the quality of the luminaire. The quality is, in turn, determined by the energy efficiency, luminaire design, thermal management, lamp life, and illumination of the luminaire. These factors also affect the overall cost of the fixture, and hence, we

Table 6.1 IP codes for protection against solid and liquid intrusions. *IP*, ingress protection.

Code value	Meaning of code	
	Protection against solids	**Protection against liquids**
0	No protection is assured.	No protection is assured.
1	Protection is assured against solid objects that are bigger than 50 mm.	Protection is assured against drops of condensed water.
2	Protection is assured against solid objects that are bigger than 12.5 mm.	Protection is assured against drops of condensed water when the product is tilted at any angle up to 15 degrees from the vertical position.
3	Protection is assured against solid objects that are bigger than 2.5 mm.	Protection is assured against rain or spray of water falling on the product at any angle up to 60 degrees from the vertical position.
4	Protection is assured against solid objects that are bigger than 1 mm.	Protection is assured against splashing of water or liquid from any angle.
5	Complete protection is assured against moving solid objects. Protection is assured against certain amount of dust that may interfere with the normal operation, but not completely dust-proof.	Protection is assured against water jets projected by a nozzle (6.3 mm) from any angle.
6	Completely dust-proof and protection is assured against all kinds of solid objects.	Protection is assured against stronger water jets projected by a nozzle (12.5 mm) from any angle.
7	–	Protection is assured against immersion in water at a depth between 15 and 100 cm for maximum 30 minutes.
8	–	Protection is assured against long periods of immersion in water at a depth over 100 cm.
9K	–	Protection is assured against the effects of high-pressure water jets and steam cleaning.
X	Not tested for protection.	Not tested for protection.

may conclude that the quality of the luminaire is directly proportional to the cost of the luminaire. But it certainly will provide a much energy-efficient product that will contribute to the annual savings due to less amount of power consumption. Additionally, the reliability of the luminaire is determined based on its total hours of operation.

6.2 Light-emitting diodes for lighting applications

6.2.1 Interior lighting

SSL has pronounced applications in interior lighting, street lighting, and color-changing architectural lighting [3]. LED-based SSL for interior lighting comprises 17% of the total electricity consumption [4]. SSL technology derives three major advantages: the very first one being its inherent capability to generate light with high efficiency leading to prodigious energy savings; secondly, the durability and the efficiency of the solid-state emitters result in potentially huge environmental benefits; and finally, the flexibility to control the emission properties with much greater precision permits in customizing and tailoring the emission properties for specific applications. LEDs are the most acknowledged and highly acclaimed form of SSL. These offer an option to customize their lighting as per the buyers' needs. LED fixtures are easy to install and are also available with retrofitting options. Since there are lot many LED designs available with different specifications, buyers must be aware about their requirements and choose the product based on the analyses of their requirements. It is also essential to assure the credibility and reputation of the manufacturers as well as ensure that they offer a longer warranty period for their products.

Interior lighting often comes in three types depending upon their color temperature. White light may be warm, neutral, or cool. Warm-white light has a slightly yellow tint, and its correlated color temperature (CCT) can range from 2800 to 3800 K. Warm-white light is generally used in public places where the relaxation is given higher priority. Cool-white light glows with a bluish tint, and it lies above 6000 K temperature. Cool-white light is preferred in areas where enhanced, brighter, and concentrated illumination is necessary. Such light sources are used in offices, hospitals, work areas, and so on, where light must reach the nooks and corners of a room. Blue-enriched white light accompanied with other lighting factors such as CCT and the directional nature of light plays an important role in evoking necessary arousal in people for promoting their performance at work [5,6]. Neutral-white light lies in the intermediate temperature range, from 3800 to 6000 K, and is usually a combination of the previous two types. None of the aforementioned white light is superior over the other. The choice depends upon the necessity. Human emotions, health, and vision are strongly influenced by the lighting condition. The choice of the white light depends upon the levels of visual comfort perceived by a human. People experience higher degree of comfort, pleasantness, clarity, colourfulness, and less degree of haziness and oppression when luminaires provide appropriate levels of illuminance in the room [7]. The visual difference between the white light having different CCT values can be seen in Fig. 6.2.

The most preferred choice of CCT for the residential areas is between 2700 and 3000 K. The luminaires for residential buildings are designed to produce a wide beam angle to ensure that proper illumination is reachable at every nook and corner of the room. But the preference varies when the lighting is meant for shops or groceries. In groceries, it is preferred to keep the CCT close to 4000 K to produce neutral-white appearance that could highlight the natural appearance of food products.

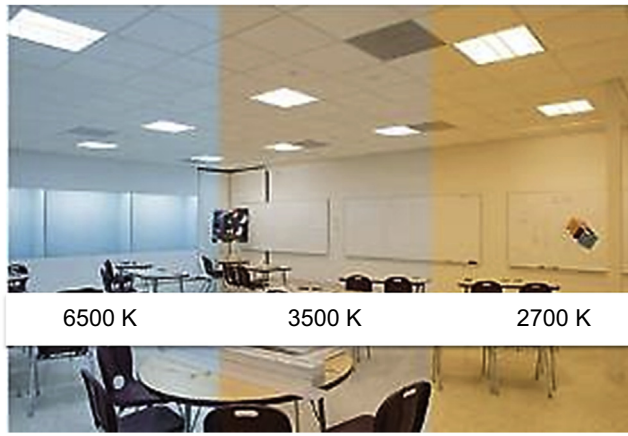

Figure 6.2 Difference in the appearance of white light produced with different CCT values. *CCT*, correlated color temperature.

The merchandise put on display in the retail shops that are illuminated with narrow floodlights or spotlights so as to enable the customers to differentiate between their colors. Proper illumination is highly essential to grab the attention of customers onto the merchandise. Shops and groceries illuminated with lights having higher CRI were found to be more successful as their products were displayed with their true color identity in front of the customers. In restaurants, the lights are kept dimmed to provide a comfortable and warm ambience to the diners. In jewellery shops, LEDs with neutral-white emission can make the jewels and ornaments look sparkling to the customer. Hence, jewellers prefer to keep their lighting with a CCT of near about 4000 K. For schools and offices, it is essential to install cool-white light with CCTs higher than 4500 K to create a sense of work among the students and employees in addition to enhanced performance in their work. Fig. 6.3 illustrates the LED interior lighting used for office rooms and homes.

The most convenient and commonly used method to obtain the white-LED is combining phosphors with GaN-based LED chip. Most of the WLED products are gained by pumping the yellow phosphor (YAG:Ce) with blue LEDs chip, which has a low color rendering index of less than 75 and high temperature due to the lack of red component. To solve these problems, red-enhanced YAG:Ce or a small amount of red phosphor was introduced in YAG. Currently, there are three viable options for achieving white-emitting LEDs:

(a) Blue LED with yellow phosphor
(b) UV-LED with RGB phosphors
(c) Three or more LEDs of different colors

Each of these approaches has its own advantages and limitations. To overcome the issues arising in these three approaches, a fourth approach was instigated wherein an NUV-emitting chip is combined with a single-phase white-emitting phosphor. The semiconductor chip and the phosphors are incorporated in a single LED package.

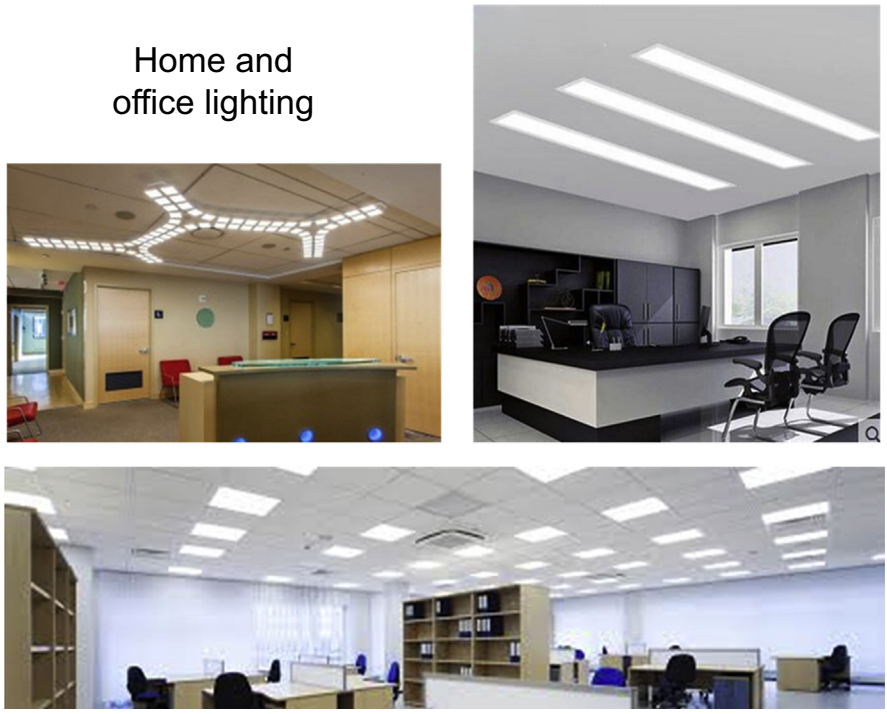

Figure 6.3 LED lighting for home and office rooms. *LED*, light-emitting diode.

There are three different types of approaches considered for the LED packaging system [8]:

(a) SMD) package
(b) Chip-on-board (COB)
(c) LED unit with remote phosphor plate

In SMD, LED chips are permanently soldered on the printed circuit board (PCB) with a predefined pitch. The phosphor is mixed with a silicone resin and then coated on the chip. The number of chips on the board can vary. They appear like a collection of smaller lights arranged on the board. The sum of the luminous fluxes of all the LEDs on the board will give the total flux of the board. Due to their versatility, SMD LEDs are highly popular. SMD package is preferred for large-sized luminaire meant to illuminate huge indoor spaces such as offices, schools, hospitals, or art galleries. They are found in LED bulbs, string of LED lights, and as notification lights in mobile phones. They are bright and can produce 50−100 lumens per watt. SMD LEDs are small, and they resemble the design of a square, flat computer chip. They are also available in different sizes and can accommodate LED chips with complicated designs. SMDs can have more than two contacts and up to three diodes, with an individual circuit arrangement for each diode. Each diode would have a cathode and an anode that can lead to a maximum of six contacts on a single SMD. This feature

makes SMDs a distinct packaging technology than the other ones and demonstrates the versatility of SMD LEDs. An SMD can include a red, green, and blue LED chip, which can be tuned to any color by adjusting the output levels of each of the LEDs. The secondary optics used for SMDs can be microprism plates or a separate lens for each SMD LED. For diffuse SMD lighting, diffuse plastic plates made of polycarbonate or poly(methyl methacrylate) (PMMA) are used. The second type of packaging is the COB, which is a step ahead in technology and more efficient than SMDs. Similar to SMDs, COB also can bear multiple diodes on the same surface. Unlike SMDs, there are only two contacts available for COBs regardless of the number of diodes attached on them. Another distinction is that COBs can have a more number of diodes on them (typically nine or more), which are all connected to the two contact points by a single circuit. This arrangement gives a panel-like appearance to COB packages. Since all the diodes are connected by a single circuit, COB LEDs cannot be used to develop color changing bulbs or luminaires. COBs are not versatile like SMD LEDs, but they are much more efficient than the SMDs. They have better thermal management and give higher lumens per watt owing to the cooling ceramic substrate and the design of COB LEDs. COBs have made it possible to realize heavy duty lights such as flood lights and spot lights. Such kinds of lights were not feasible with SMDs as more number of LED sources will be required to produce such a high lumen output with SMDs. COBs can produce a high luminous flux from a small light-emitting surface. They can produce a minimum of 80 lumens per watt. The features of COB make them suitable for high-power LEDs operating between 50 and 300 W power. COB LEDs are used for industrial lighting, downlight luminaires in shops, hotels, or restaurants, and in camera flash. The third type of packaging is the remote phosphor technology. Usually, manufacturers prefer to coat the phosphor directly on the semiconductor die. In such a case, the phosphors undergo thermal degradation at a faster rate due to the direct contact between the phosphor and the die. The remote phosphor LED package separates the phosphor coating from the LED die and makes provision to interchange different phosphors in the package. This helps in effectively changing the color temperature of the LED package by incorporating different phosphors. This has also resulted in achieving stable white light with high CRI. The phosphors are not subjected to heat degradation due to their separation from the die.

The latest development in the interior lighting segment is the entry of organic LEDs (OLEDs) for general illumination. OLEDs are thin sheets of bendable or rigid materials that can offer untold advantages while lighting up a space more efficiently [9]. This amazing lighting technology offers vivid designs and better light quality. OLED technology has the potential to create efficient, attractive, and healthy luminaires. Although OLEDs offer untold advantages, they are yet to make the inroads in the general lighting sector. OLEDs were well set to make the inorganic LEDs to bow down and take over their place [10]. OLEDs have established themselves as the mainstay in the display industry [11,12]. Citing this, many companies started exploring the possibilities to introduce OLEDs in the general illumination market. However, there were many casualties that happened in this endeavor. One of the foremost companies to introduce OLEDs in general lighting, LG, has almost quit the OLED lighting market and shifed its focus towards OLED displays and OLED automotive lighting only [13].

Several other large manufacturers in the lighting sector such as OSRAM, General Electric Company, Philips, Panasonic, and others were also active in the OLED lighting programme. But they too slowly pulled back from the business. One of the major reasons was the challenge faced by the manufacturers in bringing down the high price of production. Still none of the manufacturers has managed to overcome this difficulty. This challenge has overshadowed other hurdles such as product longevity, which were holding back the OLED lighting industry. Many optimists believe that OLEDs could nudge into the lighting industry, only if the production prices come down. OLEDs emit a softer, glare-free, and diffuse light that is more appeasing to the human eye. Thus, OLEDs have an opportunity to produce human-centric light with a diffuse surface source of SSL having a bendable form factor. Fig. 6.4 illustrates some of the OLED lighting panels used for the interior lighting applications. While LEDs are known for their throwing of intense light from a small package, OLEDs are known to produce diffuse rays of light with minimal amount of blue wavelengths. OLEDs are perfect for the rooms and locations where blue-rich light should be avoided. OLEDs also cut down the risk of infrared (IR) and ultraviolet (UV) emissions from the luminaire, and hence, they are preferable for applications such as exhibition lighting, illumination of the food products in shops or supermarkets, lighting artwork, and so on. In addition, OLEDs require lesser accessories to turn into a luminaire. In comparison with LEDs, there are fewer components in OLEDs in terms of the drivers, diffusers, optics, heat sinks, wave-guides, etc. This itself can lower the cost of the finished OLED luminaires and make their overall pricing comparable with the traditional LED luminaires.

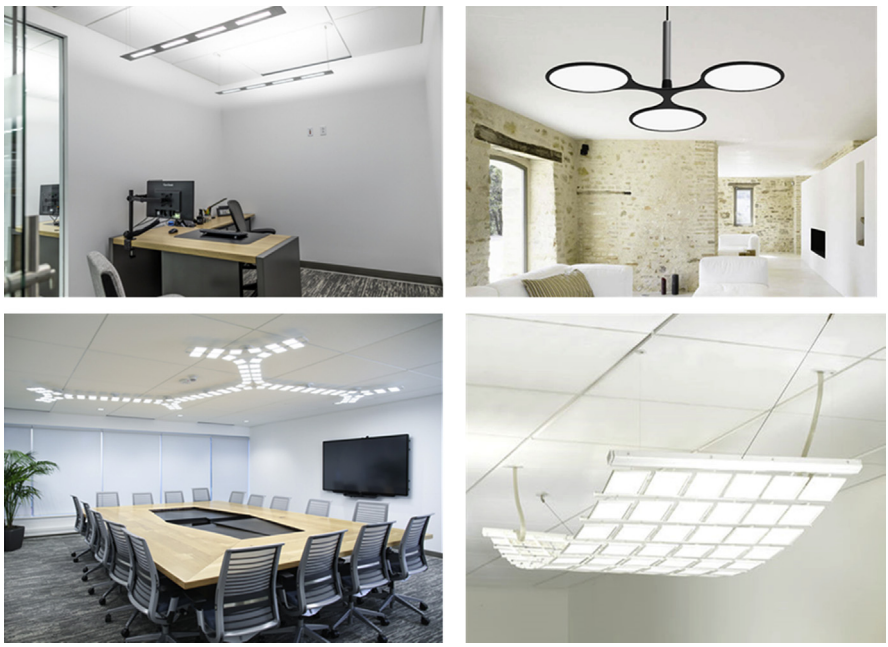

Figure 6.4 OLED indoor lighting panels. *OLED*, organic light-emitting diode.

OLED panel makers have also tried to lower the pricing by improving the energy efficiency of the luminaires to a value over 100 lm/W [14]. The longevity of OLED luminaires is still not obvious. Although there are claims that OLED luminaires can last for 100,000 hours, it is yet to be confirmed with thorough and effective tests. But it is certainly true that the rate of lumen depreciation of OLEDs has decreased with the use of multiple stacks. In some cases, people have expressed their doubts over the longevity of the OLED luminaires. Although OLEDs can show an earlier failure, it is difficult to completely blame the quality of the product. The way the luminaire is installed and handled can also be a factor deciding its longevity.

6.2.2 Street lighting

In terms of the general illumination area, the biggest growth market for LED-based SSL is provided by the outdoor lighting. Street lighting forms an essential element for urbanization. However, these street lights form the largest reason of energy drains for a city. One of the major reasons for the huge energy consumption in street lighting is the prevalence of age-old incandescent and sodium-vapor lamps in one-third of the world's roads. Almost 40% of the city's electricity needs are consumed by these lamps. In recent years, governments of various countries have become aware of the jeopardies occurring due to the use of such lamps, and thus, they are being replaced by the energy-efficient LED street lights. The roads lit by LEDs were well illuminated, and the use of these lights reduced the energy consumption for street lights by about 80%–90% as compared with the sodium vapor lamps. The adoption of LED-based lighting was mainly aimed to achieve better safety to the community and accelerating the progress towards sustainable development. An illustration of the LED lights illuminating the roads is shown in Fig. 6.5. In the initial phase, cool white–emitting LEDs (with higher CCT but lower CRI values) were installed in the streets, replacing the previously installed yellow-orange-emitting sodium vapor lamps [15]. However, the people commuting on these roads were unhappy with the unusual glare and color appearance of these LED lights [16]. This case was thoroughly studied, and a conclusion was derived that blue-rich LED lights created an unpleasant and less comfortable

Figure 6.5 LED street lights. *LED*, light-emitting diode.

atmosphere for the commuters, whereas yellow-rich LEDs created a comfortable and pleasant condition for them [17]. On separate occasions, the International Dark-Sky Association (IDA) and the American Medical Association (AMA) recommended the use of LED packages with CCTs not exceeding 3000 K for street lighting [18]. Although both the associations agreed upon this common resolution, their interests were different. IDA's recommendation was based on the fact that cool-white light from the LEDs had some adverse effects on the biological cycle of birds living on the trees, nocturnal animals, and also the sky glow and the nightscapes. On the other hand, AMA came forward to lessen the negative effects of the exposure to blue-rich light at night on the human health. Therefore, the municipalities were bound to install LED packages with lower CCT. In 2011, the difference in the luminous efficacies between the 4000 K neutral white and 3000 K warm-white was about 20%. As a result, neutral-white LEDs were installed in the streets to replace the cool-white LED lights. But, as of now, the difference in their luminous efficacies has come down to 6%, and hence, this factor should not be used as the selection criterion for preferring neutral-white light for street lighting. Further, studies revealed that pedestrians and motorists prefer to have warm-white light on the streets than the neutral-white light [18]. LED street lights comprise multiple LED units assembled in a panel and sealed by an encompassing lens. They are designed in such a way that maximum light is focused on the streets, and very less amount of light is allowed to stray away. The fixtures are provided with heat sinks to dissipate the heat generated by the driver circuits and to ensure longer life span of the luminaire. Nowadays, the LED fixtures are available in different shapes and sizes. The lens of the luminaire is specially designed to cast a wider pattern of light on the streets.

The levels of comfort enjoyed by motorists in driving through roadways lit by yellow-rich lights were the main reason that high-pressure sodium (HPS) lamps remained the mainstay in street lighting all these years. HPS lamps were highly efficient and used to beat the efficiency of all other lighting technology before the 1970s. But it loses out when it comes to competition with LEDs. LEDs dissipate negligible amount of heat as compared to the HPS lights. Also, the light emitted from LEDs is directional and can be focused maximum on to the roads. On the other hand, HPS lights produce more dispersion, and much of the light falls outside the path. The nocturnal animals and the birds nested on the trees are adversely affected due to the dispersed light from the HPS. HPS lamps produce a lower-quality light with a monochromatic yellow emission. Hence, it may damage the color vision of the motorists if they gaze on the HPS lamps for a while. The sodium present in the HPS lamps is susceptible to catch fire if it is exposed due to breakage. This also makes HPS lamps difficult to dispose and lead to concerns over the safety of the people and animals near the light poles. But with the availability of LED lights with a wide range of color temperatures, many municipalities started weighing the benefits of LEDs over HPS lamps. The extremely long life span and high energy efficiency of LEDs have provided them with an upper edge over the HPS lights. LEDs offer superior color-rendering properties than HPS. Additionally, LEDs provide higher quality of light, and their maintenance is hassle-free with lower costs. The requirement of fewer accessories makes LED lights more profitable. A comparison between the LED and the HPS street

Figure 6.6 Comparison between the LED and the HPS street lights. *HPS*, high-pressure sodium; *LED*, light-emitting diode.

lights is illustrated in Fig. 6.6. Another advantage is that LEDs reduce the light pollution caused by the street lights. Prior to LEDs, the HPS lamps used to spread light in all the directions and a fraction of the emitted light escaped into the sky to cause light pollution. Hence, they were integrated with reflector cups to capture the light emitted upward and direct them towards the road [19]. But the use of reflectors can be avoided in LEDs as the light emanating from them covers only the lower half-spherical space. In LED-based lighting, the secondary optics play an important role in delivering a prescribed beam of light from an array of LEDs that act as point sources. On the contrary, the optics used in HPS has very little to do. They are just meant to protect the lamp and offer some diffusion properties to the light emitted from the HPS.

The LED street lights were designed specially keeping in mind that the light emitted from them should not produce any harm to the wildlife or the birds living on the trees. Several agencies have surveyed and studied the effect of LED hues on the wildlife [20]. From the survey, the biologists concluded that green, amber, and yellow light were gentle and benevolent for the wildlife, whereas blue and white light has adverse effects on their metabolism [21,22]. The nocturnal animals and the birds having their nests on the trees near the light poles are the most vulnerable creatures. Already the wildlife species are experiencing negative impact of the rapidly changing environments. To add to their woes, humankind has introduced artificial lighting during the night that disturbs their lifecycles and metabolism. The street lights illuminate so brightly in big cities that the earth appears like a big glowing ball when viewed from a distance. Researchers have made a deep and thorough study to find out how the wildlife is affected by the light and its brightness. They have found that the circadian rhythms, migration, reproduction, and predator−prey relationships can be adversely affected due to exposure to improper lighting.

The introduction of LED street lighting systems has delivered extensive benefits to both the economy and the environment equally. In recent years, there has been a

considerable amount of decrease in the CO_2 emissions owing to lesser burning of coals for the generation of power in the thermal plants, and this indirectly ensued from the use of energy-efficient LED lights. Many cities across the globe have adopted LED lighting to cut down the energy needs for street lighting and direct the saved energy to other purposes. However, switching to LED street lights was not enough to meet the targets, and adaptive interoperable lighting was adopted to achieve bigger savings in energy. A central control system can be connected with all the LED street lights, and the operators can remotely monitor and regulate the light levels as per the requirements in unprecedented ways. Huge energy savings can be achieved by using these networked street lighting. The replacement of incandescent and HPS bulbs by LEDs in street lighting systems has brought about 50% energy savings, and an additional 30% increase was achieved by adopting smart lighting integrated with central control system. The LED-based smart street lighting systems have provided wider potential for the progress of cities accompanied with the benefits of energy and cost savings. Now, street lights are not seen just as a means of illuminating the roads in the dark. With the addition of cameras and sensors, the infrastructure for street lighting has become a platform for a variety of applications [23]. Certain cities have installed environmental monitoring systems with the street lights. The day-to-day operations of the city are collected at the microscopic level using the electronics integrated with the street lights. The sensors installed in them are capable of monitoring the temperature, humidity, motion, noise, and the air quality in the surroundings. The lighting infrastructures are also integrated with motion sensors and cameras to help the motorists in parking their vehicles. This innovation was developed by certain companies to assist the drivers and help reduce the congestion in cities and improve the traffic movement. The cameras and sensors installed on the street lights are also beneficial in improving the public safety of the urban residents. When the pedestrians approach a lighting pole, the motion sensors can detect their presence and brighten the illumination in the surroundings to increase the visibility. After the pedestrian crosses the lighting pole, the lighting levels can dim to 60% of its original brightness. In some areas, the pedestrian counters are integrated with the lighting systems to guide the pedestrians with the most appropriate path to walk at night. The invention of Li-Fi for digital communications using the light medium has enabled the use of LED luminaires for data transmission. The LED street lights in some well-developed cities are being used to provide public Li-Fi and the communication network for the internet-of-things (IoT).

Traffic signals are now widely run with LED lamps, as shown in Fig. 6.7. This has now made possible to view the signals from a faraway distance even during broad daylight with clear visibility. Earlier, incandescent bulbs suffered from the disadvantage of poor visibility in day light and higher energy consumption. Lower energy requirements made it possible to install solar energy—powered LED signals with greater ease. On an average, LEDs consume 85% less energy than incandescent lamps [24]. The replacement of incandescent bulbs for traffic signals with LED lights came up with several wonderful upsides. Based on a survey of LED traffic signal maintenance practices, it was reported that the use of LED traffic signals had been expected to reduce the lifetime cost per module compared with incandescent modules. LED traffic lights consume very less power, and subsequently, they save a lot

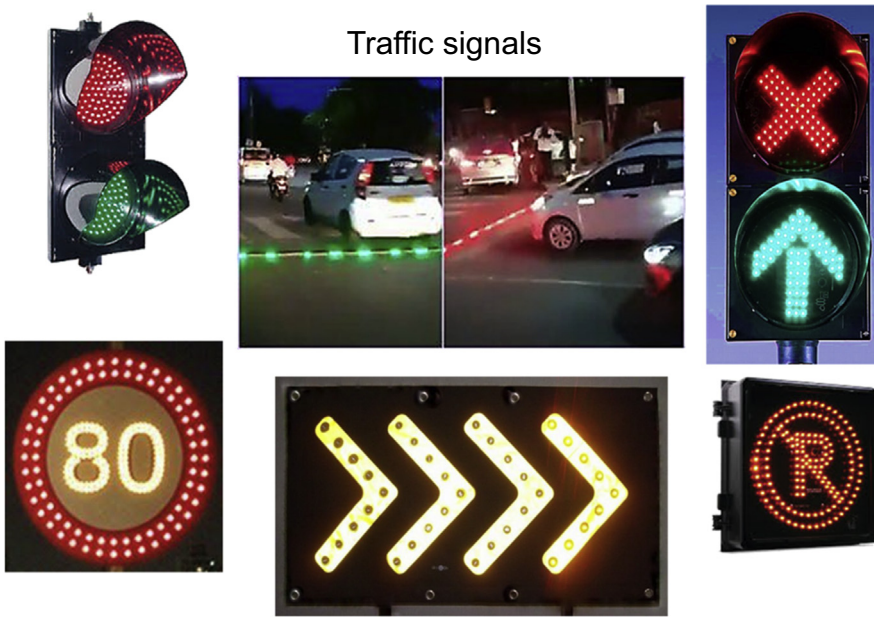

Figure 6.7 LEDs being used for traffic signal lights and signboards. *LED*, light-emitting diode.

of money. In addition to reduced energy expenditures, the extended lifetime of the LED modules had been expected to reduce the relamping material and labor costs by reducing the frequency of the incurring costs. Although LEDs offer a myriad of advantages over incandescent bulbs, there is one feature where the latter scores ahead. LEDs do not heat up during their operation, and this feature has proved to be a curse for the LED traffic lights in the regions experiencing snowfall. While the traffic lights based on tungsten filament heating lamps produced enough heat to melt the snow clad on the traffic lights, LEDs fail to do so. The snow deposited on the lights would often obscure the vision of the vehiclists. But the excess heat produced by the incandescent bulbs melted the snow even in the worst weather conditions. Soon, solutions to this unexpected and unusual issue were also found. The traffic signals in the snow-clad regions are now installed with LED arrays featuring built-in heating modules. The thermal sensors detect the temperature of the traffic signal, and when the temperature falls beyond a critical point, the heating module is switched on to melt the snow accumulation. LEDs are also known for their compact size that has allowed in modifying the design of traffic signals. From the traditional traffic signal poles, LEDs have transformed the signals into simple strips of light, as shown in Fig. 6.7. Besides, LEDs are now used for signposts to give better visibility to vehicle drivers.

6.2.3 Automobile lighting

In almost all machineries, LEDs have found their role as headlamps and indicator lamps due to their portable size, low energy consumption, and low maintenance requirements. Most of the roads and highways outside the urban area are left without

Figure 6.8 LED lamps used in different parts of cars and motorcycles. *LED*, light-emitting diode.

any illumination by the road lighting, and hence, it is necessary to have very bright and efficient headlamps to be installed on the automobiles for their journey through such paths. Automotive lighting on cars, motorcycle, and bicycle lights has gained more efficiency due to the mechanical robustness and long lifetime of LEDs [25]. Fig. 6.8 illustrates some of the applications of LED lamps in automobiles. The LEDs were introduced in the automotive lighting through the higher-class car models. But the advancements in the technology led to the shifting of the LED lighting towards the midrange and lower-class car models too. In higher-class car models, the space left out by the LEDs is being filled up by laser lights. But the laser light supplies are limited, and hence, their use will be limited to only the top-class models.

Until a few years ago, the use of LED lights in the automotive industry was just limited to only the premium car models. But their use has now extended to lower-priced car models too. Apart from the headlights and taillights, LEDs are now available in the car interiors also. LEDs are now an omnipresent entity in the automotive industry. LEDs are featured with long lifetime, durability, high output and focus, clear visibility during broad daylight, and fast switching times. These features have been considered while applying them to automotive industrial applications. They are used to make brake lights for cars, buses, and trucks. Their use in brake lights improves safety, as they quickly respond by lighting up fully and giving a correct signal of braking to the vehicles that are following from behind. They glow fully at least 0.5 seconds faster than the incandescent bulbs, thereby, giving the drivers behind to react more quickly and avoid any type of accidental collision. White LED headlamps are on the rise recently, for providing better visibility during the night and stylish looks to automobiles. These lamps accompany parabolic reflectors. Additionally, the vehicle headlights are integrated with flexible driving beam control that can shut off the

specific portions of the lighting beam and stop the glaring issues from the arriving vehicles by optimizing the illumination. Such lights offer more security and higher brightness levels due to which many automotive manufacturers are focusing on including them in their premium model cars. LEDs are known for their bright emission of light with lower power consumption. As a result, LEDs have become the first choice for signal lights or indicator lights on the vehicles. The signal lights are necessary for the vehicle drivers to communicate with other drivers on the road about their actions such as turning or stopping their vehicle. These lights must be equally visible during the day and night. In majority of the countries, yellow light is used as signal lights, as it is more visible than any other color to other drivers at a distance. Red LED lights are used as brake lights for vehicles. Brake lights are turned on when the driver presses the brakes of the vehicle. On pressing the brakes, LED brake lights illuminate instantly and give a signal to other drivers behind. The time taken for the LEDs to turn on is very less as compared to the halogen bulbs that were earlier used in the vehicles [26]. This will aid the drivers behind to make a quicker response and stop their vehicles immediately.

In the recent times, vital strides were made in the automotive forward-lighting applications with the development of high-luminance white LEDs. The manufacturers and the suppliers of the automobile products and their components have gained increased understanding about the advancements in the LED products and their designs. The thermal management of the LED headlamps has been improved to extend their life span in automobiles. The advancements in the automotive lighting were also contributed by the development of new materials and the emerging optics and electronics associated with the LED headlights. The use of plastics in the base and housing materials has been replaced by the ceramics. The joining layers in the LED packages are now being made of solder and gold, instead of adhesives. Similarly, the use of epoxy resins as encapsulants has become outdated, and they are now being replaced by silicone that demonstrates higher heat resistance, thereby enabling the LEDs to operate at higher temperatures. Even the optics is being redesigned to give superior performance. Earlier, the optics for the LED lights was adapted from the lens and the reflector applications. These are now being replaced by the miniature lenses and the index-coupled light guides and lenses. Other factors that contributed to the progress of LED forward lighting are the improvements in the luminance, luminous flux, and efficacy as well as the control over the color temperatures. The newer LED packages offer higher drive current and thermal resistance as well as lower optical magnification that lead to higher luminance levels. But there are certain limitations in achieving higher thermal resistance for a lamp. Under such circumstances, all other elements and parameters associated with the LED package must be improved to ensure optimum performance of the LED headlight. Thus, less-efficient LED packages with lower thermal resistance can also achieve higher luminance levels through the optimization of other parameters. The optics of the LED package is essential in achieving high luminance levels and for the style and structure of the headlight design. The light output necessary to produce the required light beam from the headlamp is decided by the luminous flux and the luminance levels. Improvements in the efficacy of the LED packages were achieved in the recent years, and this has influenced the

headlight design to a great extent. The enhancements in the phosphor and the chip epitaxy have some role in extracting higher lumens per watt from the LED package. The luminous efficacy is also influenced by the temperature. When the operating temperature of the LED package increases, there is a drop in its efficacy. This drop can be even greater than 10%. Therefore, it is necessary that the LEDs are operated in a cooler environment and provided with better thermal management systems to enhance their efficiency. One of the areas that need to be improved is the color control of LEDs. Till now, the color range of the LED headlamps went unnoticed as they were not in prominence like the LEDs used for the general illumination. But the available color range of LEDs is not acceptable for the forward lighting of premium model cars. Research is going on to find an optimum color control to develop LED headlights with ideal color output. In the past few years, significant enhancement in the operating performance and thermal resistance has been achieved to improve the cost-effectiveness of LEDs. These improvements have resulted in higher power density of the LED package and, consequently, brought out higher luminance levels. This has allowed the development of smaller, high-temperature packages that demonstrate better thermal stability.

There has been a lot of improvement in the system integration and mounting capabilities for LED headlamps owing to the joint development work carried out by the automotive manufacturers and suppliers. The need to satiate the safety standards for motor vehicles has led to several big industrial collaborations among major motor companies. Besides, the competition among the major players in the automotive industry has demanded to exhibit something extra to make their products more attractive. As a result, many additional features that were not demanded from the current range of headlights have also been included in them. The quality of the components used in the LED package has a big role in improving the overall efficiency of the luminaire. Hence, the manufacturers of each of the individual components are focusing on improving the quality of their components. The suppliers of heat sinks, electronic substrates, and silicone resins are taking utmost care to provide the finest components that works the best in the package.

6.3 Advantages of light-emitting diode lighting

LED lamps have loads of advantages in comparison with other artificial light sources. They are inevitably better in quality with unrivaled performance in all sectors. Although they are not the optimum solution to all the problems associated with lighting, LEDs have proved themselves to be a distinct technology that has brought a revolution in the lighting industry. Some of the benefits offered by LED lights are described in the following [27]:

- **Mercury-free and eco-friendly:** The biggest advantage of using LED-based lighting is to the environment that has been striving all these years due to the toxic and polluting technologies introduced by humankind. LEDs are free from any kind of mercury. This also ensures that the environment will not be polluted with poisonous mercury vapors or liquid mercury as a result

of the breakage or improper disposal of LED lamps. To make LED lamps more eco-friendly, they are being manufactured with lead-free circuit boards. Lead was the primary material used to solder the LED lights with the electronic circuit boards. With the move to replace lead with other eco-friendly materials, LED lamps have become friendlier to the environment.

- **Low power consumption:** LEDs require very less power to operate. They consume just 10% of the power required to illuminate a fluorescent lamp. Hence, they are also useful in battery-powered and energy-saving devices.
- **Fully recyclable:** The components of LED are fully recyclable and can be disposed as a normal household waste. The glass and the metal components of the LED lamp can be separated and recycled and reused. LEDs incorporated with phosphor or organic materials are also non-hazardous to the environment. The hydrometallurgy and other extraction processes can be implemented to separate the rare-earth elements from the used phosphor.
- **Miniature size:** LEDs are very small in size, and each luminaire is manufactured by arranging a specific number of LED lights in an array that is then connected to an electronic driver circuit. The small size of LEDs decreases their chances of getting damaged. The miniature size of LEDs also makes them a bankable option for small indicator lights in electronic equipments, backlights for LCD screens, displays, flashlights, keypad lights, etc.
- **Radiates very little heat:** LED bulbs are designed in such a way that the heat is least dissipated from them. Although LEDs do not emit heat themselves, their driver circuits can often heat up. But unlike other illumination sources such as incandescent bulbs, LEDs are not hot enough to burn the skin. The exception is IR-emitting LEDs, which can heat up their enclosures and surroundings with their emission of infrared (IR) waves. There are also certain instances where the lower-quality semiconductor light-emitting chips are used, and the inefficient semiconducting processes occurring in these chips can lead to higher degree of heat generation. Still, such LEDs will also give a relatively cold feeling on the touch as compared with incandescent bulbs or fluorescent tubes.
- **Low operating temperature:** Lighting sources such as fluorescent lamps, incandescent bulb, high-intensity discharge lamps, and so on require a hot cathode or a ballast to illuminate the lamps. On the other hand, LED luminaires are designed to operate at low temperatures and are free of any hot cathode or ballasts. With the rising temperatures, phosphors also lose their intensity, and the emission spectra gradually decrease in intensity. Hence, it is also essential to keep the operating temperatures from crossing a critical limit. LEDs attain the maximum temperature of 150 °C during operation. Such low operation temperatures ensure that the phosphor coating of LEDs does not degrade easily and enjoys a longer lifetime.
- **Fire safe:** Switching to LED luminaires can reduce the probability of fire accidents to a significantly low level. The traditional lamps, which emit heat along with light, are at a higher risk of igniting fire. LED luminaires do not heat up. Also, LEDs are accompanied with a heat sink that can draw up all the heat and keep the temperature of the luminaire under control. This makes them eligible to be used for lighting in cold-refrigerated rooms, storage places, and temperature-controlled surroundings.
- **Nonbreakable:** LEDs are resistant to breakage and do no break into pieces like incandescent bulbs or fluorescent lamps. They are made of epoxy lens that are shatterproof and a lot sturdier than the normal glass covering.
- **Mechanically robust and resistant to vibrations and shocks:** LEDs are free of glass enclosures or filaments that can be otherwise susceptible to breakage even with the slightest of the mechanical impacts or shocks.
- **Long operating life:** LEDs have relatively longer operating lifetime than all other artificial lighting sources. A good-quality LED can last anywhere from 5 to 10 years on an average and can operate for 50,000 to 100,000 hours. This is against the 1000 hours life span of

incandescent bulbs and 10,000 hours of fluorescent lamps or CFLs. If used judiciously, LED luminaires can last beyond 15 years.

- **Less maintenance required:** LED luminaires boast of 50,000 to 100,000 hours of working lifetime. This means these luminaires can last for upto 35 years. Yet they may face the failure of other components or driver circuits, which can lead to relatively lesser operating life. Choosing the right luminaire with better quality driver circuits and components can help in reducing the maintenance needs of the LED luminaire. Although it is imperative to claim it as a maintenance-free lighting, there is no doubt that LEDs can offer a lighting technology requiring the least maintenance.

Besides the previously discussed advantages, LEDs are also benefited by the following features:

- Slow failure
- Less quantity of materials required for manufacture
- Faster response time
- Ideal for uses subject to frequent on−off cycling
- Efficient even in harsh conditions
- Emits light of an intended color without using filter
- Emits light with constant temperature regardless of its intensity
- Varied spatial distribution of illumination
- Highly reliable lighting sources

6.4 Innovations in light-emitting diode lighting

LED lighting has come a long way since its induction into the lighting industry. They underwent several technological improvements and innovations to finally appear in different shapes and sizes. Now, consumers can select from a wide range of LED fixtures or modules that specifically fit the requirements of their home or offices. The most standard form of the LED light is the basic LED bulb. They depict the shape of the traditional incandescent bulb. LEDs have also mimicked the shape of a fluorescent tube. LED tubes are found in many offices as they are designed specially to fit into structures similar to fluorescent tubes. There are foldable strips of lights, too, in which individual LEDs are arranged in an array. Such strips are more commonly used along the hallways, ceilings of office rooms, decorations, etc. In office settings, panel lights are also found to be common. Apart from these, LED lights are available in some innovative designs too. LED lights take the form of candle bulbs wherein they are shaped like a narrow flame. Candle bulbs are used in decorative lamps or chandeliers. Another one is the globe bulbs that are round and have a classic appearance. These are also used as decorative lights. Besides the size and shape, the functions of LED lights are also popular among the consumers. Their ability to produce dimmable light as per the needs is highly appreciated. Dimmable LEDs are customized with a dimmer switch. Such functions can reduce the energy consumption by the lighting sources to a significantly low level. Smart bulbs have also attracted a huge number of the global population.

Smart bulbs, as the name suggests, are totally the smartest among the artificial lighting technologies that have descended on the earth. They can be connected to a smartphone, which perform as a remote to control the appliances at home. They also make it possible to build a centralized control system that connects all the appliances to a single smartphone. For interior commercial spaces, the automatic light control systems can save a lot of electricity. The automatic lighting controls can be categorized as zone controls, connected lighting, and luminaire-integrated controls [28]. In zone controls, multiple luminaires are controlled by a single photosensor/motion sensor. In connected lighting, a central control system is connected to a group of luminaires, and the control system can be remotely controlled and monitored over the Internet. In luminaire-integrated controls, each of the luminaire has one motion sensor/photosensor. In this system, a mesh network is used to group the luminaires and establish a direct communication between them. Unlike connected lighting system, luminaire-integrated controls require less capital and labor for their installation and also have the advantage of higher energy savings than the zone controls. Due to finer spatial granularity, luminaire-integrated controls with manual switches reduce energy use to a value between 32% and 47% in open offices [29,30]. In contrast, the decrease in energy use is limited to just 10% for zone controls with manual switches [31]. This is because the zone controls are programmed to switch on all the lights even if there is only one occupant present in the room.

Another innovative feature that came with the LED lighting is the ability to change the color of the light over a wide range. LEDs became dominant in this feature, which found many applications. Depending on the composition of the phosphor, LEDs can emit different colors, and their combinations can be effectively used to give a new color emission. The color gamut presented by LEDs is highly impressive. Some manufacturers claim to produce millions of colors by mixing the color emissions from LED arrays in different proportions. The color-changing LEDs are used in both indoor and outdoor lightings. The elegance of the color-changing cove lighting has defined the indoor applications of color changing LEDs. The color-changing lighting schemes are used in outdoor wall washing or facade lighting, as shown in Fig. 6.9.

6.5 Conclusions

LED lighting is anticipated to provide a promising future for the human society. The limitations put on by Haitz's law were already surpassed by the LEDs, and the present LEDs are way ahead than any other form of artificial lighting that existed till date. The introduction of LED lamps for the general lighting has significantly reduced the energy demands in the lighting sector and also eliminated the danger of mercury vapor exposure at offices and homes that used to be found during the era of fluorescent lamps and CFLs. Although the consumers find the LED fixtures a bit expensive than the incandescent or fluorescent lamps, the reality is that LEDs grant a higher luminous efficiency and a longer operating lifetime that turn out with huge savings for the

Figure 6.9 LED facade lighting for the offices, buildings, bridges, and monuments. *LED*, light-emitting diode.

consumer annually. The innovations achieved in the LED lighting industry has made it possible to obtain lights of different color hue, shapes, and sizes that suits the needs of the consumer. Therefore, it is possible to obtain LEDs in the form of bulbs, tube light, retrofits, wallpaper lighting, etc. Yet, to achieve a better future for the LED lighting, there is a need to sort out the issues of thermal management and driver electronics that pose as a hindrance in attaining an extended operating life for LED luminaires.

References

[1] N. Yeh, J.P. Chung, High-brightness LEDs-Energy efficient lighting sources and their potential in indoor plant cultivation, Renew. Sustain. Energy Rev. 13 (2009) 2175−2180, https://doi.org/10.1016/j.rser.2009.01.027.

[2] J.J. Zhang, R. Hu, X.J. Yu, B. Xie, X.B. Luo, Spectral optimization based simultaneously on color-rendering index and color quality scale for white LED illumination, Optic Laser. Technol. 88 (2017) 161−165, https://doi.org/10.1016/j.optlastec.2016.08.006.

[3] R. Sinnadurai, M.K.A.A. Khan, M. Azri, Vikneswaran, Development of white LED down light for indoor lighting, in: 2012 IEEE Conf. Sustain. Util. Dev. Eng. Technol., IEEE, 2012, pp. 242−247, https://doi.org/10.1109/STUDENT.2012.6408412.

[4] K.R. Wagiman, M.N. Abdullah, M.Y. Hassan, N.H. Mohammad Radzi, A.H. Abu Bakar, T.C. Kwang, Lighting system control techniques in commercial buildings: current trends and future directions, J. Build. Eng. 31 (2020) 101342, https://doi.org/10.1016/j.jobe.2020.101342.
[5] I. Iskra-Golec, A. Wazna, L. Smith, Effects of blue-enriched light on the daily course of mood, sleepiness and light perception: a field experiment, Light. Res. Technol. 44 (2012) 506–513, https://doi.org/10.1177/1477153512447528.
[6] A.H. Cockram, J.B. Collins, A study of user preferences for fluorescent lamp colours for daytime and night-time lighting, Light. Res. Technol. 2 (1970) 249–256, https://doi.org/10.1177/14771535700020040301.
[7] B. Wilhelm, P. Weckerle, W. Durst, C. Fahr, R. Röck, Increased illuminance at the workplace: does it have advantages for daytime shifts? Light. Res. Technol. 43 (2011) 185–199, https://doi.org/10.1177/1477153510380879.
[8] Q.T. Vinh, T.Q. Khanh, Optimization and characterization of LED luminaires for indoor lighting, in: LED Light, Wiley-VCH Verlag GmbH & Co. KGaA, Weinheim, Germany, 2014, pp. 399–442, https://doi.org/10.1002/9783527670147.ch7.
[9] J.F. García, S. Höfle, M. Zhang, J. Dlugosch, T. Friedrich, S. Wagner, A. Colsmann, O.L.E.D. Luminaires, Device arrays with 99.6% geometric fill factor structured by femtosecond laser ablation, ACS Appl. Mater. Interfaces 9 (2017) 37898–37904, https://doi.org/10.1021/acsami.7b12356.
[10] D. Chitnis, N. Thejo kalyani, H.C. Swart, S.J. Dhoble, Escalating opportunities in the field of lighting, Renew. Sustain. Energy Rev. 64 (2016) 727–748, https://doi.org/10.1016/j.rser.2016.06.041.
[11] Y. Choi, R. Ha, H. Cha, Fully automated OLED display power modeling for mobile devices, Pervasive Mob. Comput. 50 (2018) 41–55, https://doi.org/10.1016/j.pmcj.2018.07.006.
[12] S. Logothetidis, Flexible organic electronic devices: materials, process and applications, Mater. Sci. Eng., B 152 (2008) 96–104, https://doi.org/10.1016/j.mseb.2008.06.009.
[13] Y. Zhu, L. Guo, Y. Lee, X. Xu, J. Xie, G. Zhang, Y. Hu, 57.4: OLED in automotive lighting applications, SID symp, Dig. Tech. Pap. 50 (2019) 628–631, https://doi.org/10.1002/sdtp.13592.
[14] A. Kumar, W. Lee, T. Lee, J. Jung, S. Yoo, M.H. Lee, Triarylboron-based TADF emitters with perfluoro substituents: high-efficiency OLEDs with a power efficiency over 100 lm W −1, J. Mater. Chem. C (2020), https://doi.org/10.1039/C9TC06204A (in press).
[15] W. van Bommel, Road Lighting – Fundamentals, Technology and Application, Springer International Publishing, Cham, 2015, https://doi.org/10.1007/978-3-319-11466-8.
[16] J. Hecht, The early-adopter blues, IEEE Spectr 53 (2016) 44–50, https://doi.org/10.1109/MSPEC.2016.7572537.
[17] D. Beckwith, X. Zhang, E. Smalley, L. Chan, M. Yand, LED streetlight application assessment project, Transp. Res. Rec. J. Transp. Res. Board. 2250 (2011) 65–75, https://doi.org/10.3141/2250-09.
[18] M. Davidovic, L. Djokic, A. Cabarkapa, M. Kostic, Warm white versus neutral white LED street lighting: pedestrians' impressions, Light. Res. Technol. 51 (2019) 1237–1248, https://doi.org/10.1177/1477153518804296.
[19] R. Ciriminna, L. Albanese, F. Meneguzzo, M. Pagliaro, LED street lighting: a looking ahead perspective, Greenpeace 5 (2015), https://doi.org/10.1515/green-2015-0020.
[20] University of Southern California, Putting animals in their best light: Some shades of LED lamps threaten wildlife: New tool to help protect animals from harmful hues of light, ScienceDaily. www.sciencedaily.com/releases/2018/06/180612090618.htm (accessed March 20, 2020).

[21] A.M. Dimovski, K.A. Robert, Artificial light pollution: shifting spectral wavelengths to mitigate physiological and health consequences in a nocturnal marsupial mammal, J. Exp. Zool. Part A Ecol. Integr. Physiol. 329 (2018) 497−505, https://doi.org/10.1002/jez.2163.
[22] V.J. Alaasam, R. Duncan, S. Casagrande, S. Davies, A. Sidher, B. Seymoure, Y. Shen, Y. Zhang, J.Q. Ouyang, Light at night disrupts nocturnal rest and elevates glucocorticoids at cool color temperatures, J. Exp. Zool. Part A Ecol. Integr. Physiol. 329 (2018) 465−472, https://doi.org/10.1002/jez.2168.
[23] K.R. Wagiman, M.N. Abdullah, M.Y. Hassan, N.H.M. Radzi, A new optimal light sensor placement method of an indoor lighting control system for improving energy performance and visual comfort, J. Build. Eng. 30 (2020) 101295, https://doi.org/10.1016/j.jobe.2020.101295.
[24] R.H. Iwasaki, LED traffic signal modules as an incandescent lamp alternative, ITEA J. 73 (2003) 42.
[25] S. Landau, J. Erion, Car makers embrace LED signals, Nat. Photon. 1 (2007) 31−32, https://doi.org/10.1038/nphoton.2006.31.
[26] J.D. Bullough, LEDs and automotive lighting applications, in: Nitride Semicond. Light. Diodes, Elsevier, 2018, pp. 647−658, https://doi.org/10.1016/B978-0-08-101942-9.00020-4.
[27] G.B. Nair, S.J. Dhoble, A perspective perception on the applications of light-emitting diodes, Luminescence 30 (2015) 1167−1175, https://doi.org/10.1002/bio.2919.
[28] J. Snyder, Energy-saving strategies for luminaire-level lighting controls, Build. Environ. (2018), https://doi.org/10.1016/j.buildenv.2018.10.026.
[29] A.D. Galasiu, G.R. Newsham, C. Suvagau, D.M. Sander, Energy saving lighting control systems for open-plan offices: a field study, Leukos 4 (2007) 7−29, https://doi.org/10.1582/LEUKOS.2007.04.01.001.
[30] F. Rubinstein, A. Enscoe, Saving energy with highly-controlled lighting in an open-plan office, Leukos 7 (2010) 21−36, https://doi.org/10.1582/LEUKOS.2010.07.01002.
[31] J. Jennings, N. Colak, F. Rubinstein, Occupancy and time-based lighting controls in open offices, J. Illum. Eng. Soc. 31 (2002) 86−100, https://doi.org/10.1080/00994480.2002.10748395.

Digital communications and display devices

7

7.1 Introduction

Light-emitting diodes (LEDs) can be used to transmit digital and analog signals through fiber optic cables due to their ability to achieve very high data bandwidth by virtue of their very high frequency. During his TED Global talk, Prof. Harald Haas mentioned about Li-Fi, which is analogous to Wi-Fi, referring to a bidirectional, high-speed, and fully networked wireless communications using visible light. Li-Fi is a subset of visible light communication (VLC) system, which is a data communication medium using the visible light spectrum (375-780 nm). Many attractive advantages of VLC over the radio frequency (RF)−based wireless systems have been reported such as its ignorance to electromagnetic interference, high network security, integration with indoor lighting, availability throughout the world with unlicensed bandwidth, and so on. In many cases, LEDs are also used as sensors or as a photodiode in light detection. LEDs can be used both as a source and as a detector, especially as a photodiode that is useful in bidirectional communications [1].

LED displays are fast replacing other display screens due to their incomparable merits over the previously known displays and far superior quality of picture with utmost clarity preloaded with them, thereby, putting a marked distinction over their stature in the display market. Large LED displays are being used as dynamic decorative displays, stadium displays. Seven segment LED displays or alphanumeric displays are used in the informative displays at railway stations and airports, in destination displays on buses, trains, and trams, in calculators, and in other portable devices. Monocolor light is extensively used in the emergency vehicle lighting, lanterns, ships' navigation lights, decorative light bulbs, etc. Often, indicator lamps are required to retain the vision at night for navigation through seas or via air. Submarines and ships while sailing through the waters send the signals of their arrival to the coast by flashing coherent, monochromatic, and clearly visible lights. Aircraft cockpits, astronomy observatories, military fields, and so on use LED lamps to retain the night-time vision.

In the ensuing sections, the breakthrough achievements put forward by LEDs in the field of display devices and digital communication will be focused on. We shall also put light on the progress made in these fields by the previous technologies and the take-over executed by the LEDs to embark a revolution.

7.2 Digital communications

Personal communication using wireless data transfer has become a core part of human life. There are about 5 billion people in the world that use Internet on a daily

The Fundamentals and Applications of Light-Emitting Diodes. https://doi.org/10.1016/B978-0-12-819605-2.00007-0

basis. And the numbers are going on increasing day by day. The world has experienced a sharp increase in the number of people using smartphones and other wearable smart devices such as health trackers, smart watches, and digital glasses. The big cities and houses are now underpinned by the devices requiring Internet connections. The requirement of signal strength and networking speed has increased manifold, and new technologies have been introduced to satisfy the data communication needs of the people. The world mostly relies on the digital wireless communication system to surf through the Internet and communicate across the globe. Even the space programmes rely on wireless digital communications to maintain contact with the artificial satellites launched into the space. At present, RF waves dominate the wireless communication systems. RF waves are part of the wider electromagnetic spectrum that requires very sensitive electronic equipments during the wireless data transmission. The past decade witnessed the compound annual growth rate (CAGR) of 60% for the wireless traffic at the global level [2]. Assuming that the spectrum efficiency will remain the same for the next 20 years, it is estimated that the bandwidth requirement in the future shall rise to 12,000 times than that available at present [3]. Wireless fidelity (Wi-Fi) network uses 500 MHz bandwidth in the 5.4 GHz region of the RF spectrum. Citing the 12,000 times increase in the bandwidth requirement, the demand for the bandwidth for the future wireless network would have reached up to 6 THz. But the entire RF spectrum accounts to only 0.3 THz; thus, it is practically impossible to achieve the bandwidth requirements for the future, and the situation will ultimately lead to a spectrum crunch. Consequently, there is a huge shortfall in the available RF spectrum for Wi-Fi as compared with the rising bandwidth demands for the future.

The lower frequency waves of the electromagnetic spectrum are much easy to use, but these were ignored for data transmission until recently. The bandwidth offered by the optical spectrum is several orders higher than that offered by the RF spectrum. The size of the spectrum covered by the visible light and the infrared (IR) together can range up to 2600 times the size of the 300 GHz RF spectrum, as illustrated in Fig. 7.1 [4]. This spectrum requires only eye safety regulations and can be subjected

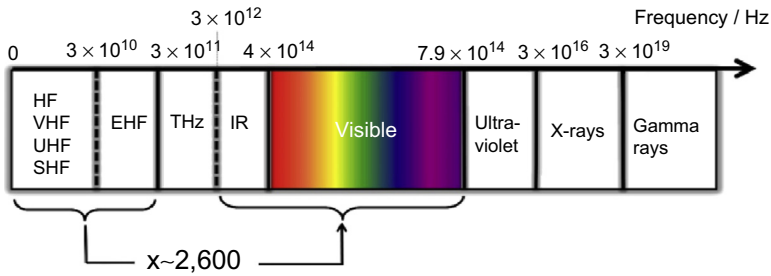

Figure 7.1 The optical spectrum comprising the visible and the IR regions is 2600 times larger than the RF spectrum. *EHF*, extremely high frequency; *HF*, high frequency; *IR*, infrared; *RF*, radio frequency; *SHF*, superhigh frequency; *UHF*, ultrahigh frequency; *VHF*, very high frequency.

Reprinted with permission from H. Haas, LiFi is a paradigm-shifting 5G technology, Rev. Phys. 3 (2018) 26−31. https://doi.org/10.1016/j.revip.2017.10.001. Copyright 2017, Elsevier B.V.

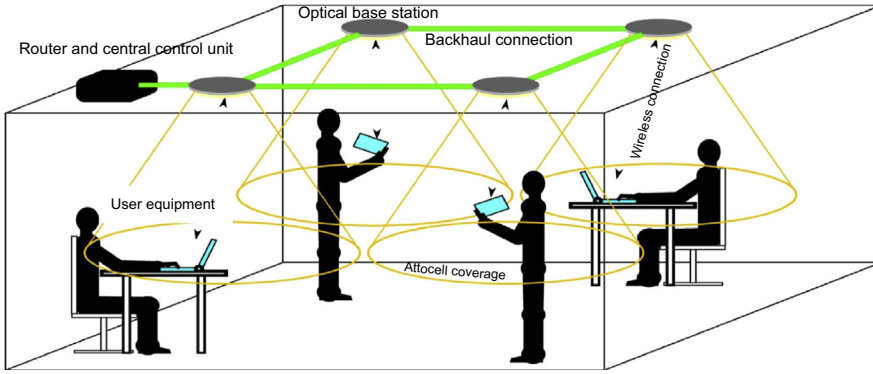

Figure 7.2 Indoor wireless networking based on the concept of Li-Fi attocell networks. *Li-Fi*, liquid fidelity.
Reprinted with permission from H. Haas, LiFi is a paradigm-shifting 5G technology, Rev. Phys. 3 (2018) 26−31. https://doi.org/10.1016/j.revip.2017.10.001. Copyright 2017, Elsevier B.V.

to unlicensed utilization. Also, the 6 THz bandwidth demand for the future will account to only 0.8% of the optical spectrum, which offers a bandwidth of 780 THz. There are several lasers and LEDs that cover the visible light and IR spectra. Also, the availability of photodiodes as receivers in the optical spectrum paved way for the optical wireless communication systems, which will potentially attract the new-generation networking and wireless communications [5]. This led to the establishment of Li-Fi as a means for high-speed data communication.

The concept of Li-Fi can be understood from a typical Li-Fi attocell (LAC), as illustrated in Fig. 7.2 [3]. Several light fixtures are suitably fit in the room and are driven by a modem or chip to set up the Li-Fi system. Each of the light fixtures in the room serves as an access point (AP) or an optical base station for the Li-Fi system. There is a high-speed backhaul connection between the core network and the APs. To receive signals from the terminal points, the light fixtures are provided with an integrated IR detector. The light emitted from the optical base stations is modulated at very high rates, such that their flickering does not appear to a naked human eye. Techniques such as power line communication and power over ethernet are implemented for providing data and power to each light fixture [6,7]. An IR source is embedded as a transmitter onto the user equipment for the implementation of optical uplink. The use of IR transmitters renders the visibility of the transmission signals to the user. The light fixtures create optical attocells, which are extremely small cells with radii less than 5 m. Each of the light fixtures can contain an AP. However, only selected fixtures are made to contain the AP, and the rest are utilized only for illumination. This will ensure that less expenditure is incurred to create the attocells and more coverage is provided by each of the access points. The selection of APs is made on the basis of the requirements, and it is made sure that no extra APs are created whose coverage shall overlap with that of the already existing AP. Li-Fi makes provision for connecting multiple user equipments through its multiple APs that will cover a larger area. This shall also ensure that each of the user equipment is receiving and transmitting the data

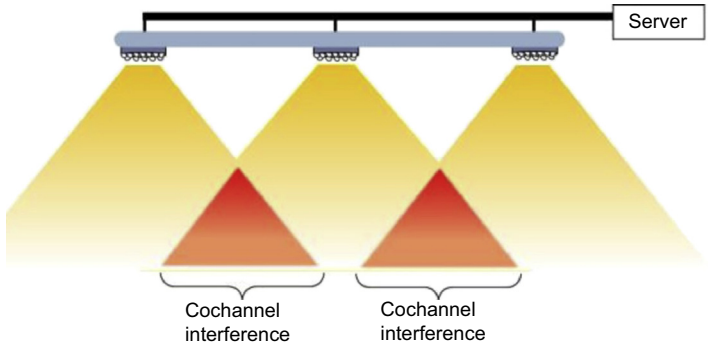

Figure 7.3 Occurrence of cochannel interference in the regions where the same light spectrum of neighboring access points overlap.
Reprinted with permission from H. Haas, LiFi is a paradigm-shifting 5G technology, Rev. Phys. 3 (2018) 26–31. https://doi.org/10.1016/j.revip.2017.10.001. Copyright 2017, Elsevier B.V.

more efficiently than the single AP offered by a Wi-Fi hotspot. The light emitted by multiple APs using the same channel can interfere and produce co-channel interference (CCI) in the optical attocell network, as shown in Fig. 7.3. The occurrence of CCI can help in achieving very high data density.

Li-Fi networking layers enjoy certain advantages over Wi-Fi. Some of the key advantages of Li-Fi are listed in the following:

1. **Speed**: The data communication speeds achieved through Li-Fi are greater by three orders of magnitude than the currently achievable speeds in Wi-Fi. Better communication and better service quality can be offered with such faster communication systems.
2. **Security**: Li-Fi systems are much safer and secure than the Wi-Fi systems. The RF spectrum used in Wi-Fi systems can be vulnerable to unauthorized access from the areas beyond the walls. On the other hand, Li-Fi uses the optical spectrum that cannot be accessed beyond the walls and the data transmission can be protected from hackers. Since light cannot penetrate opaque objects, it is difficult for the hackers from the other side of the walls to breach the security offered by Li-Fi.
3. **Availability**: Li-Fi can be made available everywhere by replacing the existing regular LED bulbs with Li-Fi-compatible LED bulbs, as illustrated in Fig. 7.4.
4. **Cost and efficiency**: Li-Fi systems are much cheaper than the Wi-Fi systems. Also, they consume lesser quantity of power than the latter. Li-Fi is mainly facilitated through LED bulbs. LED bulbs are already meant for providing the household lighting, and additionally, they are given the charge of communication and data transmission too. This shall avoid the extra expenses that would have arisen in setting up an additional hardware for data transmission. Unlike Wi-Fi, the cost incurred in implementing Li-Fi is far reduced.
5. **Safety**: Li-Fi is safer than Wi-Fi or any other wireless communication system relying on the RF spectrum. Since Li-Fi relies on the visible light emitted by the LED bulbs, no humans or animals are affected. On the other hand, RF spectrum has raised concerns over the human health and other living beings of the ecosystem [8,9].

Li-Fi is an emerging technology that makes use of the LED bulbs for data transmission. The Li-Fi-compatible LED bulbs demonstrate dual functioning of illumination as well as data transmission by embedding the data in the light waves. There is a

Figure 7.4 Li-Fi-compatible LED bulbs serving as transmitters and receivers for data transmission. *LED*, light-emitting diode; *Li-Fi*, liquid fidelity.

widespread misconception prevailing among the consumers that the LED bulb must be kept on bright illumination for the Li-Fi system to operate. But the Li-Fi system is so sensitive that even the lowest levels of light can be easily detected. So the LED bulbs can be dimmed to such a level that they appear turned off but are enough to carry out the data transmission. Since light cannot pass beyond the four walls of a room, its range is limited but more secure than Wi-Fi. Although Li-Fi technology is regarded as the future of Internet, it needs to overcome certain limitations for achieving data transmission on a massive scale. The major limitations suffered by the Li-Fi system currently are as follows:

1. **Limited range**: The inability of light to penetrate through opaque objects and walls of a room as well as the dispersion of light waves pose as a major hindrance in achieving larger coverage by the Li-Fi systems. The limited range of Li-Fi is still a boon-in-disguise as the vulnerability to unauthorized access to data transmission can be circumvented.
2. **Confusion about uplink**: The downlink speeds demonstrated by Li-Fi are exceptional. But there is not enough clarity about the uplink speeds offered by this system. Neither there is any mention about the implementation of uplink through Li-Fi.
3. **Large-scale implementation**: Currently, there is no specialized hardware available to implement Li-Fi on a large scale.
4. **Interference**: Li-Fi signals are susceptible to interference by other light waves. Sunlight and other common lighting can obstruct the Li-Fi signals that are also in the form of visible light. As a result, Li-Fi will face challenges while setting up data transmission systems in public places or open areas.

7.2.1 Evolution of light-emitting diode technology for communication

Researchers discovered the potential of LEDs to provide free-space optical wireless VLC for both indoor and outdoor applications. However, the use of phosphor-converted white LEDs suffers from poor modulation bandwidth, and hence, it is essential to undertake measures to overcome them for a better VLC data transmission rate, and use of different types of analogy equalizers at both the transmitter (Tx) and receiver (Rx) sides has been proposed [10].

In 2012, Jonathan McKendry et al. demonstrated a 400 MHz modulation bandwidth using a μ-LED array [11]. But this setup faced a limitation in the transmission rate (∼1.5 Gb/s) of mere on−off keying (OOK) modulation as a result of its limited carrier lifetime (∼1 ns). Much higher transmission rate of 3 Gb/s was also achieved using orthogonal frequency-division modulation (OFDM) [12]. In 2014, Yeh et al. experimentally demonstrated a 380 (2 × 190) Mbps phosphor LED−based VLC [13]. They claimed that their RLC bias-tee design can act as a simple Tx pre-equalization circuit in addition to its functioning of combining the DC and data signal. Using the OFDM-QAM (quadrature amplitude modulation) with bit loading, they achieved enhanced transmission rate, and the modulation bandwidth of the LED was extended from ∼1 to 30 MHz. They reported the achievement of 380 and 176.88 Mbps data rates at high and low illuminations, respectively.

A demonstration on a VLC system based on a white LED for indoor broadband wireless access was made after investigating the nonlinear effects of the LED and the power amplifier. A data rate of 1 Gb/s has been achieved at the standard illuminance level, by using an optimized discrete multitone modulation technique and adaptive bit- and power-loading algorithms, and this was twice the highest capacity that had been previously reported [14]. Another group reported a 3.75-Gb/s VLC system that uses single-carrier frequency-domain equalization (SC-FDE) based on a single red−green−blue (RGB) LED [15]. An optical free-space wavelength-division multiplexing (WDM) transport system employing vertical cavity surface emitting lasers and spatial light modulators with 16-quadrature amplitude modulation orthogonal frequency-division multiplexing modulating signals over a 17.5-m free-space link was proposed and demonstrated [16]. A novel bidirectional light wave transport system employing phase modulation scheme and light injection-locked distributed feedback laser diode as a duplex transceiver for passive optical network (PON), as well as employing laser pointer lasers with directly modulating data signals for WDM VLC, was experimentally demonstrated with an impressive and low bit error rate operation for PON integration with VLC application [17]. Yuanquan Wang et al. experimentally demonstrated a novel integrated PON and indoor VLC system based on Nyquist SC-FDE modulation with direct detection, in which a directly modulated laser and a commercially available red LED served as the transmitters of the PON and VLC, respectively [18].

The VLC based on RGB white LED can obtain high communication rate owing to a wide bandwidth obtained by modulating each color of the RGB white light source, respectively. A demonstration was made on a simple and efficient color demultiplexer

based on the volume holographic gratings that can separate RGB light and focus each color on different directions. The expression of the volume holographic grating vector with curved interference fringes was derived with an inference that spectral selectivity and angular selectivity change on the different positions of volume holographic grating [19].

7.2.2 Future prospects

The available RF spectrum is limited for wireless data traffic. This has constricted the growth of high-speed data transfer. VLC has dramatically overcome this limitation. VLC network offers a broad range of spectrum, even in the frequencies of terahertz (THz) range. Also, it is benefited due to noninterference with the RF spectrum and nonrequirement of sensitive electronic equipments for its operation. LEDs have successfully demonstrated high-speed data transmission through visible light and established VLC as the future of wireless data transfer. But there are still some limitations faced by LED-based VLC that limits the data transmission rates. In case of white LEDs, the slow yellow signals are often blocked by a blue filter with a target to increase the transmission rate. But this strategy also resulted in a narrow bandwidth of $\sim$20 MHz because of the narrow bandwidth of the LED source and the diminished power from the filter. Hence, it is quite essential to obtain a considerable increase in the modulation bandwidth to achieve high data transmission rates in VLC network.

The Li-Fi technology, which started with LED lighting, has switched over to laser-based lighting due to much better transmission speeds. It is estimated that Li-Fi systems based on laser can demonstrate 10 times faster data transmission than the LED-based Li-Fi system. Lasers have better light output than LEDs, and hence, laser diodes are considered to be the next wave of energy-efficient lighting systems for Li-Fi. In general, the data are embedded on the light emitted by the Li-Fi-compatible LEDs. These data are continuously being exchanged with the user equipment through the light transmitted and received by the LEDs. This process is accompanied with the flickering of LEDs that occurs at a rapid pace such that a naked human eye cannot detect it. However, the flickering can be read by a receiver in computers or mobile devices, and the devices can send back the signals to the transceiver. In this way, a two-way communication is established. In pc-LEDs, the phosphor coating is used for converting the blue light to white, and this coating hampers the overall speed for modulation and transmission of the data from the device. But there is a drastic improvement witnessed in the transmission speeds when the laser diodes replaced the LEDs. Laser can be modulated at 10 times faster than the LEDs owing to the high optical efficiency and energy demonstrated by the former. Unlike LEDs that produce white light with the help of phosphors, laser-based lighting produces white light by blending different wavelengths emitted from several lasers. Lots of data can be optically transmitted through these wavelengths, and each of the wavelengths can be used as a separate channel for data transmission. Against the speed of 10 Gb/s offered by the LED-based Li-Fi, the Li-Fi systems based on laser diodes can easily reach the speeds of 100 Gb/s.

Much significant improvement was achieved in the modulation bandwidth by introducing the GaN laser diode in the VLC system [20]. This was demonstrated by a blue-emitting 450 nm laser diode that produced a VLC system of 1 GHz. Watson et al. demonstrated an error-free transmission of data at the rate of 2.5 Gbps with a sensitivity of 11.5 dBm showing modulation bandwidths of up to 1.4 GHz using a 422 nm laser diode [21]. This is thrice the value of the bandwidth that has been recorded for the VLC based on blue LEDs. The only demerit of VLC based on the blue-emitting laser diode is that there are no high-speed photodetectors available in the blue region of the spectrum. As a result, the bandwidth of the laser-based VLC system suffers to some degree, and there is a limit put on the measurement of the bandwidth above the GHz level. This issue is not experienced while using LED-based VLC system as the silicon photodetectors could easily cover the LED bandwidths. But the LED-based systems are affected by lesser response from the phosphor than the laser-based system, as the latter has larger inherent bandwidth and operates at higher power at high current density. Oubei et al. successfully demonstrated the high-speed underwater wireless optical communication using a modulated 520 nm laser diode [22]. Another laser-based technique to tackle the Internet capacity crunch and maintain faster, instant, and better Internet connectivity with the global network was conceived in the form of optical phase conjugation (OPC) [23]. Almost 99% of the global data traffic is managed through optical communications. To keep the technology ahead of the project growth in demand for the bandwidth, it is essential to tackle the nonlinear distortions of the signals traveling through the optical cables. These distortions form the major reason for the increasing data transmission rates. OPC can be implemented to curb the distortions caused by the nonlinearities in the optical waves and increase the distance traveled by the data in the fiber cables.

7.3 Display technology

Gone are the days of liquid crystal displays (LCDs) that were used to present images and videos with relatively poor clarity and inconsistency in the contrast of pictures at different viewing angles. Although LCD technology easily surpassed the primitive cathode ray tubes (CRTs), they found a tough time to survive when newer LED-based technologies evolved in the display market. In the initial days, LEDs gained recognition in the display market as a supporting performer and not as a full-fledged display product. Their prime role was to provide backlight to the LCD displays, which they performed quite efficiently. Although LED displays are credited to be in existence from the late 1960s, it was through LCDs that LEDs gained more recognition in the display market. Prior to that, LEDs were just limited to the seven-segment displays that were often used in calculators or sign boards. The advancement in the technology witnessed the evolution of LED displays with higher efficiency and wider viewing angles. Such displays offer an array of LEDs that act as pixels that are independently illuminated. On the other hand, LCDs use a matrix of liquid crystal cells that require a backlight to illuminate. These liquid cells are influenced by the electric field to change their color or become opaque while displaying a picture. The liquid molecules of

organic nature are influenced by the electric field during their transition from the transparent state to the opaque state. The backlight source provides the light to the entire LCD screen, and the pixels on the pixel panel block the light coming from the backlight source to produce images on the screen. These pixels do not emit their own light. The liquid crystals rotate the polarized light for electronically switching the pixels on or off on the LCD screen. As a result, it is nearly impossible to obtain a complete black image on an LCD screen, no matter how well the LCD is constructed. Additionally, the colors produced on LCD screens do not offer a natural appearance as compared with those on the LED screens. On the contrary, LED screens can produce a perfect black screen by stopping the emission of light from the pixels (since the LEDs themselves act as pixels on the screen). LED screens also provide a more realistic and vivid color presentation to the images due to their ability to switch each of their pixels on or off independently. Also, the brightness levels offered by LED screens are much higher than the LCD screens. LED displays are much thinner than the LCDs due to the non-requirement of backlights for the former. The power consumption of LED screens is much brilliant than the LCD screens, especially for battery-operated portable devices such as smartphones. LEDs can completely enable/disable each of the pixels independently while displaying an image and thereby modulate the amount of power consumed depending on the color shown on the screen. The maximum power consumed by the LED screen is the moment when it shows a completely white image. On the other hand, LCD screens consume the same amount of power irrespective of the color being displayed on the screen. The numerous benefits offered by LED screens have made them popular among the consumers. The market is rapidly focusing on the newer LED products and is slowly ignoring the LCD technology. The recent innovations have granted newer variants of LED displays with much better resolution and brightness. This has made possible to realize different sizes of displays ranging from extremely large-sized television (TV) to miniature wearable display devices.

7.3.1 Advancement in display devices

Display devices have formed to be an imperative part of human life. On an average, an individual stares on displays for around 6−7 hours daily. This is a proof about the depth of influence imposed by displays on human life. The importance of display devices in human life is closely watched by the manufactures, and this has motivated them to work out on newer technologies at regular intervals and attract consumers towards newer trends in the market. The display market has evolved to meet the requirements of the consumer and has gone through several phases wherein different technologies were implemented to upgrade the quality and efficiency of the display. The CRTs were the earliest known display devices that were invented in the late 19th century. These displays were quite bulky and consisted of the vacuum tube with one or more electron guns and a phosphorescent screen, as shown in Fig. 7.5. The bulky size of CRTs made them impossible to be realized in small-sized display devices, and hence, they were often found in TV sets, monitors, or oscilloscopes. CRT displays were available in monochrome, color, raster scan, and random scan versions. The Braun tube, which was invented in 1897 by the German physicist Ferdinand

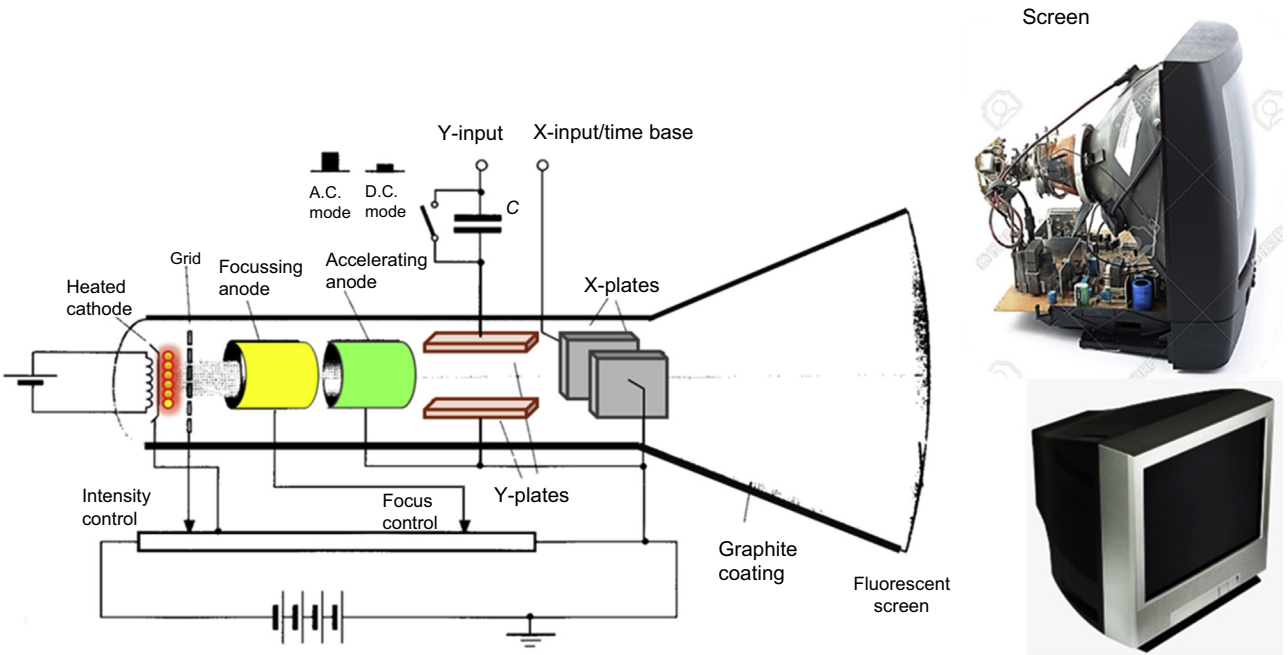

Figure 7.5 Cathode ray tube (CRT) and the television sets based on CRT.

Braun, was the first known version of the CRT [24]. It almost took another three decades to realize the first prototype of a CRT display. John L. Baird, a Scottish engineer, demonstrated the first prototype of the CRT TV in 1925. Kenjiro Takayanagi, a Japanese innovator, succeeded in the transmission of human image through his CRT TV with a 40-line resolution at the rate of 14 frames per second in 1928. By 1931, he further improved the resolution and frame rate to 100 and 20, respectively. In the early 1950s, color TV sets encoded with chrominance and luminance were released. The CRT TV sets continued to improve, and they ruled the display market till the beginning of the 21st century.

In 1964, the first working LCD panel and the first plasma display panel (PDP) were developed. This marked the beginning of the flat panel displays that were much thinner and lighter than the CRT displays. But they were gradually inducted into the mainstream displays, and it took nearly four decades for the LCDs to completely dominate the market. The plasma devices struggled to a larger extent than the LCDs and faced many challenges to get launched into the market. The monochrome PDP, invented by Prof. Donald L. Bitzer, Prof. H. Gene Slottow, and Robert H. Wilson in 1964, used neon gas and was connected to a leaking vacuum system that resulted in the mixing of a small quantity of air with the neon gas. As a result, the orange glow of the neon discharge inherited a hysteresis that would not have been there if the vacuum system worked perfectly. It was later found that the hysteresis worked as an inherent memory and the group purposely started introducing a fraction of nitrogen gas with the neon gas to produce this hysteresis [25]. In 1966, the same group developed a plasma panel with more than one pixel and capable of demonstrating matrix addressability. In the succeeding years, many obstacles came in and delayed the commercialization of PDP TVs. The popularity and cheap price of CRTs also formed the reason for PDPs not gaining the expected recognition. However, in the 1990s, plasma panels were at its best when manufacturers unveiled the 21- and 42-inch plasma TVs with 852×480 resolution. Plasma displays continued to be the first choice for consumers who preferred to buy high-definition television (HDTV). These displays offered a deeper black screen, wider viewing angle, higher brightness, faster response time, better contrast, and larger color spectrum as compared to LCDs. In those days, LCDs were limited to only smaller display devices and small- to midsized TVs. PDPs dominated the large-sized TV industry for almost a decade until the LCDs started entering the market with a cheaper version of the large-sized displays. By 2010, plasma TVs lost its popularity, and most of the major manufacturers stopped the production. Panasonic, which was the largest manufacturer of plasma TVs, ended their production in the late 2013. The decreasing demand compelled LG and Samsung to follow the footsteps of Panasonic and put an end to the plasma TV in the market. Meanwhile, LCDs emerged as the leading technology for display applications. The emergence of cell phones and other portable handheld devices was boosted due to the availability of thin display panels offered by LCDs. Although they were invented in 1964, LCDs took nearly 40 years to gain the commercial recognition and overtake the CRTs in the mainstream TV sets. However, LCDs were able to survive in the display market due to their success in small-screen devices such as calculators.

Austrian botanist and chemist, Friedrich Reinitzer laid the foundation for the LCD technology long back before the first commercial versions of CRT [26]. In 1888, he examined the strange properties of several derivatives of cholesterol extracted from carrots [27]. It was observed that the cholesterol derivative exhibited a mesophase between its solid and liquid phases. The cholesterol derivative was found to be cholesteryl benzoate. It melted at 145 °C to form a viscous and cloudy white substance. The substance turned into a clear and isotropic liquid after reaching the temperature of 179 °C. German physicist, Otto Lehman studied the two melting points of the material and the properties of the mesophase existing between the two points. He discovered the double refraction phenomenon, which is generally shown by crystals, being exhibited by the mesophase. The mesophase demonstrated the characteristics of both liquids and crystals, and hence, he termed the mesophase as "fliessende krystalle" [28]. This German terminology was later on accepted, and the mesophase came to be widely known as "liquid crystals." But the liquid crystals remained unpopular till the middle of the 20th century, and it took almost 80 years from the date of its discovery for these materials to be really considered for some application. Till then, liquid crystals were viewed as a scientific curiosity, and no major progress was achieved in understanding the prerequisites for their development. Although liquid crystals were unknown to a large part of the scientific society, few institutions were known to investigate the properties of liquid crystals in the early 1960s. The electrooptic characteristics of the liquid crystals were discovered by Richard Williams of the Radio Corporation of America (RCA) in 1962. At around the same time, George Heilmeier was pursuing his PhD under the sponsorship of RCA. He got fascinated by the experiments of Williams and starting working on the liquid crystals. He along with his coworkers developed several prototypes such as liquid crystal cockpit displays, electronic clock with a liquid crystal readout, alphanumeric displays, and so on. Finally, RCA declared the invention of LCDs in its press conference at the Rockefeller Plaza, New York, in 1968. George Heilmeier was credited for the invention of the LCDs, which operated at about 80 °C. His LCDs were based on the dynamic scattering method (DSM) wherein the molecules of the liquid crystals rearrange to scatter the light under the influence of an electrical charge. LCDs gained recognition for their lower power consumption, lesser weight, and the thinness as compared with the CRT displays. The attention of the scientific community was drawn towards this invention, and many countries started adapting this technology to build their gadgets at a lower cost. Many Japanese companies started developing pocket calculators using DSM LCDs as they considered them to be the best available flat display technology. Heilmeier's invention paved way to realize the dream of hanging a flat TV on the walls like a picture. It was his vision to witness the evolution of his invention into RCA products. He convinced RCA to start the business of LCDs and then approached several companies and corporate industries to collaborate with RCA in this endeavor. But he faced several harsh comments from the critics who termed his invention as "dirty" with regard to the semiconductor standards. Some of the comments from the critics were that liquid crystals were difficult to be synthesized or they can be duplicated easily or they are just liquids. Such disheartening comments led to the downfall of liquid crystals, and their commercialization for displays delayed further. In addition,

the top members of the RCA management were against the invention as they held a significant share of business in CRTs and regarded LCDs as a threat to their business profit. Nevertheless, many Japanese companies found success with the LCDs in their small devices such as calculators. But the ultimate goal of achieving a flat TV set hanging on the wall was yet to be realized. But the then existing DSM LCDs demonstrated a very slow response time, which was disagreeable for TVs. Fast response and multiplexing were essential for the LCDs to realize a television.

In the late 1960s, Wolfgang Helfrich from the RCA started working on the twisted-nematic (TN) mode of the liquid crystals, wherein two polarizers were required, as shown in Fig. 7.6 [33]. He left the RCA and collaborated with Martin Schadt to make further progress in the TN mechanism of the liquid crystals by reporting about the dielectric torques that realigned the liquid crystal molecules [29]. They filed a patent application on the TN mode of liquid crystals in 1970 in Switzerland. At about the same time, James Fergason of the International Liquid Xtal Company at Kent, Ohio in the USA also filed a patent on the liquid crystals. The invention of TN cells at a simultaneous period in different locations marked the breakthrough moment for LCDs that led to greater efforts in the field of nematic crystals. The first wristwatch based on the TN-LCD was launched in 1972. In the same year, T. Peter Brody and his coworkers introduced the prototypes of active-matrix thin-film transistor (AM TFT) LCD panels [30]. In 1973, George W. Gray of the University of Hull, Great

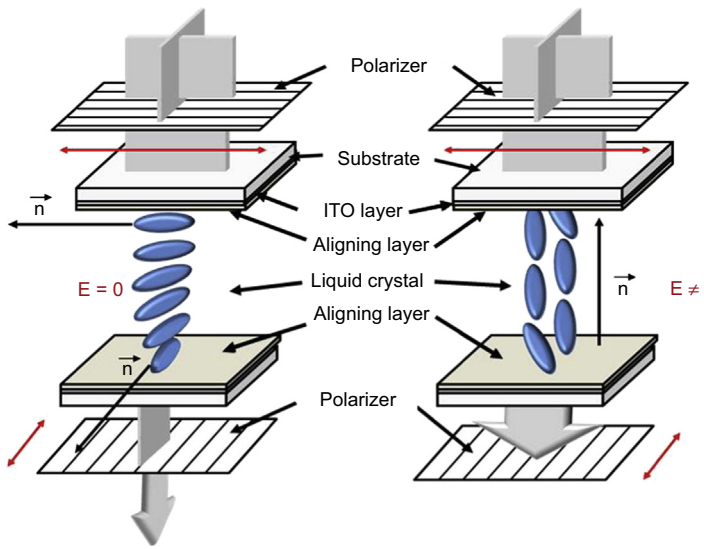

Figure 7.6 The mechanism of TN-mode liquid crystals with two polarizers. *ITO*, indium tin oxide; *TN*, twisted-nematic.
Reprinted with permission from R. Węgłowski, W. Piecek, A. Kozanecka-Szmigiel, J. Konieczkowska, E. Schab-Balcerzak, Poly(esterimide) bearing azobenzene units as photoaligning layer for liquid crystals, Opt. Mater. 49 (2015) 224–229. https://doi.org/10.1016/j.optmat.2015.09.020. Copyright 2015, Elsevier B.V.

Britain, reported about the cyanobiphenyls and cyanoterphenyls that exhibited positive dielectric anisotropy [31]. These organic compounds gave stable nematic liquid crystals at room temperature. The Merck group also started investigating the cyclohexanoates for the liquid crystals meant for pocket calculators. They got the breakthrough, in 1976, with the discovery of phenyl cyclohexane (PCH) that exhibited lower viscosity and thereby, demonstrated a rapid time response and smaller birefringent effects [32]. This facilitated in reducing the switching time of LCD displays from several hundreds of milliseconds to 20 ms. TN cells and, later, AM TFT LCDs widely used PCH owing to their superior properties. The Merck group further improved the time response by introducing cyclohexylcyclohexanes (CCHs) in 1978.

The 1980s witnessed a sudden flourishing in the LCD market with lots of surprise inventions and product launches. Several multinational companies launched their own versions of handheld LCD TVs or pocket TVs in different parts of the world. There were also launching of the color LCD TVs, TFT computer monitors, and full-color LCD projectors. All these products were just in their production stage and required a long way to gain the commercial success. The high price tag attached to these products also played a role in delaying the recognition of these products in the market. In 1983, a research team led by Terry J. Scheffer presented an LCD with an improved image quality and better than the TN display multiplexed at the same high level [26]. The principle of this new electrooptic effect was termed as supertwisted birefringence effect (SBE). The terminology was derived from the fact that the layer twist angle (∼240 or 260 degree) of this new technology was thrice the twist angle of the originally developed TN display. The interference of the two optical normal modes provided the contrast to the SBE display as compared with the TN display that relied on the guiding of single mode [34]. The SBE was later named as the super twisted-nematic (STN) mode. This technology helped in achieving a color display, and the background color was often chosen as blue or yellow to provide better contrast to the pictures. It was essential prerequisite to get a white background for the full color display. This was finally achieved by incorporating two back-to-back STN panels: the first panel would twist the liquid crystals by 240 degree, and the second panel would untwist them by 240 degree. The use of two STN panels in this technology led to its naming as double super twisted-nematic (DSTN) mode. It was also called as neutralized twisted-nematic (NTN) mode by some others. Nevertheless, the use of two STN panels made the displays bulkier, and hence, the second panel was replaced by a birefringent film. This decreased the overall weight of the display and also helped in achieving full color display for portable display devices. The new mode was known as the film super twisted-nematic (FSTN) mode. Since a single-layer birefringent film failed to compensate completely for the coloring in the large-sized LCDs, a new structure was defined with the STN panel sandwiched between two layers of film. This new mode was called triple super twisted-nematic (TSTN) mode. The STN panels were completely replaced by the FSTN and the TSTN panels for the portable devices and large-sized devices, respectively. Yet there were some limitations faced by these modes such as bad color reproduction, low-quality color images, and bad viewing angle. To solve these issues, alternatives to STN panels were conceived. The 1990s witnessed the arrival of new technologies such as in-plane

switching (IPS) and vertical alignment (VA) to address the issues put forward by the STN panels. IPS involves the horizontal alignment of the liquid crystals to the screen. There are two interdigital electrodes or the glass substrates kept parallel to the liquid crystals, and a lateral electric field is applied between them to rearrange and switch the orientation of the liquid crystals. The robustness and the stability of the hard-wired liquid crystal molecules protect them from the external forces. As a result, there are least chances of picture distortion or the non-generation of the picture color while encountering the external forces. Although they are relatively expensive than the STN panels, their superior display properties and wider viewing angles have boosted the commercial demand for IPS panels in the display industry.

With the progress in LED technology, the manufacturers gradually shifted their focus towards the LED displays and started replacing the LCD technology wherever possible. In between, there were some other forms of displays that came to the display market but were unable to gain enough popularity among the consumers. Electroluminescent displays (ELDs) were one such technology that appeared in the early 1970s. ELDs consisted of an electroluminescent (EL) material that was sandwiched between two conductors to form a flat display panel. Most of the ELDs are found to be monochromatic. But, unlike LCDs, they can operate even in rugged temperatures ranging from 200 to 400 K. Also, they offer a higher operating lifetime than the organic LEDs (OLEDs) and lose only 80% of its initial brightness after 100,000 hours of operation. Another noteworthy feature is the clarity and the sharpness of the pictures as well as the wider viewing angles offered by the ELDs. Yet they are rarely found in the household or personal display devices, and most of their applications were found in the instrumentation for the industrial and the transportation sectors. Another sort of display device is the electronic paper (e-paper), which was developed in the 1970s but gained popularity from the beginning of the 21st century. As the name suggests, e-paper was designed to mimic the appearance of an ordinary paper with the texts written using the ink. Similar to OLED displays, e-papers can illuminate their own and do not require any backlight. They are flexible and reusable displays on which texts can be written and erased numerous times without losing the luster of a traditional paper.

LEDs are currently the most popular among the recent technologies available in the display market. LEDs were first implemented in the seven-segment displays, before coming into the limelight for its backlight applications in LCD panels. The seven-segment LED displays were first adopted in the sophisticated laboratory equipment, and later on, they found their way into more common gadgets such as wristwatches, calculators, and so on. Soon LEDs also found way into large billboard displays that used discrete or individually mounted LEDs of RGB colors. The cluster of red-, green-, and blue-emitting LEDs form a full-color pixel. The pixels generally depict a square shape and are arranged in such a way that they are evenly separated from each other on a panel. Apart from the discrete-mounted LED panels, there is another type of LED panel that uses surface-mount devices (SMDs) or the surface-mount technology (SMT), as shown in Fig. 7.7. SMDs were preferred to build most of the indoor screens, whereas discrete-mounted LED panels were popular for the outdoor screens. A pixel on the SMD panel comprises red-, green-, and blue-emitting diodes that are

Figure 7.7 Examples of LED panels based on discrete-mounted LEDs and SMD LEDs. *LED*,light-emitting diode; *SMD*, surface-mount device.

mounted on the chipset. Each of these diodes is smaller than a pinhead, and they are all arranged very close to each other. The chipset is then mounted on a driver printed circuit board (PCB). A new revolution in the LED display industry emerged with the introduction of OLEDs. The first report on organic electroluminescent diodes came in 1987 by Tang and VanSlyke [35]. It was a two-layered OLED that consisted of a bottom emission layer. This was followed by the invention of OLEDs based on conjugated polymers in 1990 [36]. In 1994, white-emitting OLEDs were reported that led to the development of full-color OLED displays that used color filters [37]. The first OLED display was commercially introduced in 1997 by Pioneer. It was a green monochrome passive-matrix (PM) display specially designed for car audio. In 1998, Baldo et al. reported the phosphorescent emission from OLEDs [38]. Unlike fluorescent dyes that could transfer energy only through the singlet states, phosphorescent dyes demonstrated emission from both triplet and singlet states and, thus, much improved efficiency in their light emission was observed. The first prototype of the polymer OLED display was fabricated in 1999 using the inkjet printing by Epson [39]. It was an AM full-color display. AM-OLEDs have several advantages over the PM-OLEDs. The former has higher refresh rates and consumes less power than the latter. Also, the response time of AM-OLEDs is smaller than a millisecond. A prototype of a 13-inch full-color AM-OLED display with a screen resolution of 800 × 600 pixels was unveiled by Sony in 2001 [40]. In the following year, Toshiba fabricated a

prototype of a 17-inch full-color polymer AM-OLED display using inkjet printing. In 2003, Philips and SK Display (Company formed as a result of the joint venture between Eastman Kodak and Sanyo Electric), respectively, launched the world's first commercial versions of polymer OLED display and AM-OLED display [41]. In 2007, Sharp fabricated a prototype of the 3.6-inch full-color polymer OLED display using the inkjet printing [42]. This display achieved a resolution of 202 ppi, which was the highest ever achieved in that time. The first commercial OLED TVs were launched by Sony in 2007. It had a full-color AM-OLED display with a size of 11-inch and 960 × 540 pixels with 600 ppi. In the same year, Samsung introduced a full-color AM-OLED displays to its mobile phones. In 2010, the world's largest OLED TV was revealed that carried PM-OLEDs with a tiling system on a 155-inch display [43]. This achievement got a significant recognition as it ended all the barriers to realize a full-color large-sized display. In 2012, Samsung and LG unveiled their respective prototypes of 55-inch OLED TVs. In the succeeding year, Sony and Panasonic also revealed their respective prototypes of 56-inch OLED TVs. Semiconductor Energy Laboratory (SEL) and Sharp introduced their prototypes of 3.4- and 13-inch flexible OLED display, respectively, in 2012. LG and Samsung materialized on it and launched their own versions of flexible OLED displays in the commercial market in 2013 [44]. SEL developed a high-resolution AM-OLED display in the 8 K format (664 ppi) with a display size of 13.3 inch in 2014 [45]. They also developed an ultrahigh-definition AM-OLED display with the size of 2.8 inch and resolution of 1058 ppi in 2015 [46].

More recently, microLEDs also marked their entry into the display market. In 2019, Samsung demonstrated their 75-, 146-, and 219-inch versions of their microLED TVs and named them as "The Wall." At the same time, quantum dots (QDs) are also making their way into the display industry. Currently, QDs are used as backlights in LCD TVs, and the commercial TVs are named as QLEDs, which may misguide a consumer to think these products to be purely made of QD-LEDs. QDs in these LCD TVs use photoemissive particles. Although electroemissive QD displays have been realized in the laboratory, they are not yet launched into the commercial market. QDs are much cheaper than the OLEDs and hence, they can easily replace the latter in the mainstream display market.

7.3.2 Current and future prospects in display technology

The emerging technologies in the LED industry have made it possible to realize all sorts of display devices ranging from the large-sized screens to ultrasmall wearable devices, as illustrated in Fig. 7.8. Currently, the 16,000 m^2 Suzhou Sky Screen located in the Harmony Times Square at Suzhou, China, is the largest screen on earth. This display is also based on the LED technology. The advent of LEDs into the display industry has removed all sorts of barriers that were earlier faced while constructing miniature or very large display devices. Apart from the device dimensions, LEDs have also made it possible to realize ultrathin displays. LG introduced a superthin prototype of OLED display in 2015. This was a 55-inch flexible and paper-thin TV weighing just 1.9 kg and measuring 0.04 inches thick.

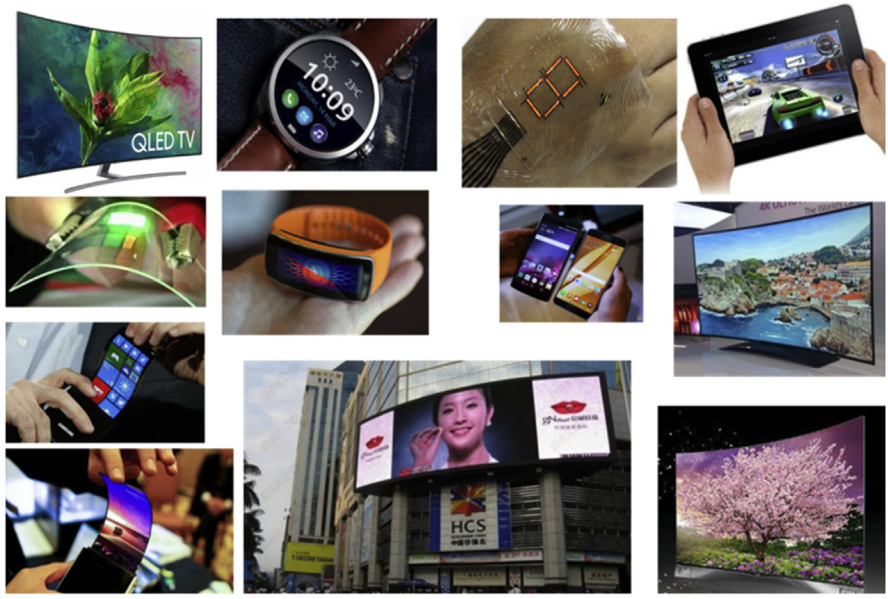

Figure 7.8 Different types of LED displays for TVs, watches, mobile phones, public screens, etc. *LED*, light-emitting diode; *TV*, television.

Among the offshoots of the LED technology, OLEDs are, currently, the most popular in the display market. OLEDs are made of either the organic small molecules or the polymers. Displays made from OLEDs use either the PM-OLEDs or the AM-OLEDs. OLEDs consume very less power. They can shut down their pixels completely to produce a perfect black display. They do not require backlights, and hence, they are thinner than the LCDs. OLEDs have wider viewing angles and very high contrast ratios. OLEDs are fabricated on lighter, yet stronger plastic substrates. The substrates and the organic layers coated on them are flexible, thinner, lighter, and durable. These advantages have granted a significant growth of OLEDs in the global market. But the existing technologies applied for mass production of OLEDs will soon put a halt on their market growth and new, but cheaper production technologies must be adopted to maintain their hold in the market. Flexible substrate process and solution printing technologies can be adopted to boost the OLED display production and reduce the costs of the OLED products. Foldable or bendable TVs can be manufactured using the flexible substrate process. Soluble printing process can improve the efficiency in the use of organic layers, and hence, manufacturers are trying to switch to this method to develop OLED TV panels. Since 2015, the sales of OLED TVs have soared up. LG was the first to enter the OLED business, and they held 100% of the market share in the production of OLED TVs. Soon, the Korean manufacturers such as Samsung and Chinese manufacturers such as Hisense, Skyworth, Haier, and Changhong entered the OLED TV production business and gave a tough competition

to LG. However, the rapid growth in OLED TV sales and the tough competition between the manufacturers did not help in cutting down the prices of OLED TVs. Meanwhile, there was a significant increase in the demand for OLED panels in smartphones. Microsoft launched their first Windows 10 mobile with AM-OLED displays. They also launched their second-generation fitness tracker or the smart band with a curved flexible OLED display. The adoption of OLEDs in the smartphones has been driven rapidly owing to the vibrant color, low power consumption, and flexibility of OLEDs. The cutthroat competition in the LCD market, the declining demand for LCD TVs, and the oversupply of LCD panels compelled the Korean giants Samsung and LG to shift their focus on the OLED technology. Samsung obtained a US patent for the flexible OLED displays meant for foldable TVs, smartphones, and tablet PCs. Although the market for smartphones has saturated to some extent, the demand for OLED panels is still increasing rapidly due to the rapid growth in the sales of wearable devices. The global sales of LCD panels experienced a decline by 2%, and this gap was filled up by the OLED panels. It is anticipated that OLED panels will experience consistent growth with an estimated CAGR of 14.27% from 2018 to 25. Over the forecast period of 2016−23, the global market for OLED TVs is anticipated to register a CAGR of 17.6%.

Inspite of several advantages, there are certain limitations that paved way for other offshoots of LEDs to enter the competition in the display industry. One of the flaws lies in the blue-emitting organic layer that shows faster degradation, thereby causing misbalance in the color and decrease in brightness. Therefore, manufacturers often double the size of the blue subpixel than the red and the green subpixels. Also, the blue organic layer shows shorter operating lifetime than the other layers. The organic layers are easily damaged by water, and they are quite expensive. To overcome these limitations, display manufacturers are trying to revert back to inorganic semiconductor form of LEDs. MicroLEDs were found to be a perfect solution to all the issues put forward by OLEDs. MicroLEDs have just entered the market and are forecasted to gain the market share and progressively inch ahead of OLEDs very soon. Mini-LEDs and microLEDs are well poised to become the latest sensation in the LED display industry. This new wave of technology promises better visual appearance, enhanced display performance, and improved efficiency. Similar to OLEDs, microLED displays do not require backlight and are self-emissive. Samsung and Sony have already rolled out their respective prototypes of microLED TVs. Samsung has further announced about its expansion with the microLED TV range and will be introducing the 437- and 587-inch TVs with 8 K resolution. A comparison between the LCD, OLED, and microLED TVs is illustrated in Table 7.1.

More recently, new TVs were launched based on QDs and were named as QLED. Although this marks the debut for QDs into the mainstream display market, the terminology provided is misleading. QLEDs are LCD panels that are backlit by photoemissive QDs. The display market is yet to witness the prowess of QD-LED, which shall be seen only when the electroemissive QD-LED TVs will be rolled out in the market.

Table 7.1 Comparison between the LCD, OLED, and microLED TVs.

Display technology	LCD	OLED	MicroLED
Type of displaying	Backlight + color filter	Self-emissive	Self-emissive
Contrast	Medium	High	High
Contrast ratio	5000:1	Infinite	Infinite
Power consumption	Medium	Medium	Low
Operating life	Long	Medium	Long
Luminous efficacy	Low	Medium	High
Response time	ms	μs	ns
Operating temperature	−20 to 80°C	−30 to 70°C	−100 to 120°C
Flexibility	Low	High	Medium
Viewing angle	Low	Medium	High

7.4 Conclusions

The future of the digital communications and data transmissions will rely heavily on the visible light spectrum. The LED-based Li-Fi system will be cybersecure and would make things complicated for the hackers to break through the strong security offered by the system. Since the Li-Fi signals are confined within the four walls of a room, it is difficult for anyone to get an unauthorized access to the network unless he or she manages to coerce into the room. Even if the coercive entry happens, the Li-Fi signals must be intercepted from both the ends, and this will be obstructed by several other barriers. LED lights form separate downlink and uplink channels, and at the moment, they are the best available option to utilize the readily available light spectrum for networking. There will be a huge Internet capacity crunch in the near future due to the limited bandwidth in the RF spectrum. The switching over from Wi-Fi to Li-Fi system can circumvent this crunch and provide a platform to connect the network to almost anything lying within the ubiquitous coverage range. The Internet of things will also find the Wi-Fi systems falling short of the spectrum availability and hence, would prefer to have the light spectrum for networking. The day will not be far when all the equipment or devices will be connected to one network through the Li-Fi system and they will be operated using a single remote control.

The display market also visualizes LEDs as the future for the all sizes of display devices. The consumers assign primary importance to the performance, durability, longevity, and adaptability before choosing a product, and all these factors are pretty fulfilled by the display devices based on LEDs. The availability of the spare parts and the expenses incurred in their replacements are a lot cheaper than the LCDs or the CRT displays. LEDs have also made it possible to achieve full color displays for both large-sized and microsized devices. The things that seemed to be unreal once are now reality.

Even the wearable displays such as wristwatches have achieved brighter and ultrathin device structure owing to OLEDs. The flexibility of OLEDs has granted handheld devices like mobile phones to get a foldable display. This feature has also enabled the TVs to obtain a curved structure for better vision, clarity, and panoramic viewing. The newer technologies such as micro-LEDs and QDs will further boost the performance of LED TVs. Since they are in the initial stages of their production, the TVs based on these technologies are priced at the higher end. But soon they are expected to become affordable for the general consumers and will hit the market pretty soon.

References

[1] S. Bent, A. Moloney, G. Farrell, LEDs as both optical sources and detectors in bi-directional plastic optical fibre links, in: IET Irish Signals Syst. Conf. (ISSC 2006), IEE, 2006, pp. 345–349, https://doi.org/10.1049/cp:20060461.

[2] P.J. Winzer, D.T. Neilson, From scaling disparities to integrated parallelism: a decathlon for a decade, J. Lightwave Technol. 35 (2017) 1099–1115, https://doi.org/10.1109/JLT.2017.2662082.

[3] H. Haas, LiFi is a paradigm-shifting 5G technology, Rev. Phys. 3 (2018) 26–31, https://doi.org/10.1016/j.revip.2017.10.001.

[4] H. Haas, C. Chen, D. O'Brien, A guide to wireless networking by light, Prog. Quant. Electron. 55 (2017) 88–111, https://doi.org/10.1016/j.pquantelec.2017.06.003.

[5] J. Jiang, Y. Huo, F. Jin, P. Zhang, Z. Wang, Z. Xu, H. Haas, L. Hanzo, Video streaming in the multiuser indoor visible light downlink, IEEE Access 3 (2015) 2959–2986, https://doi.org/10.1109/ACCESS.2015.2513010.

[6] A. Papaioannou, F.-N. Pavlidou, Evaluation of power line communication equipment in home networks, IEEE Syst. J. 3 (2009) 288–294, https://doi.org/10.1109/JSYST.2009.2023202.

[7] W. Ni, R.P. Liu, I.B. Collings, X. Wang, Indoor cooperative small cells over ethernet, IEEE Commun. Mag. 51 (2013) 100–107, https://doi.org/10.1109/MCOM.2013.6588657.

[8] E. Karaca, B. Durmaz, H. Altug, T. Yildiz, C. Guducu, M. Irgi, M.G.C. Koksal, F. Ozkinay, C. Gunduz, O. Cogulu, The genotoxic effect of radiofrequency waves on mouse brain, J. Neuro Oncol. 106 (2012) 53–58, https://doi.org/10.1007/s11060-011-0644-z.

[9] T. Takebayashi, N. Varsier, Y. Kikuchi, K. Wake, M. Taki, S. Watanabe, S. Akiba, N. Yamaguchi, Mobile phone use, exposure to radiofrequency electromagnetic field, and brain tumour: a case–control study, Br. J. Cancer 98 (2008) 652–659, https://doi.org/10.1038/sj.bjc.6604214.

[10] C.H. Yeh, Y.F. Liu, C.W. Chow, Y. Liu, P.Y. Huang, H.K. Tsang, Investigation of 4-ASK modulation with digital filtering to increase 20 times of direct modulation speed of white-light LED visible light communication system, Opt. Express 20 (2012) 16218, https://doi.org/10.1364/OE.20.016218.

[11] J.J.D. McKendry, D. Massoubre, S. Zhang, B.R. Rae, R.P. Green, E. Gu, R.K. Henderson, A.E. Kelly, M.D. Dawson, Visible-light communications using a CMOS-controlled micro-light- emitting-diode array, J. Lightwave Technol. 30 (2012) 61–67, https://doi.org/10.1109/JLT.2011.2175090.

[12] D. Tsonev, H. Chun, S. Rajbhandari, J.J.D. McKendry, S. Videv, E. Gu, M. Haji, S. Watson, A.E. Kelly, G. Faulkner, M.D. Dawson, H. Haas, D. O'Brien, A 3-Gb/s single-LED OFDM-based wireless VLC link using a gallium nitride μLED, IEEE Photon. Technol. Lett. 26 (2014) 637−640, https://doi.org/10.1109/LPT.2013.2297621.
[13] C.H. Yeh, H.Y. Chen, Y.L. Liu, C.W. Chow, Polarization-multiplexed 2×2 phosphor-LED wireless light communication without using analog equalization and optical blue filter, Opt. Commun. 334 (2015) 8−11, https://doi.org/10.1016/j.optcom.2014.08.003.
[14] A.M. Khalid, G. Cossu, R. Corsini, P. Choudhury, E. Ciaramella, 1-Gb/s transmission over a phosphorescent white LED by using rate-adaptive discrete multitone modulation, IEEE Photonics J 4 (2012) 1465−1473, https://doi.org/10.1109/JPHOT.2012.2210397.
[15] N. Chi, Y. Wang, Y. Wang, Ultra-high-speed single red − green − blue light-emitting diode-based visible light communication system utilizing advanced modulation formats, Chin. Opt. Lett. 12 (2014) 10−13, https://doi.org/10.3788/COL201412.010605.Visible.
[16] C.-Y. Lin, Y.-P. Lin, H.-H. Lu, C.-Y. Chen, T.-W. Jhang, M.-C. Chen, Optical free-space wavelength-division-multiplexing transport system, Opt. Lett. 39 (2014) 315, https://doi.org/10.1364/OL.39.000315.
[17] C.Y. Chen, P.Y. Wu, H.H. Lu, Y.P. Lin, C.H. Chang, H.C. Lin, A bidirectional lightwave transport system based on PON integration with WDM VLC, Opt. Fiber Technol. 19 (2013) 405−409, https://doi.org/10.1016/j.yofte.2013.05.006.
[18] Y. Wang, J. Shi, C. Yang, Y. Wang, N. Chi, Integrated 10 Gb/s multilevel multiband passive optical network and 500 Mb/s indoor visible light communication system based on Nyquist single carrier frequency domain equalization modulation, Opt. Lett. 39 (2014) 2576−2579, https://doi.org/10.1364/OL.39.002576.
[19] Z. Shen, T. Lan, L. Wang, G. Ni, Color demultiplexer using angularly multiplexed volume holograms as a receiver optical end for VLC based on RGB white LED, Opt. Commun. 333 (2014) 139−145, https://doi.org/10.1016/j.optcom.2014.07.075.
[20] C. Lee, C. Zhang, M. Cantore, R.M. Farrell, S.H. Oh, T. Margalith, J.S. Speck, S. Nakamura, J.E. Bowers, S.P. DenBaars, 4 Gbps direct modulation of 450 nm GaN laser for high-speed visible light communication, Opt. Express 23 (2015) 16232, https://doi.org/10.1364/OE.23.016232.
[21] S. Watson, M. Tan, S.P. Najda, P. Perlin, M. Leszczynski, G. Targowski, S. Grzanka, A.E. Kelly, Visible light communications using a directly modulated 422 nm GaN laser diode, Opt. Lett. 38 (2013) 3792, https://doi.org/10.1364/OL.38.003792.
[22] H.M. Oubei, C. Li, K.-H. Park, T.K. Ng, M.-S. Alouini, B.S. Ooi, 23 Gbit/s underwater wireless optical communications using directly modulated 520 nm laser diode, Opt. Express 23 (2015) 20743, https://doi.org/10.1364/OE.23.020743.
[23] G. He, Optical phase conjugation: principles, techniques, and applications, Prog. Quant. Electron. 26 (2002) 131−191, https://doi.org/10.1016/S0079-6727(02)00004-6.
[24] F. Braun, Ueber ein Verfahren zur Demonstration und zum Studium des zeitlichen Verlaufs variabler Ströme, in: Ann. Der Phys. Und Chemie, 3rd series, 1897, pp. 552−559.
[25] L.F. Weber, History of the plasma display panel, IEEE Trans. Plasma Sci. 34 (2006) 268−278, https://doi.org/10.1109/TPS.2006.872440.
[26] H. Kawamoto, The history of liquid-crystal displays, Proc. IEEE 90 (2002) 460−500, https://doi.org/10.1109/JPROC.2002.1002521.
[27] F. Reinitzer, Beiträge zur Kenntniss des Cholesterins, Monatshefte Für Chemie − Chem. Mon. 9 (1888) 421−441, https://doi.org/10.1007/BF01516710.
[28] O. Lehmann, Über fliessende Krystalle, Zeitschrift Für Phys. Chemie. 4U (1889), https://doi.org/10.1515/zpch-1889-0434.

[29] M. Schadt, W. Helfrich, Voltage-dependent optical activity of a twisted nematic liquid crystal, Appl. Phys. Lett. 18 (1971) 127−128, https://doi.org/10.1063/1.1653593.
[30] T.P. Brody, The birth and early childhood of active matrix — a personal memoir, J. Soc. Inf. Disp. 4 (1996) 113, https://doi.org/10.1889/1.1985000.
[31] G.W. Gray, K.J. Harrison, J.A. Nash, New family of nematic liquid crystals for displays, Electron. Lett. 9 (1973) 130, https://doi.org/10.1049/el:19730096.
[32] R. Eidenschink, D. Erdmann, J. Krause, L. Pohl, Substituted phenylcyclohexanes—a new class of liquid-crystalline compounds, Angew. Chem. Int. Ed. Engl. 16 (1977), https://doi.org/10.1002/anie.197701001, 100−100.
[33] R. Węgłowski, W. Piecek, A. Kozanecka-Szmigiel, J. Konieczkowska, E. Schab-Balcerzak, Poly(esterimide) bearing azobenzene units as photoaligning layer for liquid crystals, Opt. Mater. 49 (2015) 224−229, https://doi.org/10.1016/j.optmat.2015.09.020.
[34] T.J. Scheffer, J. Nehring, A new, highly multiplexable liquid crystal display, Appl. Phys. Lett. 45 (1984) 1021−1023, https://doi.org/10.1063/1.95048.
[35] C.W. Tang, S.A. VanSlyke, Organic electroluminescent diodes, Appl. Phys. Lett. 51 (1987) 913−915, https://doi.org/10.1063/1.98799.
[36] J.H. Burroughes, D.D.C. Bradley, A.R. Brown, R.N. Marks, K. Mackay, R.H. Friend, P.L. Burns, A.B. Holmes, Light-emitting diodes based on conjugated polymers, Nature 347 (1990) 539−541, https://doi.org/10.1038/347539a0.
[37] J. Kido, K. Hongawa, K. Okuyama, K. Nagai, White light-emitting organic electroluminescent devices using the poly(N−vinylcarbazole) emitter layer doped with three fluorescent dyes, Appl. Phys. Lett. 64 (1994) 815−817, https://doi.org/10.1063/1.111023.
[38] M.A. Baldo, D.F. O'Brien, Y. You, A. Shoustikov, S. Sibley, M.E. Thompson, S.R. Forrest, Highly efficient phosphorescent emission from organic electroluminescent devices, Nature 395 (1998) 151−154, https://doi.org/10.1038/25954.
[39] T. Shimoda, S. Kanbe, H. Kobayashi, S. Seki, H. Kiguchi, I. Yudasaka, M. Kimura, S. Miyashita, R.H. Friend, J.H. Burroughes, C.R. Towns, 26.3: multicolor pixel patterning of light-emitting polymers by ink-jet printing, SID Symp. Dig. Tech. Pap. 30 (1999) 376, https://doi.org/10.1889/1.1834036.
[40] T. Sasaoka, M. Sekiya, A. Yumoto, J. Yamada, T. Hirano, Y. Iwase, T. Yamada, T. Ishibashi, T. Mori, M. Asano, S. Tamura, T. Urabe, 24.4L: late-news paper: a 13.0-inch AM-OLED display with top emitting structure and adaptive current mode programmed pixel circuit (TAC), SID Symp. Dig. Tech. Pap. 32 (2001) 384, https://doi.org/10.1889/1.1831876.
[41] M. Fleuster, M. Klein, P.v. Roosmalen, A.d. Wit, H. Schwab, 44.2: mass manufacturing of full color passive-matrix and active-matrix PLED displays, SID Symp. Dig. Tech. Pap. 35 (2004) 1276, https://doi.org/10.1889/1.1821342.
[42] T. Gohda, Y. Kobayashi, K. Okano, S. Inoue, K. Okamoto, S. Hashimoto, E. Yamamoto, H. Morita, S. Mitsui, M. Koden, 58.3: a 3.6-in. 202-ppi full-color AMPLED display fabricated by ink-jet method, SID Symp. Dig. Tech. Pap. 37 (2006) 1767, https://doi.org/10.1889/1.2433379.
[43] Z. Hara, K. Maeshima, N. Terazaki, S. Kiridoshi, T. Kurata, T. Okumura, Y. Suehiro, T. Yuki, 25.3: the high performance scalable display with passive OLEDs, SID Symp. Dig. Tech. Pap. 41 (2010) 357, https://doi.org/10.1889/1.3500456.
[44] S. Hong, C. Jeon, S. Song, J. Kim, J. Lee, D. Kim, S. Jeong, H. Nam, J. Lee, W. Yang, S. Park, Y. Tak, J. Ryu, C. Kim, B. Ahn, S. Yeo, 25.4: invited paper : development of commercial flexible AMOLEDs, SID Symp. Dig. Tech. Pap. 45 (2014) 334−337, https://doi.org/10.1002/j.2168-0159.2014.tb00090.x.

[45] S. Kawashima, S. Inoue, M. Shiokawa, A. Suzuki, S. Eguchi, Y. Hirakata, J. Koyama, S. Yamazaki, T. Sato, T. Shigenobu, Y. Ohta, S. Mitsui, N. Ueda, T. Matsuo, 44.1: distinguished paper : 13.3-in. 8K x 4K 664-ppi OLED display using CAAC-OS FETs, SID Symp. Dig. Tech. Pap. 45 (2014) 627−630, https://doi.org/10.1002/j.2168-0159.2014.tb00164.x.

[46] K. Yokoyama, S. Hirasa, N. Miyairi, Y. Jimbo, K. Toyotaka, M. Kaneyasu, H. Miyake, Y. Hirakata, S. Yamazaki, M. Nakada, T. Sato, N. Goto, 70.4: a 2.78-in 1058-ppi ultra-high-resolution OLED display using CAAC-OS FETs, SID Symp. Dig. Tech. Pap. 46 (2015) 1039−1042, https://doi.org/10.1002/sdtp.10376.

Biomedical applications

8

8.1 Introduction

LEDs are the latest sensation in the field of medical treatment, light-assisted skin rejuvenation, and photodynamic therapy. LEDs have paved way for several new prospects in the medical field, especially in the improved and better treatment of joint or tissue inflammation, skin abnormality, arthritis, rhinitis, seasonal affective disorders (SAD), stress relief, and biological clock disorders. Optimization of the effectiveness is the major requirement in the medical treatment, and this is easily matched by the capability of LEDs in providing a true spectral composition that matches the wavelengths desired for the treatment [1]. The newest designs and applications of LEDs have been inspired by the pursuit of scientific innovation that has been encouraged by the latest demands of consumers in the lighting industry working in the medical field.

LEDs were successful in expanding its wings in diverse fields and not just limiting itself in the general lighting applications. The benefits of light therapy in enhancing the facial beauty came as a surprise package that received a massive response from all over the world. This ensured that the skin-related issues such as acne, wrinkles, and aging were tackled without any medications and the impending side effects. The light therapy was extended to cure a number of skin diseases and LEDs soon took over the charge from the conventionally used UV-emitting arc lamps. LED light therapy enjoys the advantage over other skin treatments such as laser therapy, dermabrasion, and chemical peeling in the sense that it does not lead to side effects and is a painless, noninflammatory treatment to a number of skin disorders and diseases. Although it is mostly claimed to be free from any side effects, certain rare occasions may result in some redness, rashes, or mild facial erythema in the skin following LED light therapy [2,3]. However, these effects are very rare and considering the huge benefits and profit derived from the LED light therapy, the minor side effects (highly negligible chance to occur) can be conveniently ignored.

The applications of LED therapy are not just limited to skin diseases. It has a full-fledged application in many mental, dental, and other physical disorders in human beings. This chapter is especially dedicated to get a clear view of the advantages of LEDs in light therapy for curing several disorders and diseases in the human body. There is an extended review, in the latter part of this article, describing the applications of LEDs in food processing units that enable the food products to enjoy a longer shelf-life and protection from fungal or bacterial growth on them.

The Fundamentals and Applications of Light-Emitting Diodes. https://doi.org/10.1016/B978-0-12-819605-2.00008-2

8.2 Skin rejuvenation

Gradual aging of skin is often accompanied by the breakdown of collagen in the skin. This leads to the appearance of fine lines and deeper grooves on the skin surface [4]. Several factors such as sleeping positions, constant pulling of gravity on the body, repetitive facial movements, smoking, and hormones can accelerate the aging process. Patients with diverse skin disorders and conditions can approach cosmetic surgery to repair their skin. Most of the procedures adopted in cosmetic surgery can be really painful. Light therapy is a painless solution to numerous skin problems. Wrinkles and aging issues can be solved by generating a dermal matrix using ablative or nonablative resurfacing. Laser ablative resurfacing is often followed by expensive nonablative laser treatments to avoid the redness, bruises, and pain on the skin. However, accomplishing all the complex requirements for effective skin rejuvenation just by a single modality is not feasible [5]. Combining different modalities at sublative thresholds through combination phototherapy, prevention of anti-aging of the skin can be materialized by irradiation of skin by specific wavelengths with a low level of photon energy. This fact is based on the photobiological findings that claim the stimulation of dermal and epidermal cells by the light of certain wavelengths with low photon energies. LEDs can enhance the action potentials of the skin cells and lead to an increase in the local blood and lymphatic flow in a noninvasive manner. LED-based systems can be less expensive but clinically useful light sources against photoaging [4]. LEDs provide effective and safe treatment with a nonpainful experience that results in high satisfaction among the patients [6]. Skin rejuvenation is performed either by exposing the facial skin under a bunch of LEDs emitting specific wavelengths or by wearing a mask fitted with the LEDs of desired wavelengths, as shown in Fig. 8.1.

LEDs initiate photobiomodulation in the damaged tissues of the skin by providing certain specific wavelengths to be absorbed by the skin to modulate the cell functions and repairing of the tissues [7]. Photobiomodulation is a medical treatment that involves the exposure of the affected part of the body to LEDs or low-level laser light to bring about beneficial clinical effects by stimulating the cellular function of that part of the body. Photobiomodulation is also known as low-level light therapy (LLLT). Skin can absorb infrared light and initiate regeneration of cells using infrared light as the energy source. It is scientifically proven that LED light therapy can produce wondrous results on human skin [8–10]. LED light therapy is a noninflammatory, painless, relaxing, and cool treatment to the skin. This type of therapy can repair numerous skin problems. LEDs can repair the wrinkles, remove acne, rosacea, and calm eczema and also heal the scars from the skin through a painless light therapy. It can also offer rejuvenation and energization of the skin by relieving stress from them. It can clean the blemishes, tighten the skin, remove dark spots, soften the redness of the skin, and shrink the pores on them. The dermal cells exposed to LEDs show twice the growth than those that are not exposed. Some case studies showing significant improvement in the skin wrinkles, acnes, and other skin-related issues, as a result of LED-assisted skin rejuvenation, are shown in Fig. 8.2.

Figure 8.1 LED masks for skin rejuvenation.

Skin layers are more inclined to absorb the red light owing to their high blood and water content. Red light (630−700 nm) from LEDs can penetrate the tissues of about 10 mm and contribute to the treatment of wounds, scars, infections, and cuts. It also heals the production of intracellular Adenosine triphosphate (ATP) and collagen by stimulating the fibroblasts. An example of skin rejuvenation using red light exposure from LEDs can be seen in Fig. 8.3. Infrared light (800−1000 nm) can go deep down up to 40 mm and provide relief from the ailments of muscle tissues, joints, bones, etc. Orange light can help in lightening up the skin tone, while green light can heal rosacea due to its antiinflammatory property. Blue LEDs can cure acne, while violet LEDs can heal blackheads due to their antibacterial characteristics. Acne-causing bacteria reside deep within the skin, and they can be easily perished using blue LEDs [11]. Acne is one of the biggest skin problems faced by common people, and dermatologists are visited mostly by patients encountered with acne problems [12,13]. Conventional ways of treating acne included systemic and topical antibiotics, chemical peelings,

Figure 8.2 Improvement in the skin health and cure of various skin-related issues after LED treatment.

and retinoids, which witnessed different success rates in the treatment [14−16]. The bacteria primarily responsible for commencing acne in human skin is *Propionibacterium acnes* (*P. acnes*) that prefers anaerobic conditions for growth. It releases cytokines after acting on the triglycerides and triggers the inflammatory reaction in the skin.

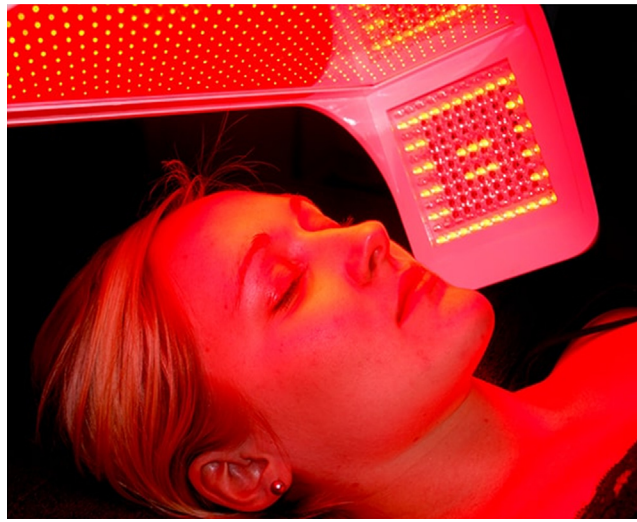

Figure 8.3 Skin rejuvenation under red LED lights.

Recently, all the conventional treatments are found to be resistant against *P. acnes*, and hence these treatments to acne is currently not that effective as it used to be earlier. This has motivated dermatologists to seek the benefits of LED treatment for destroying the *P. acnes* bacteria from the skin and reduce the acne problem significantly. The success rate for the treatment of acne using blue LEDs has been amazingly higher than all other conventional methods [17,18]. *P. acnes* produces bacterial porphyrins as part of its routine metabolism. These are deposited in the skin and when exposed to blue light, the bacterial porphyrins lead to a photodynamic reaction that stimulates the production of singlet oxygen species and reactive free radicals [19–21]. These species ultimately cause the destruction of bacteria from the skin.

LEDs do not emit harmful UV rays along with the visible light, and this proves to be a major safety to the people undergoing light therapy for long durations. This noninvasive procedure does not produce any damage to the skin. Different from laser light therapy, there is no skin burn or pain associated with LED therapy. People with sensitive skin or with darker complexion are recommended to approach LED light therapy to derive more fruitful results as compared to any other therapy. The risks and side effects of LED light therapy are minimal. However, there are chances of some side effects if the LED therapy is conducted with some medication that makes the skin more sensitive. Taking oral medications or applying cream on the skin that makes it sensitive to light can often lead to conditions such as hives, rashes, pain, tenderness, inflammation, and redness on the skin following LED light therapy. Accutane is a powerful drug for treating acne and is derived from vitamin A. Using Accutane can increase the skin's sensitivity to light and cause scars on the skin after a mild dose of LED therapy. Post treatment with LED light, no recovery time is needed and the person subjected to the therapy can continue with his/her daily routine almost immediately. Generally, 10 or more sessions of therapy each spaced at an interval of a week are required for better

results. Still, minor results come to visibility even after first session of therapy. After completing certain number of therapy sessions, the results become more noticeable and fascinating. Despite multiple therapy sessions, the results are not permanent on the skin and once the cells turn over, the collagen gets reduced and the skin starts showing the signs of aging or acne breakouts. This can be averted only if the person sticks to maintenance treatments in the gap of every few months.

8.3 Photodynamic therapy

The light-assisted treatment of skin disorders are basically classified into three types based on the method involved during the treatment. They are phototherapy, photodynamic therapy (PDT), and photochemotherapy involving psolaren and ultraviolet A (PUVA). Phototherapy usually employs the ultraviolet light A (UVA) or ultraviolet light B (UVB) or a combination of both for the therapeutic applications. Phototherapy does not require any photosensitizers and the UV radiations can be directly exposed on to the affected skin. On the other hand, PUVA requires the UVA in association with a photosensitizing chemical drug named psoralen, which is orally administered into the body, to improve the skin's sensitivity towards the UVA light and effectiveness of the treatment on the skin. PDT also works on the similar grounds, but PUVA is generally considered to be a different class from PDT. PDT mostly involves radiations in the visible range (generally blue or red light) along with the nontoxic chemicals that are sensitive to light. These light-sensitive chemicals are nontoxic to healthy parts of the skin and tissues but toxic to the microbial and malignant cells. Porphyrins were the first photosensitizers that were approved by the US Food and Drug Administration for PDT in 1975 [22]. However, the applications of these chemicals were limited due to their inability to get excited by a wavelength outside the visible range and hence, were able to treat only superficial tumors. This led to the development of new modified versions of porphyrins, among which 5-aminolevulinic acid and methyl ester aminolevulinate became more popular for PDT applications. Temoporfin and indole-3-acetic acid are also considered as potential photosensitizers for PDT. Each of the colors in the visible light spectrum is known to produce certain therapeutic applications and they are tabulated in Table 8.1. The longer the wavelength, the more deeper will be the penetration of light into the skin, as shown in Fig. 8.4 [23].

LED-based PDT was evaluated by conducting a split-face study on actinic keratosis, or solar keratosis patients that proved to be safe and effective [24]. Photodynamic therapy is a form of phototherapy using nontoxic light-sensitive compounds that are exposed selectively to light, whereupon they become toxic to targeted malignant and other diseased cells. The wavelength in phototherapy is more important than the coherence. In 1982, McDonald conducted a study on the rheumatoid arthritis patients and concluded that exposure to blue light provides pain relief depending on the exposure time [25]. Greater relief could be experienced with longer exposure to blue light. A therapeutic light source device consisting of a set of 350−1000 nm LEDs and fiber optic connections was patented by Hart and Malak for the treatment of arthritis or joint inflammation and reducing both internal and external edema to joints, muscles,

Table 8.1 The therapeutic applications of different color LEDs.

LED color	Wavelength range	Applications
Violet	400−459 nm	• Treatment to psoriasis • Antibacterial • Acne • Vitiligo • Dermatitis
Blue	460−499 nm	• Treatment to psoriasis • Antibacterial • Treatment to acne breakouts • Treatment to Seasonal Affective Disorders (SAD) • Soothes sebaceous glands • Relief from pain due to rheumatoid arthritis • Reduces Parkinsonian neural circuitry • Treatment of newborn jaundice • Eradication of dental decay
Green	500−564 nm	• Treatment to Rosacea • Treatment to skin inflammation • Fading age spots and pigmentation • Treatment to broken red capillaries • Lessens erythema following treatments and procedures • Reduces Parkinsonian neural circuitry
Yellow and orange	565−609 nm	• Reduces photoaging, pigmentation, and age spots • Lightning the skin tone • Reduces wrinkles and fine lines on the skin • Deeper level attack on acne and prevention of future acne breakouts • Tightening of skin
Red	610−700 nm	• Stimulation and production of collagen • Skin rejuvenation • Relieves inflammation of sebaceous glands • Relieves age spots and wrinkles • Enhanced circulation and cell repair • Treatment to ulcers • Treatment to Allergic rhinitis • Healing of wounds • Treatment of Osteoporosis

nerves, and skin tissues. Allergic rhinitis can be effectively treated by narrow-band red light illumination of the nasal mucosa at 660 nm [26]. However, there is a failure observed in the treatment when the situation is complicated by chronic sinusitis or polyps and no significant improvement can be predicted in this condition. Based on

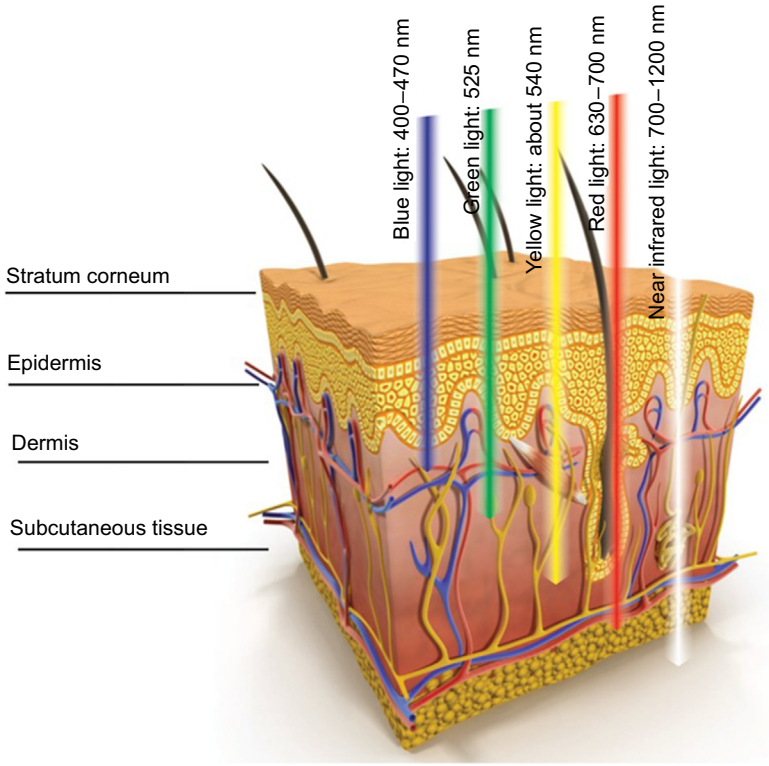

Figure 8.4 Penetration of different wavelengths into the human skin.
Reprinted under the Creative Commons Attribution 4.0 International License from E. Sorbellini, M. Rucco, F. Rinaldi, Photodynamic and photobiological effects of light-emitting diode (LED) therapy in dermatological disease: an update, Lasers Med. Sci. 33 (2018) 1431−1439. https://doi.org/10.1007/s10103-018-2584-8. Copyright © 2018, Elisabetta Sorbellini, Mariangela Rucco, Fabio Rinaldi.

a randomized placebo-controlled double-blind study, a hypothesis was made that LED phototherapy with combined 660 nm and 890 nm light will promote the healing of chronic venous ulcers, particularly large recalcitrant ulcers that do not respond to conventional treatment [27]. An investigative study suggested that irradiation by a 635 nm red LED appears to be useful as an anti-inflammatory tool [28]. Mucositis is a dose-limiting complication of cancer treatment that disturbs the treatment plan and leads to serious or life-threatening consequences. Lang-Bicudo et al. have evaluated the effectiveness of oral mucositis prevention in a cancer patient via phototherapy using LEDs and declared that LED therapy is a safe and effective method for the prevention of oral mucositis [29]. Recently, Chen et al. reported a more effective management of oral leukoplakia by a topical 5-aminolevulinic acid-mediated photodynamic therapy [30]. Fig. 8.5 shows the clinical effects of PDT on oral leukoplakia. Newborn jaundice, a case of yellowing of the skin and other tissues of a newborn infant, could be treated and its symptoms may be reduced by considerable exposure to sunlight or

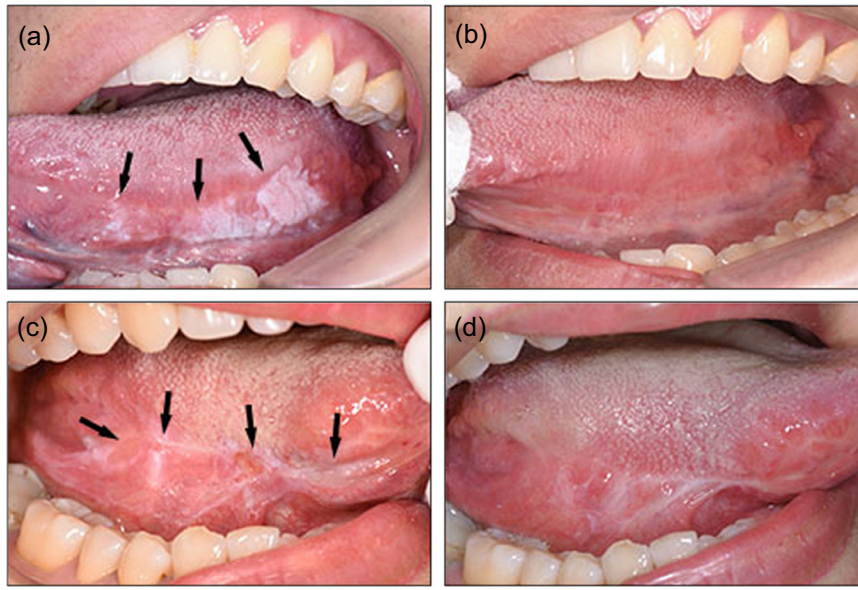

Figure 8.5 Clinical effects of photodynamic therapy (PDT) on oral leukoplakia (OLK). A patient with a primary OLK lesion (a) and the appearance of the site 1 month after PDT (b). No recurrence at the 6-month follow-up; the site of recurrent OLK after scalpel excision (c) and its appearance 1 month after PDT, with some scarring from the surgery before PDT (d). No recurrence at the 8-month follow-up. The lesions are indicated by *black arrowheads*. Reprinted under the Creative Commons Attribution 4.0 International License from Q. Chen, H. Dan, F. Tang, J. Wang, X. Li, J. Cheng, H. Zhao, X. Zeng, Photodynamic therapy guidelines for the management of oral leucoplakia, Int. J. Oral Sci. 11 (2019) 14. https://doi.org/10.1038/s41368-019-0047-0. Copyright © 2019, Springer Nature.

blue light [31]. The affected child is kept under the blue-emitting LED fixture, as shown in Fig. 8.6.

A phototherapy garment containing the surface-mounted LEDs arranged in a densely packed array facing the liner and capable of emitting uniform, high-intensity light was developed for the treatment of newborn jaundice. The garment can be wrapped around the newborn baby to provide uniform, high-intensity blue light exposure to a large portion of the skin. The advancement in the technology has led to the application of compact-sized LEDs in the treatment of newborn jaundice and thereby, assisted in reducing the size of the phototherapy equipment from a large-sized incubator to a compact wearable garment. LED-assisted PDT is also effective for the treatment of rosacea. It is an inflammatory skin condition that causes visible blood vessels and redness on the skin. It is characterized by the conditions such as inflammatory papules, inflammatory pustules, vascular inflammation, dryness in skin, watery eyes, skin inflammation, telangiectasia, facial erythema, or redness in eyes [32]. Several oral medications and topical therapies are on offer to reduce the complications arising from rosacea. However, none of them provide a complete and clear

Figure 8.6 LED phototherapy for the treatment of neonatal jaundice in newborn babies.

solution, and the patients are often not able to tolerate such harsh treatment methods. However, LED light therapies proved much more effective in reducing and controlling this disease [33]. Similarly, eczema or atopic dermatitis has also found proper treatment using LEDs. It is a chronic condition causing inflammation on the skin and affecting about 2% of the adult population and 20% of children globally [34]. There are limited reports on the beneficial treatment of LED therapy on the severe conditions of eczema. Still, its anti-inflammatory effect on the eczema-affected skin is widely accepted.

8.4 Cure for mental disorders

Before the artificial lighting came into picture, the sun was the lone source of light during the day and moon during the night. However, the intensity of moonlight is such low that it did not interfere with the circadian rhythm of human beings. Hence, the rhythm was well in sync only with the sunlight. Circadian rhythm is a cellular process that is responsible for synchronizing the biological and behavioral processes in living beings. This process is mostly influenced by the reception of light from the surrounding environment, with the strongest influence being produced by the blue light. Other than rods and cones, light is perceived by human eye through a third type of

photoreceptor known as intrinsically photoreceptive retinal ganglion (ipRGC) cells. A light-sensitive protein known as melanopsin is present in ipRGCs that make them highly photosensitive and capable of performing nonimage-forming functions and gives a steady representation of the ambient light intensity. It also plays a significant role in performing a cellular process known as circadian phototransduction, wherein the light signals are transformed into electrical signals. Blue light is the most influential component of visible light on ipRGCs. Blue light from the natural sunlight has the peak intensity during midday and its intensity starts declining as evening approaches. The daily cycle of sunrise and sunset is so planned that exposure to blue light is maximum during the day and minimum during the night. At night, the human body produces a hormone known as melatonin that plays a major role in regulating the circadian sleep phase and provides a peaceful night's sleep to the human body. Too much exposure to blue light at night can inhibit the production of melatonin and create sleep disorders in human beings. These, in turn, will suppress several biological processes in the human body and give an invitation to lots of metabolism disorders and mood swings. Suprachiasmatic nucleus (SCN), which is present in the hypothalamus of the brain, is responsible for temperature control and melatonin regulation in the human body. SCN shows a cyclic fluctuation, but to maintain a consistent 24-hour cycle it must be provided by an external stimulus. The alternate light and dark periods during the day and night, respectively, prove to be the crucial external stimulus that maintains this cycle. During day, the human body is exposed to very high levels of light and at night, the body is exposed to darkness. This helps SCN to sync with the 24-hour cycle and assures that the body responds to the physiological rhythm throughout the cycle. In other words, the body is kept alert and awake during the day and it is commanded to rest and sleep during the night. Delayed sleep phase syndrome (DSPS), also known as delayed sleep phase disorder, is a type of circadian rhythm disorder or a neurological sleep disorder in which a person's sleep/wake cycle is delayed with respect to the external day/night cycle. Affected people often report that while they do not get to sleep until the early morning, they do fall asleep around the same time every day. There is an intractable delay in the phase of the major sleep period in relation to the desired clock time, as evidenced by a chronic or recurrent complaint of inability to fall asleep at a desired conventional clock time together with the inability to awaken at a desired and socially acceptable time [4].

SAD is another disorder associated with mood and sleep. It is also known as winter blues, winter depression, summer blues, summer depression, or seasonal depression. People suffering from this mood disorder remained normal throughout the year but suffered from depression or symptoms of excessive depression during winter or summer. One of the symptoms of this disorder can be observed in the form of depression during the seasons when the length of the daylight time is reduced. Patients suffering from SAD generally show normal mental health, but they tend to show some irregularities in their physical and mental health at times. They can experience irritability, social withdrawal, anxiety, fatigue, and a lack of alertness in the seasons with less sunlight. One of the theoretical assumptions holds inhibition in melatonin production as the cause of SAD. Melatonin secretion is controlled by the endogenous circadian clock, but can also be suppressed by bright light [35]. A group of researchers tracked

sleep, activity levels, melatonin rhythms and depression symptoms of 68 SAD patients who took either low doses of melatonin or a placebo in the morning or afternoon for a winter month. From the results of the experiment, the researchers proposed that most patients will respond best to a low dose of the light-sensitive hormone melatonin in the afternoon in addition to 30 minutes of bright light in the morning. Without determining an optimal wavelength combination for SAD treatment, they suggested that clinical benefit of light treatment is greater than melatonin treatment [36]. A light therapy study on 68 SAD patients using 468 nm blue LEDs demonstrated the positive influence of short-wavelength blue light for melatonin suppression and circadian phase shifting [37]. Light therapy has also been suggested in the treatment of nonseasonal depression and other psychiatric disturbances, including major depressive disorder, bipolar disorder, and postpartum depression [38,39].

The selection of luminaires for indoor lighting is essentially based on the type of requirement associated with the room. The blue light is known to produce alertness in humans by suppressing the melatonin secretion in them. Luminaires with a higher amount of blue wavelengths can be effective in study rooms and offices. However, this same light can be disturbing when used in bedrooms. Selectively reducing the short-wavelength (blue) components of the bedroom light can decrease the level of alertness caused in humans. This will help to provide effective sleep and give a refreshing health after the long night's sleep. A specially designed C-LED luminaires have multiple benefits that help to subdue the alertness in the brain by suppressing the melatonin secretion [40].

8.5 Cure for other disorders

LEDs have proven its worth in curing a number of diseases and disorders in the human body. It has been quite effective in regulating the intracellular signaling pathways and regulation network of genes in the cell, which is collectively referred as optogenetics [41,42]. Optogenetics is a very powerful tool in the treatment of neurological diseases using light therapy. Parkinson's disease, which is a degenerative, progressive disorder affecting the brain cells and nerves, can be arrested to a certain extent and the Parkinsonian neural circuitry can be destroyed using the LEDs emitting at 473 nm and 561 nm [43]. Neuronal health can be arrested with an effective and safe therapy using red to infrared light therapy, in the wavelength range 600−1070 nm [44]. Treatment to a chronic case of traumatic brain injury (TBI) proved effective using LED therapy by combining the 633 nm and 870 nm [45]. The treatment involving these LEDs initiated photobiomodulation that resulted in the neurogenesis and anti-inflammatory effects leading to improvement in the verbal memory and executive functioning of the brain cells of the patients suffering from TBI. The presence of high amount of reactive oxygen species and deficient amount of ATP are some factors leading to several neurological disorders. The excessive amount of reactive oxygen species cannot be balanced by antioxidants, and they result in oxidative stress that can lead to Alzheimer's disease and major depressive disorder. The photobiomodulation effects produced by LEDs can

improve the metabolic activities in the brain by decreasing the proinflammatory cytokines and oxidative stress, and by promoting the ATP production and neurogenesis [46,47]. Blue LED emitting at 473 nm can attenuate the pathological conditions associated with Alzheimer's disease by reducing the amyloid-β levels [48].

LEDs find applications in the treatment of bone issues like osteoporosis. Osteoporosis is a disorder in the human body that comes up with a gradual loss in the bone mass. Women are at a higher risk of developing osteoporosis than men. It is caused by the imbalance in the skeletal turnover lead by the prolonged and excessive resorption of bones. The major pathophysiological activity responsible for this bone resorption is the activation of osteoclasts. The treatment of this disorder can be initiated by both chemically or physically. Chemical methods involve the medication to reduce the resorption of bones and to stimulate an increase in the bone mass [49]. Physical methods involve treatment with laser light or by ultrasound [50,51]. The LED treatment has been found effective in treating this disorder. The exposure to 635 nm red LED has significantly reduced the osteoclastogenesis by decreasing the generation of reactive oxygen species in the cells [47].

The presence of cariogenic bacteria in the mouth due to foul local conditions in the oral environment and low host immunity causes tooth decay. Dental caries progress with the bacterial growth and it also leads to the formation of cavities and dental plaque. If not treated in time, these bacteria can cause severe damage to the dental system. There are several oral medications suggested to reduce the microbial growth in the mouth [52]. However, the use of such chemicals often leaves numerous side effects such as burning sensation in the mouth, alteration in taste, and staining of teeth [53,54]. An alternate and nonharmful treatment for dental issues is the photodynamic therapy that makes use of the LEDs. LEDs are also used to fabricate the light-curing unit (LCU) that tends to polymerize dental composites. Although the irradiance of LED LCUs is relatively lower than their halogen counterparts, their efficiency is approximately the same as that of the halogen LCUs of twice the irradiance. The light outputs of halogen LCUs decrease with time, which may result in a low degree of monomer conversion of the composites. Studies have shown that blue light LED LCUs tend to polymerize dental composites without the previously mentioned drawback of decreasing light. This is mainly possible due to the use of photosensitizing agents or dyes that suppress the microbial growth. Red dyes such as Bengal rose, curcumin, and erythrosine can get activated by absorbing the blue light in the presence of oxygen and eradicate the dental decay, thus letting the use of blue LEDs in dentistry [55−58].

Healing of wounds can also be accelerated using the near-infrared (NIR) LEDs. On treating the wound with NIR and visible LEDs, the growth of fibroblast cells can be accelerated. The healing process takes place in three phases, namely (1) inflammatory phase, (2) proliferative phase, and (3) remodeling phase. The latter two phases are greatly influenced by the fibroblast cell growth [59]. Healing of wounds is a complex process involving the cells, their cytokines, mediators, and extracellular matrix. Exposure to light can accelerate the activation and proliferation of lymphocytes and increase the motility of epithelial cells to quicken the closure of wounds [47,59]. Some clinical studies report that during the healing of wound, irradiation of certain wavelengths has

antiinflammatory effects that are caused by inhibiting cyclo-oxygenase prostaglandin E_2 that protects the cells against the cell injury in specific pathophysiological situations such as inflammation and oxidative stress. Healing of wounds can be accelerated by exposing them to light in the wavelength range 630−1000 nm covering the red to NIR region of the spectrum. The effect of LEDs on the proliferation of blood vessels were conducted on rats induced with wounds by Corazza et al. [60]. The results were interesting and the LED exposure resulted in excellent blood vessel proliferation effects. Postoperative incisions and cuts can also be healed rapidly using a 670 nm LED. A study conducted by Erdle et al. about the effect of 670 nm emitting red LED on the healing of burn injuries and wounds on hairless mice showed that the mice rapidly recovered from their wounds due to the incisions after red light therapy, but the light therapy seemed not so effective on burn injuries [61]. A comparative study between the wound healing effects of laser and LED lights were made by Agnol et al. [62]. The study was conducted on 36 rats that were induced with surgical dorsum lesions. The rats were irradiated either by a 660 nm laser light with a full width at half maximum (FWHM) of 30 nm or by a 640 nm LED with an FWHM of 40 nm. All the rats induced with lesions showed similar treatment effects after the 168 hours of exposure to light. On the other hand, diabetic rats expressed better healing properties after 72 hour exposure of LED light as compared to that observed for a similar duration of exposure of laser light. Thus, LEDs emerge as an economical, effective, and great alternative to lasers for LLLT. NASA developed an NIR LED to access the effect of NIR on plant growth. Whelan et al. used these LEDs to study the effect of NIR on the wound-healing effects of a diabetic mouse [63]. Some of the tissue-regenerating genes in the diabetic mouse were found to be regulated positively after the LED irradiation. This group also made an in-vivo and in-vitro analysis on the effects of LED parameters such as intensity and wavelength to optimize the biostimulation for wound healing [64]. Another study discovered that LED light therapy improved energy metabolism and production by stimulating the photoacceptor cytochrome oxidase and also accelerated the recovery of wound-healing in ischemic and diabetic rat models [65]. NIR LED light therapy can stimulate the mitochondrial oxidative mechanism and accelerate the repair of cells and tissues [65].

8.6 Food safety

The food and beverages industry has slowly adopted LED light fixtures to provide safe and hygienic lighting while handling the food products. This industry is a specialized sector that lays down stringent requirements for the lighting fixtures. Proper visibility is the major requirement while making a choice on the luminaires. While handling the machinery, it is of utmost significance for the employees to get a clear view of their operation to avoid injuries or accidents. The risks of dropping tools, nuts, and bolts in the food products or their raw materials can also be averted if proper lighting is provided in the food-processing units. Employees can avoid injuries to themselves from slips or accidents if they have proper visibility in the area. A single incident can prove

fatal and demand a mass recall of all the food products processed in that unit, thus making a hefty loss. To obviate these issues, LED luminaires have started replacing the traditional lamps in almost every food industry. Another important characteristic of the luminaire should be its color rendering index (CRI), and LEDs are known to provide the best CRI than other traditionally used lamps [4]. A luminaire with high CRI can enable the employees to detect any kind of discoloration of food products, fungal growth, or other defects quite easily.

The lighting conditions and requirements are diverse for the processing, packaging, and storage units of a food-processing plant. Food-processing units often give out bulk proportion of contaminants that can get deposited on the luminaires and affect their performance. Steam, oils, water vapors, dust, mist, effluents, and grime are prone to affect the luminaires in the food-processing units. As a result, luminaires should be chemically inert to its surroundings and must not react with these contaminants to create toxicity in the environment. Sometimes, flammable dust can also get accumulated over the luminaires and the bulbs working on the principle of incandescence hold a very high chance of setting fire in the entire workplace due to the heat eliminated from the bulb. This risk is applicable to all those light sources that emit some form of heat during their operation. LED luminaires are the best choice in this regard. They are much efficient and safer to be used in the food-processing chambers as compared to any other light source. They produce a very small amount of heat during their operation, and it is not huge enough to ignite anything in its surrounding. Different from other light sources, they do not stand a chance to burst out due to failure and spread the glass pieces all across the room, thereby contaminating the food with glass fragments. Most of the LED luminaires have an impact-resistant construction that eliminates any chance of the luminaire bursting and allowing the debris from finding its path into food products. LEDs are free from toxic gases and mercury vapors. Hence, a failure in their working will not produce any leakage of toxic gases that can poison the food. On the other hand, mercury-vapor lamps, fluorescent lamps, sodium vapor lamps, or metal halide lamps can leak out the toxic vapors and spoil the food. In addition, these light sources can burst out with an explosion and ruin the foodstuffs with glass fragments. Yet another big issue with these types of luminaires is their act of attracting bugs and insects, which can contaminate and poison the food and thereby, spread disease-causing microbes through the food.

LED luminaires are the major eliminators of bugs and insects. They attract very few insects and can be considered negligible when compared to other light sources. LED lights can eliminate most of the pathogens that spread diseases. Bacteria such as *Salmonella typhimurium* and *Escherichia coli* (*E. coli*) are known to produce food-poisoning and a number of health issues in humans. These bacteria can be easily destroyed when they are exposed to light from LED luminaires [66]. The blue-emitting LEDs are more effective in eliminating the pathogens under its exposure. Several pathogens produce amalgam that is sensitive to light, and the continued exposure to blue light triggers the amalgam to absorb this light and lay the foundation for the termination of bacteria. In most cases, the food need not be added with preservatives and the exposure to blue light itself can prolong its shelf life. LEDs are more effective for preserving fruits and other food products in cold temperatures and in

acidic environment. This new method of preservation is known to be eco-friendly and chemical-free.

LED luminaires are much effective and energy saving when used in cold storage facilities. All other extensively used light sources are suffering from their drawback of heat generation during their operation. This makes it difficult for these lighting systems to illuminate the cold storages without affecting the temperature of the storage. The heat generated by the luminaires must be eliminated to safeguard the food from being spoiled, and this shall require more energy consumption to manage the temperature of the storage. Moreover, most of the light bulbs and tubes perform to its full potential only after warming up. The temperature of the cold storage shall delay this warming up and hence, the lighting system itself faces a delay in giving out its full brightness. Low temperatures can often degrade the quality and reduce the lifespan of several of these lamps. LEDs serve better in these conditions. LED luminaires instantly illuminate even in cold conditions. They do not heat up during their operation and help in maintaining the temperatures within the cold storage. Workers employed in the cold storages are required to frequently get in and out of the subfreezing temperatures of the storage facilities. The use of LEDs in these places enables the workers to quickly perform their work inside and avoid lingering in the dismal light. They can thwart the potential danger that must have been posed by the use of traditional lamps. Moving beyond the safety advantages of LEDs, there is more on offer from these energy-efficient luminaires. LEDs require very less amount of energy as compared to other light sources, and this proves to be a massive profit for the food industries. The energy savings retrieved from the use of LEDs can be utilized to increase the product yield from the industry. In addition, LEDs can play the role of bactericides in cold storages [67].

It is more often realized that the shelf-life of food products improved when they were kept under LED lights. The fats present in meat can be impacted by light, and this can cause rancidity in the meat on trade. Light can also initiate a reaction in the meat on exposure to oxygen and result in its discoloration. The light-induced discoloration of meat can make the buyers to forfeit from taking that meat [68]. LED lights cut down the chances of discoloration in meat and extend the shelf-life of most of the food products. Food items such as fruits and dairy products are treated with UV light to improve its shelf-life. Ultraviolet C (UVC) light covers the wavelength from 200 to 280 nm, and these are more effective in killing the pathogens due to the overlap of the UVC range with the wavelength absorbed by the DNA at 260 nm. UVC LEDs can disinfect the food without any need of chemicals or heat. Many food-borne pathogens can be eliminated using UVC LEDs [69]. Nowadays, many water filters make use of UVC rays to kill disease-causing bacteria and germs. Due to the absence of mercury, LEDs do not stand a chance to contaminate the drinking water with deadly mercury even if the installation of the lamp in the filter is inappropriate.

Storage under LED lights is now a viable option to protect the postharvest agricultural goods from many types of damage. In most cases, the postharvest yield from crops suffers losses due to over-ripening, decay, senescence, and other physiological processes [70]. Using LED lighting in the storage chambers for postharvest yield can significantly increase the shelf life of the yield by maintaining the quality of the

products and decreasing the loss in their weight. Based on the requirement in the market, the ripening of fruits and vegetables in the storage can be either accelerated or delayed using the color combination of different LEDs. For example, consider the case of tomatoes. Tomato is a vegetable that is generally gathered in an unripe stage. This is mainly to facilitate the handling and distribution of tomatoes without causing any damage, as unripe green tomatoes are firm and can withstand the shocks and jerks experienced during the distribution in the market. The ripening of tomatoes is mainly carried out during the storage. By introducing different light exposure on these unripe tomatoes, it is possible to bring about certain effects on its ripening and lycopene content [71]. Green tomatoes exposed to red LEDs and a combination of UV and red LEDs were able to ripe in five days less than those that were not treated with LEDs [71]. The combination of red and UV-LEDs also resulted in the enhancement of phenolic, flavonoids, lycopene, and β-carotene contents in tomatoes [72]. One of the ways to extend the storage life of tomatoes is by inhibiting its ripening process. The tomatoes that were subjected to blue LED treatment for seven days followed by its storage in darkness led to a delay in the accumulation of lycopene and development of redness in them [73]. On the other hand, the tomatoes that were stored in darkness without any LED treatment experienced quicker lycopene accumulation and they ripened much faster. Thus. blue LED treatment has the potential to delay the ripening of tomatoes and thereby, extend its storage life. A comparison of the appearance of tomatoes kept in darkness and irradiation by red and blue LEDs can be seen in Fig. 8.7.

Senescence and yellowing of green vegetables is a major problem during the postharvest storage. The yellowing of broccoli florets can be delayed by decreasing the reduction of ascorbate and ethylene production in them, and this can be achieved by subjecting them to exposure under red LEDs [74]. Storage of broccoli under green light also produced fruitful results, and they were able to stay without deteriorating for a period, which is three times more than the ones stored in dark [75]. Green light can increase the phenolic and glucosinolate contents in broccoli. It also prevents the bioactive compounds in broccoli from decreasing and thus, extends the shelf life of broccoli.

8.7 Other health and environmental benefits

LED lighting has shown several biomedical benefits, which were discussed in the previous sections. Apart from them, there are some more biological applications that do not completely come under the medical field applications but can be included in the biological coverage. One such application is the ability of LEDs to keep the insects at bay. Several studies have shown that LEDs do not attract nuisance causing insects and hence, can provide much comfortable illumination with the insect-free environment. Most of the insects are fascinated by the heat emitted by the lamps and hence, are known to get attracted to traditional lamps such as incandescent bulbs and fluorescent lamps. Fig. 8.8 shows a comparison of different lamps surrounded by insects. Many insects that are attracted to lamps are carriers for disease-causing pathogens and can transmit

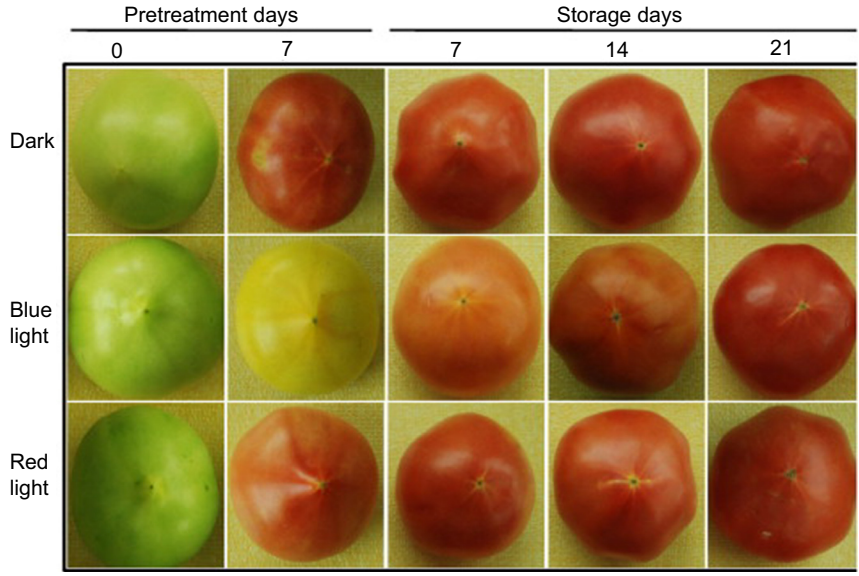

Figure 8.7 Appearance of mature green tomatoes stored in darkness (without any irradiation) and stored after continuous irradiation of blue and red LEDs. Mature green tomatoes were pretreated with darkness or continuous irradiation of blue and red light for 7 days, then stored in darkness at 25 ± 2°C for 7, 14, and 21 days. Each column represents the pretreatment and storage days, while rows 1, 2, and 3 represent tomatoes pretreated for 0 and 7 days with darkness, blue light, and red light followed by 7, 14, and 21 days of storage in darkness, respectively.
Reprinted with permission from R. Dhakal, K.-H. Baek, Short period irradiation of single blue wavelength light extends the storage period of mature green tomatoes, Postharvest Biol. Technol. 90 (2014) 73−77. https://doi.org/10.1016/j.postharvbio.2013.12.007. Copyright © 2013 Elsevier B.V.

diseases. A study was conducted by the Natural Environment Research Council (NERC), UK and a UK-based LED manufacturing company, Integral LED to determine the percentage of insects that were attracted by different types of lighting [76]. They developed customized traps illuminated by a series of incandescent lamps, fluorescent lamps, and LEDs at 18 trap sites across south-west England. More than 4000 insects were observed for their affinity towards different light sources. LEDs were the ones to attract the least number of insects. Fluorescent lamps attracted twice the number of insects and incandescent lamps attracted four times more insects as LEDs. Among the insects observed were the midges or the biting flies from the genus *Culicoides* that act as vectors for a number of diseases. The incandescent lamps attracted almost 80% of the midges, while fluorescent lamps attracted 15% of the midges. LEDs attracted only 2% of the midges. It is assumed that the insects are drawn in towards these lamps by the thermal energy emitted from them. LEDs being the least heat-emitting lamps were, thus, able to attract much lesser insects as compared to other lamps. By keeping these insects at bay, it is possible to prevent a number of vector-borne diseases.

Figure 8.8 Comparison between LEDs and other lamps in attracting insects.

8.8 Conclusions

LEDs have proved their worth in curing numerous diseases and disorders in the human body through their much acclaimed light therapy. The advantages of LED therapy are countless and the benefits derived from them are worthy enough to quote LEDs as the most promising technology for biomedical fields. LEDs are the mainstay of phototherapy and have held their roots in the field following their success in treating several skin diseases, mental disorders and dental issues. However, the expenses incurred in the treatment are still a bit out of control. It is essentially needed to bring the cost around the LED therapy within the limits for making it viable to more people. The biological applications of LEDs are not just limited in the medical field; it extends its applications in food storage and preservation too. LEDs of different color emissions have shown diverse preservation and storage effects on food. LEDs have also proven its ability to enrich the nutrient contents in fruits and vegetables as well as extend the shelf-life of a number of food products.

References

[1] N.G. Yeh, C.H. Wu, T.C. Cheng, Light-emitting diodes-Their potential in biomedical applications, Renew. Sustain. Energy Rev. 14 (2010) 2161−2166, https://doi.org/10.1016/j.rser.2010.02.015.

[2] D. Goldberg, B. Russell, Combination blue (415 nm) and red (633 nm) LED phototherapy in the treatment of mild to severe acne vulgaris, J. Cosmet. Laser Ther. 8 (2006) 71−75, https://doi.org/10.1080/14764170600735912.

[3] B. Michael Terman, J. Su Terman, M. Terman, Light therapy for seasonal and nonseasonal depression: efficacy. Protocol, safety, and side effects, CNS Spectr. 10 (2016) 647−663, https://doi.org/10.1017/S1092852900019611.

[4] G.B. Nair, S.J. Dhoble, A perspective perception on the applications of light-emitting diodes, Luminescence 30 (2015) 1167−1175, https://doi.org/10.1002/bio.2919.

[5] M.A. Trelles, S. Mordon, R.G. Calderhead, Facial rejuvenation and light: our personal experience, Lasers Med. Sci. 22 (2007) 93−99, https://doi.org/10.1007/s10103-006-0418-6.

[6] F. Baez, L.R. Reilly, The use of light-emitting diode therapy in the treatment of photoaged skin, J. Cosmet. Dermatol. 6 (2007) 189−194, https://doi.org/10.1111/j.1473-2165.2007.00329.x.

[7] N.S. Sadick, Update on non-ablative light therapy for rejuvenation: a review, Lasers Surg. Med. 32 (2003) 120−128, https://doi.org/10.1002/lsm.10127.

[8] B.A. Russell, N. Kellett, L.R. Reilly, A study to determine the efficacy of combination LED light therapy (633 nm and 830 nm) in facial skin rejuvenation, J. Cosmet. Laser Ther. 7 (2005) 196−200, https://doi.org/10.1080/14764170500370059.

[9] J.H. Hong, D.Y. Kim, Y.C. Kye, S.H. Seo, D.H. Kim, H.H. Ahn, Lightning effect of a light-emitting diode mask on facial skin: a colorimetric assessment, Ann. Dermatol. 31 (2019) 247, https://doi.org/10.5021/ad.2019.31.2.247.

[10] L. Rocha Mota, L.J. Motta, I. da S. Duarte, A.C.R.T. Horliana, D. de F.T. da Silva, C. Pavani, Efficacy of phototherapy to treat facial ageing when using a red versus an amber LED: a protocol for a randomised controlled trial, BMJ Open 8 (2018) e021419, https://doi.org/10.1136/bmjopen-2017-021419.

[11] S.Y. Lee, C.E. You, M.Y. Park, Blue and red light combination LED phototherapy for acne vulgaris in patients with skin phototype IV, Lasers Surg. Med. 39 (2007) 180−188, https://doi.org/10.1002/lsm.20412.

[12] M.M.S. Mulder, V. Sigurdsson, E.J. Van Zuuren, E.J. Klaassen, J.A.J. Faber, J.B.F. De Wit, W.A. Van Vloten, Psychosocial impact of acne vulgaris: evaluation of the relation between a change in clinical acne severity and psychosocial state, Dermatology 203 (2001) 124−130, https://doi.org/10.1159/000051726.

[13] J.J. Leyden, Therapy for acne vulgaris, N. Engl. J. Med. 336 (1997) 1156−1162.

[14] H.P.M. Gollnick, A. Krautheim, Topical treatment in acne: current status and future aspects, Dermatology 206 (2003) 29−36, https://doi.org/10.1159/000067820.

[15] S.J. Longshore, K. Hollandsworth, Acne vulgaris: one treatment does not fit all, Cleve. Clin. J. Med. 70 (2003) 670−680.

[16] H. Pawin, C. Beylot, M. Chivot, M. Faure, F. Poli, J. Revuz, Physiopathology of acne vulgaris: recent data, new understanding of the treatments, Eur. J. Dermatol. 14 (2004) 4−12. http://ovidsp.ovid.com/ovidweb.cgi?T=JS&PAGE=reference&D=emed8&NEWS=N&AN=38187090.

[17] T.-Y. Tzung, K.-H. Wu, M.-L. Huang, Blue light phototherapy in the treatment of acne, Photodermatol. Photoimmunol. Photomed. 20 (2004) 266–269, https://doi.org/10.1111/j.1600-0781.2004.00109.x.
[18] C.A. Morton, R.D. Scholefield, C. Whitehurst, J. Birch, An open study to determine the efficacy of blue light in the treatment of mild to moderate acne, J. Dermatol. Treat. 16 (2005) 219–223, https://doi.org/10.1080/09546630500283664.
[19] H. Ashkenazi, Z. Malik, Y. Harth, Y. Nitzan, Eradication of Propionibacterium acnes by its endogenic porphyrins after illumination with high intensity blue light, FEMS Immunol. Med. Microbiol. 35 (2003) 17–24, https://doi.org/10.1016/S0928-8244(02)00423-6.
[20] E. V Ross, Optical treatments for acne, Dermatol. Ther. 18 (2005) 253–266, https://doi.org/10.1111/j.1529-8019.2005.05024.x. DTH05024[pii]\r.
[21] B. Kjeldstad, A. Johnsson, An action spectrum for blue and near ultraviolet inactivation of Propionibacterium acnes; with emphasis on a possible porphyrin photosensitization, Photochem. Photobiol. 43 (1986) 67–70, https://doi.org/10.1111/j.1751-1097.1986.tb05592.x.
[22] T.J. Dougherty, G.B. Grindey, R. Fiel, K.R. Weishaupt, D.G. Boyle, Photoradiation therapy. II. Cure of animal tumors with hematoporphyrin and Light23, JNCI J. Natl. Cancer Inst. 55 (1975) 115–121, https://doi.org/10.1093/jnci/55.1.115.
[23] E. Sorbellini, M. Rucco, F. Rinaldi, Photodynamic and photobiological effects of light-emitting diode (LED) therapy in dermatological disease: an update, Lasers Med. Sci. 33 (2018) 1431–1439, https://doi.org/10.1007/s10103-018-2584-8.
[24] P. Babilas, R. Travnik, A. Werner, M. Landthaler, R.-M. Szeimies, Split-face-study using two different light sources for topical PDT of actinic keratoses: non-inferiority of the LED system, J. Dtsch. Dermatol. Ges. 6 (2008) 25–32, https://doi.org/10.1111/j.1610-0387.2007.06555.x.
[25] S.F. McDonald, Effect of visible lightwaves on arthritis pain: a controlled study, Int. J. Biosoc. Res. 3 (1982) 49–54. http://search.ebscohost.com/login.aspx?direct=true&db=psyh&AN=1984-12710-001&%5Cnlang=de&site=ehost-live.
[26] I. Neuman, Y. Finkelstein, Narrow-band red light phototherapy in perennial allergic rhinitis and nasal polyposis, Ann. Allergy Asthma Immunol. 78 (1997) 399–406, https://doi.org/10.1016/S1081-1206(10)63202-4.
[27] K.S. Caetano, M.A. Frade, D.G. Minatel, L.A. Santana, C.S. Enwemeka, Phototherapy improves healing of chronic venous ulcers, Photomed. Laser Surg. 27 (2009) 111–118, https://doi.org/10.1089/pho.2008.2398.
[28] W. Lim, S. Lee, I. Kim, M. Chung, M. Kim, H. Lim, J. Park, O. Kim, H. Choi, The anti-inflammatory mechanism of 635 nm light-emitting-diode irradiation compared with existing COX inhibitors, Lasers Surg. Med. 39 (2007) 614–621, https://doi.org/10.1002/lsm.20533.
[29] L. Lang-Bicudo, F.D.P. Eduardo, C.D.P. Eduardo, D.M. Zezell, LED phototherapy to prevent mucositis: a case report, Photomed. Laser Surg. 26 (2008) 609–613, https://doi.org/10.1089/pho.2007.2228.
[30] Q. Chen, H. Dan, F. Tang, J. Wang, X. Li, J. Cheng, H. Zhao, X. Zeng, Photodynamic therapy guidelines for the management of oral leucoplakia, Int. J. Oral Sci. 11 (2019) 14, https://doi.org/10.1038/s41368-019-0047-0.
[31] R. Cremer, P. Perryman, D. Richards, Influence of light on the hyperbilirubinaemia of infants, Lancet 1 (1958) 1094–1097, https://doi.org/10.1542/pir.32-8-341.
[32] L.E. Maier, Rosacea: advances in understanding pathogenesis and treatment, Clin. Investig. 1 (2011) 739–755, https://doi.org/10.4155/cli.11.50.

[33] M. Triesscheijn, P. Baas, J.H.M. Schellens, F.A. Stewart, Photodynamic therapy in oncology, Oncologist 11 (2006) 1034−1044, https://doi.org/10.1634/theoncologist.11-9-1034.
[34] A. Wollenberg, S. Barbarot, T. Bieber, S. Christen-Zaech, M. Deleuran, A. Fink-Wagner, U. Gieler, G. Girolomoni, S. Lau, A. Muraro, M. Czarnecka-Operacz, T. Schäfer, P. Schmid-Grendelmeier, D. Simon, Z. Szalai, J.C. Szepietowski, A. Taïeb, A. Torrelo, T. Werfel, J. Ring, Consensus-based European guidelines for treatment of atopic eczema (atopic dermatitis) in adults and children: part II, J. Eur. Acad. Dermatol. Venereol. 32 (2018) 850−878, https://doi.org/10.1111/jdv.14888.
[35] R.W. Lam, R.D. Levitan, Pathophysiology of seasonal affective disorder: a review, J. Psychiatry Neurosci. 25 (2000) 469−480.
[36] A.J. Lewy, B.J. Lefler, J.S. Emens, V.K. Bauer, The circadian basis of winter depression, Proc. Natl. Acad. Sci. U.S.A. (2006) 7414−7419, https://doi.org/10.1073/pnas.0602425103.
[37] G. Glickman, B. Byrne, C. Pineda, W.W. Hauck, G.C. Brainard, Light therapy for Seasonal Affective Disorder with blue narrow-band light-emitting diodes (LEDs), Biol. Psychiatry 59 (2006) 502−507, https://doi.org/10.1016/j.biopsych.2005.07.006.
[38] F. Benedetti, C. Colombo, A. Pontiggia, A. Bernasconi, M. Florita, E. Smeraldi, Morning light treatment hastens the antidepressant effect of citalopram: a placebo-controlled trial, J. Clin. Psychiatry 64 (2003) 648−653, https://doi.org/10.4088/JCP.v64n0605.
[39] M. Terman, Evolving applications of light therapy, Sleep Med. Rev. 11 (2007) 497−507, https://doi.org/10.1016/j.smrv.2007.06.003.
[40] S.A. Rahman, M.A. St. Hilaire, S.W. Lockley, The effects of spectral tuning of evening ambient light on melatonin suppression, alertness and sleep, Physiol. Behav. 177 (2017) 221−229, https://doi.org/10.1016/j.physbeh.2017.05.002.
[41] K. Zhang, B. Cui, Optogenetic control of intracellular signaling pathways, Trends Biotechnol. 33 (2015) 92−100, https://doi.org/10.1016/j.tibtech.2014.11.007.
[42] E.J. Olson, J.J. Tabor, Optogenetic characterization methods overcome key challenges in synthetic and systems biology, Nat. Chem. Biol. 10 (2014) 502−511, https://doi.org/10.1038/nchembio.1559.
[43] V. Gradinaru, M. Mogri, K.R. Thompson, J.M. Henderson, K. Deisseroth, Optical deconstruction of parkinsonian neural circuitry, Science 324 (2009) 354−359, https://doi.org/10.1126/science.1167093.
[44] D.M. Johnstone, C. Moro, J. Stone, A.-L. Benabid, J. Mitrofanis, Turning on lights to stop neurodegeneration: the potential of near infrared light therapy in Alzheimer's and Parkinson's disease, Front. Neurosci. 9 (2016), https://doi.org/10.3389/fnins.2015.00500.
[45] M.A. Naeser, A. Saltmarche, M.H. Krengel, M.R. Hamblin, J.A. Knight, Improved cognitive function after transcranial, light-emitting diode treatments in chronic, traumatic brain injury: two case reports, Photomed. Laser Surg. 29 (2010) 351−358, https://doi.org/10.1089/pho.2010.2814.
[46] M. Hennessy, M.R. Hamblin, Photobiomodulation and the brain: a new paradigm, J. Opt. 19 (2017), https://doi.org/10.1088/2040-8986/19/1/013003.
[47] J. Dong, D. Xiong, Applications of light emitting diodes in health care, Ann. Biomed. Eng. 45 (2017) 2509−2523, https://doi.org/10.1007/s10439-017-1930-5.
[48] H.F. Iaccarino, A.C. Singer, A.J. Martorell, A. Rudenko, F. Gao, T.Z. Gillingham, H. Mathys, J. Seo, O. Kritskiy, F. Abdurrob, C. Adaikkan, R.G. Canter, R. Rueda, E.N. Brown, E.S. Boyden, L.H. Tsai, Gamma frequency entrainment attenuates amyloid load and modifies microglia, Nature 540 (2016) 230−235, https://doi.org/10.1038/nature20587.

[49] P. Mc Donnell, P.E. Mc Hugh, D. O' Mahoney, Vertebral osteoporosis and trabecular bone quality, Ann. Biomed. Eng. 35 (2007) 170–189, https://doi.org/10.1007/s10439-006-9239-9.

[50] B. Atalay, S. Yalcin, Y. Emes, I. Aktas, B. Aybar, H. Issever, N.M. Mandel, O. Cetin, B. Oncu, Bisphosphonate-related osteonecrosis: laser-assisted surgical treatment or conventional surgery? Lasers Med. Sci. 26 (2011) 815–823, https://doi.org/10.1007/s10103-011-0974-2.

[51] D.G. Woo, C.Y. Ko, H.S. Kim, J.B. Seo, D. Lim, Evaluation of the potential clinical application of low-intensity ultrasound stimulation for preventing osteoporotic bone fracture, Ann. Biomed. Eng. 38 (2010) 2438–2446, https://doi.org/10.1007/s10439-010-9983-8.

[52] K.J. Anusavice, Chlorhexidine, fluoride varnish, and xylitol chewing gum: underutilized preventive therapies? Gen. Dent. 46 (1998).

[53] N.B. Arweiler, T.M. Auschill, E. Reich, L. Netuschil, Substantivity of toothpaste slurries and their effect on reestablishment of the dental biofilm, J. Clin. Periodontol. 29 (2002) 615–621, https://doi.org/10.1034/j.1600-051X.2002.290705.x.

[54] C.H. Charles, K.M. Mostler, L.L. Bartels, S.M. Mankodi, Comparative antiplaque and antigingivitis effectiveness of a chlorhexidine and an essential oil mouthrinse: 6-month clinical trial, J. Clin. Periodontol. 31 (2004) 878–884, https://doi.org/10.1111/j.1600-051X.2004.00578.x.

[55] A.C.B.P. Costa, V.M. de Campos Rasteiro, C.A. Pereira, E.S.H. da Silva Hashimoto, M. Beltrame, J.C. Junqueira, A.O.C. Jorge, Susceptibility of Candida albicans and Candida dubliniensis to erythrosine- and LED-mediated photodynamic therapy, Arch. Oral Biol. 56 (2011) 1299–1305, https://doi.org/10.1016/j.archoralbio.2011.05.013.

[56] C. Chui, A. Aoki, Y. Takeuchi, Y. Sasaki, K. Hiratsuka, Y. Abiko, Y. Izumi, Antimicrobial effect of photodynamic therapy using high-power blue light-emitting diode and red-dye agent on *Porphyromonas gingivalis*, J. Periodontal. Res. (2013), https://doi.org/10.1111/jre.12055 n/a-n/a.

[57] D.F. Oda, M.A.H. Duarte, F.B. Andrade, L.T. Moriyama, V.S. Bagnato, I.G. de Moraes, Antimicrobial action of photodynamic therapy in root canals using LED curing light, curcumin and carbopol gel, Int. Endod. J. 52 (2019) 1010–1019, https://doi.org/10.1111/iej.13092.

[58] M.A. Paschoal, C.C. Tonon, D.M.P. Spolidório, V.S. Bagnato, J.S.M. Giusti, L. Santos-Pinto, Photodynamic potential of curcumin and blue LED against Streptococcus mutans in a planktonic culture, Photodiagnosis Photodyn. Ther. 10 (2013) 313–319, https://doi.org/10.1016/j.pdpdt.2013.02.002.

[59] W. Posten, D.A. Wrone, J.S. Dover, K.A. Arndt, S. Silapunt, M. Alam, Low-level laser therapy for wound healing: mechanism and efficacy, Dermatol. Surg. 31 (2005) 334–340, https://doi.org/10.1097/00042728-200503000-00016.

[60] A.V. Corazza, J. Jorge, C. Kurachi, V.S. Bagnato, Photobiomodulation on the angiogenesis of skin wounds in rats using different light sources, Photomed. Laser Surg. 25 (2007) 102–106, https://doi.org/10.1089/pho.2007.2011.

[61] B.J. Erdle, S. Brouxhon, M. Kaplan, J. Vanbuskirk, A.P. Pentland, Effects of continuous-wave (670-nm) red light on wound healing, Dermatol. Surg. 34 (2008) 320–325, https://doi.org/10.1111/j.1524-4725.2007.34065.x.

[62] M.A. Dall Agnol, R.A. Nicolau, C.J. De Lima, E. Munin, Comparative analysis of coherent light action (laser) versus non-coherent light (light-emitting diode) for tissue repair in diabetic rats, Lasers Med. Sci. 24 (2009) 909−916, https://doi.org/10.1007/s10103-009-0648-5.

[63] H.T. Whelan, E.V. Buchmann, A. Dhokalia, M.P. Kane, N.T. Whelan, M.T.T. Wong-Riley, J.T. Eells, L.J. Gould, R. Hammamieh, R. Das, M. Jett, Effect of NASA light-emitting diode irradiation on molecular changes for wound healing in diabetic mice, J. Clin. Laser Med. Surg. 21 (2003) 67−74, https://doi.org/10.1089/104454703765035484.

[64] M.A. Liebert, H.T. Whelan, R.L. Smits, E. V Buchman, N.T. Whelan, S.G. Turner, D.A. Margolis, V. Cevenini, H. Stinson, R.O.N. Ignatius, T. Martin, J. Cwiklinski, A.F. Philippi, W.R. Graf, D. Ph, B. Hodgson, L. Gould, M. Kane, G. Chen, J. Caviness, Effect of NASA light-emitting diode irradiation on wound healing, J. Clin. Laser Med. Surg. 19 (2001) 305−314, https://doi.org/10.1089/104454701753342758.

[65] M.A. Liebert, J.T. Eells, D. Ph, M.T.T. Wong-riley, M.M. Henry, E. V Buchmann, M.P. Connelly, J. V Dovi, H.L. Liang, D.S. Henshel, R.L. Yeager, D.S. Millsap, J. Lim, L.J. Gould, R. Das, M. Jett, B.D. Hodgson, D. Margolis, H.T. Whelan, Clinical and experimental applications of NIR-LED photobiomodulation, Photomed. Laser Surg. 24 (2006) 121−128, https://doi.org/10.1089/pho.2006.24.121.

[66] M.L. Bhavya, H. Umesh Hebbar, Efficacy of blue LED in microbial inactivation: effect of photosensitization and process parameters, Int. J. Food Microbiol. 290 (2019) 296−304, https://doi.org/10.1016/j.ijfoodmicro.2018.10.021.

[67] M.M. Hasan, T. Bashir, R. Ghosh, S.K. Lee, H. Bae, An overview of LEDs' effects on the production of bioactive compounds and crop quality, Molecules 22 (2017) 1420, https://doi.org/10.3390/molecules22091420.

[68] P.N. Haughton, E.G. Grau, J. Lyng, D. Cronin, S. Fanning, P. Whyte, Susceptibility of Campylobacter to high intensity near ultraviolet/visible 395±5nm light and its effectiveness for the decontamination of raw chicken and contact surfaces, Int. J. Food Microbiol. 159 (2012) 267−273, https://doi.org/10.1016/j.ijfoodmicro.2012.09.006.

[69] L.M. Hinds, C.P. O'Donnell, M. Akhter, B.K. Tiwari, Principles and mechanisms of ultraviolet light emitting diode technology for food industry applications, Innov. Food Sci. Emerg. Technol. 56 (2019) 102153, https://doi.org/10.1016/j.ifset.2019.04.006.

[70] F. Bantis, S. Smirnakou, T. Ouzounis, A. Koukounaras, N. Ntagkas, K. Radoglou, Current status and recent achievements in the field of horticulture with the use of light-emitting diodes (LEDs), Sci. Hortic. 235 (2018) 437−451, https://doi.org/10.1016/j.scienta.2018.02.058.

[71] S. Chomchalow, N.M. El Assi, S.A. Sargent, J.K. Brecht, Fruit maturity and timing of ethylene treatment affect storage performance of green tomatoes at chilling and nonchilling temperatures, HortTechnology (2002) 104−114, https://doi.org/10.21273/HORTTECH.12.1.104.

[72] L. Panjai, G. Noga, A. Fiebig, M. Hunsche, Effects of continuous red light and short daily UV exposure during postharvest on carotenoid concentration and antioxidant capacity in stored tomatoes, Sci. Hortic. 226 (2017) 97−103, https://doi.org/10.1016/j.scienta.2017.08.035.

[73] R. Dhakal, K.-H. Baek, Short period irradiation of single blue wavelength light extends the storage period of mature green tomatoes, Postharvest Biol. Technol. 90 (2014) 73−77, https://doi.org/10.1016/j.postharvbio.2013.12.007.

[74] G. Ma, L. Zhang, C.K. Setiawan, K. Yamawaki, T. Asai, F. Nishikawa, S. Maezawa, H. Sato, N. Kanemitsu, M. Kato, Effect of red and blue LED light irradiation on ascorbate content and expression of genes related to ascorbate metabolism in postharvest broccoli, Postharvest Biol. Technol. 94 (2014) 97−103, https://doi.org/10.1016/j.postharvbio.2014.03.010.

[75] P. Jin, D. Yao, F. Xu, H. Wang, Y. Zheng, Effect of light on quality and bioactive compounds in postharvest broccoli florets, Food Chem. 172 (2014) 705−709, https://doi.org/10.1016/j.foodchem.2014.09.134.

[76] LED Lights Attract Fewer Insects than Other Lights, BizLED, 2016. http://bizled.co.in/led-lights-attract-fewer-insects-than-other-lights/. (Accessed 31 July 2019).

Horticultural applications

9

9.1 Introduction

It is a very well-known reality that adequate proportion of light, water, oxygen, and mineral nutrients are essential for the productive growth of plants [1]. Plants prefer to grow in those geographical locations where they meet the climatic conditions required for their growth. Different parts of the world show great amount of variation in their climatic conditions. As a result, the regional temperature differs along with the availability of light, water, and nutrients. Natural sunlight is the cheapest source of light available, but it is not always attainable in sufficient quantities in every nook and corner of the world. Consequently, farmers started relying on the artificial sources of light for cultivating plants in gloomy, misty, or overcast conditions. The rising human population has led to the mounting food demands and, thereby, need for expansion in the agricultural productivity [2]. On the other hand, agricultural productivity is being threatened by frequent floods, droughts, pest attack on crops, and uneven climatic changes. Indoor farming gained momentum owing to the rising issues faced by conventional agriculture that led to decline in the overall product yield in recent years [3]. Indoor farming is not affected by weather conditions, floods or droughts, and unavailability of arable land. It also assures availability of uninterrupted food supply all round the year to quench the demands of the rising population. This type of vertical farming makes use of artificial light sources as grow-lights for the crops to carry out photosynthesis in the absence of natural sunlight. The use of artificial lighting is not just limited to indoor farming, but its application has also been extended to several greenhouses as supplementary light source when sunlight is not available in the desired intensity. Particularly in winter, artificial grow-lights come to the rescue as the sun does not shine bright enough for the crop plants to gain adequate light for carrying out photosynthesis.

The light from the sun is entirely different as compared with that received from an artificial source. Vast amount of energy is received from the sun along with highly intense red and blue regions of the light spectrum. Sunlight is composed of different wavelengths of the visible light spectrum with approximately the same photon flux. In addition, there are ultraviolet (UV) and infrared (IR) components, too, present in the sunlight. In general, plants have affinity towards the intense blue and red components of light provided by the sun. Most artificial light sources do not emit as much energy in the red and blue region of the light spectrum as sunlight does. This has inspired researchers to develop much better and powerful artificial sources that are completely dedicated to grow plants. The lighting requirements in horticulture are complex, and farmers need artificial light sources that not only mimic the natural sunlight but also show the caliber to reap benefits beyond that. Over time, these

The Fundamentals and Applications of Light-Emitting Diodes. https://doi.org/10.1016/B978-0-12-819605-2.00009-4

artificial light sources developed into more sophisticated plant grow-lights that were specially designed to suit the needs of plants. The technological advancement paved way to a number of grow-lights that worked on various principles, and each of them was surpassed by a technologically newer kind of light source.

Light-emitting diodes (LEDs) have advanced fast and become the front runners in the agricultural grow-light industry. They can be customized to meet the requirements of indoor farming. LEDs can be closely optimized to tune the color precisely needed by a plant to grow or a seed to germinate. The advanced system controls that are assembled with the LED fixtures further facilitate the tuning of their spectral intensity and output based on the growth stage of a plant and the type of plant. The selection of a grow-light must be made by taking into consideration a number of factors. The farmers desiring to reap good yield from their harvest using grow-lights must be aware of the precise terms associated with the measurement of light in photosynthesis light applications, viz., photosynthetically active radiation (PAR), photosynthetic photon flux (PPF), and photosynthetic photon flux density (PPFD). PAR defines the type of light spectrum required to support plant growth. PPF defines the number of photons emitted by the light source per unit time, and PPFD defines the density of the photons being distributed across a unit area per unit time by the light source. The selection of a grow-light is made on the basis of the following three points:

(1) The quality and quantity of light produced by the grow-light.
(2) The quality and quantity of light that is made available for the plants to grow.
(3) The quality and quantity of light received by the plant from the grow-light during the photoperiod.

It is worthwhile to know that a grow-light may produce lumen output with high PPF. But it is not necessary that the quantity of lumens measured per unit area under the grow-light shall be equally interesting. The uniformity in the lumen output throughout the luminaire shall be the deciding factor to conclude if the PPFD will be consistent or not. LEDs provide uniform lighting resulting in quantitative and qualitative improvement in the crop yield. The continuous advancement in LED technology has attracted huge benefits into the horticulture domain, and now, the market is well poised for the mass adoption of LEDs into the horticulture business.

9.2 Plant's response to light

Plants show an entirely different sensitivity to light as compared to human beings. The quality and quantity of light becomes much important for plants to attain optimum growth and good health. The portion of the light spectrum between 400 nm and 700 nm, wherein plants show maximum sensitivity, is used by plants for their photosynthesis. This specific portion of the light spectrum is called the PAR light. This quantified amount of radiation is often expressed in the units of energy flux (W/m^2) or photon flux ($mol/m^2/s$). A comparison between the solar spectrum and the relative sensitivity of human vision and PAR is shown in Fig. 9.1. The PAR consists of full spectrum of light colors, with special emphasis on red and blue light. Light is perceived by plant photoreceptors such as phytochromes, cryptochromes, and phototropins, and

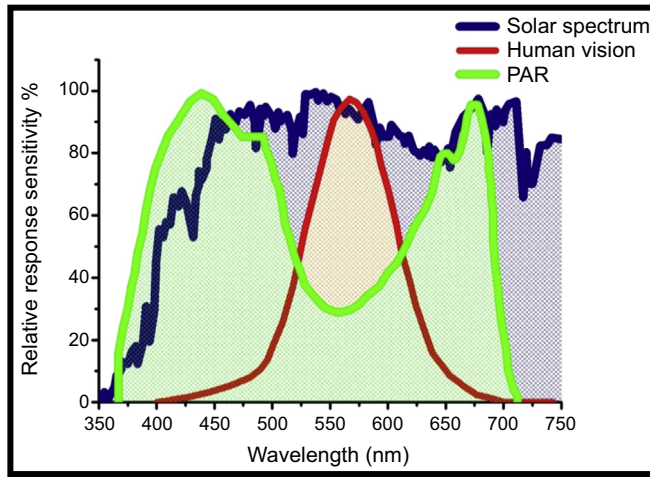

Figure 9.1 Comparison of the solar spectrum with the relative sensitivity of human vision and photosynthetically active radiation (PAR).

plants generate a wide range of specific physiological responses through these receptors [4]. Plants use light as an environmental signal and respond to its intensity, wavelength, and direction. Plants have developed sophisticated processes for receiving various wavebands from the solar radiation and perceive them as signals to initiate certain growth or development mechanisms in them. The absorbed light induces processes such as photomorphogenesis, photosynthesis, phototropism, and photoperiodism in plants. Photomorphogenesis is induced in plants by the far-red region (700−735 nm) of the electromagnetic spectrum. This is a light-mediated process that produces development of cells, tissues, and organs in plants during its growth. Photosynthesis is a chemical process by which plants synthesize the essential carbohydrates required for their growth by utilizing the light, water, and CO_2 from the environment. A plant's capacity to sense, assess, and respond to the quality, quantity, and direction of light grants it with the ability to maximize its productivity in photosynthesis. The role of light-harvesting antenna in plants is enacted by protein chlorophyll−carotenoid complexes present in chloroplasts. They harvest the photons from a light source and send them to the photosystem reaction center where electrons are generated [5]. If the lighting levels are not appropriate, there will be disruption in the photosynthetic processes. Too much lighting leads to the production of oxygen radicals that result in photoinhibition [6]. On the other hand, weak lighting can lead to etiolation symptoms and reduce the photosynthetic activity in plants [7]. Phototropism is the growth movement of plants towards a light source. This process often leads to the bending of plants toward or away from the light source by a chemical called auxin. Auxins are present in plant cells that are farthest away from the light, and they compel the plant cells that are farthest from the light to elongate and bend towards the light source. When the plants bend towards the light source, it is called positive phototropism. Most of the plants prefer to exhibit positive tropism. When plants move away from the light source, it is called negative phototropism, and this is rarely

seen, for instance, in certain vine shoots. Phototropism is generally triggered by visible light in the range of 400−500 nm. Photoperiodism is a physiological response given by plants to the duration of day and night. The development processes occurring in the plants are relative to the duration of days and nights, and this is decided by the plants with respect to the light and dark periods.

The first photoreceptor to be identified in plants is the phytochrome, which is a photoreversible red receptor in plants [8]. In long-day plants, flowering is essentially stimulated by far-red light [9]. Cryptochromes were the first blue receptors identified in plants. Several photomorphogenesis processes such as stomatal opening, stem elongation, leaf expansion, and seed germination are regulated by cryptochromes. Phototropins are another class of blue receptors found in plants. They play a major role in the optimization of light harvesting from a source and prevention of photoinhibition by regulating the pigment content and position of the photosynthetic organelles [10]. Blue light supports strong root growth and intense photosynthetic process in plants that lead to productive vegetative growth [11]. In most cases, blue or red LEDs are used for target lighting for the plants. Goins et al. investigated the effect of red light on wheat (*Triticum aestivum* L., cv. 'USU-Super Dwarf) crops by comparing the photomorphogenesis, photosynthesis, and seed yield of wheat under simple red LEDs, daylight fluorescent (white) lamps, and red LEDs supplemented with 1% or 10% blue light from the fluorescent lamps [12]. The wheat crops grown under red LEDs showed complete full life cycle, but with lesser seed yield and shoot dry mass accumulation as compared to those grown under white fluorescent lamps and the red LEDs supplemented by blue light.

In addition, infrared (IR) LEDs too proved their worth in horticulture. Seedlings of oat (*Avena sativa* cv. Seger) were irradiated with IR LEDs by Johnson et al. [13]. The IR radiations were allowed to pass through a visible-light-blocking filter before making it to fall on the seedlings. The irradiated seedlings showed dissimilarities in the growth and development as compared to those seedlings that were grown in the dark at the same temperature. These seedlings showed a gravitropic response pattern that was distinct from those grown in the dark. On the other hand, the seedlings that grew in the dark did not show any bending and was uniformly directed in the direction of endosperm crease away from the seed.

9.3 Light-emitting diode versus other types of grow-lights

LEDs have gained huge reputation in recent years due to loads of features that resulted in huge energy savings and environment-friendly source of lighting applications in diverse fields [14]. Researches were fascinated by the upcoming popularity of LEDs and started testing them for their effectiveness in vertical/indoor farming. Experiments were conducted to evaluate the influence of individual monochromatic LEDs and their combinations on the growth and development of various plants. LEDs were preferred over all other light sources as grow-lights owing to a number of reasons. LEDs are feasible alternatives to existing artificial sources of lighting owing to their durability, flexibility, stability, and low energy consumption [15]. They provide an excellent

flexibility in their operation allowing to control their intensity, pulse mode, and wavelength of the light emitted from them [16]. They offer a life span that is unmatchable by any other source of artificial lighting [17]. They are miniature in size and less in mass and do not involve any ballast for operation. LEDs can significantly reduce the expenses incurred in electricity, and all the initial investments will turn out to be huge profits in the long-term operations in the greenhouse industry [18]. They have proved themselves as the most effective artificial source of lighting that is flexible for plant tissue culture [19]. The spectral quality and the intensity of light emitted by an LED can be precisely manipulated as per the requirement [20]. For in-vitro plants and bioregenerative life support systems, LEDs can be considered as a primary source of lighting [21]. Based on the plant response that is targeted, LEDs can offer specific wavelengths for desired output. Also, they do not heat up much during their operation and hence, can be kept near the plants for maximum effectiveness [22]. This will ensure that plants do not suffer from the lack of light.

To highlight the effective performance of LEDs in plant growth, a comparison is essential between the LEDs and the other types of grow-lights that are available in the market. This section focuses on the features offered by different types of grow-lights and their demerits as opposed to their LED counterparts.

9.3.1 Incandescent lamps

Bare incandescent lights generally illuminate with a red-yellowish tone and a low color temperature of approximately 2700 K. They do not truly behave like a plant-growing light but are sometimes used to highlight indoor plant groupings. Some incandescent grow-lights come with a blue filter coating, as shown in Fig. 9.2, which reduces the

Figure 9.2 Incandescent grow-lights (left), incandescent bulb with blue filter coating (right top), and mushroom-shaped white-coated incandescent bulb (right bottom).

amount of red light given off by them. An extremely small amount of light is expended as compared with the amount of energy needed to illuminate the bulb, and almost 90% energy is given off as heat. Incandescent lights generate a lot of heat and should be placed farther away from the plant foliage. On a precautionary note, incandescent bulbs must always maintain a minimum distance of 24 inches from the plants. The lack of light intensity can be remedied by increasing the number of hours the plant is exposed to the light or by adding reflective surfaces to make the available light reach more areas of the plant. Because red light tends to encourage bud and flower growth, bare incandescent lights are better used on flowering plants. Incandescent bulbs can be used to prolong the short days during autumn, winter, and spring. While the initial expenditure to purchase incandescent bulbs is very cheap, they are much costlier to operate when compared with other grow-lights. Such grow -lights have a brief life expectancy of about 750 hours and are energy inefficient, producing more heat than useable light. Incandescent light bulbs show no match with LED lights, when it comes to the efficiency, durability, and lifetime.

9.3.2 Fluorescent lamps

Fluorescent lamps are available in cool, warm, or full spectrum with the color temperatures ranging from 2700 to 10,000 K. Fluorescent lights, which are as shown in Fig. 9.3, have an average useable life span of up to 20,000 hours. Fluorescents put out very little heat, which allows them to be hung close to the plants. These are

Figure 9.3 Fluorescent grow-lights.

very affordable and convenient for use. They give a light output that is twice as that of the incandescent lamps. These are quite popular for propagation, early vegetative growth, and overwintering semi-hardy and tender plants. T5 and T8 fluorescents are the most modern type of fluorescent lamps that are available as single, daisy-chainable strips or in panel arrays. A fluorescent grow-light's electronic ballast does not emit noise or vibration. A smaller version of the fluorescent tubes are the compact fluorescent lamps (CFLs), which work in specially designed reflectors to direct their light to plants. High-output fluorescent lights produce twice as much light as the standard fluorescent lights. However, a fluorescent tube makes use of highly pressurized mercury vapor and neon, argon, krypton, or xenon gases within the tube. This can prove hazardous to the environment if not disposed of safely. LEDs prove their beneficence to the environment in this regard. They never pose any threat either when in use nor at the time of disposal. Although fluorescent lamps seem to be cheaper at the initial stage, they turn out to pierce the money bags of plant growers with the frequent replacement of lamps. Hence, it is more profitable to go with the LEDs, which prove their worth with lesser expenses on maintenance.

9.3.3 High intensity discharge

Although the initial costs of setting up the high intensity discharge (HID) grow-lights seem affordable for plant growers, the initial saving gets overshadowed by the additional costs that cannot be avoided. HID lighting creates light by passing an electric current through the metal vapors that charge the electrons and cause them to bump into each other. HID lights take a few seconds to give a full output, and once it is turned off, it needs to be cooled down completely before another use. Some variants of HID grow-lights are shown in Fig. 9.4. The HID lights are very bright and powerful but produce a large amount of heat that has to be diffused by airflow systems. Their maintenance requirements force the plant growers to deal with an extra cost, which can incredibly turn to be an overexpensive affair when they are being run on a daily basis. They will effectively grow plants at any stage of life, but it will come at a cost, and they require a great deal of attention. On the other hand, LED grow-lights are efficient in every imaginable way, and this has made people to turn toward LEDs for efficient and productive plant growth.

9.3.4 Metal halide

Metal halide (MH) lights are a subset of HID lights. Generally, an abundant amount of light in the blue spectrum is produced by MH bulbs, as shown in Fig. 9.5. Blue light promotes plant growth and is excellent for green leafy growth and keeping plants compact. They also contain some ultraviolet (UV) radiation that is useful for combating pests and molds and promoting the production of essential oils in aromatic crops. It is the best type of light to be used as a primary light source when the scarcity of natural sunlight is felt. Although the bulb will continue to light up even after its average life span of 10,000 cumulative hours, it is not worth to use beyond this span due to its gradual decline of light intensity. Metal halides produce up to

Figure 9.4 High intensity discharge grow-lights.

125 lumens per watt as compared to the 39 lumens per watt produced by the standard fluorescent lights and 18 lumens per watt produced by the standard incandescent bulbs. Horticultural metal halide lamps have an enhanced red spectrum, hardly noticeable to the naked eye, which is added for improved fruiting and flowering without compromising with the plant appearance. The major disadvantage of a metal halide lamp is their lower efficacy and shorter life span, and hence, it easily gets beaten up by a more durable and sustainable LED grow-lights.

9.3.5 High-pressure sodium

Like MHs, high-pressure sodium (HPS) lights are also based on the same working principle as that of HID lights. Although they are not the best at present, HPS lighting systems are more efficient than several others in the past. They usually emit an orange light that is incredibly bright and powerful, as it is seen in Fig. 9.6. Sometimes, a combination of HPS and MH lamps are assembled in the same reflector, with either a single integrated ballast assembly or two separate ballast assemblies. The combination of blue MH light and orange HPS light creates an ideal spectral blend and extremely high outputs. HPS has a life span twice as that of MH lamps and a light output of 140 lumens per watt. Unfortunately, for the plant growers, these lights require a lot of power to run effectively and produce a large amount of heat in addition to hazardous

Figure 9.5 Metal halide grow-lights.

levels of CO_2 emission. In comparison, LED lighting has the ability to make use of more effective wavelengths that actually provide benefits to plants. The energy requirement for LEDs is much less, thereby making them cheaper than HPS lighting systems. LEDs certainly cost much more than HPS grow-lights in the initial phase, but the savings over time can make a huge difference as the plant growers reap out huge profits with LED grow-lights.

9.3.6 Plasma

Plasma grow-lights, as shown in Fig. 9.7, are often viewed as a relatively new and most advanced lighting technology, which is still proving to be excessively expensive for the massive majority of the consumers. Unlike traditional lighting systems, plasma grow-lights are free from the use of electrodes or filaments but have higher efficiency and longer lamp life on offer. Although very expensive, they are incredibly powerful and efficient enough to provide improved light spectrum, especially for the vegetative

Figure 9.6 High-pressure sodium grow-lamps.

Figure 9.7 Plasma grow-light fixtures.

growth. Plasma grow-lights save a lot of space and offer a great amount of benefits over other types of grow-lights that require ballasts and extensive wiring harnesses. Plasma grow-lights are much larger than their LED counterparts, although they are still smaller than the massive HID systems. Even though plasma light shows comparable efficiency with LED grow-lights, the former is placed at a higher price tag. Therefore, consumers prefer to go with the cheaper LED lights for indoor farming.

9.3.7 Induction light

Induction lights create light by using an electromagnetic field to excite mercury particles mixed in an inert gas. The mercury, present inside the lamp, creates a UV light that excites the phosphor coating inside the walls of the bulb to emit visible light. They do not use electrodes or filaments to get power to the light. Since those are the parts of a light bulb that tend to break first, induction lights have a much significantly longer life span than any other kind of light in the market today. The absence of electrodes also means a better sealed bulb, resulting in a high-quality grow-light that will stand the test of time. This also rules out the possibility of the phosphor material reacting with the metal electrodes and giving out hazardous products. Induction lights use 80% less mercury and produce five times less heat in comparison with the HPS or MH lamps. Some of the induction grow-lights in action can be seen in Fig. 9.8. Although induction grow-lights are cheaper than their LED counterparts, LEDs turn out to produce more savings and prove cheaper than the induction light in the long run. Induction grow-lights are efficient and let off almost no heat. However, LED grow-lights use less electricity than induction grow-lights and are more flexible in design due to each LED bulb having a different spectrum.

9.4 Light-emitting diodes in horticulture

Horticulture has developed the prospect to utilize artificial lighting sources of specific wavelengths for enhancing the productivity yield from crop plants. LEDs offer the choice of narrow spectral bands of desired wavelength for optimal absorption by chlorophyll to carry out the photosynthetic process [23]. The use of LED grow-lights has made it possible to cultivate crop plants even in space. On prolonged space expeditions, the supply of food often falls short and does not suffice the needs of space trekkers. A round trip space journey from the Earth to Mars would require atleast 1000 days, and this is exclusive of the stay on Mars by the crew members. It is indeed not a solution to carry huge stocks of food that could actually get spoiled and be nonedible with time. Fresh vegetables and fruits have a very short shelf-life in space. They must be consumed within a week of the space voyage. Most of the food for the space journey is kept unrefrigerated in lockers, which are in close proximity with the electrical equipment of the space shuttle. These equipment often heat up and transfer the heat to the nearby lockers containing food. As a result, the fresh food kept in the lockers experiences rapid increase in their spoilage. The other option is to send an unmanned lightweight rocket from the Earth to the destination in space with sufficient amount of food supply. But this will take a long time to reach the destination and

Figure 9.8 Induction grow-light fixtures.

can prove to be risky and nonreliable at several occasions. The best alternative is to cultivate crops locally in space and acquire fresh fruits and vegetables from them. This will also provide sufficient oxygen supply to the surrounding environment. LED grow-lights are the best available source for lighting up the crop plants in space. These are the safest source of lighting that shows least chances of damage, highest life span, and are miniature in size, specific in the emitted wavelength and maximum in efficiency. Using limited energy resources, it is possible to replicate the environment that a plant experiences on the Earth. LEDs can produce target lighting that suits well with the light requirements of a plant. The LED grow-lights have been specially designed to suit all types of farming in the horticulture domain. It has provided endless opportunities to farmers by offering various modules of lighting that includes toplighting, interlighting, supplemental light, and lights for multilayer cultivation.

Multilayer farming or the vertical farming requires grow-lights solely for providing light to plants. It is practiced indoors by maintaining the conditions such as heat, light, carbon dioxide, ventilation, and air condition under control [24]. Such type of farming has facilitated large scale of vegetation growth in a limited available land. This means that farming can be carried out in urban areas and the harvest obtained need not be transported to long distances for trade as it used to be done in case of field agriculture. Multilayer faming has the capacity to produce 100 times more crop yield annually as compared with an agricultural field. It also cannot be affected by the seasonal environmental conditions that occur outdoors. Farmers practicing multilayer farming are also benefited in terms of the expenses incurred for transportation and storage of their harvest. Since the distance between the production farms and the trade markets is reduced, the fuel consumption for transportation is reduced. Also, the harvest need not be kept for long durations under cooling during storage or transportation, and the time required for transporting these harvested products will be much shorter. All these benefits shall prove very profitable for farmers, and this will indirectly benefit the consumers too, who will be paying much lesser price for the food products yielded from multilayer farming. Vertical farms can be established in almost any empty area inside a city. This also proves to be a massive job opportunity for the people living in cities. However, vertical farming is limited for growing only high-value crop plants that are compact and grow quickly. Preferably, the height of the crops must be less than 30 cm, and it should be ready to be harvested in a month.

Bula et al. were the first group to investigate and acclaim the role of LEDs in the growth of a whole crop plant [25]. They conducted their trials on lettuce plants and observed their behavior under LED lights. Since lettuce is compact high-value plant that shows fast growth under controlled conditions, it formed the best choice to carry out the trials. The growth of potato, wheat, and spinach was also tested under the LED lights at about the same time [17,26]. During those days, the blue LEDs were still in their development and hence, were unavailable to conduct experiments on plants. Consequently, most of the plant growth experiments were conducted using the red LEDs in combination with the blue fluorescent lamps [27]. The results were fascinating enough to attract more research on LED-based plant grow-lights for the study of the plant physiological changes under LED lights [28,29]. But the high expenses incurred in manufacturing the LEDs, and their scarce availability in the

market compelled most of the people to continue with traditional fluorescent lamps or arc-based lamps for indoor farming. Thus, LED grow-lights were restricted only for research in greenhouses and growth chambers. Tissue cultures based on LEDs were suggested by Miyashita et al. for regulating the plantlet morphology by light [30]. A major portion of LED-based horticultures were investigated by the space research centers such as National Aeronautics and Space Administration (NASA) and Kennedy Space Center (KSC) to find ways to cultivate crops in space and meet the food requirements there itself [26,31]. The space odyssey to explore the moon and Mars with manned space vehicles has made it necessary to develop plant-based regenerative life support systems to fulfill the food requirements without requiring any need to carry huge loads of food along with them. This has even inspired many researchers to invest more on the indoor farming research and the methods to derive higher crop yield with better quality. Soon LEDs gained huge recognition for their ability to provide spectral quality suitable for plant growth in greenhouse chambers and space stations. It has also been possible to thwart the attacks of disease causing pathogens on plants by controlling the spectral quality [32].

There are significant anatomical changes observed in the leaf and stem morphologies of plants grown under LEDs. The anatomical morphologies of pepper (*Capsicum annuum* L.) plants grown under LED arrays and MH lamps were studied and compared by Schuerger et al. [33]. LED lights of different colors produced different morphology and phytochemical characteristics in basil plants. They can exert antifungal, antibacterial, and antimicrobial action too [24]. On maintaining the red/blue ratio as 0.7, the nutraceutical properties improved and the nitrate content decreased in basil leaves [34]. The phenolic content of basil (*Ocimum basilicum*) plants also increased under the LED grow-lights [35]. Phenolic compounds such as chicoric, p-coumaric, chlorogenic, caffeic, rosmarinic, and caftaric acids are richly available in basil [36,37]. Phenolic acids and flavonoids are the secondary metabolites that are produced by plants. To adapt with the biotic and abiotic alterations in the environment, plants make use of both the primary and secondary metabolites. The primary metabolites are the carbohydrates and amino acids. Phenolic compounds can act as ultraviolet screens, antioxidants as well as red and blue pigments in plants. Flavonoids such as quercetin, rutin, apigenin glucuronide, and kaempferol glucoside are known to have metal ion chelating properties. They also exhibit antimicrobial and antibacterial action, antioxidant activity, and radical scavenging [24]. Anthocyanins are another class of compounds that exhibit antimicrobial activity. They also attract insects and provide color to fruits and flowers. In addition, they give a protective shield to the plant cells against damage due to higher intensities of light by absorbing the blue and ultraviolet light [24]. Carotenoids can also serve protection to cell membranes against the damage due to excess light. These are terpenoid compounds that act as free radical scavengers and provide orange or yellow pigmentation to fruits and flowers [38]. Carotenoids have the ability to absorb in those regions of the visible light spectrum, which cannot be absorbed by chlorophyll. This light energy is then efficiently dissipated to the chlorophylls to enhance the photosynthetic activity. Green light is essential for increasing the carotenoid content in plants. A study on the lettuce plant showed that white light lacking the green component resulted in reduced carotenoids as well as

dry weight of roots and shoots [39]. In Chinese cabbage (Brassica campestris L.), the carotenoid concentrations and chlorophyll suffered a negative impact under the influence of red light [40]. The negative effects were extended to the chlorophyll biosynthetic precursors such as protoporphyrin IX, protochlorophyllide, Mg-protoporphyrin IX, and 5-aminolevulinic acid. Yet there were positive effects of red light on the plant's height. The combination of red and blue light as well as monochromatic blue lights favored to increase the carotenoids, soluble proteins, and chlorophyll in them but resulted in diminished plant height. The dry mass, soluble protein, and sugar concentrations were reduced when grown under monochromatic yellow light. Carotenoid accumulation was found to increase in mustard and mizuna microgreens when the light intensities were increased [41].

The impact of red and blue lights on the plant growth and yield is pointed out in a number of reports [42−44]. The quality and flavor of vegetables are often affected by the composition and accumulation of carbohydrates in them, which is impacted by the exposure of red and blue light on the plants [45,46]. In the case of *Oncidium* protocorm-like bodies, red light proved beneficial for the accumulation of carbohydrates, whereas blue light promoted the antioxidant enzyme activities and the protein content improvement in them [47]. Similarly, the tissue culture seedlings of upland cotton (*Gossypium hirsutum* L.) showed higher accumulation of sucrose and starch accompanied with increased root activity when they were grown under red LEDs alone [44]. The combination of red light and a higher amount of blue light from their respective LEDs resulted in higher biomass content, a larger and healthier plant of upland cotton [44]. Chen et al. investigated the enhancement in the accumulation of sucrose, starch, and biomass in lettuce that were exposed to alternating red and blue LEDs for different time intervals [48]. In another study, the combination of red, blue, and white lights increased the sucrose content in lettuce as compared with simple combination of red and blue LEDs [49]. As compared with the lettuce plant grown under normal white light, the lettuce grown under the white light lacking green component showed reduced net rate of photosynthesis, chlorophyll *a* and *b* contents, and dark respiration [39]. Metallo et al. investigated the influence of blue/red light treatment using LEDs on kale (*Brassica oleracea*), which were grown hydroponically [50]. When the kale plants were exposed for a short duration under LEDs with higher blue/red ratio, the biomass content increased, and there was a decrease in the chlorophyll fluorescence; also the height was shorter than that of the plant grown under a normal white LED. The exposure of kale plants to lower the blue/red ratio increased the potassium content but decreased the fructose content in them. The biomass content in cucumber can be promoted by exposing them under blue LEDs [51]. The exposure of red LEDs, on the other hand, suppressed the dry mass production in cucumber. When the cucumber plants were exposed to different combinations of red and blue LEDs, it was found that there was an increase in the leaf mass per unit area, stomatal conductance, chlorophyll content, and photosynthetic rate and decrease in the biomass, leaf area, plant height, and length of hypocotyl and epicotyl on having more blue light amount in these combinations. Cucumber's leaf area index is positively affected by exposure under green LEDs but results in the suppression of the chlorophyll concentration [52]. Red LEDs have contributed in significant enhancement of β-carotene contents and

antioxidant activity in pea seedlings, whereas blue LEDs have contributed towards their chlorophyll induction and seedling weight [53]. The root growth of *Cunninghamia lanceolata* tissue culture seedlings was most benefited with a combination of red, blue, purple, and green lights in the ratio of 8:1:1:1 [54].

9.5 Significance of light-emitting diode grow-lights

As such, grow-lights do not have any other special applications other than acting as an artificial light source to stimulate the plant growth by emitting an electromagnetic spectrum appropriate for photosynthesis. Grow-lights are used for horticulture, indoor gardening, plant propagation, and food production, including indoor hydroponics and aquatic plants [55]. LED grow-lights provide a safe and reliable supplement or replacement to natural light for the growth of potted, bedding, and young plants in greenhouse/climate chambers [56]. It improves the quality of seeding, cultivates healthy seedlings, and provides effective heat management. The heat management, provided by LED grow-lights, remarkably extends the service life of the electrical system by making huge savings on the air-conditioning expenditures. It also facilitates adjustable and controllable photoperiod to control the vegetative and reproductive growth of plants. A high-quality light recipe is achieved that fulfills the growth needs of young plants, seedlings, cuttings, or tissue culture. A major problem solved by LED grow-lights is the disruption of quality and growth of crop plants due to natural weather conditions such as cloudy, rainy, and snowy days. With the adoption of LED lights, farmers can precisely provide the desired light wavelength required for high-quality yields.

LED grow-lights maintain the uniformity of illumination with high luminous efficiency and reduce the distance between layers. It improves high-quality seeding rate and shortens the production cycle. The feasibility of city farms and kitchen indoor farming with huge energy savings becomes more possible with LED grow-lights. This achieves a reduction in the production costs and a continuous supply of high and stable yields with improved quality, nutrient content, and flavor. It also improves the possibility to deliver fresh vegetables at a relatively shorter period [57]. LEDs are also known to improve the taste and flavor of vegetables and fruits. They promote the growth of plants rapidly and can also help treat the plants affected by pathogens. LEDs are currently known to provide effective treatment to humans from a number of diseases [14]. This feature can be extended to plants as well. This will probably limit the usage of expensive and harmful pesticides that degrade the quality of the soil and the crops. Blue LEDs were successful in suppressing the gray mold disease caused by *Botrytis cinerea* in lettuce [58]. Downey mildew and powdery mildew pathogens that cause disease in the foliage and plants, respectively, are vulnerable when exposed to LEDs of some specific wavelengths. Thus, LED grow-lights have solved the challenge that farmers faced while growing vegetables, fruits, and flowers in high-density areas without using pesticides. LED grow-lights effectively improve the land-use rate and increase the yield per unit area by implementing multilayer cultivation as shown in Fig. 9.9. By utilizing the low heat characteristics of LEDs, interlighting among vegetables and flowers can be used to increase the vegetable production in

Figure 9.9 Multilayer farming using LED grow-lights. *LED*, light-emitting diode.

greenhouses. Since LEDs do not heat up unlike other artificial sources such as HID or MH grow-lights, less water can be provided to the crop plants. In a way, use of LED grow-lights reduces the water consumption, and this shall make indoor farming more effective in drought-affected areas. LED grow-lights complement the natural light with a spectrum and light intensity combination designed to promote plant growth. The scientifically designed illumination angle and light position allow plants to make maximum use of the light, thereby stabilizing and improving the plant yield and quality. Farmers also confronted the challenge of growing diverse crops that need different light spectra at different phases of the growth cycle. Here also, LED grow-lights had the advantage. They have the ability to tune the spectral quality of the light at various stages of plant growth. Farmers can regulate the spectral quality and quantity for different crops and different requirements at different phases of crop's growth cycle. LEDs can also be adjusted to offer photon energy at wavelengths optimum for plant photosynthesis. This leads to faster growth of plants accompanied by a higher yield. Implementation of LED grow-lights has enabled plant growers to harvest huge amounts of profit through vegetable production. One of the major concerns for farmers practicing indoor farming was the expenses incurred in setting up artificial lighting for their crops, and their anxieties were incredibly reduced with the induction of LED grow-lights.

9.6 Current market scenario

The proven efficiency of LED agricultural grow-lights in the indoor farming has helped them to snatch the global market at a very swift pace. The advanced technology made it possible to design the LED lights to increase the crop yield and quality of crops, vegetables, and fruits. Urban farming is greatly benefited from these advancements, and farmers are now able to reap huge profits. The biggest breakthrough came from the understanding that although plants require light, they do not need the

same amount of light to grow, nor do they require the same type of light source. This allowed farmers to adjust their resources as per the crop and inspired many farmers to take up indoor farming. LED grow-lights have been tailored to meet the requirements of plants and control the intensity of light, its duration, and color. This has facilitated the growth of LED lights as a major industrial asset in the horticulture domain. With the inclusion of LED lights, agriculture has become a large profitable industry that has opened up many business opportunities. As a result, plant growers of all dimensions are embracing LEDs to meet the demands of their farming. By application, horticulture is classified into subsections like greenhouse, indoor farming, vertical farming, and so on. Greenhouse farming is the most widely practiced and possessing the largest revenue shares in the global market. The dominance of greenhouse in the horticulture industry shall continue even in the upcoming years. Such type of farming enjoys the advantage of higher plant growth and crop yield owing to better protection from external elements such as strong wind and harsh sunlight as well as protection against pests and insects. In the near future, vertical farming is also expected to be more prevalent in urban environments. The shortage experienced in the availability of agricultural lands has boosted vertical farming techniques to optimize the available space. It enables the farmers to maximize the crop capacity in the limited land and optimize the cultivation conditions for its proper growth. The market of grow-lights is mainly driven by the growth of greenhouse farming, indoor, and vertical type of farming techniques. The harsh climatic conditions can be conveniently ignored, and the loss of crop yield due to such conditions will be almost none for the farmers practicing indoor farming. Currently, the replacement of HID grow-lights by LEDs has brought out much more profit in this farming.

The global market of grow-lights in 2018 accounts for $2.51 billion and is forecasted to register a compound annual growth rate (CAGR) of 20.44% by the end of the year 2023 [59]. The largest revenue earned by the grow-lights was from the commercial greenhouses, and it is estimated to lead the market share in the coming years too, owing to the rising demand of food supply and popularity of urban farming. If the regional markets are analyzed, the grow-light market in Europe has earned the highest share of revenues. The European market is driven by the government initiatives and the presence of key companies related to the manufacturing and marketing of grow-lights for the agricultural sector. The second highest share of revenues is currently held by North America, and this can be attributed to the adoption of novel farming methodologies and the increasing number of greenhouse chambers in the region [60]. The Asia−Pacific region is not far behind and is forecasted to overtake the North American region in terms of the revenue share very soon. In the global level, most of the farmers were using HID lamps for indoor farming. But the awareness among the farmers regarding the benefits of LED grow-lights has grown ever since its arrival in the market. This has led to a massive replacement of the existing grow-lights with LEDs, and now, LEDs comprise more than 40% of the global market in horticultural lamps. From Fig. 9.10, the growing share of LED grow-lights in the global market can be witnessed. The global market in this forecast period shall also experience a higher number of retrofit installation of grow-lights as compared to the new installations. The government initiatives to replace the existing hazardous

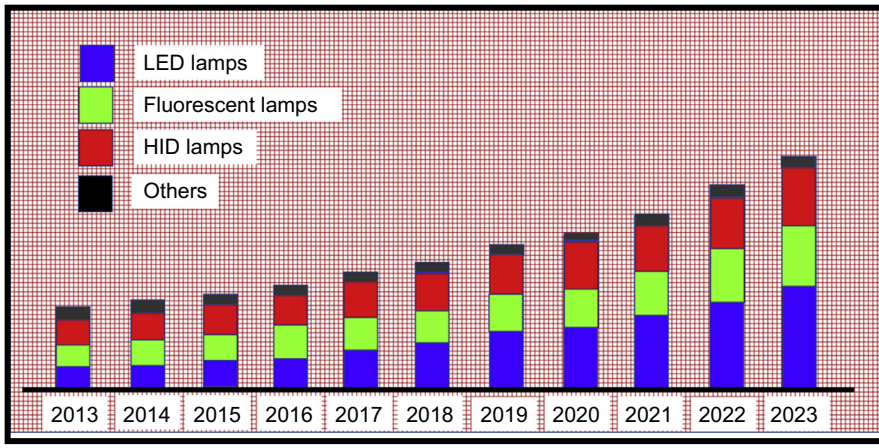

Figure 9.10 Global market share of different types of grow-lights (2013–23). *HID*, high intensity discharge; *LED*, light-emitting diode.

artificial light sources with LEDs has driven the LED grow-light markets in several countries. At the global level, the demand to reduce the energy consumption on lighting is on the rise, and hence, the governmental bodies are seeking the transition towards LED-dominated lighting industry. This has encouraged the governmental bodies to provide subsidiaries on LED lights and regulations on the use of incandescent and fluorescent lamps. Countries such as Brazil, United States, Venezuela, South Korea, Russia, Argentina, Mexico, Switzerland, Australia, Canada, Malaysia, and so on have already began on the phasing out of incandescent lamps and are replacing them with energy-efficient LED lamps. This has also supported the ongoing research on the photobiological effects of LEDs on plant physiology and morphology. Additionally, many companies have come forward to make investment in the profitable LED grow-light business and build a bright future for LEDs in the horticultural sector.

With the growth of business opportunities in the horticulture market, major LED-manufacturing companies such as Philips, Osram, and so on are dealing with ways to understand the effect of growing fruits, flowers, and vegetables in diverse weather conditions under various LED light wavelengths. The key players rooted in the horticultural light business involve the names of Signify (Philips lighting, Netherlands), Osram (Germany), General Electric Company (GE, United States), Gavita (Netherlands), Agrolux (Netherlands), Hortilux Schreder (Netherlands), PARsource (United States), Heliospectra (Sweden), Lumileds (Netherlands), Illumitex (United States), Lumigrow (United States), Maxigrow (United Kingdom), Bridgelux (United States), Hubbell (United States), and Eye Hortilux (United States). These companies have contributed a humongous share for the growth of LED grow-lights in the horticultural market. To further increase their market share and boost the profit in the sector, the companies are engaged in a stiff competition with each other. This has proven a golden opportunity for the farmers in the horticultural sector, as the competition has provoked these companies to come out with a better grow-light that could provide better

performance and benefits than the existing ones. Their research activities have boosted the knowledge regarding the impact of the spectral quality and quantity on the growth and quality of plants and, thereby, paved way for more specifically designed LED grow-lights. Philips lighting is a leading multinational company in LEDs. In 2018, Philips lighting has renamed its lighting products under the brand name of Signify. They launched an energy-efficient Philips GreenPower LED flowering lamp to extend the daylight and interrupt the night growing cycles in greenhouse chambers for farmers growing strawberries, bedding plants, cut flowers, and plant cuttings. The newer version of Philips GreenPower modules are built on the first generation of Philips GreenPower LEDs, and they are optimized for closed, climate-controlled cultivation facilities such as vertical farms, propagation, and research chambers that make use of multilayer farming to cultivate crops such as herbs, young tender plants, lettuce, spinach, and other green leafy vegetables and soft fruits. These highly energy-efficient grow-lights can steer the growth of crop plants with better precision and flexibility and aims to increase the crop yield, quality, and consistency. It holds the ability to accelerate flowering and serve the needs of farmers practicing indoor farming. They are designed with a standard E26 or E27 fitting to allow their installation in the existing setup and avoid unnecessary expenses in modifications. Philips lighting has developed certain recipes of light that makes use of the light intensity, spectrum, positioning, uniformity, and duration. By altering these characteristics as per the requirement of plant, farmers were able to achieve better yield from their crops. This has led to the pushing away of the boundaries of farmers that are used to restrict them from gaining control over the crop yield and quality. Philips GreenPower lamp also follows a similar policy and is available in two different variants. The first variant consists of a combination of white and deep red, whereas the other offers the combination of white, deep-red, and far-red colors. The first variant is effective in inhibiting the flowering in short-day plants, whereas the second variant is effective in providing photoperiodic lighting for perennials and bedding plants. It can monitor and interrupt the night cycle to extend the daylight availability to plants and promote the growth and strength of stems of plants such as strawberries and stimulate the flowering in them. Philips GreenPower lamps come with an appearance of an incandescent lamp but are purely made of LEDs assembled inside a robust plastic dome. Such type of design is provided keeping the safety of crop plants in the front line. This will help to mitigate the jeopardy of damage to crop plants from the broken pieces of glass lamps. Philips claims that GreenPower lamps can last for about 25,000 hours with 90% flux maintenance and is rated for IP44 and UL dry and damp conditions indoors. It is also found to perform much better on the energy grid in comparison with the incandescent and CFL grow-lights.

Osram Sylvania has released its Zelion HL300 series of horticulture LED fixtures that are available for various phases of plant growth. This series of lamps can be dimmable and tunable along the full spectrum of light so as to adjust to the plant requirements. The series consists of three variants, namely, Zelion HL300 Grow-Light, Zelion HL300 Grow White, and Zelion HL300 Sunlight. Zelion HL300 Grow-Light is designed to commercially boost the horticulture market and are generally used as supplemental light for crops to give better yield and quality. Zelion HL300

Sunlight is recommended for providing natural daylight artificially to crops that require natural sunlight. Zelion HL300 Grow White is a combination of the spectrum provided by the other two variants. Such fixtures are most recommended for the climate chambers wherein higher photosynthetic activity among the crop plants is required. These horticulture lamps use superior quality Osram Oslon LEDs that are manufactured by the Osram optosemiconductors and are merited with long life. They emit light in the visible light region covering the spectrum from 400 to 700 nm, which is the photosynthetically active region and suitable for plant growth. These lights are designed to withstand the greenhouse environment for optimum crop production. They provide the essential spectral quantity and quality needed for superior photosynthetic performance accompanied by optimum energy savings. The Zelion HL300 series have kept a nice attention on two important parameters. The first one is the maintenance of the temperature of the fixture during its operation. It has a patented active cooling system that enables the lamp to maintain a low temperature during operation and ensure long life over the span of the fixture. The second parameter is the uniformity of the spectral distribution on the plant canopy, and this is also taken good care of by the HL300 series lamps.

Optimization of LEDs to enhance the photosynthetic activity by bringing about technological advancements in them can lead to the growth of grow-light market. This can be achieved by utilizing the profound knowledge gained on the plant physiology and the photosynthetic activity to systematically adjust the LEDs to function as per the plant's requirement. Modern LED grow-lights come with the ability to control temperature and spectral parameters depending on the crop to optimize the photosynthesis. Another advantage is the emergence of advanced softwares and calculators for horticultural lighting that can intelligently maneuver the light output. Several manufacturers of grow-lights have begun developing softwares with the help of botanical researchers to provide a reliable agricultural lighting for better yield from crops and achieve the targeted harvest. The amount of light wasted on the walls or illuminating the aisles can be focused precisely on the plants by using these softwares.

9.7 Conclusions

The virtues hailed by LEDs during their operation have tremendously benefited farmers practicing vertical farming and have also shielded them from the wrath of unpredictable weather conditions. The use of artificial lighting systems as primary and supplemental light sources for the cultivation of crops has not been a new idea, but this concept became more feasible with the entry of LEDs in to the market. The use of conventional light sources such as incandescence lamps, fluorescence lamps, HID lamps, and so on proved uneconomical and risky for the farmers. However, all the apprehensions of adopting artificial lighting for plant cultivation were removed when LEDs stepped into the pivotal role of grow-lights. The clear-cut advantages of LEDs over other artificial sources have put them on the driving seat and increased the potential to reap out huge profits from vertical farming.

References

[1] H. Poorter, O. Nagel, The role of biomass allocation in the growth response of plants to different levels of light, CO_2, nutrients and water: a quantitative review, Funct. Plant Biol. 27 (2000), 1191−1191.

[2] R. Singh, P. Srivastava, P. Singh, S. Upadhyay, A.S. Raghubanshi, Human overpopulation and food security, in: Urban Agric. Food Syst., IGI Global, 2019, pp. 439−467, https://doi.org/10.4018/978-1-5225-8063-8.ch022.

[3] W.D. Dar, C.L. Laxmipathi Gowda, Declining agricultural productivity and global food-security, J. Crop Improv. 27 (2013) 242−254, https://doi.org/10.1080/15427528.2011.653097.

[4] W.R. Briggs, Photoreceptors in plant photomorphogenesis to date. Five phytochromes, two cryptochromes, one phototropin, and one superchrome, Plant Physiol. 125 (2001) 85−88, https://doi.org/10.1104/pp.125.1.85.

[5] K. Solymosi, A. Keresztes, Plastid structure, diversification and interconversions II. Land plants, Curr. Chem. Biol. 6 (2013) 187−204, https://doi.org/10.2174/2212796811206030003.

[6] J. Barber, B. Andersson, Too much of a good thing: light can be bad for photosynthesis, Trends Biochem. Sci. 17 (1992) 61−66, https://doi.org/10.1016/0968-0004(92)90503-2.

[7] K. Solymosi, B. Schoefs, Etioplast and etio-chloroplast formation under natural conditions: the dark side of chlorophyll biosynthesis in angiosperms, Photosynth. Res. 105 (2010) 143−166, https://doi.org/10.1007/s11120-010-9568-2.

[8] W.L. Butler, K.H. Norris, H.W. Siegelman, S.B. Hendricks, Detection, assay, and preliminary purification of the pigment controlling photoresponsive development of plants, Proc. Natl. Acad. Sci. U.S.A. 45 (1959) 1703−1708, https://doi.org/10.1073/pnas.45.12.1703.

[9] G.F. Deitzer, R. Hayes, M. Jabben, Kinetics and time dependence of the effect of far red light on the photoperiodic induction of flowering in wintex barley, Plant Physiol. 64 (2008) 1015−1021, https://doi.org/10.1104/pp.64.6.1015.

[10] E.P. Spalding, K.M. Folta, Illuminating topics in plant photobiology, Plant Cell Environ. 28 (2005) 39−53, https://doi.org/10.1111/j.1365-3040.2004.01282.x.

[11] M. Rehman, S. Ullah, Y. Bao, B. Wang, D. Peng, L. Liu, Light-emitting diodes: whether an efficient source of light for indoor plants? Environ. Sci. Pollut. Res. 24 (2017) 24743−24752, https://doi.org/10.1007/s11356-017-0333-3.

[12] G.D. Goins, N.C. Yorio, M.M. Sanwo, C.S. Brown, Photomorphogenesis, photosynthesis, and seed yield of wheat plants grown under red light-emitting diodes (LEDs) with and without supplemental blue lighting, J. Exp. Bot. 48 (1997) 1407−1413, https://doi.org/10.1093/jxb/48.7.1407.

[13] C.F. Johnson, C.S. Brown, R.M. Wheeler, J.C. Sager, D.K. Chapman, G.F. Deitzer, Infrared light-emitting diode radiation causes gravitropic and morphological effects in dark-grown oat seedlings, Photochem. Photobiol. 63 (1996) 238−242, https://doi.org/10.1111/j.1751-1097.1996.tb03020.x.

[14] G.B. Nair, S.J. Dhoble, A perspective perception on the applications of light-emitting diodes, Luminescence 30 (2015) 1167−1175, https://doi.org/10.1002/bio.2919.

[15] A. Wishkerman, E. Wishkerman, Application note: a novel low-cost open-source LED system for microalgae cultivation, Comput. Electron. Agric. 132 (2017) 56−62, https://doi.org/10.1016/j.compag.2016.11.015.

[16] C.M. Bourget, An introduction to light-emitting diodes, HortScience 43 (2008) 1944−1946.

[17] R.C. Morrow, LED lighting in horticulture, HortScience 43 (2008) 1947−1950, https://doi.org/10.21273/HORTSCI.43.7.1947.
[18] D. Singh, C. Basu, M. Meinhardt-Wollweber, B. Roth, LEDs for energy efficient greenhouse lighting, Renew. Sustain. Energy Rev. 49 (2015) 139−147, https://doi.org/10.1016/j.rser.2015.04.117.
[19] S. Jatothu, B. Dutta Gupta, Fundamentals and applications of light-emitting diodes (LEDs) in in vitro plant growth and morphogenesis, Plant Biotechnol. Rep. 7 (2013) 211−220, https://doi.org/10.1007/s11816-013-0277-0.
[20] K.M. Folta, L.L. Koss, R. McMorrow, H.H. Kim, J.D. Kenitz, R. Wheeler, J.C. Sager, Design and fabrication of adjustable red-green-blue LED light arrays for plant research, BMC Plant Biol. 5 (2005), https://doi.org/10.1186/1471-2229-5-17.
[21] N. Yeh, J.P. Chung, High-brightness LEDs-Energy efficient lighting sources and their potential in indoor plant cultivation, Renew. Sustain. Energy Rev. 13 (2009) 2175−2180, https://doi.org/10.1016/j.rser.2009.01.027.
[22] G.D. Massa, H.H. Kim, R.M. Wheeler, C.A. Mitchell, Plant productivity in response to LED lighting, HortScience 43 (2008) 1951−1956.
[23] C.A. Mitchell, M.P. Dzakovich, C. Gomez, R. Lopez, J.F. Burr, R. Hernández, C. Kubota, C.J. Currey, Q. Meng, E.S. Runkle, C.M. Bourget, R.C. Morrow, A.J. Both, Light-emitting diodes in horticulture, in: Hortic. Rev., vol. 43, John Wiley & Sons, Inc., Hoboken, New Jersey, 2015, pp. 1−88, https://doi.org/10.1002/9781119107781.ch01.
[24] F. Bantis, S. Smirnakou, T. Ouzounis, A. Koukounaras, N. Ntagkas, K. Radoglou, Current status and recent achievements in the field of horticulture with the use of light-emitting diodes (LEDs), Sci. Hortic. 235 (2018) 437−451, https://doi.org/10.1016/j.scienta.2018.02.058.
[25] R.J. Bula, R.C. Morrow, T.W. Tibbitts, D.J. Barta, R.W. Ignatius, T.S. Martin, Light emitting diodes as a radiation source for plants, HortScience 26 (1991) 203−205.
[26] D.J. Barta, T.W. Tibbitts, R.J. Bula, R.C. Morrow, Evaluation of light emitting diode characteristics for a space-based plant irradiation source, Adv. Space Res. 12 (1992) 141−149, https://doi.org/10.1016/0273-1177(92)90020-X.
[27] M.E. Hoenecke, R.J. Bula, T.W. Tibbitts, Importance of 'Blue' photon levels for lettuce seedlings grown under red-light-emitting diodes, HortScience 27 (1992) 427−430, https://doi.org/10.21273/HORTSCI.27.5.427.
[28] D.J. Tennessen, E.L. Singsaas, T.D. Sharkey, Light-emitting diodes as a light source for photosynthesis research, Photosynth. Res. 39 (1994) 85−92, https://doi.org/10.1007/BF00027146.
[29] D.J. Tennessen, R.J. Bula, T.D. Sharkey, Efficiency of photosynthesis in continuous and pulsed light emitting diode irradiation, Photosynth. Res. 44 (1995) 261−269, https://doi.org/10.1007/BF00048599.
[30] Y. Miyashita, T. Kimura, Y. Kitaya, C. Kubota, T. Kozai, Effects of red light on the growth and morphology of potato plantlets in vitro: using light emitting diodes (LEDS) as a light source for micropropagation, Acta Hortic. 418 (1997) 169−173.
[31] B.C. Tripathy, C.S. Brown, H.G. Levine, A.D. Krikorian, Growth and photosynthetic responses of wheat plants grown in space, Plant Physiol. 110 (1996) 801−806, https://doi.org/10.1104/pp.110.3.801.
[32] A.C. Schuerger, C.S. Brown, Spectral quality affects disease development of three pathogens on hydroponically grown plants, HortScience 32 (1997) 96−100.
[33] A.C. Schuerger, C.S. Brown, E.C. Stryjewski, Anatomical features of pepper plants (*Capsicum annuum* L.) grown under red light-emitting diodes supplemented with blue or far-red light, Ann. Bot. 79 (1997) 273−282, https://doi.org/10.1006/anbo.1996.0341.

[34] C. Piovene, F. Orsini, S. Bosi, R. Sanoubar, V. Bregola, G. Dinelli, G. Gianquinto, Optimal red:blue ratio in led lighting for nutraceutical indoor horticulture, Sci. Hortic. 193 (2015) 202−208, https://doi.org/10.1016/j.scienta.2015.07.015.
[35] F. Bantis, T. Ouzounis, K. Radoglou, Artificial LED lighting enhances growth characteristics and total phenolic content of *Ocimum basilicum* , but variably affects transplant success, Sci. Hortic. 198 (2016) 277−283, https://doi.org/10.1016/j.scienta.2015.11.014.
[36] E.M. Kwee, E.D. Niemeyer, Variations in phenolic composition and antioxidant properties among 15 basil (*Ocimum basilicum* L.) cultivars, Food Chem. 128 (2011) 1044−1050, https://doi.org/10.1016/j.foodchem.2011.04.011.
[37] G. Zgórka, K. Glowniak, Variation of free phenolic acids in medicinal plants belonging to the Lamiaceae family, J. Pharmaceut. Biomed. Anal. 26 (2001) 79−87, https://doi.org/10.1016/S0731-7085(01)00354-5.
[38] A.E. Solovchenko, M.N. Merzlyak, Screening of visible and UV radiation as a photoprotective mechanism in plants, Russ. J. Plant Physiol. 55 (2008) 719−737, https://doi.org/10.1134/S1021443708060010.
[39] H. Liu, Y. Fu, M. Wang, H. Liu, Green light enhances growth, photosynthetic pigments and CO_2 assimilation efficiency of lettuce as revealed by 'knock out' of the 480−560 nm spectral waveband, Photosynthetica 55 (2017) 144−152, https://doi.org/10.1007/s11099-016-0233-7.
[40] X. Fan, J. Zang, Z. Xu, S. Guo, X. Jiao, X. Liu, Y. Gao, Effects of different light quality on growth, chlorophyll concentration and chlorophyll biosynthesis precursors of non-heading Chinese cabbage (*Brassica campestris* L.), Acta Physiol. Plant. 35 (2013) 2721−2726, https://doi.org/10.1007/s11738-013-1304-z.
[41] J.K. Craver, J.R. Gerovac, R.G. Lopez, D.A. Kopsell, Light intensity and light quality from sole-source light-emitting diodes impact phytochemical concentrations within Brassica microgreens, J. Am. Soc. Hortic. Sci. 142 (2017) 3−12, https://doi.org/10.21273/JASHS03830-16.
[42] Z. Yang, Y. Qin, G. Hu, T. Wang, H. Wang, X. Huang, Patterns of enzyme activities and gene expressions in sucrose metabolism in relation to sugar accumulation and composition in the aril of Litchi chinensis Sonn, J. Plant Physiol. 170 (2013) 731−740, https://doi.org/10.1016/j.jplph.2012.12.021.
[43] H. Li, C. Tang, Z. Xu, The effects of different light qualities on rapeseed (*Brassica napus* L.) plantlet growth and morphogenesis in vitro, Sci. Hortic. 150 (2013) 117−124, https://doi.org/10.1016/j.scienta.2012.10.009.
[44] H. Li, Z. Xu, C. Tang, Effect of light-emitting diodes on growth and morphogenesis of upland cotton (*Gossypium hirsutum* L.) plantlets in vitro, Plant Cell Tissue Organ Cult. 103 (2010) 155−163, https://doi.org/10.1007/s11240-010-9763-z.
[45] L.S. Magwaza, U.L. Opara, Analytical methods for determination of sugars and sweetness of horticultural products-A review, Sci. Hortic. 184 (2015) 179−192, https://doi.org/10.1016/j.scienta.2015.01.001.
[46] D.M. Beckles, Factors affecting the postharvest soluble solids and sugar content of tomato (*Solanum lycopersicum* L.) fruit, Postharvest Biol. Technol. 63 (2012) 129−140, https://doi.org/10.1016/j.postharvbio.2011.05.016.
[47] L. Mengxi, X. Zhigang, Y. Yang, F. Yijie, Effects of different spectral lights on Oncidium PLBs induction, proliferation, and plant regeneration, Plant Cell Tissue Organ Cult. 106 (2011) 1−10, https://doi.org/10.1007/s11240-010-9887-1.
[48] X. Chen, L. Wang, T. Li, Q. Yang, W. Guo, Sugar accumulation and growth of lettuce exposed to different lighting modes of red and blue LED light, Sci. Rep. 9 (2019) 6926, https://doi.org/10.1038/s41598-019-43498-8.

[49] K.-H. Lin, M.-Y. Huang, W.-D. Huang, M.-H. Hsu, Z.-W. Yang, C.-M. Yang, The effects of red, blue, and white light-emitting diodes on the growth, development, and edible quality of hydroponically grown lettuce (*Lactuca sativa* L. var. capitata), Sci. Hortic. 150 (2013) 86−91, https://doi.org/10.1016/j.scienta.2012.10.002.

[50] R.M. Metallo, D.A. Kopsell, C.E. Sams, N.R. Bumgarner, Influence of blue/red vs. white LED light treatments on biomass, shoot morphology, and quality parameters of hydroponically grown kale, Sci. Hortic. 235 (2018) 189−197, https://doi.org/10.1016/j.scienta.2018.02.061.

[51] R. Hernández, C. Kubota, Tomato seedling growth and morphological responses to supplemental led lighting red:blue ratios under varied daily solar light integrals, Acta Hortic. (2012) 187−194, https://doi.org/10.17660/ActaHortic.2012.956.19.

[52] M.C. Snowden, K.R. Cope, B. Bugbee, Sensitivity of seven diverse species to blue and green light: interactions with photon flux, PLoS One 11 (2016) e0163121, https://doi.org/10.1371/journal.pone.0163121.

[53] M. Wu, C. Hou, C. Jiang, Y. Wang, C. Wang, H. Chen, H. Chang, A novel approach of LED light radiation improves the antioxidant activity of pea seedlings, Food Chem. 101 (2007) 1753−1758, https://doi.org/10.1016/j.foodchem.2006.02.010.

[54] Y. Xu, Y. Liang, M. Yang, Effects of composite LED light on root growth and antioxidant capacity of *Cunninghamia lanceolata* tissue culture seedlings, Sci. Rep. 9 (2019) 9766, https://doi.org/10.1038/s41598-019-46139-2.

[55] N. Yeh, T.J. Ding, P. Yeh, Light-emitting diodes′ light qualities and their corresponding scientific applications, Renew. Sustain. Energy Rev. 51 (2015) 55−61, https://doi.org/10.1016/j.rser.2015.04.177.

[56] E. Darko, P. Heydarizadeh, B. Schoefs, M.R. Sabzalian, Photosynthesis under artificial light: the shift in primary and secondary metabolism, Philos. Trans. R. Soc. B Biol. Sci. 369 (2014), https://doi.org/10.1098/rstb.2013.0243, 20130243−20130243.

[57] J. Fanwoua, G. Vercambre, G. Buck-Sorlin, J.A. Dieleman, P. de Visser, M. Génard, Supplemental LED lighting affects the dynamics of tomato fruit growth and composition, Sci. Hortic. 256 (2019) 108571, https://doi.org/10.1016/j.scienta.2019.108571.

[58] H.-S. Kook, S.-H. Park, Y.-J. Jang, G.-W. Lee, J.S. Kim, H.M. Kim, B.-T. Oh, J.-C. Chae, K.-J. Lee, Blue LED (light-emitting diodes)-mediated growth promotion and control of Botrytis disease in lettuce, Acta Agric. Scand. Sect. B Soil Plant Sci. 63 (2013) 271−277, https://doi.org/10.1080/09064710.2012.756118.

[59] Horticulture Lighting Market 2019 Global Analysis by Industry Size, Growth, Business Strategies, Opportunities, Leading Companies, Emerging Technology and Forecast 2023, 2019. https://www.reuters.com/brandfeatures/venture-capital/article?id=117970. (Accessed 29 July 2019).

[60] Horticulture Lighting Market 2019 Global Share, Trend, Segmentation and Forecast to 2028, 2019. https://www.marketwatch.com/press-release/horticulture-lighting-market-2019-global-share-trend-segmentation-and-forecast-to-2028-2019-04-11. (Accessed 29 July 2019).

Current trends and innovations 10

10.1 Introduction

For the past two decades, the optoelectronics industry has witnessed a strong growth that was fueled by the back-to-back emergence of high-profile devices. LEDs are one of the key contributors to the growth of optoelectronics market in all these years. High-brightness LEDs (HB-LEDs) have already surpassed the luminous efficacy demonstrated by the once efficient CFLs. From the beginning of the last decade, HB-LEDs have made strong sales in the backlighting systems for the displays of LCD TVs, computers, smartphones, and tablets [1]. The penetration of HB-LEDs into these applications has almost reached 100%. This compelled the manufacturers to increase the production capacity of HB-LEDs. They have also focused on improving the efficiency and quality of light as well as cutting down the costs on its production [2]. HB-LEDs have now captured the lighting market in the major sectors such as outdoor lighting, automotive lighting, digital signs, and indoor lighting.

The tremendous growth and change experienced by the LED industry have led to several new opportunities and businesses for many industries. The lowering costs, increasing efficiencies, and improving device structures have made the LED industry a leader in the lighting industry. LEDs have achieved many great strides to become an inevitable part of all the new recent technologies to make human life more comfortable and easier. They ended the realm of incandescent bulbs and fluorescent tubes in a short span of time. The LED lights meant for general illumination have got modified to deliver additional features too. The newer versions of LED luminaires are specially designed to provide a dynamic beam spread without any moving parts. This feature has found applications in the systems requiring customized control over the beam. Another modification is the removal of the external circuit board drivers that were earlier highly essential for the LED lighting systems. Traditionally, external drivers were meant for the conversion of electricity supply from the mains to a form suitable for the stable operation of LEDs. The removal of external drivers from the emerging new LED products has made them compact and the LEDs have itself become capable to handle the power requirements. Newer manufacturing processes have led to the creation of LED arrays in flexible foils. A roll-to-roll manufacturing process was found suitable for developing flexible LED displays that comprise printed electronics. The ultra-thin design of LEDs has made them applicable in various fields. Newer models of TVs and smartphones feature flexible thin displays made of such LEDs that contribute to reducing the size and weight of the device.

The Fundamentals and Applications of Light-Emitting Diodes. https://doi.org/10.1016/B978-0-12-819605-2.00010-0

LEDs are not just a mere means of lighting, but it has brought about a revolution in the life of mankind. It has touched innumerable fields of application wherein no other lighting sources were able to reach. They have captured two-thirds of the global lighting market and have extended their influence on other sectors such as display industry, horticulture, food storage, data transmission and digital communication, skin rejuvenation, and medical treatment. [3]. A number of organizations have shifted their research on LEDs citing their omnipotent applications in diverse fields. Efforts are being put to design appropriate LED products that can fit into each of the individual applications and initiate their actual commercialization for the world to enjoy a more comfortable and luxurious life.

10.2 Overview on the past and present trends in LEDs

Light has become an inseparable part of human life. Light decides how productive an individual can be at his work, how quickly he can recover from an illness, and how well he can learn. Over a century ago, people accustomed to oil lamps and candles were amazed with the popularity of the incandescent bulbs. This invention was seen as the ultimate and ideal light source. Years passed by and the society witnessed newer technologies, which were far better in efficiency and performance. Yet none were as amazing and innovative as the LEDs. In the early days of LEDs' emergence, R. Haitz made some observations and forecasted about the future of LEDs and its steady improvement accompanied by declining prices, as shown in Fig. 10.1 [4].

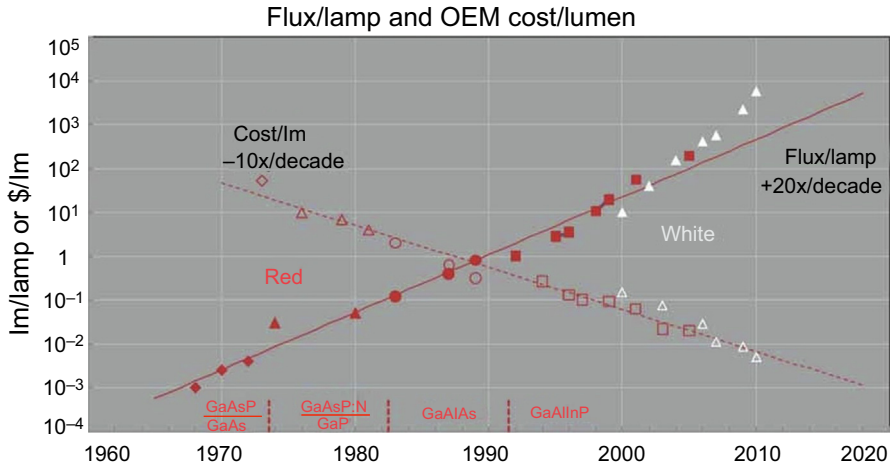

Figure 10.1 Haitz Law forecasting about the variation of light output and cost per lumen for every decade.
Reproduced with permission from Ref. R. Haitz, J.Y. Tsao, Solid-state lighting: 'The case' 10 years after and future prospects, Phys. Status Solidi 208 (2011) 17−29. doi:10.1002/pssa.201026349, Copyright. 2011 WILEY-VCH Verlag GmbH and Co. KGaA, Weinheim.

According to Haitz, the quantity of light generated from an LED will increase by a factor of 20 and the cost incurred per lumen output will fall by a factor of 10, in every decade. This trend was supposed to level off by 2016, but the improvements still continue to appear in the LED technology. Every year, LED packages come out with new streamlined mechanical and optical designs, improved electronic drivers, and enhanced performance. LED fixtures have evolved, not only in the design but also in the range of applications. LEDs have successfully found applications in diverse fields such as horticulture, food storage, dentistry, medical treatment, display devices, high-speed digital communication, and indoor and outdoor lighting, The LED lighting fixtures are becoming smarter and now, and they are not just limited to general lighting. LEDs are designed to send high-frequency modulation signals that can be picked up by a smartphone or other devices. It is, now, possible to control the color hue of the LED lamp using a smartphone and automatically switch it on/off.

Although consumers usually just want their lights to be turned on or off as per their needs, many consumers always desire to extract something more from their luminaires. LEDs have stood up to the demands of these consumers, and now, LED luminaires are twice as efficient as the ones that were introduced half a decade ago. The introduction of several new materials and technologies boosted the efficacy and performance of LED luminaires and has brought down the production costs to a considerable level. The cost of LED luminaires is now comparable to that of CFLs, and this has accelerated the adoption of LED lighting in almost every segment. Their prices have now declined to a point that every sector relies on LEDs as the most economical choice available in the market. The market potential offered by the LEDs is acting as a driving force for its development and growth. There is a rapid growth of LED lighting in the global market and the projected growth is mainly propelled by the rising demand from an ever-growing population and the progressive development of nations. The annual global shipment of LED products is projected to reach 14 billion units in the year 2022 [5]. The global lighting market is anticipated to reach USD 92.4 billion in the same year.

10.3 Innovations in the structure and designing of LEDs

To achieve a more effective connection between humans and electronics, researchers are now focusing their attention on the development of wearable electronics. This has propelled the research on the related materials like e-textile, wherein human-friendly fabrics were integrated with electronic components to provide some additional features to the human wear. A research group headed by Kyung Cheol Choi developed a fiber-based polymer LED that can be woven to create wearable fabric [6]. These fibers can be subjected to mass production just as polyethylene or nylon fibers. These polymer fibers will open the door for flexible wearable displays and lower the barriers encountered while introducing flexible wearable displays into the market. Earlier, wearable displays were produced by coating the emitting layer on a hard substrate and then attaching them onto the surface of the fabric. However, such

displays were not flexible and were susceptible to damage. With the introduction of polymer fibers, it has become possible to LED displays that carry the features of a display device as well as a fabric. The light-emitting fibers were developed in the laboratory using the dip-coating process. This method involved a lot of dipping and drying and was assumed to be a more efficient process than any heat-treatment method for the application of LED fibers over small cylindrical structures. In addition, dip coating is much more effective than the inkjet printing, screen printing, or spin coating methods, as the former allows concentric coating of fibers easily. The process involved the dipping of a fiber of polyethylene terephthalate (PET) into a solution of PEDOT:PSS (poly(3,4-ethylene dioxythiophene) polystyrene sulfonate). This was, then, dried at 130 °C for half an hour. After drying, the fiber was again dipped in a bath of super yellow (poly-(*p*-phenylenevinylene) polymer OLED) solution. The dipped fiber was, then, dried in an oven and coated with LiF/Al cathode material. This process is a simple, cheap, and effective method that can accelerate the production of wearable displays. Fig. 10.2 shows the microscopic images of the polymer fiber emitting light when operated at 8 V and a bare fiber.

Currently, most of the wearable displays are fabricated using OLEDs. In most cases, OLEDs are fabricated on a glass substrate and encapsulated using a glass lid. However, the flexibility of OLEDs is lost with the use of glass encapsulation. The next generation of tablets, smartphones, and wearable displays shall be completely based on flexible displays, for which the glass-encapsulated OLEDs will not be appropriate. For such flexible displays, graphene-based ultrabarrier materials will suit the best. Graphene is granted with an excellent thermal and chemical stability accompanied by a fine carbon lattice and a densely packed structure [7]. Graphene can turn out to be an amazing barrier to liquids and gases [8]. Due to its flexibility, robustness, and transparency to visible light, it is considered as an excellent barrier film for the encapsulation of flexible OLEDs. In addition, the high conductivity of graphene acts as an added advantage in the development of graphene LEDs with more efficiency, long-lasting life, and brightness. Seo et al. used multistacked graphene films

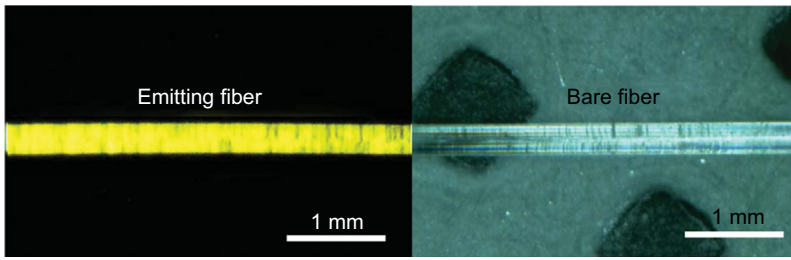

Figure 10.2 Microscopic images of the polymer fiber emitting light when operated at 8 V and a bare fiber.
Reproduced with permission from Ref. S. Kwon, W. Kim, H. Kim, S. Choi, B.-C. Park, S.-H. Kang, K.C. Choi, High luminance fiber-based polymer light-emitting devices by a dip-coating method, Adv. Electron. Mater. 1 (2015) 1500103. doi:10.1002/aelm.201500103, Copyright. 2015 WILEY-VCH Verlag GmbH and Co. KGaA, Weinheim.

with a polydimethylsiloxane buffer on a PET substrate to demonstrate a simple, low-cost, scalable, transparent, and flexible lamination encapsulation for OLEDs [9]. The graphene innovation is hugely led by the United Kingdom (UK), whose market in graphene is expected to touch GBP 800 million by 2023. The University of Cambridge, the National Physical Laboratory, the Centre for Process Innovation, and the business partner FlexEnable Ltd. have joined hands to work together on a combined project on graphene to scale-up its manufacturing landscape in the UK. They investigated the feasibility of producing graphene-based barrier films for the next-generation flexible OLED lighting and display products. Graphene is impervious to many molecules and hence, will provide significant blocking of liquids and gases, thereby enabling them to be a perfect barrier material for OLEDs. Another competitive technology that has been regarded as an appealing product for high-quality display panels and solid-state lighting (SSL) devices is the solution-processed OLEDs (s-OLEDs). The s-OLEDs have shown superior properties than the vacuum-evaporated OLEDs (v-OLEDs). The production costs involved in the development of s-OLEDs is far less than the v-OLEDs [10,11]. Burroughes et al. reported the first conjugated polymer-based s-OLEDs in 1990 [12]. Since then, several huge achievements were made in this field [13−17]. The need to achieve s-OLEDs, which are consuming a lesser amount of energy, has led to several serious efforts for the exploration of the methods and designs suitable for realizing energy-efficient s-OLEDs. Quantum dots (QDs) have also set a mark in the LED industry and are set to outperform the phosphor-converted LEDs (pc-LEDs) in general lighting. QDs have already put up a tough competition with the OLEDs in the display industry. QDs are known to produce tunable emission with low back-scattering loss. Their dominance in the display and general illumination has been long anticipated. However, they were held back due to certain difficulties in withstanding the on-chip LED temperature and photoflux intensity. The passivation of QDs turned out to be a solution to many such difficulties that hindered their path to commercial applications [18]. This resulted in the improvement of the spectral luminous efficacies of QDs way better than pc-LEDs, as illustrated in Fig. 10.3. In the case of bare QDs (nonpassivated QDs), the electrons from the conduction band can get trapped in the surface states that can decay

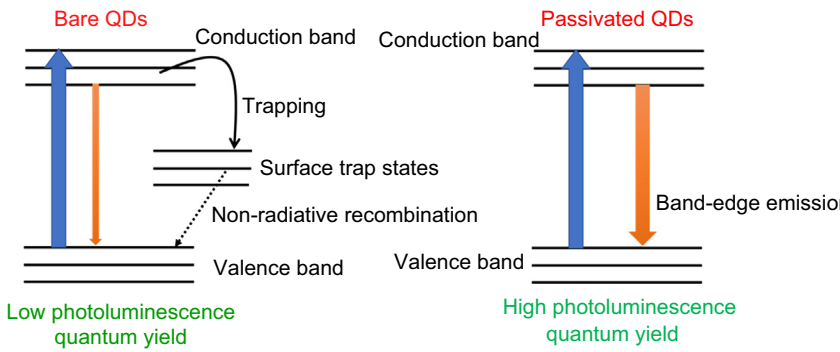

Figure 10.3 Difference in the PLQY obtained for bare QDs and surface passivated QDs.

non-radiatively to give a weak trap emission. On the contrary, QDs with the surface states passivated by inorganic or organic shells remove the occurrence of trap emission and allow only the band-to-edge emission [19]. Consequently, the photoluminescence quantum yield (PLQY) is low for the bare QDs and high for the surface-passivated QDs. In recent years, perovskite materials based on the metal halides have grabbed the attention of the scientific community working in the field of optoelectronics [20]. Particularly, hybrid organic−inorganic metal halide perovskite nanocrystals (NCs) of the form $MPbX_3$ (where M = MA [CH_3NH_3], FA [$CH_3(NH_2)_2$]; X = Cl, Br, I) have shown great potential in the luminescence industry. CsPbX QDs have also been regarded as excellent luminescent materials owing to their high PLQY. The next generation of LEDs is certainly going to adopt these perovskite materials that offer several intrinsic advantages owing to their direct bandgap. They are also known to produce high PLQY that can reach close to unity, high carrier mobility, and long exciton diffusion length [21]. The introduction of perovskite NCs for photovoltaic applications led to an epiphany that these materials can be used for LEDs too.

For an LED bulb, the driver circuit forms an integral part that converts the electricity from the mains supply into a form that can be used to operate the LEDs. Unfortunately, the driver circuits are the first ones to fail in an LED package and virtually shorten the life of the luminaire. As a solution to this, certain manufacturers have started eliminating the driver component out of the equation. Some others adopted multichannel LED drivers instead of single-channel drivers to increase device efficiency and reduce the production costs [22]. For each of the individual LED channels, the drivers can operate at different brightness levels. This enables optimization of the lighting applications as compared to single-channel drivers. LED retrofits are also a solution to reduce the maintenance costs by enabling the replacement of only the faulty components of the system, rather than replacing the entire luminaire.

10.4 Innovations in the applications of LEDs

There is a lot of buzz going on in the lighting industry with the new-found applications of LEDs. LEDs have made a strong and comprehensive presence in human life. Their suitability for applications in diverse areas has aided them to go beyond the frontiers that were never reachable by its preceding light technologies. LEDs have also paved way to achieve smart lighting solutions, wherein the luminaire can be controlled remotely just by a touch on the smartphone. LED luminaires can be connected with a smartphone, and thus, the smartphones can be used to control the lights that can be controlled. The lights can be switched on/off, dimmed, and its color hue can be varied as per the need. The biggest potential benefit of this feature is the greater energy savings attained by the smart utilization of the light. In commercial airlines, passengers often experience jetlag during their international travel across the longitudes of the earth. As illustrated in Fig. 10.4, the aircrafts are installed with color-tunable LEDs to provide comfortable lighting to the passengers and make them adjust with the jetlag faced while traveling to different time zones.

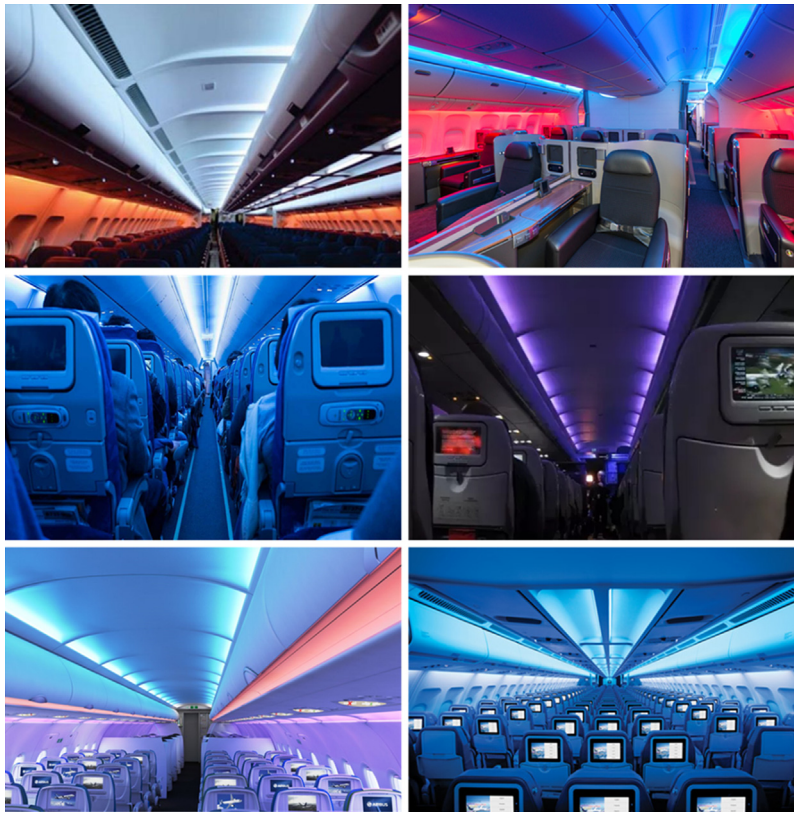

Figure 10.4 Color tunable aircraft cabin-lighting.

Apart from smartphones, LED luminaires now offer the ability to connect with the Internet of Things (IoT). The term IoT is usually meant for describing the set of gadgets (in addition to computers or smartphones) that are connected with the networking web. Thus, all sorts of household equipment such as fridge, air-conditioners, TVs, and lamps can be included in IoT as they can be connected to the internet. The best way to connect all the things at once is through the ideal network provided by lighting. As light fixtures are already installed on the ceilings and walls of a building, it is easy to connect them to all possible things on which light will fall on. The only requirement will be the additional installation of some sensors and a data connection. Commercial outlets, museums, indoor spaces, railway stations, and airports are all transforming into internet hubs, and this will be further facilitated by the new Li-Fi system. The smart lighting feature of LEDs enables them to operate the Li-Fi system and connect all the things to a single network. These light bulbs are becoming smarter and can be controlled by voice commands too. LIFX, a pioneer in smart LED lamps, has collaborated with Google to add voice controls for the LED lamps through smartphones or other devices that run on the Google's Android operating system. The voice

commands can control the lighting system connected to it through the LIFX app or can be controlled using Google without the app. The lights can be switched on or off, and the lamp's color hue and brightness can be adjusted just by giving voice commands on the Android device. The Android device must be always kept connected to the network for enabling the voice command feature. Philips Hue is another android app that has been introduced to control the lighting system. Fig. 10.5 illustrates the LIFX app and Philips Hue app.

LEDs have made promising future for the horticulture and indoor farming. These innovative sources of artificial lighting have improved the nutrient quality in plants, microgreens, and sprouts [23]. LEDs not only provide supplementary illumination for plants but may also prove to be useful sole-source lighting at times when no other light source (including solar energy) is available. The exposure of sprouts and microgreens to the LED source can help in the regulation of a series of structural genes in them. These are of utmost importance for the biosynthesis of phytochemical compounds such as carotenoids and flavonoids. It is predicted that the number of greenhouses and horticulture farms depending on LED light sources will be on a

Figure 10.5 Android-based LIFX and Philips Hue apps for controlling the LED lighting system.

rise [24]. The introduction of LEDs into the food industry has provided huge health benefits and opened up possibilities to produce enough grains and vegetation to sustainably feed the ever-expanding population.

10.5 Innovations in fashion

The best way to express fashion in society is through the clothes worn by an individual. The fabric materials used for clothes are meant to be both seasonal wear and attractive. Gone are the days when people used to prefer clothes just on the basis of fashion. The modern era demands something extra in addition to fashion. Swedish designer, Malin Bobeck, made efforts to bring life into the fabrics by inducting LEDs into them. She created a glowing fabric by weaving optical fibers in them. She developed a grand textile of wonder by incorporating 500 programmable LEDs into the fabric that responded to human touch. Several other textile industries experimented by developing jackets and coats embedded with LEDs. They are also embedded in the skirts for ladies and girls to light up their thighs and give a more fashionable appearance to the user. Depending on the movement of the user, the LEDs change colors with the help of gyro sensors that keep track of the user's movements. The gyro sensors are miniature in size that is capable of sensing even the rotational movement of skirts. Consequently, the skirt shows different patterns and colors of light, thereby giving a vivid appearance to the skirt. Another wonderful piece of LED skirt was launched by ThinkGeek, a US online retailer. They named the skirt as "Twinkling Stars Skirt" because of the fancy pattern of LED lights that twinkle like a star constellation as shown in Fig. 10.6. There are more than 250 LED lights embedded within the blue skirt to mimic the star constellations. There are three layers that give a fascinating appearance to the skirt. The layers include the white liner, the gauze layer, and the

Figure 10.6 "Twinkling Stars Skirt" created by ThinkGeek.

transparent constellation layer. The battery-powered LED lights are attached to the gauze layer that consists of 30 elastic snap tabs. The battery pack is held within a built-in pocket in the gauze layer. The blue skirt can be worn with the lights on or off. If the battery pack is removed, it becomes just like a regular skirt. However, when the lights are powered on, the 45 feet of the LED strip will shine within the layers to appear like fairy lights twinkling through the fabric.

Apart from the fancy appearance for fashion, LED clothing has also been brought to certain life-saving applications. LED embedded apparels are recommended for cyclists at night to prevent them from accidents. The National Highway Traffic Safety Administration (NHTSA), a US federal agency, has reported that the number of cyclists dying due to accidents has increased particularly because they are not visible to other vehicle drivers at night. The Centers for Disease Control and Prevention, a US federal agency under the Department of Health and Human Services, recommended the cyclists to wear apparel with active lighting and reflective panes. Visijax, which is a leading company in the world for the production of wearable electronic apparel and clothing, has developed a coat with LED lights embedded on the back of its sleeves. The lights would flash whenever the cyclist wearing the coat would lift his arm to signal his turn and thereby, alert other vehicle drivers on the path or behind the cyclist. A narrow strip of red LEDs is also embedded at the back bottom of the coat to mimic like a brake-light. However, the coat is incapable of sensing the braking of the cycle and hence, the red strip of LEDs is a mere indicator of the presence of the rider. A line of apparel embedded with smarter LED lights was developed by Lumens. When the lights are not on, the jacket looks like a regular, fashionable one. These LED lights are customized to conduct several functions in the jacket. Lumens app, which is available in both Android and iOS versions, can pair with these LED lights and perform several actions. They can be configured to use GPS navigation through Google Maps and the gyros with the help of this app. The jacket worn by the cyclist can give signals of his movements to other vehicle drivers and warn them about the cyclist's next move. For example, the jacket shall stimulate a red brake light when the cyclist stops, flash an orange light to signal his turn, and switch on the strobe mode while crossing an intersection, as shown in Fig. 10.7. The lights can also be customized to indicate different activities of the wearer. Another British brand, Lumo, has also introduced a wide range of apparel and backpacks with built-in LEDs. The LED lights on the clothes may go unnoticed during the day but will never miss any admirers during the night. As per Lumo's claims, these LEDs are visible from a distance of 400 m in the dark. Other added advantages of these clothes are that they are stain-resistant, waterproof, and can be machine-washed. The LED lights are powered by a light-weight rechargeable battery that can last for 2−6 h on a single charge. Lumo's Herne Hill Harrington jackets boast of bike-friendly features that consist of a dropped tail, stretchable shoulders, and inner cuffs capable of resisting the entry of cold air. This range of apparel also includes a polo shirt with white LEDs (WLED) in the front placket and red LEDs at the back seam. The Bermondsey backpack is decorated with WLEDs on its straps and red LEDs on its back. Impulse has also created a jacket to increase the rider's

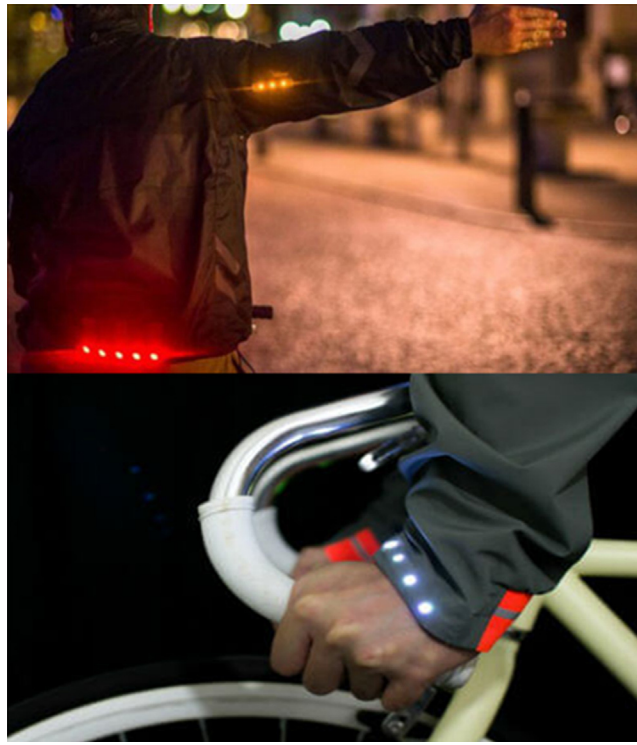

Figure 10.7 Jacket embedded with LEDs for the cyclists.

visibility to other vehicle drivers through the illumination of its high-output LEDs. These jackets offer a wireless link with the motorcycle that aids in stimulating the illumination of certain LEDs based on the movement of the motorcycle.

LED lights have also been embedded in clothes to detect the Wi-Fi and Bluetooth signals in the nearby premises. Matt Martin created a perfect shirt with a combination of electronic devices powered by Li-polymer batteries to detect the Wi-Fi and Bluetooth signals. 31 Neo pixel strips comprising more than 100 LEDs were hand sewn into the shirt. LED-embedded goggles are another piece of innovation that combines the utility with fashion. The implantation of LEDs into swim-goggles has facilitated swimmers to swim from one end of the swimming pool to the other in a straight line. The goggles are easy to use in water. They are powered by high-precision compass, accelerometer, and a microprocessor. To set the target destination, the user needs to look at the far-off target and switch on the button by pushing it on the side of the goggles. This will set the target and the swimmer can swim to the destination under water. If the swimmer is swimming correctly in the direction of the destination, then the two LEDs situated above each eye of the goggles will illuminate green. If the swimmer strays away from the destination or follows a wrong path, then the LEDs

will illuminate yellow or red light depending on the level of straying. After reaching the target destination, the swimmer can set a new destination by looking at the new target and pushing the button again.

10.6 Current scenario of LED market

Manufacturers have explored the potential for LEDs by introducing new lighting designs and producing the luminaires as per the requirement of the situation in which it is to be mounted. Special care has been taken to optimize the lighting needs and provide the best experience to consumers through integrated lighting. LEDs have achieved great heights by meeting the demands of the consumers in terms of the efficiency, color tone, and operating life. Although there is seemingly little room left for improvement, LEDs continue to amaze again and again with its new developments that pushed its performance limits.

Recently, UV-LEDs have gained huge popularity owing to its disinfecting properties. The rising number of bacterial and viral infections/diseases has provided an urge to disinfect the surroundings. Of late, the mayhem caused by the COVID-19 disease has increased the demand for disinfection. The continuing global spread of the disease has fueled great concerns over the future and this has increased the need for sterilizing. Consequently, the sales for the UV-LED products have gone up significantly. Several Chinese automotive companies have relied on the UV-LEDs to develop sterilization systems for the vehicle's interiors. UV-LEDs are also used by space research centers like NASA to provide a germ-free environment for astronauts aboard the International Space Station. One of the major developments in this technology is the improvement in its lifetime. Earlier, UV-LEDs were highly expensive and offered a short lifetime of just 10,000 h. This disheartened many manufacturers and they refrained from the production of UV-LEDs. However, a South Korean company, Seoul Viosys Co. started developing Violed UV-LEDs that offered a higher lifetime of 50,000 h. They claim that 1 min of UVC exposure using UV-LEDs can sterilize about 90% of the coronavirus and 97% of the influenza-type viruses [25]. Everlight has also designed a 280-nm emitting UVC LED that can kill pathogens effectively. These LEDs are packaged in inorganic quartz and can be mounted in direct contact with the water, thereby, making them eligible to disinfect the drinking water more efficiently. The US Department of Energy's Ames Laboratory has developed an OLED that can emit near-ultraviolet light [26]. These OLEDs could emit light in the wavelength range of 370−430 nm.

The market trend for the LEDs has always been ascending since its penetration into the lighting and display industries. Although LEDs were priced much higher than their counterpart technologies, their efficiency and longer lifespan compensated for the initial investments [3]. There has been a rise in the LED market at a global level. It is projected that 67% of the energy will be saved by the year 2030 with the implementation of LEDs [27].

Unfortunately, there has been a down graph in 2020 in the market for packaged LEDs in overall. Compared to its preceding year, the year 2020 witnessed a decline

of 4% in the market for packaged LEDs. There were a plethora of negative factors that resulted in this scenario. There was an oversupply of LEDs in the late 2018 that led to a drop in the prices during the first quarter of 2019 and the situation worsened further with the price erosion of LEDs in mid-2019. This led to a significant drop in LED prices during the fourth quarter of 2019. Compared to the fourth quarter of the previous year, the mid-power LED price dropped by 20%−30%, while the prices of high-power LED dropped by 5%−10%. The overall decline in the revenues of the LED market for 2019 was about 4% than the previous year. Another factor that put a dent in the LED market was the US−China trade war. It was anticipated that the repercussions of the trade war will be sorted out in 2020 and the LED market will resume its recovery with the pickup in its demand. However, things got worse with the outbreak of the coronavirus disease (COVID-19) in December 2019. It is still not clear how the pandemic will impact the LED business in 2020 and the succeeding years. The year 2019 also witnessed the shutting down of many troubled manufacturing companies that were later acquired by the giant players such as Signify, GE, and Acuity; yet, the manufacturers are optimistic that the LED market will gain positive momentum and recover all its losses incurred due to the global crisis. By 2024, the LED market is expected to show 5% growth to reach the revenues of $20 billion. Huge growth is anticipated in the sales of mini-LED and micro-LED based displays. This sector earned $200 million revenue in 2019 and is expected to grow to $1.6 billion by 2024. The 5-year forecast predicts that the revenue of the initial 3 years will be mainly contributed by the mini-LEDs that would serve as backlighting for displays in a more fashionable way than the present displays. The last two years of the forecast will be mainly dominated by the self-emissive displays developed from micro-LEDs.

10.7 Limitations and challenges

LEDs have become the backbone for the SSL industry and many other related sectors. LEDs have successfully overcome most of the limitations faced by the previous lighting sources. Some of the advantages accompanied by the LEDs were the superior color rendering ability and spectral output, higher efficiency, longer lamp life, lower power consumption, etc. All these attributes made LEDs distinct from other lighting sources and hence, LEDs became the most desirable lighting technology. Yet, certain limitations put LEDs on the back foot at certain points. The LED industry has made massive strides in growth and processing technologies. Regardless of the breath-taking progress made by LEDs, there are still certain issues that require further improvement. The performance and reliability of LEDs are sensitive to the temperature and other environmental conditions. In addition, there are certain challenges faced in the cost-control during production and thermal management. LEDs exhibit optimum performance in the ambient temperature of the operating environment. In high-power LEDs, this feature is highly critical. In recent years, there has been significant improvement in the energy efficiency of LEDs. Yet, there has been a lot of heat

dissipation from LED packages mainly because of the electronic drivers installed in them. LEDs can be permanently damaged if they are exposed to heat very often. It may also result in the degradation of the LED's performance, decrease in the quality and quantity of the light output, or premature failure of the device. It is highly crucial to provide proper heat sink or cooling systems to the luminaires to ensure proper heat dissipation. This would guarantee a long lifetime for the LEDs and allow its operation in a wide range of temperatures. The involvement of heat sinks in the LED package is one of the prime reasons that the manufacturers are facing difficulty in bringing down the production costs of the LED. Heat sinks are unavoidable components of the package and are essential to curb the problem of overheating. Generally, materials with high thermal conductivity are used to propagate the heat out of the package. However, these materials come with a substantial amount of weight and cost. As a result, the weight of the LED package increased along with its cost. Additionally, the higher weight of the package means that the cost of shipping the LED products is also raised. An LED package generally consists of three features [28]:

(a) Heat generation and dissipation
(b) Fluid flowing and molding
(c) Lighting extraction and control.

The first two features strongly influence the lighting extraction and control of the LED package. The heat generation in the LED package can arise from multiple reasons. The prime reason for the generation of heat in the package is the non-radiative recombination processes in the LED chips. In addition, the driver circuits add to the overall heat generation in the package. The phosphor coated on the chip is also affected by the heating of the LED chip. The heat generated in the chip will be conducted by the phosphor coating, and during operation the phosphors themselves can generate additional heat. A phosphor is coated on the chip by embedding them in a silicon matrix. The phosphor can be considered as a non-Newtonian fluid that also exhibits the flowing processes of contacting, wetting, spreading, and stabilizing [28]. When a phosphor gel is dispensed over the LED chip, it makes a contact with the chip and wets it to cover the chip. The phosphor spreads over the heat slug and then stabilizes over the chip to form a convex shape. However, the phosphors particles can form non-uniform distribution on the chip as a result of gravity. The non-uniform distribution of phosphors can adversely affect the optical characteristics of the LED package [29,30].

Sometimes, flickering and other visual anomalies are observed in LED lamps, which appear due to the occurrence of large ripples in the DC power supplied to the lamps. The temporal variation in the power supply causes flickering in the lighting. When an unbalanced current waveform is supplied to the LED, flickering happens. The LED drivers supply a regulated power supply to the LEDs from an AC power input. The regulated power supply provides a stable and balanced power for the LED to operate. Any kind of instability in the power supply would result in the LEDs to flicker indicating a malfunction in its operation. It is a challenge to develop appropriate driver circuits and power supplies for an LED that can avoid the flickering

of light from the LEDs. The glare from the LEDs remains to be an obstacle, which must be addressed by the manufacturers to improve the overall lighting experience. LED lights are also facing certain challenges in the automotive lighting sector. WLEDs have found suitable applications in the automotive forward-lighting applications. Although their mechanical packaging and thermal resistance were appropriate for this purpose, their luminance and luminous flux remain a matter of concern. Still, high-intensity discharge (HID) lamps show higher luminance and luminous flux than the LEDs. The LED headlamps are now just limited to the premium model cars due to their high pricing.

10.8 Future prospects and scope

The new decade has ascended with higher aspirations and planning to tackle the newer challenges in the lighting industry. The industry has experienced rapid digitalization and dazzling transformation to exhibit some key advances in the technology due to which the SSL industry will touch the greatest heights in the next 10 years. The manufacturers are trying to take advantage of every opportunity by designing the LED products with the involvement of the latest technologies that are at their pike. The LED industry has gone through certain ups and downs in the recent past. However, in the long run, LEDs have proven a profitable track and will keep continuing to do so. LEDs have successfully penetrated various sectors such as automotive lighting, traffic signals, communications, signage lighting, medical sector, horticulture, and food industry. However, its main objective was to dominate the general lighting sector and to eliminate the existence of incandescent and fluorescent lamps. The emergence of LEDs has not only lowered the energy consumption but also reduced the carbon footprint. The whole new range of applications is now driven by the new LED technology that has presented a novel approach to the lighting products.

During the early days, there used to be a belief that LEDs are not meant for every application. However, things have changed and now LEDs have spread their wings in almost every field. Some fields have adopted LED technology a bit slower than others, but this did not halt the penetration of LED technology in those fields. Rather, the old technologies were forcefully thrown out by the consumers who were overwhelmed by the richness of the LED technology. Nowadays, everything is turning wireless and eliminating the long tangling wired connections that often resulted in a mess. The lighting controls are also not an exception and they are slowly approaching the wireless trend. Wireless communication devices such as tablets or smartphones can be used to control the luminaires and set the desired color hue. The retrofit modules of LEDs are the most appealing as they eliminate the need for replacing the entire luminaire and just concentrate on the replacement of the faulty component of the module. In short, LED luminaires are transforming into plug-and-play devices that do not require a professional electrician to come and replace the faulty luminaire.

10.9 Conclusions

It is a daunting task to predict the position of LEDs or SSL in the next 10 or 20 years. However, identifying the present conditions as clues to the future, it can be assumed that LEDs will head-on to become the prime technology for lighting and other related applications. The rise and popularity of LEDs have helped in the cause of lowering their prices and making them easily available in the market. The boundaries projected on the LED efficacy and costs by the Haitz's law have been shattered long back. One of the reasons for the LEDs exceeding the limits set by this law is the incorporation of phosphors into the device structure. Phosphors have become an integral part in the fabrication of WLEDs. The innovations introduced in the design and applications of LEDs have grabbed global attention. Despite the present global economic conditions, the LED market has maintained its vibrancy. It has not only established a strong position in the market but also eliminated the existence of its rival technologies. Although there are certain limitations and issues, LEDs hold the ability to overcome them and emerge as a flawless technology very soon. Owing to the rapid improvements in the mechanical, electrical, optical, and thermal components, it is guaranteed that the LED technology will advance rapidly to reach the pinnacle very soon.

References

[1] A. Mills, Trends in HB-LED markets, III-vs Rev. 14 (2001) 38−42, https://doi.org/10.1016/S0961-1290(01)80124-1.

[2] J.-W. Park, Y.-B. Yoon, S.-H. Shin, S.-H. Choi, Joint structure in high brightness light emitting diode (HB LED) packages, Mater. Sci. Eng. A 441 (2006) 357−361, https://doi.org/10.1016/j.msea.2006.09.043.

[3] G.B. Nair, S.J. Dhoble, A perspective perception on the applications of light-emitting diodes, Luminescence 30 (2015) 1167−1175, https://doi.org/10.1002/bio.2919.

[4] R. Haitz, J.Y. Tsao, Solid-state lighting: 'The case' 10 years after and future prospects, Phys. Status Solidi 208 (2011) 17−29, https://doi.org/10.1002/pssa.201026349.

[5] LED Lighting Market by Installation Type (New Installation and Retrofit Installation), End-Use Application (Indoor Lighting and Outdoor Lighting), Product Type (Lamps and Luminaires), and Geography - Global Forecast to. 2022, https://www.marketsandmarkets.com/Market-Reports/led-lighting-market-201130554.html?gclid=CjwKCAjwvOHzBRBoEiwA48i6AirGOClHfY21qoY_eUIWaVO5beoOc34YBS1zYZy4kXjvKY_iDbZ73RoCt4wQAvD_BwE (accessed March 23, 2020).

[6] S. Kwon, W. Kim, H. Kim, S. Choi, B.-C. Park, S.-H. Kang, K.C. Choi, High luminance fiber-based polymer light-emitting devices by a dip-coating method, Adv. Electron. Mater. 1 (2015) 1500103, https://doi.org/10.1002/aelm.201500103.

[7] A.K. Geim, K.S. Novoselov, The rise of graphene, Nat. Mater. 6 (2007) 183−191, https://doi.org/10.1038/nmat1849.

[8] T.-H. Han, Y. Lee, M.-R. Choi, S.-H. Woo, S.-H. Bae, B.H. Hong, J.-H. Ahn, T.-W. Lee, Extremely efficient flexible organic light-emitting diodes with modified graphene anode, Nat. Photon. 6 (2012) 105−110, https://doi.org/10.1038/nphoton.2011.318.

[9] H.-K. Seo, M.-H. Park, Y.-H. Kim, S.-J. Kwon, S.-H. Jeong, T.-W. Lee, Laminated graphene films for flexible transparent thin film encapsulation, ACS Appl. Mater. Interfaces 8 (2016) 14725−14731, https://doi.org/10.1021/acsami.6b01639.
[10] M.C. Gather, A. Köhnen, K. Meerholz, White organic light-emitting diodes, Adv. Mater. 23 (2011) 233−248, https://doi.org/10.1002/adma.201002636.
[11] D. Di, A.S. Romanov, L. Yang, J.M. Richter, J.P.H. Rivett, S. Jones, T.H. Thomas, M. Abdi Jalebi, R.H. Friend, M. Linnolahti, M. Bochmann, D. Credgington, High-performance light-emitting diodes based on carbene-metal-amides, Science 356 (2017) 159−163, https://doi.org/10.1126/science.aah4345.
[12] J.H. Burroughes, D.D.C. Bradley, A.R. Brown, R.N. Marks, K. Mackay, R.H. Friend, P.L. Burns, A.B. Holmes, Light-emitting diodes based on conjugated polymers, Nature 347 (1990) 539−541, https://doi.org/10.1038/347539a0.
[13] F. Huang, P.-I. Shih, C.-F. Shu, Y. Chi, A.K.-Y. Jen, Highly efficient polymer white-light-emitting diodes based on lithium salts doped electron transporting layer, Adv. Mater. 21 (2009) 361−365, https://doi.org/10.1002/adma.200802179.
[14] B. Zhang, G. Tan, C.-S. Lam, B. Yao, C.-L. Ho, L. Liu, Z. Xie, W.-Y. Wong, J. Ding, L. Wang, High-efficiency single emissive layer white organic light-emitting diodes based on solution-processed dendritic host and new orange-emitting iridium complex, Adv. Mater. 24 (2012) 1873−1877, https://doi.org/10.1002/adma.201104758.
[15] C. Min, C. Shi, W. Zhang, T. Jiu, J. Chen, D. Ma, J. Fang, A small-molecule zwitterionic electrolyte without a π-delocalized unit as a charge-injection layer for high-performance PLEDs, Angew. Chem. Int. Ed. 52 (2013) 3417−3420, https://doi.org/10.1002/anie.201209959.
[16] S. Höfle, A. Schienle, C. Bernhard, M. Bruns, U. Lemmer, A. Colsmann, Solution processed, white emitting tandem organic light-emitting diodes with inverted device architecture, Adv. Mater. 26 (2014) 5155−5159, https://doi.org/10.1002/adma.201400332.
[17] A. Perumal, H. Faber, N. Yaacobi-Gross, P. Pattanasattayavong, C. Burgess, S. Jha, M.A. McLachlan, P.N. Stavrinou, T.D. Anthopoulos, D.D.C. Bradley, High-efficiency, solution-processed, multilayer phosphorescent organic light-emitting diodes with a copper thiocyanate hole-injection/hole-transport layer, Adv. Mater. 27 (2015) 93−100, https://doi.org/10.1002/adma.201403914.
[18] D.B. Straus, E.D. Goodwin, E.A. Gaulding, S. Muramoto, C.B. Murray, C.R. Kagan, Increased carrier mobility and lifetime in CdSe quantum dot thin films through surface trap passivation and doping, J. Phys. Chem. Lett. 6 (2015) 4605−4609, https://doi.org/10.1021/acs.jpclett.5b02251.
[19] J. Lim, W.K. Bae, J. Kwak, S. Lee, C. Lee, K. Char, Perspective on synthesis, device structures, and printing processes for quantum dot displays, Opt. Mater. Express 2 (2012) 594, https://doi.org/10.1364/OME.2.000594.
[20] N. Wang, L. Cheng, R. Ge, S. Zhang, Y. Miao, W. Zou, C. Yi, Y. Sun, Y. Cao, R. Yang, Y. Wei, Q. Guo, Y. Ke, M. Yu, Y. Jin, Y. Liu, Q. Ding, D. Di, L. Yang, G. Xing, H. Tian, C. Jin, F. Gao, R.H. Friend, J. Wang, W. Huang, Perovskite light-emitting diodes based on solution-processed self-organized multiple quantum wells, Nat. Photon. 10 (2016) 699−704, https://doi.org/10.1038/nphoton.2016.185.
[21] M. Cao, Y. Xu, P. Li, Q. Zhong, D. Yang, Q. Zhang, Recent advances and perspectives on light emitting diodes fabricated from halide metal perovskite nanocrystals, J. Mater. Chem. C. 7 (2019) 14412−14440, https://doi.org/10.1039/C9TC03978C.
[22] C. Ye, H.W. Chan, D. Lan, P. Das, S.K. Sahoo, Efficiency improvement of multichannel LED driver with selective dimming, IEEE Trans. Power Electron. 35 (2020) 6280−6291, https://doi.org/10.1109/TPEL.2019.2951629.

[23] X. Zhang, Z. Bian, X. Yuan, X. Chen, C. Lu, A review on the effects of light-emitting diode (LED) light on the nutrients of sprouts and microgreens, Trends Food Sci. Technol. 99 (2020) 203−216, https://doi.org/10.1016/j.tifs.2020.02.031.

[24] Y.A. Berkovich, I.O. Konovalova, S.O. Smolyanina, A.N. Erokhin, O.V. Avercheva, E.M. Bassarskaya, G.V. Kochetova, T.V. Zhigalova, O.S. Yakovleva, I.G. Tarakanov, LED crop illumination inside space greenhouses, Reach. Out. 6 (2017) 11−24, https://doi.org/10.1016/j.reach.2017.06.001.

[25] COVID-19 Increases Demand for Disinfecting UVLEDs, https://www.photonics.com/Articles/COVID-19_Increases_Demand_for_Disinfecting_UVLEDs/a65629 (accessed March 19, 2020).

[26] E. Manna, F. Fungura, R. Biswas, J. Shinar, R. Shinar, Tunable near UV microcavity OLED arrays: characterization and analytical applications, Adv. Funct. Mater. 25 (2015) 1226−1232, https://doi.org/10.1002/adfm.201403313.

[27] A. Nardelli, E. Deuschle, L.D. de Azevedo, J.L.N. Pessoa, E. Ghisi, Assessment of Light Emitting Diodes technology for general lighting: a critical review, Renew. Sustain. Energy Rev. 75 (2017) 368−379, https://doi.org/10.1016/j.rser.2016.11.002.

[28] X. Luo, R. Hu, S. Liu, K. Wang, Heat and fluid flow in high-power LED packaging and applications, Prog. Energy Combust. Sci. 56 (2016) 1−32, https://doi.org/10.1016/j.pecs.2016.05.003.

[29] N.T. Tran, F.G. Shi, Studies of phosphor concentration and thickness for phosphor-based white light-emitting-diodes, J. Lightwave Technol. 26 (2008) 3556−3559, https://doi.org/10.1109/JLT.2008.917087.

[30] R. Yu, S. Jin, S. Cen, P. Liang, Effect of the phosphor geometry on the luminous flux of phosphor-converted light-emitting diodes, IEEE Photon. Technol. Lett. 22 (2010) 1765−1767, https://doi.org/10.1109/LPT.2010.2085080.

Index

Note: 'Page numbers followed by "f" indicate figures and "t" indicates tables.'

WOODHEAD PUBLISHING SERIES IN ELECTRONIC AND OPTICAL MATERIALS

Traditional light sources are fast being replaced by the light-emitting diodes (LEDs). The fourth generation of lighting is completely dominated by LED luminaires. Apart from lighting, LEDs have extended their hold on other fields such as digital communications, horticulture, medical fields, space research, art and culture, display devices, entertainment, and so on. The technological promises offered by LEDs have elevated them as a front-runner in the lighting industry. This book explores the journey of LEDs for readers belonging to the scientific community.

This book reviews the general understanding of the luminescence processes and the background of solid-state lighting. It includes special emphasis on the phosphor-converted LEDs that are based on inorganic phosphors. It also explores the different types of LEDs that are based on inorganic, organic, quantum dots, perovskite-structured materials, and biomaterials. A detailed description has been included about the diverse applications of LEDs in fields such as lighting, displays, horticulture, biomedical, and digital communication. Considerable importance has been given to discussion of the challenges that must be solved before using LEDs in commercial applications.

Key features:

- Presents a concise overview of different types of LEDs based on inorganic phosphors, organic materials, quantum dots, perovskite-structured materials, and biomaterials
- Includes a discussion of current and emerging applications in lighting, communications, horticulture, and medical fields
- Addresses fundamentals, luminescence mechanisms, and key optical materials (including synthesis methods)

About the Authors

Dr. Govind B. Nair is currently a Postdoctoral researcher at the University of the Free State, Bloemfontein, South Africa. During his PhD, he was awarded with an INSPIRE Fellowship, which is a prestigious fellowship program conducted by the Department of Science and Technology (DST), India. His areas of research include the synthesis and characterization of optical materials, theoretical analysis of luminescence processes, structural analysis of materials, etc.

Dr. S.J. Dhoble is presently working as a Professor in the Department of Physics, R.T.M. Nagpur University, Nagpur, India. Dr. Dhoble has published more than 600 research papers in international and national reviewed journals and presented more than 1300 research papers in international and national conferences on solid-state lighting, LEDs, radiation dosimetry, phototherapy, and laser materials.

Technology and Engineering / Electronics / General

ISBN 978-0-12-819605-2

9 780128 196052

WP
WOODHEAD PUBLISHING
An imprint of Elsevier
elsevier.com/books-and-journals

ELSEVIER